Prevention of oxidative stress for cytoprotection of intestinal epithelial cells

Dinesh Babu

2015

Thesis submitted as partial fulfilment of the requirements for the degree
of Doctor in Medical Sciences

**Dedicated to my
FAMILY
(**F**ather **A**nd **M**other **I **L**ove **Y**ou)**

Faculty of Medicine and Health Sciences

Heymans Institute of Pharmacology

Promotor: Prof. Dr. R.A. Lefebvre

Prevention of oxidative stress for cytoprotection of intestinal epithelial cells

Dinesh Babu

2015

Thesis submitted as partial fulfilment of the requirements for the degree
of Doctor in Medical Sciences

List of abbreviations

AMPs	antimicrobial peptides
ANOVA	analysis of variance
APC	allophycocyanin
AP-1	activator protein-1
ATP	adenosine triphosphate
BHA	butylated hydroxyanisole
BHT	butylated hydroxytoluene
BVR	biliverdin reductase
carboxy-H_2DCFDA	5-(and-6)-carboxy-2′,7′-dichlorodihydrofluorescein diacetate
CCCP	carbonyl cyanide 3-chlorophenylhydrazone
cGMP	intracellular cyclic guanosine monophosphate
CHX	cycloheximide
CLP	cecal ligation and puncture
CM-H_2DCFDA	5-(and-6)-chloromethyl-2′,7′-dichlorodihydrofluorescein diacetate, acetyl ester
CO	carbon monoxide
COHb	carbon monoxide-hemoglobin
CoPP	cobalt protoporphyrin IX
CoQ	coenzyme Q
CO-RM	carbon monoxide-releasing molecule
COX	cyclo-oxygenase
Cu/ZnSOD	copper/zinc superoxide dismutase
DAMPs	damage-associated molecular patterns
DCF	dichlorofluorescein
DCs	dendritic cells
DFO	desferrioxamine
DHR123	dihydrorhodamine 123
DMEM	Dulbecco's modified Eagle's medium
DMOG	dimethyloxallyl glycine
DMSO	dimethyl sulfoxide
DNA	deoxyribonucleic acid
DPI	diphenylene iodonium
DUOX	dual oxidase
ECAR	extracellular acidification rate
EGDT	early goal-directed therapy
eNOS	uncoupled endothelial nitric oxide synthase
ERK	extracellular signal-regulated kinase
ETC	electron transport chain

E2	17-β-estradiol
FAEEs	fatty acid ethyl esters
FCCP	carbonyl cyanide p-trifluoromethoxyphenylhydrozone
Fe^{2+}	ferrous iron
FITC	Fluorescein isothiocyanate
GALT	gut-associated lymphoid tissue
GI	gastrointestinal
GPx	glutathione peroxidase
GSH	reduced glutathione
GSSG	glutathione disulfide
GTPase	guanosine triphosphate hydrolase
Hb	hemoglobin
HBSS	Hanks' balanced salt solution
HO	heme oxygenase
HOCl	hypochlorous acid
H_2DCFDA	2'7'-dichlorodihydrofluorescein diacetate acetyl ester
H_2O	water
H_2O_2	hydrogen peroxide
IBD	inflammatory bowel disease
ICAM	intercellular adhesion molecule
IECs	intestinal epithelial cells
IFNγ	interferon gamma
IL	interleukin
iNOS	inducible nitric oxide synthase
i.p.	intraperitoneal
I/R	ischemia/reperfusion
i.v.	intravenous
JNK	c-Jun amino-terminal kinases
KC	keratinocyte chemoattractant
KCN	potassium cyanide
LDL	low-density lipoprotein
LPS	lipopolysaccharide
LSCM	laser scanning confocal microscopy
MAPK	mitogen-activated protein kinase
MCP-1	monocyte chemoattractant protein-1
MDA	malondialdehyde
MFI	mean fluorescence intensity
Mito-TEMPO	2-(2,2,6,6-tetramethylpiperidin-1-oxyl-4-ylamino)-2-oxoethyl triphenylphosphonium chloride monohydrate
MnSOD	manganese superoxide dismutase
MOF	multiple organ failure

MPO	myeloperoxidase
mtDNA	mitochondrial DNA
m$^\phi$	macrophages
NAC	N-acetylcysteine
NADPH	nicotinamide adenine dinucleotide phosphate
Nalp	Nacht domain-, Leucine-rich repeat-, and PYD-containing protein
NDUFB8	NADH dehydrogenase [ubiquinone] 1 beta subcomplex subunit 8
NEC	necrotizing enterocolitis
NEMO	nuclear factor-κB essential modulator
NF-κB	nuclear factor-κB
NLRs	nucleotide-binding oligomerization domain-like receptors
NO$^\bullet$	nitric oxide
NOD	nucleotide-binding oligomerization domain
NOX	nicotinamide adenine dinucleotide phosphate oxidase
Nrf2	nuclear factor erythroid 2-related factor 2
NSC23766	N^6-[2-[[4-(Diethylamino)-1-methylbutyl]amino]-6-methyl-4-pyrimidinyl]-2-methyl-4,6-quinolinediamine trihydrochloride
O$_2$	oxygen
O$_2^{\bullet-}$	superoxide anion radicals
OCR	oxygen consumption rate
ODQ	1H[1,2,4,]oxadiazolo[4,3-a]quinoxalin-1-one
OH$^\bullet$	hydroxyl radical
ONOO$^-$	peroxynitrite anion
PAF	platelet activating factor
PAMPs	pathogen-associated molecular patterns
PBS	phosphate buffered saline
PERK	protein kinase R-like endoplasmic reticulum kinase
PI	propidium iodide
PKC	protein kinase C
PMA	phorbol 12-myristate 13-acetate
PMNs	polymorphonuclear leukocytes
POI	postoperative ileus
ppm	particles per million
PRRs	pattern recognition receptors
RhoGDI	Rho GDP dissociation inhibitor
RNase	ribonuclease-A
RNS	reactive nitrogen species
ROO$^\bullet$	peroxyl radical
ROS	reactive oxygen species
RT	room temperature
R123	rhodamine 123

S.E.M.	standard error of the mean
sGC	soluble guanylate cyclase
sIgA	secretory immunoglobulin A
SIH	salicylaldehyde isonicotinoyl hydrazone
SIRS	systemic inflammatory response syndrome
SIRT1	silent mating type information regulator 2 homolog 1
Sir2	*Saccharomyces cerevisiae* silent information regulator 2
SOD	superoxide dismutase
SV	simian virus
TBARS	thiobarbituric acid reactive substances
TLRs	Toll-like receptors
TMRM	tetramethyl rhodamine methyl ester
TNF-α	tumor necrosis factor alpha
TNFR1	tumor necrosis factor type I receptor
TTFA	theonyltrifluoroacetone
UGT	uridine 5'-diphospho-glucuronyltransferase
VAS-2870	3-Benzyl-7-(2-benzoxazolyl)thio-1,2,3-triazolo(4,5-d)pyrimidine
VCAM	vascular cell adhesion molecule
VDAC	voltage dependent anion channels
XDH	xanthine dehydrogenase
XO	xanthine-xanthine oxidase
ZO-1	zona occludens-1
Ψm	mitochondrial membrane potential
3D	three-dimensional

Table of contents

Chapter I

LITERATURE SURVEY

Part of the information presented in sections 1.2.3, 1.3.3 and 1.4.1 of this chapter has been published in the following publication:

Chapter I   Literature survey

I. 1   The gastrointestinal tract

I.1.1   Anatomy and histology

The human gastrointestinal (GI) tract consists of a 6-9 m long canal from mouth to anus, and the associated organs that empty their content into the canal (Fig. I.1). The GI canal consists of the mouth (the pharynx), esophagus (involving upper and lower esophageal sphincters), the stomach (comprising the cardia, fundus, corpus and antrum leading to the pyloric sphincter), the small intestine (composed of the duodenum, jejunum and ileum), the large intestine (composed of the cecum, colon and rectum) and the anus (comprising the internal and external anal sphincters).
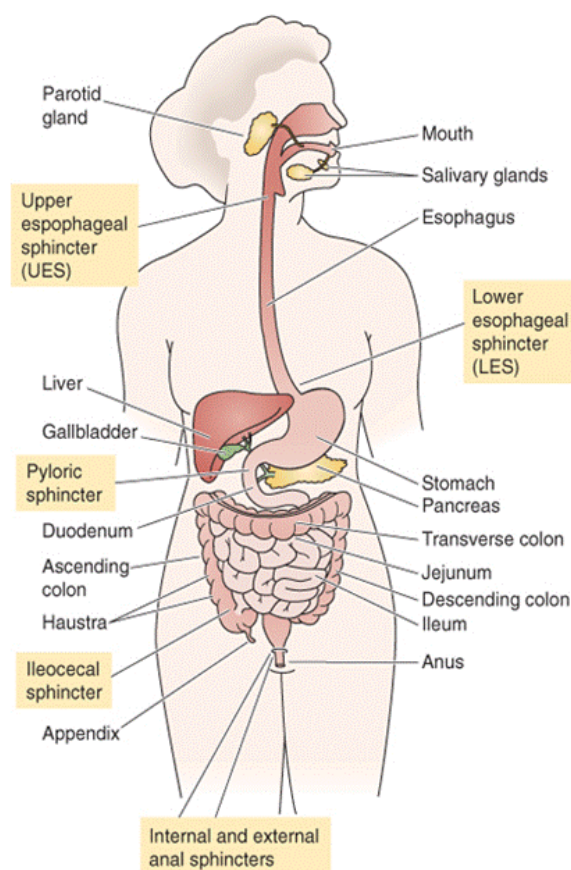
Fig. I.1   Schematic illustration of the anatomy of the gastrointestinal tract (adapted from Boron & Boulpaep, 2009).

Motility, digestion, secretion, absorption and elimination are the major physiological processes occurring in the GI tract. These processes are well coordinated by the organs of the GI tract to efficiently digest food for taking in nutrients and eliminating waste. The interplay of several humoral and neuronal mechanisms regulates the different processes of the GI tract. Apart from those major functions described above, the GI tract also plays a vital role in the *immune defense.*

The basic structural organization of the GI tract is relatively similar resembling a hollow cylindrical tube consisting of four concentric layers from inside to outside of the lumen (Fig. I.2):

- The mucosa is the innermost layer enclosing the intestinal lumen; it consists of three sublayers, namely, the epithelium, the lamina propria (a layer of loose connective tissue containing the mucosal capillaries) and the muscularis mucosae (comprising a thin smooth muscle layer).

- The submucosa is the second layer, also consisting of loose connective tissue along with the submucosal nerve plexus and blood vessels.

- The muscularis externa is the third layer, consisting of inner circular and outer longitudinal smooth muscle layers, with the myenteric nerve plexus in between.

- The adventitia is the outermost layer comprising loose connective tissue; when covered by the visceral peritoneum, it is called the serosa.
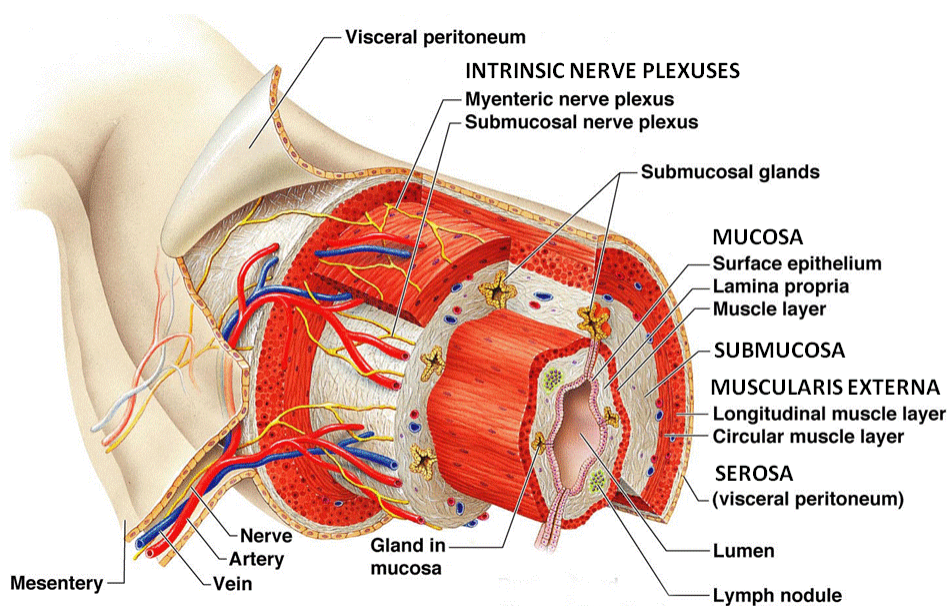
Fig. I.2 Schematic representation of the different layers of the gastrointestinal tract (adapted from Marieb *et al.*, 2004).

I.1.2   The mucosal epithelial cell layer

The surface epithelium in the mucosa forms the border between the luminal content and the body. In the oral cavity, pharynx and esophagus, it consists of non-keratinized stratified squamous epithelium; in the stomach, the small intestine and almost the entire length of the large intestine, it consists of simple columnar epithelium; in the rectum and anus, it consists of stratified columnar epithelium followed by non-keratinized stratified squamous epithelium, and finally keratinized stratified squamous epithelium towards the end of the anal canal. Starch and lipid digestion start in the oral cavity via salivary amylase and lipase, and protein digestion starts in the stomach via pepsin. But digestion is mainly covered in the small intestine via the pancreatic enzymes, entering the duodenum via the ductus pancreaticus, and via the intestinal enzymes provided by the epithelial lining of the duodenum and jejunum. All digested nutrients and the majority of water, daily passing through the GI tract via oral intake and GI secretions, are absorbed in the jejunum and ileum. The epithelial surface of the small intestine is multiplied by 600 via three mechanisms: 1) the *valvulae conniventes* hanging in the lumen (x 3); 2) the presence of finger-like projections, called intestinal *villi*, alternating with crypts in between (x 10); 3) the presence of numerous very small projections at the apical side of the epithelial cells, called *microvilli* (x 20) (Fig. I.3). This yields an estimated surface of 200 m^2 allowing the absorptive function of the small intestine but also meaning that there is a great mucosal surface in contact with luminal contents and in danger of damage. The large intestine consists of a smooth surface interspersed with crypts; a last part of water is absorbed here to maintain the water balance and indigestible material is stored till defecation occurs.

Unlike other mucosal sites, the intestinal epithelium is normally exposed to commensal bacteria and their products. The small intestine is only sparsely populated with bacteria while the large intestine contains around 10^{13} microorganisms. Thus, intestinal epithelial cells are the initial site of contact between the host and the gut microbiome. This epithelial layer prevents the uncontrolled passage of luminal contents to subepithelial tissues by forming a physical barrier between the luminal contents and the body (Karrasch & Jobin, 2009).
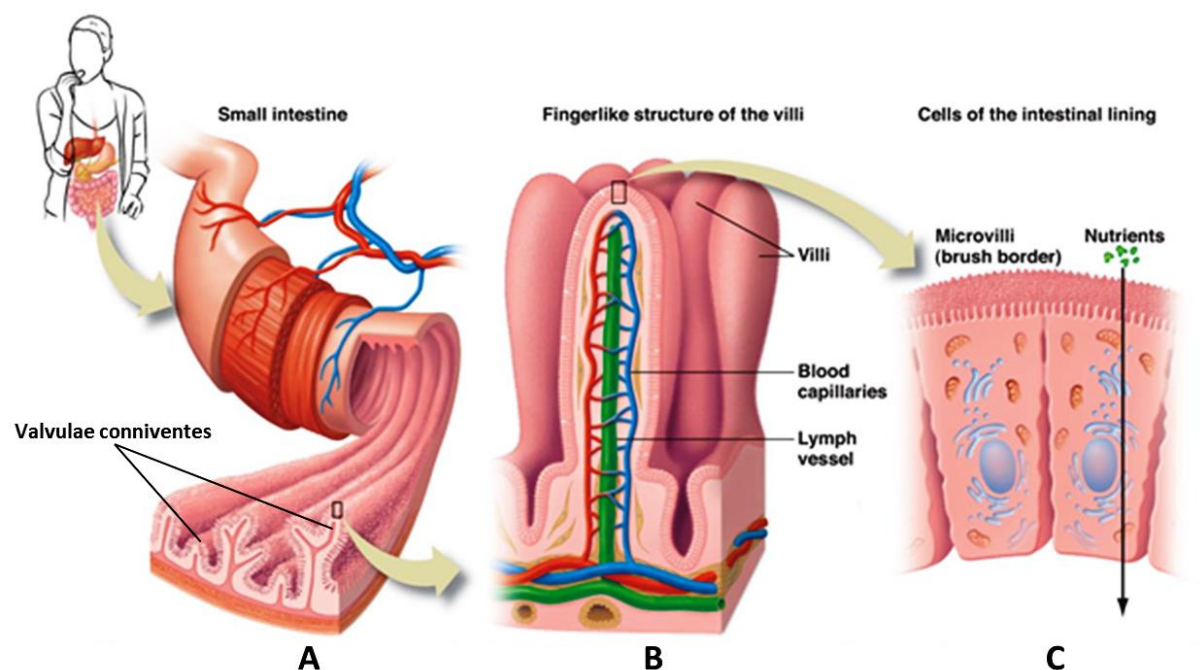
Fig. I.3 Illustration of a cross section through the small intestine with valvulae conniventes (A), villi (B) and epithelial cells featuring microvilli at the apical side (C) (from Pearson education).

The intestinal epithelium is composed of different types of cells, each of them having a specialized function. The stem cells located near (small intestine) or in (large intestine) each crypt bottom continuously produce proliferating progenitor cells, which finally result in differentiated cells along the crypt-villus axis (Sancho *et al.*, 2004; van der Flier & Clevers, 2009). These differentiated epithelial cells can be further divided into cells of the absorptive and secretory lineages (Fig. I.4A).

In the small intestine, the progenitor cells migrate to the crypt bottom to differentiate to Paneth cells or along the crypt-villus axis to proliferate several times and finally differentiate into absorptive epithelial cells, enteroendocrine cells or goblet cells (Fig. I.4B). The absorptive epithelial cells are called enterocytes in the small intestine and colonocytes in the large intestine; they represent the most numerous cell type in the intestinal epithelium contributing to the physical barrier (Sancho *et al.*, 2003; van der Flier & Clevers, 2009). In the literature, the term "intestinal epithelial cells (abbreviated as IECs)" is used to describe the absorptive epithelial cells, and hence this description will be followed from now on in this thesis. The main function of IECs is efficient absorption and transport of nutrients from the luminal side towards the circulation. The Paneth cells, goblet cells and
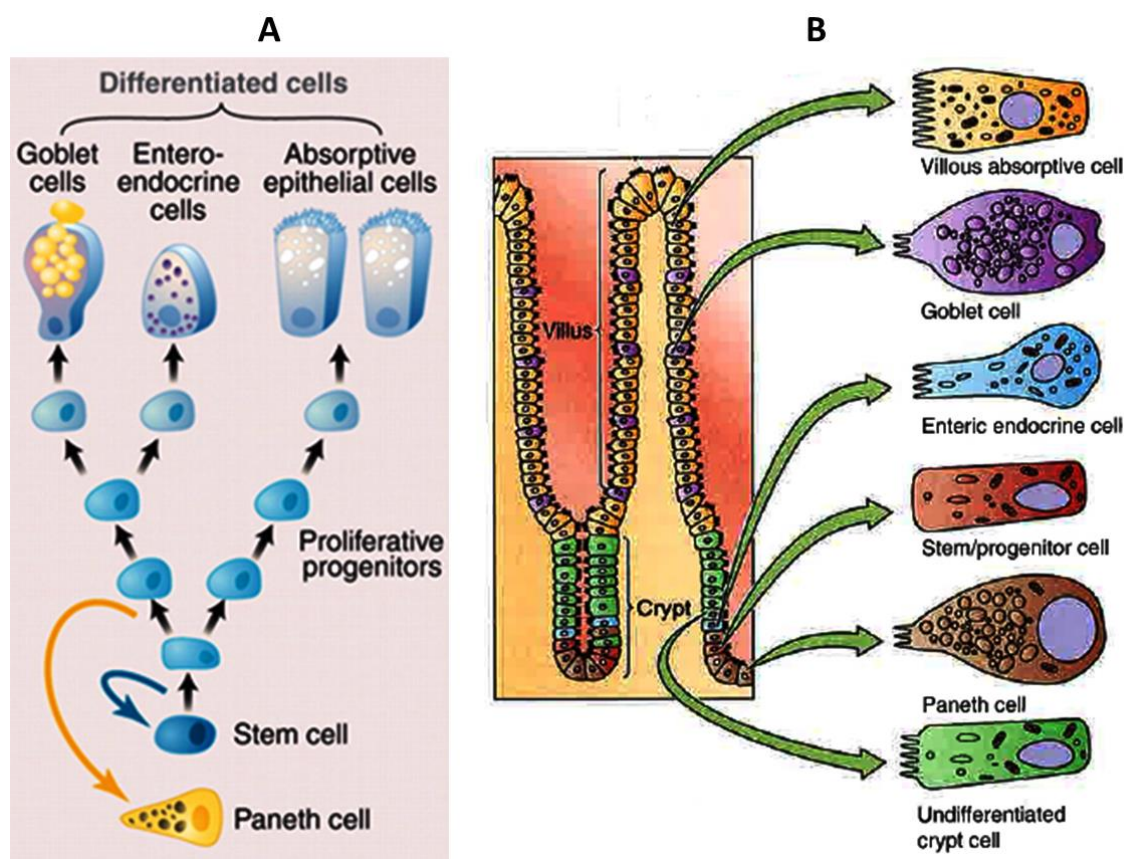
Fig. I.4 (A) Scheme depicting intestinal stem cells, progenitor cells and the two differentiated branches of cell lineages, viz., the absorptive lineage (absorptive epithelial cells) and secretary lineage (Paneth, goblet and enteroendocrine cells). (B) Different cell types along the crypt-villus axis in the small intestinal epithelium (adapted from Radtke & Clevers, 2005).

enteroendocrine cells are of secretory lineage developing from the same epithelial progenitor cells but differ from absorptive epithelial cells both in morphology and function. Paneth cells are restricted to the crypt in the small intestine and are located together with intestinal stem cells at the crypt base. They express antimicrobial peptides (AMPs) like α-defensins, lysozyme or phospholipase A, which along with the secretory immunoglobulin A (sIgA), contribute to host defence against a broad spectrum of pathogens like bacteria, fungi and viruses (Fig. I.5). Goblet cells secrete high molecular weight glycoproteins called mucins. These mucins result in the formation of a gel-like matrix covering the intestinal epithelium, which provides a protective function against physical and chemical injury. The mucin forms an IEC-adherent inner mucus layer that is largely impervious to bacterial penetration or colonization and a less densely cross-linked outer mucus layer, which is highly colonized by constituents of the microbiota. The mucus layer is thicker in the large intestine than in the

small intestine, which accounts for its effective protection against the large number of bacteria in large intestine (Fig. I.5). Finally, enteroendocrine cells coordinate the gut function by secreting specific gut hormones and are mainly found in the upper part of the small intestine.
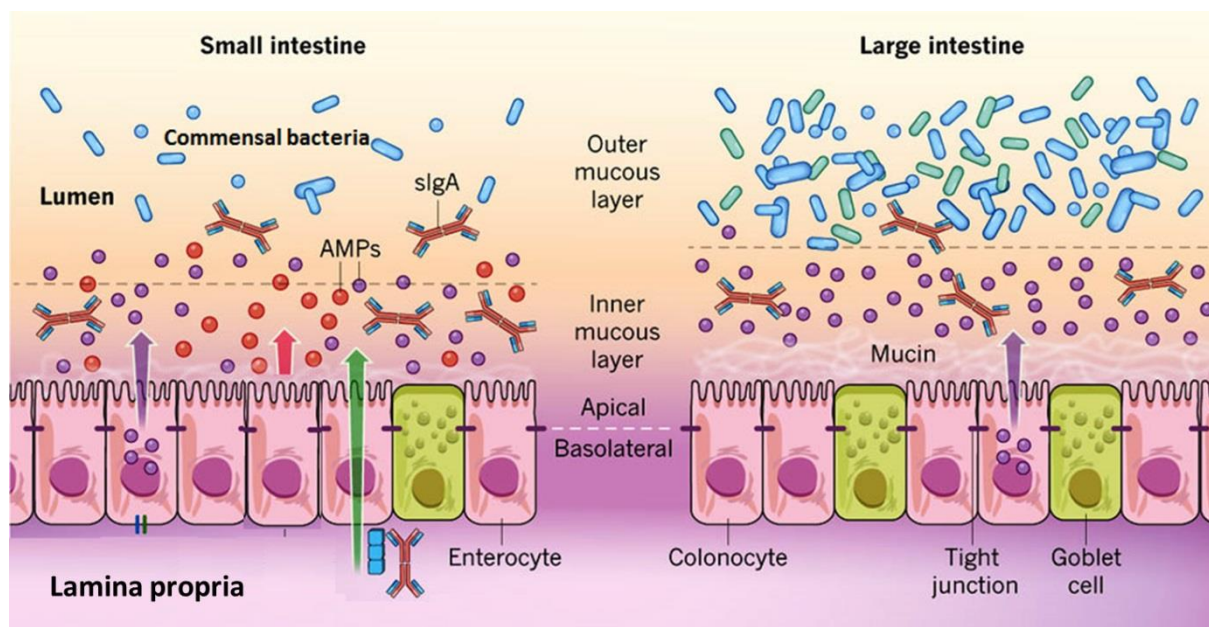
Fig. I.5 Distinct subpopulations of intestinal epithelial cells are integrated into a continuous, single cell layer that is divided into apical and basolateral regions by tight junctions to form an intact barrier in small (left) and large (right) intestine. AMPs: antimicrobial peptides; sIgA: secretory immunoglobulin A (adapted from Maynard *et al.*, 2012).

I.1.3   Intestinal epithelial homeostasis

Since the IECs (enterocytes and colonocytes) are the major targets of invasive enterobacteria to induce mucosal damage, they have several crucial functions to maintain intestinal homeostasis apart from absorption. Connected by tight junctions, they form a physical barrier separating the sterile underlying gut layer from the non-sterile contents of the lumen (Fig. I.6). Additionally, they secrete regulatory cytokines (e.g. transforming growth factor-β) and electrolytes (e.g. chlorides and bicarbonates) to influence microbial colonization, they sense differences between beneficial (commensal) and harmful (pathogenic) microbes, and they initiate immune responses when necessary to maintain epithelial barrier integrity. In order to achieve this, they work in concerted action with the
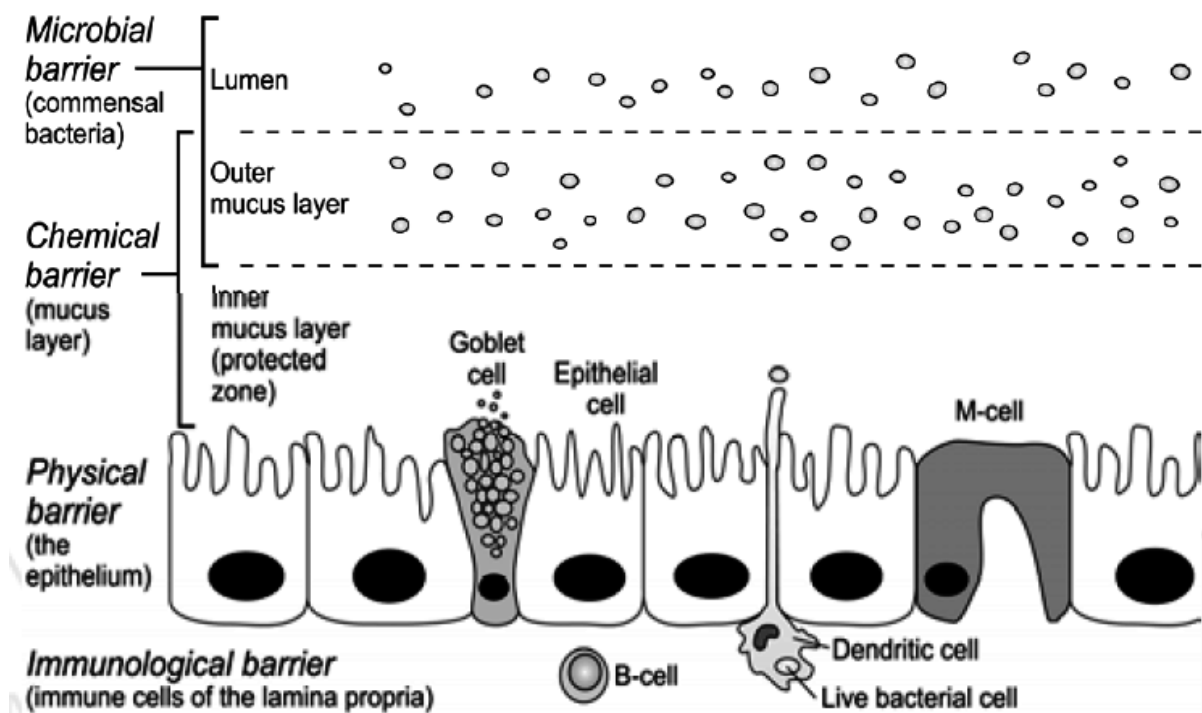
Fig. I.6 Four components of the intestinal barrier (adapted from Anderson *et al.*, 2012).

other epithelial cell types of secretory lineage and with immune cells, together with the signals provided by the gut residing commensal microbiota. The gastrointestinal microbiota is composed of several species including bacteria and eukarya. The human body benefits from the commensal microbiota as many of them live in a homeostatic symbiosis with the host. The commensal bacteria help in water and electrolyte retention, and could even modulate tissue development and repair (Leser & Molbak, 2009). However, upon ingestion of food, potential pathogens can enter the intestinal lumen. Therefore, the intestinal epithelium is constantly challenged with the discrimination between beneficial and pathogenic organisms. The mucus layer above the IECs acts as a chemical barrier to undesired invasion of foreign organisms and toxins, and thus plays a crucial role in intestinal homeostasis. The gut has a mucosal immune system called the gut-associated lymphoid tissue (GALT); this consists of both organized (e.g. Peyer's patches and M-cells) and diffuse structures (e.g. intraepithelial lymphocytes and gut-draining mesenteric lymph nodes) to maintain homeostasis. Upon exposure to bacteria, phagocytic cells like macrophages (m$^{\phi}$) and dendritic cells (DCs) detect the antigens resulting in activation of lymphocytes (like B-cells) to trigger the immune response. The GALT forms the largest immune system in the body. The two main functions of GALT are to enable protective immunity against harmful

pathogens (like bacteria, viruses and protozoans) and to ensure immunological tolerance to harmless materials (like dietary components and commensal bacteria). Additionally, non-immunogenic mechanisms like gastric acid secretion, intestinal mucin and gut motility are also important to protect against the pathogens and maintain a healthy intestinal microflora (Boron & Boulpaep, 2009).

Taken together, a tightly regulated cross-talk exists between IECs, commensal bacteria and immune cells in order to maintain intestinal homeostasis. It is now clear that the intestinal barrier comprises microbiological, chemical, physical and immunological components (Fig. I.6).

One unique feature of IECs is thus that they are constantly exposed to high concentrations of nutrients, microbes and xenobiotics. The regulation of the function of IECs is controlled by both external substances through food components and microbes, and factors like hormones and cytokines (Shimizu, 2010). IECs were once considered as an inert physical barrier, but over the last few decades it has been increasingly realized that they express a cadre of surface receptors (like pattern recognition receptors; PRRs) that allows direct communication between the human body and the intestinal microbiota. Apparently, IECs can manage the numbers and types of microbes present in the gut microbiota through regulation of their colonization and penetration of the epithelium. This is effectively achieved by secretion of AMPs by the enterocytes themselves together with the Paneth cells. This epithelial sensing of microbes is critical as the alterations in the composition of the microbiota are now believed to predispose to chronic diseases like inflammatory bowel disease (IBD) (Asquith & Powrie, 2010).

The intestinal homeostasis is primarily regulated by a delicate balance of the life and death of IECs. The intestinal epithelium has an enormous self-renewing capacity, the life span of a normal epithelial cell being four to five days. Undifferentiated stem cells proliferate within the crypt base, undergo a few rounds of cell division before they differentiate and migrate upwards along the crypt-villus axis. After three to four days, these terminally differentiated cells reach the tip of the villi (in the small intestine) or the surface epithelium (in the colon), followed by cell shedding as depicted in Fig. I.7 (Ramachandran *et al.*, 2000; Sancho *et al.*, 2004; Sato *et al.*, 2009). Minor breaks in epithelial layer continuity are rapidly resealed by a cell proliferation-independent process called epithelial restitution; however, major damage by exaggerated epithelial cell death leads to barrier impairment.
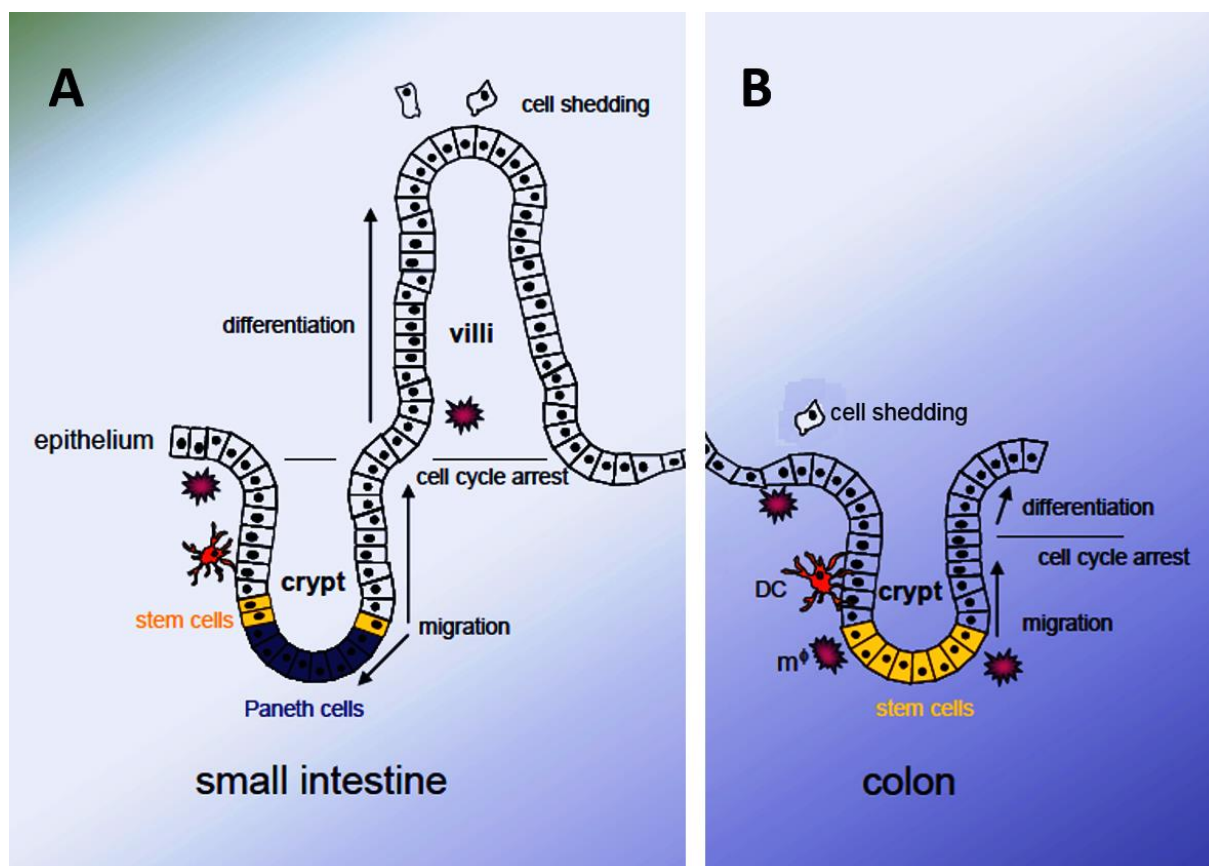
Fig. I.7 Schematic intestinal construction with crypts and villi representing the small intestine (A), and the colon (B) solely exhibiting crypts. Dendritic cells (DCs) and macrophages (mᵠ) are resident in the lamina propria.

In order to maintain an efficient intestinal barrier, the rates of epithelial cell proliferation and cell death have to be tightly regulated. During normal conditions, aged epithelial cells in the villus tip (of small intestine) or the surface epithelial cuff (of colon) are believed to die by apoptosis. Among the various ways by which cells could die, apoptosis is a programmed cell death pathway which is physiologically relevant in the intestinal epithelium (Hall *et al.*, 1994; Bullen *et al.*, 2006). The main mechanism is usually thought to be activation of caspases, which are a class of cleavage enzymes involved in the breakdown of cells into apoptotic bodies. Under normal conditions, induction of apoptosis has been observed before shedding of human IECs without compromising epithelial barrier and the rate of IEC apoptosis varies significantly across the different sections of the intestinal tract (Grossmann *et al.*, 2002). Apart from the villus tip, apoptosis also occurs at the crypt level to remove excess or unwanted stem cells (Leedham *et al.*, 2005).

Because of the complex structure and organization of the intestinal epithelium, the various processes of cell proliferation, differentiation, migration and cell death have to be

tightly controlled. Excessive cell death might result in barrier dysfunction and "leaky gut" allowing uncontrolled access of bacteria and their components to the gut wall (Fig. I.8). Increase in the rate of apoptotic cell death can create leaks contributing to barrier dysfunction. The subsequent entry of bacteria and luminal contents into the lamina propria leads to secretion of cytokines and chemokines by IECs and inflammatory cells (like macrophages, neutrophils and mast cells) to initiate an inflammatory cascade (Peterson & Artis, 2014). The accumulation of neutrophils with the release of enzymes and reactive oxygen species (ROS) enhances the inflammatory reaction. The study of Nenci *et al.*, (2007) showed an essential role for nuclear factor-κB (NF-κB) essential modulator (NEMO) in the control of IEC apoptosis. In this study, mice deficient in the gene NEMO specifically in IECs were used; NEMO deficiency in IECs led to excessive tumor necrosis factor (TNF)-dependent apoptosis within the epithelium, followed by a barrier breakdown and the translocation of bacteria into the bowel wall driving inflammation. Apoptotic cells are rapidly phagocytized by macrophages, a process that represents a critical step in tissue remodeling, immune responses and the resolution of inflammation (Henson & Bratton, 2013). Apoptotic cell death plays thus an important role in inflammatory processes and in the resolution of inflammatory reactions. However, dysregulation of cell proliferation or resistance to cell death may result in tumor development in the gut (Mehlen & Puisieux, 2006; Maloy & Powrie, 2011).

I. 2   Acute gastrointestinal inflammation

I.2.1   The role of enterocytes in the immune responses of the GI tract

Under normal situations, the immune responses maintain the intestinal mucosa in a state of 'controlled' inflammation, regulated by a delicate balance of pro-inflammatory and anti-inflammatory cytokines, to maintain intestinal homeostasis (Fiocchi, 2003). This is not surprising due to the fact that the intestinal mucosa is constantly exposed to limitless number of foreign antigens (e.g. commensal microbes, pathogenic bacteria, viruses and food-derived materials). Directly below the epithelium, numerous immune cells create a homeostasis between the commensal flora of the intestine and the host immune system.
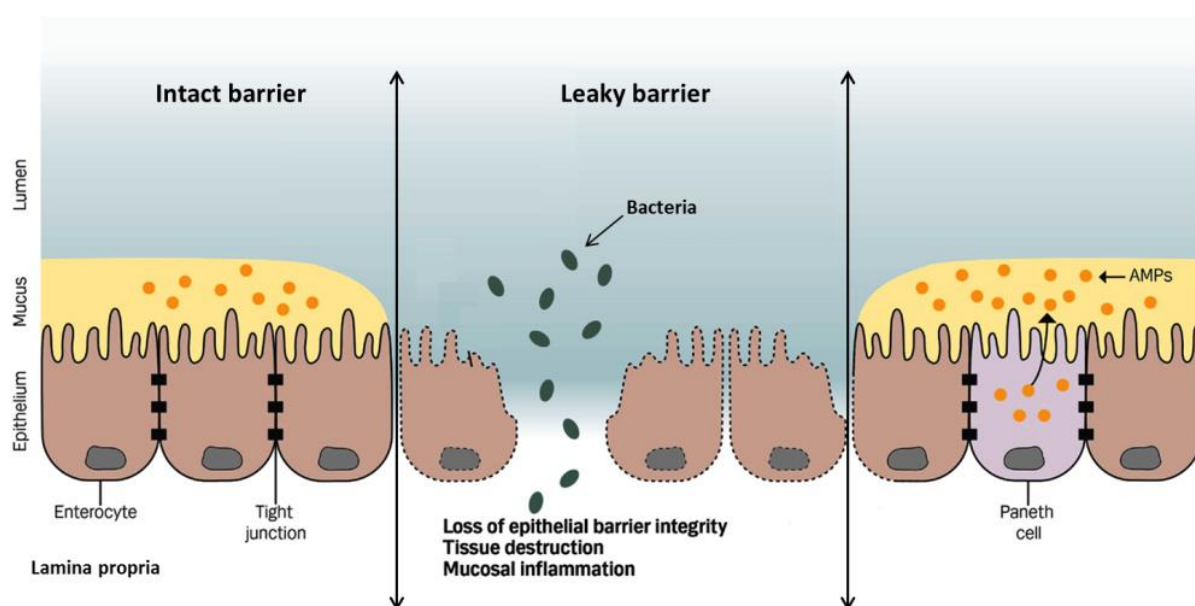
Fig. I.8 Intact versus leaky intestinal barrier: When the intestinal barrier is functioning correctly, luminal bacteria and antigens are unlikely to pass across the epithelium into the lamina propria. In contrast, disruption of the intestinal barrier due to cell death leads to increased epithelial permeability (AMPs: antimicrobial peptides; adapted from Coskun, 2014).

The innate immune system is well orchestrated by various pattern recognition receptors (PRRs) and immune cells. The Toll-like receptors (TLRs) and nucleotide-binding oligomerization domain (NOD)-like receptors (NLRs) play a key role in the innate gut immunity as they recognize the common structures on microorganisms called the pathogen-associated molecular patterns (PAMPs). TLRs are widely present on the epithelial cells, Paneth cells, mϕ and DCs (Taniguchi *et al.*, 2009; Garrett *et al.*, 2010; Wells *et al.*, 2010). The responsiveness of these cells to PRR ligands is tightly regulated in order to avoid exceeding response to commensal products. Polymorphonuclear leukocytes (PMNs; neutrophils), mϕ, DCs, T-cells and mast cells are the important team players in maintaining immunological homeostasis and host defense in the gut. The highly regulated immune responses by different epithelial and immune cells result in the induction and maintenance of intestinal homeostasis. However, defects in this equilibrium can disrupt the homeostatic mechanisms and lead to pathogenic intestinal inflammation. Damage and death of the epithelial cells lead to the breakdown of the intact barrier function resulting in access of luminal content to the immune components of the intestinal wall leading to a state of "uncontrolled" inflammation. The innate immune system of the intestine plays a vital role in initiating and perpetuating this "uncontrolled" inflammation (Fig. I.9).
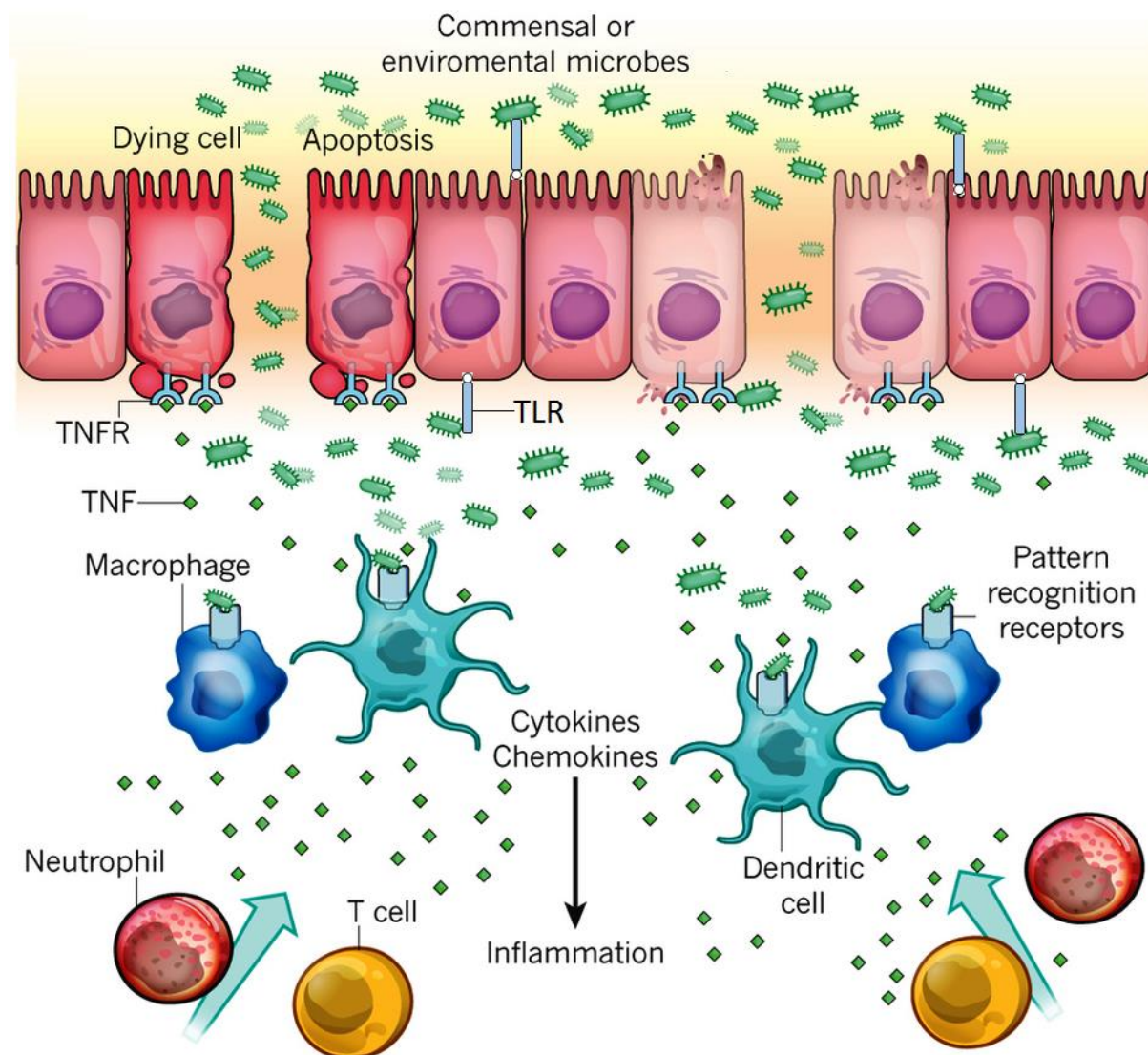
Fig. I.9 The intestinal immune reaction to epithelial barrier disruption. Epithelial cell death in barrier tissues can cause barrier disruption, allowing commensal or environmental microbes to invade the tissue. Recognition of microbial pathogen-associated molecular patterns (PAMPs) by Toll-like receptors (TLRs) on IECs, and pattern recognition receptors on dendritic cells and macrophages induces the expression of cytokines and chemokines that attract and activate immune cells resulting in inflammation. The cytokine tumor necrosis factor (TNF) binds to its receptor TNFR to initiate inflammatory signaling.

In order to fight invading pathogens, epithelial cells can recognize PAMPs by means of TLRs. Binding of PAMP to TLR can activate several downstream inflammatory signals such as NF-κB, leading to an upregulation of inflammatory cytokines like TNF-α and interleukin (IL)-6, and chemokines like IL-8 and monocyte chemoattractant protein (MCP)-1 (Medzhitov *et al.*, 1997). Thus, the redox-dependent transcription factor NF-κB in IECs plays a pivotal role as a regulator of pro-inflammatory genes involved in the onset of the mucosal

30

inflammatory response following microbial infection (Savkovic *et al.*, 1997; Elewaut *et al.*, 1999). Amongst others, TNF-α is a master orchestrator of inflammation in the intestine binding to its receptor TNFR to initiate inflammatory signaling (Dagenais *et al.*, 2014). Upon cytokine secretion, neutrophils circulating in the capillaries of the lamina propria can become activated and migrate towards the site of inflammation. Simultaneously, neutrophil production is upregulated and neutrophil lifetime increases. The neutrophilic cytosol contains granules that are filled with a variety of proteins, such as defensins, bactericidal/permeability-increasing protein, proteases (e.g. elastase, cathepsins) and myeloperoxidase (MPO). Neutrophils are well known for their bactericidal role with formation of superoxide anion radicals ($O_2^{\bullet-}$) as one of the main bactericidal mechanisms (Klebanoff, 1967; Babior *et al.*, 1973; Klebanoff & Rosen, 1978). Neutrophils can cause pathogen destruction upon the so-called "oxidative burst", marked by an increased consumption of molecular oxygen (O_2) and production of ROS and reactive nitrogen species (RNS) (Babior, 2000). $O_2^{\bullet-}$ generation by neutrophils is catalyzed by nicotinamide adenine dinucleotide phosphate (NADPH) oxidase (NOX), a membrane-bound enzyme complex (Suzuki & Lehrer, 1980). $O_2^{\bullet-}$ are dismutated into hydrogen peroxide (H_2O_2) by superoxide dismutase (SOD). MPO consumes H_2O_2 and generates hypochlorous acid (HOCl), the most bactericidal oxidant that is produced by neutrophils (Hampton *et al.*, 1998; Nauseef, 2007; Freitas *et al.*, 2009).

In addition to the barrier dysfunction resulting in aberrant recognition of microbial products by the immune cells, death of IECs in the absence of pathogens can trigger intestinal inflammation. Inflammation as a result of trauma, burn, ischemia/reperfusion (I/R) injury or chemically induced injury typically occurs in the absence of any microorganisms and has therefore been termed "sterile inflammation". In such a "sterile" setting, any stressed or injured cells release or expose certain molecules and cellular components into the extracellular environment that act as danger signals to alert the immune system to directly trigger inflammation. Such released factors are collectively called as damage-associated molecular patterns (DAMPs). DAMPs include, amongst others, cytokines (mainly of the interleukin family like IL-1β), heat-shock proteins, mitochondrial deoxyribonucleic acid (DNA), formyl peptides, cytochrome c and extracellular adenosine triphosphate (ATP). DAMPs are usually detected by PRRs that activate immune responses by inducing the expression of cytokines and chemokines by epithelial cells like IECs. Thus, apart from a

pathogen-triggered immunogenic response, in the absence of pathogens, cells can trigger inflammation through release of DAMPs.

I.2.2   Oxidative stress

I.2.2.1 ROS

Oxidative stress is described as an imbalance between oxidants and antioxidants in favor of the oxidants, which can result in cell or tissue damage (Sies, 1997). In healthy conditions, formation of oxidants is balanced by the presence of a variety of antioxidants. Oxidants can be generated by the reduction of O_2 to water (H_2O), leading to the formation of ROS. ROS are intracellular chemical species that are formed upon partial reduction of O_2, which include $O_2^{\bullet-}$, H_2O_2 and the hydroxyl radical ($OH^\bullet$). Furthermore, free radicals, in general, are also considered as oxidants. Free radicals are molecules or molecular fragments that possess one or more unpaired electrons, which are responsible for the high reactivity of the radical. Free radicals can be charged positively or negatively or be electrically neutral. They are formed from a normal molecule by either homolytic cleavage of a covalent bond, requiring high energy input (e.g. ultrasound, ultraviolet radiation), or addition or loss of a single electron. In biological processes, the electron transfer plays a major role in the generation of free radicals, as it can be initiated by enzymatic reactions (Slater, 1984; Cheeseman & Slater, 1993). In healthy conditions, oxidant formation is scavenged by various antioxidant mechanisms in the cell. The main antioxidant enzymes are SOD, catalase and glutathione peroxidase (GPx). Moreover, reduced glutathione (GSH; L-γ-glutamyl-L-cysteinyl-glycine), a tripeptide containing a thiol group, is an important intracellular antioxidant.

$O_2^{\bullet-}$ is a primary ROS generated by the one-electron reduction of O_2 and is a short-living radical (Fig. I.10).
Either spontaneously or through catalysis by SOD, $O_2^{\bullet-}$ are dismutated into H_2O_2, which is relatively stable, less toxic and capable of diffusion across membranes:

$$2O_2^{\bullet-} + 2H^+ \rightarrow O_2 + H_2O_2$$
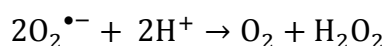
$O_2^{\bullet-}$ in the cytosolic and mitochondrial matrix are dismutated by Cu/Zn-SOD (SOD1) and Mn-SOD (SOD2), respectively.
The formed H_2O_2 leads to the generation of hydroxyl radicals ($OH^\bullet$) in the presence of ferrous iron (Fe^{2+}) through the Fenton reaction:

$$Fe^{2+} + H_2O_2 \rightarrow Fe^{3+} + OH^\bullet + OH^-$$
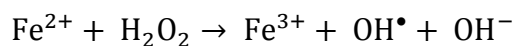
$OH^\bullet$ is a very short-lived and highly reactive radical which attacks the fatty acid side chains of the membrane phospholipids (called lipid peroxidation) to cause cell disruption. The risk of formation of $OH^\bullet$ from H_2O_2 is reduced by GPx and catalase.

GPx are a class of enzymes involved in the catalytic degradation of H_2O_2 using GSH as a substrate where it is oxidized to glutathione disulfide (GSSG), resulting in the formation of water:

$$H_2O_2 + 2GSH \rightarrow 2H_2O + GSSG$$
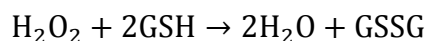
Subsequently, GSH is recovered by GSSG reductase (Sies, 1997, 1999). Determination of the changes in intracellular GSH content and the GSH/GSSG ratio is a widely used marker for cellular response to oxidative stress.

Additionally, H_2O_2 can also be degraded into water and molecular oxygen by catalase:

$$2H_2O_2 \rightarrow O_2 + 2H_2O$$
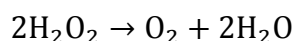
A considerable part of H_2O_2 formed is consumed by MPO in the neutrophils, for the formation of HOCl, a highly bactericidal oxidant, used for the phagocytic defense:

$$Cl^- + H_2O_2 \rightarrow HOCl + OH^-$$
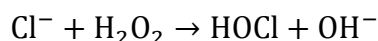
Furthermore, neutrophils and, more importantly macrophages, are capable of producing RNS, especially nitric oxide ($NO^\bullet$), via the inducible nitric oxide synthase (iNOS) by consumption of NADPH and conversion of L-arginine to L-citrulline:

$$\text{L-arginine} + O_2 + NADPH \rightarrow NO^\bullet + \text{L-citrulline} + NADP^+$$
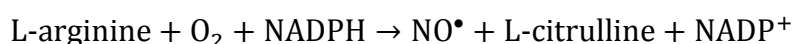
The resulting $NO^\bullet$ can further react with $O_2^{\bullet-}$ to generate the highly mutagenic and cytotoxic peroxynitrite anion ($ONOO^-$):

$$NO^\bullet + O_2^{\bullet-} \rightarrow ONOO^-$$
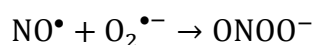
Once considered as a deleterious by-product of respiration in mitochondria and cell metabolism, ROS are now increasingly realized to be essential "second messengers" for a myriad of biological responses like cell growth, differentiation and host defense (Forman *et al.*, 2010; Vara & Pula, 2014). The distinct biological properties of each ROS like their chemical reactivity, stability and lipid diffusion capabilities determine specificity of their signaling (Reczek & Chandel, 2015). ROS could contribute to cell-survival or cell-death pathways, depending on both the site and the amount of ROS generation (Azad *et al.*, 2009). However, increased levels of ROS with compromised antioxidant defense (and hence
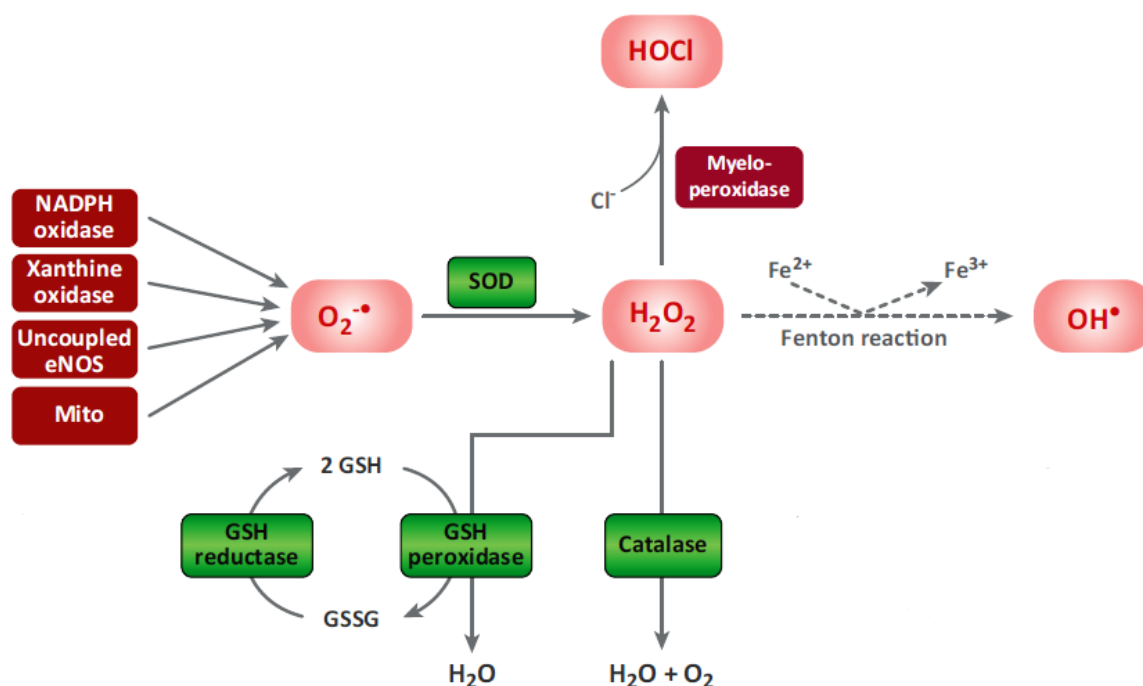
Fig. I.10 Enzymes involved in the generation and inactivation of reactive oxygen species (ROS). The superoxide anion ($O_2^{\bullet-}$) can be produced by NADPH oxidase (NOX), xanthine oxidase, uncoupled endothelial nitric oxide synthase (eNOS), and the leakage of activated oxygen (O_2) from mitochondria during respiration. $O_2^{\bullet-}$ can be converted to hydrogen peroxide (H_2O_2) by the enzyme superoxide dismutase (SOD). H_2O_2 can undergo spontaneous conversion to the hydroxyl radical ($OH^{\bullet}$) via the Fenton reaction. H_2O_2 can be detoxified by glutathione (GSH) peroxidase and catalase to H_2O and O_2. Myeloperoxidase (MPO) can use H_2O_2 to oxidize chloride to the strong oxidizing agent hypochlorous acid (HOCl).

oxidative stress) are often associated with many pathological conditions of all organ systems (including GI) and aging.

Indeed, higher levels of ROS damage almost all components of the cells including lipids, proteins and DNA resulting in lipid peroxidation, protein oxidation and nucleic acid oxidation with DNA damage, respectively. At the cellular level, the transcriptional factor nuclear factor erythroid 2-related factor 2 (Nrf2) is considered as a master regulator of antioxidant genes and hence of antioxidant status (Copple, 2012).

The major sources of ROS in a cell include the NOXs and the mitochondrial electron transport chain (ETC) where $O_2^{\bullet-}$ is formed as the main product and by-product, respectively. Other enzyme systems that generate ROS are xanthine-xanthine oxidase (XO), uncoupled endothelial nitric oxide synthase (eNOS), cyclo-oxygenase (COX), lipoxygenase, glucose oxidase and cytochrome P450 oxidases.

I.2.2.2 NOXs

NOXs are a family of enzymes solely devoted to the production of $O_2^{\bullet-}$ in cells and tissues. There are seven members in the NOX family – NOX1-5 and dual oxidase (DUOX)1-2 (Bedard & Krause, 2007). The first member, now known as NOX2, was initially discovered in neutrophils, but NOXs are now known to be present in many other cell types including epithelial cells (Bedard & Krause, 2007). NOX1 and DUOX2 are the NOX isozymes expressed in the IECs (Lambeth, 2004). They are multi-subunit membrane-bound enzyme complexes that, upon assembly in activated cells, catalyze the reduction of O_2 to $O_2^{\bullet-}$ using NADPH. NOX are present in the plasma membrane and in the membranes of intracellular vesicles and organelles. Various subunits that are located in the cytosol and in the membrane assemble to form the active NOX enzyme. The catalytic subunit of the predominantly expressed NOX2 is gp91phox, a 91-kDa glycoprotein subunit; the active enzyme complex is formed by the association of the regulatory subunit p22phox with the four other cytosolic subunits: p40phox, p47phox, p67phox and the guanosine triphosphate hydrolase (GTPase) Rac (Fig. I.11). The small G-protein Rac, in its GDP-bound form, is stabilized by Rho GDP dissociation inhibitor (RhoGDI) in the resting state. Binding of ligands to the membrane-bound receptors adjacent to NOX enzyme generally initiates the activation cascade of complexes; the ligands include lipopolysaccharide (LPS), cytokines like TNF, growth factors, increased glucose and free fatty acids. Upon activation, the cytosolic subunits migrate towards the membrane-bound subunits to bind and configure the active enzyme complex. NOX-derived ROS has been implicated in a wide array of cellular and molecular functions like cell proliferation, migration, angiogenesis and apoptosis.

I.2.2.3 Mitochondria as cellular sources of ROS

Mitochondria produce $O_2^{\bullet-}$ as an unavoidable byproduct of aerobic respiration when electron transfer occurs through the different ETC complexes I through V (Fig. I.12). At least seven distinct sites of mitochondrial $O_2^{\bullet-}$ production have been described in the mitochondria (Brand, 2010), but only the major sites are shown in Fig. I.12. During normal physiological conditions, complexes I and III are the major sites of $O_2^{\bullet-}$ production (Turrens & Boveris, 1980). During pathological conditions, complex II can also participate in $O_2^{\bullet-}$ production by reverse electron transfer (Drose, 2013). Except for complex II, all other ETC
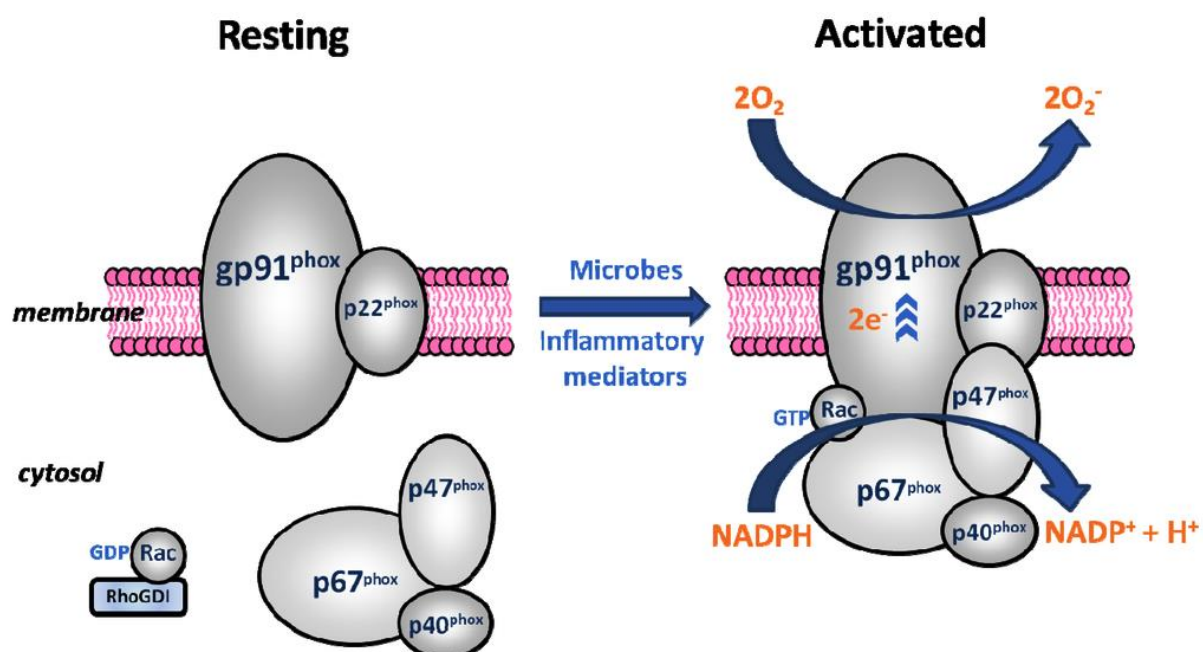
Fig. I.11 Diagrammatic representation of the resting and activated forms of NADPH oxidase2 (NOX2) upon exposure to ligands from microbes (e.g. LPS) and inflammatory mediators (e.g. TNF). Activation involves translocation of the cytosolic subunits p47phox, p67phox, p40phox and Rac to the membrane where they bind to p22phox and gp91phox subunits. The Rac protein bound to Rho GDP dissociation inhibitor (RhoGDI) in the resting state translocates to the membrane upon activation. When assembled, the enzyme generates superoxide anion ($O_2^{\bullet-}$) by accepting electrons (e^-) from cytoplasmic NADPH and donating them to molecular oxygen (O_2). (Adapted from McCann & Roulston, 2013).

complexes pump protons from the matrix into the intermembrane space, resulting in a proton gradient generating the mitochondrial membrane potential (Ψm). Ψm is utilized by complex V (ATP synthase) to synthesize ATP from ADP and phosphate, through the backflow of protons from the mitochondrial intermembrane space to the matrix. ROS production from mitochondria depends upon the availability of the substrates, type of tissue, redox state of the cells, animal species and age (Kudin *et al.*, 2008).

Recent reports suggest that activation of NOXs may increase production of mitochondrial ROS and vice versa, i.e., increase of mitochondrial ROS may activate NOXs (Daiber, 2010; Dikalov, 2011). Accordingly, NOX derived $O_2^{\bullet-}$ and H_2O_2 were reported to trigger mitochondrial dysfunction and ROS formation in angiotensin-II treated endothelial cells (Doughan *et al.*, 2008). Mitochondria are not only a target for ROS produced by NOXs but also a significant source of ROS, which under certain conditions (like serum withdrawal)
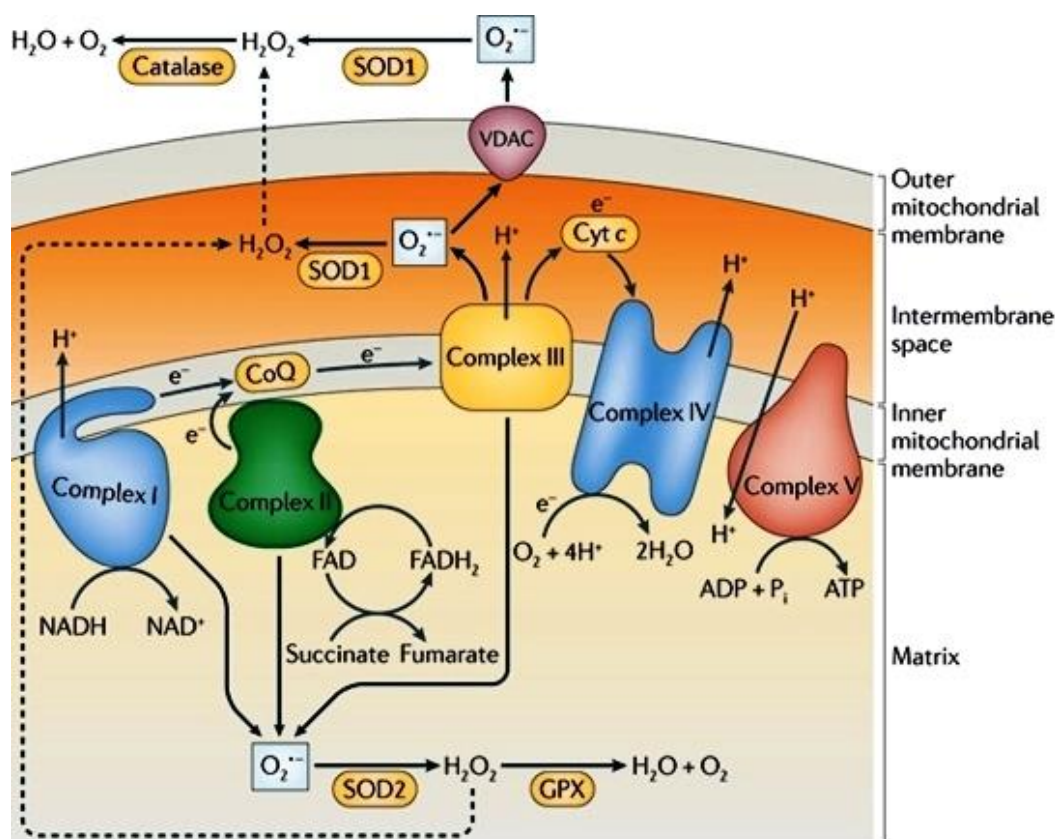
Fig. I.12 The mitochondrial respiratory chain (which carries out oxidative phosphorylation) with its five multi-subunit protein complexes (I-V) localized at the inner mitochondrial membrane. Electrons are prematurely leaked from the electron transport chain and are aberrantly transferred to molecular oxygen (O_2) resulting in mitochondrial $O_2^{\bullet-}$ generation, occurring at complexes I, II and III. Complex III can generate $O_2^{\bullet-}$ in the intermembrane space as well as into the matrix. $O_2^{\bullet-}$ can escape from the intermembrane space into the cytoplasm via voltage dependent anion channels (VDAC); in the cytoplasm $O_2^{\bullet-}$ are subsequently dismutated to H_2O_2 by SOD1. $O_2^{\bullet-}$ generated into the matrix are dismutated by SOD2 (adapted from West *et al.*, 2011).

may stimulate NOXs (Kimura *et al.*, 2005; Lee *et al.*, 2006). This crosstalk between mitochondria and NOXs, therefore, may represent a feed-forward vicious cycle of ROS production which can be pharmacologically targeted under conditions of oxidative stress. Indeed, a mitochondria-targeted antioxidant has been demonstrated to break this vicious cycle, inhibiting ROS production by mitochondria, in this way reducing NOX activity (Dikalov *et al.*, 2010).

I.2.3   Pathogenesis of acute GI inflammation: role of IEC dysfunction

Epithelial barrier dysfunction is a common phenomenon observed during several acute GI inflammatory conditions. Acute GI inflammatory conditions include, amongst others, acute gastroenteritis (of bacterial and viral origin), postoperative ileus (POI), sepsis and septic ileus, necrotizing enterocolitis (NEC), appendicitis, pancreatitis and ischemic bowel disease. Two of these conditions are considered in detail. 1) POI as the occurrence of an inflammatory process in the GI wall in the first hours after intestinal manipulation is the main trigger for sustained suppression of GI motility; oxidative stress, also in the mucosal layer, might contribute to the pathogenesis. 2) Sepsis, where inflammation and oxidative stress are important pathogenetic factors and the intestine can have a triggering role, also leading to septic ileus. As intestinal I/R injury is involved in the triggering role of the intestine during sepsis, this pathogenetic complex is also discussed.

I.2.3.1 POI

POI is defined as a transient impairment of gastrointestinal motility after major abdominal surgery; it lasts 2 to 4 days until the first passage of flatus or stool combined with adequate oral intake during 24 h. Patients suffer from abdominal discomfort, nausea and vomiting. POI can delay postoperative recovery, increase the length of hospital stay and can induce morbidity; the economic impact of POI has been estimated at $750 million per year (Doorly & Senagore, 2012). The pathogenesis of POI is multifactorial; neurogenic inhibitory reflexes, inflammatory responses and pharmacological factors are three main mechanisms known to contribute to POI (Bauer & Boeckxstaens, 2004). In the first hours after surgery, inhibition of GI motility is mainly due to activation of reflex inhibitory nervous pathways (Bauer & Boeckxstaens, 2004; Boeckxstaens & de Jonge, 2009). The prolongation of GI motility suppression during POI is due to a complex immune-regulated inflammatory process in the intestinal muscularis, with a critical role for activation of the resident muscularis macrophage network (Kalff *et al.*, 1999). The kinetically active substances NO (via iNOS) and prostaglandins (via COX-2) are released, as well as pro-inflammatory cytokines such as IL-1β, IL-6 and TNF-α, chemokines (MCP-1) and adhesion molecules like intercellular adhesion molecule (ICAM)-1. This leads to additional recruitment of circulating leukocytes and further release of inflammatory mediators (Boeckxstaens & de Jonge, 2009). Interestingly, oxidative stress might also contribute to POI. Surgical manipulation of the rat intestine resulted in

increased levels of oxidative stress in the mucosa with a significant increase in xanthine oxidase activity in the enterocytes (Anup *et al.*, 1999). In addition, in a mouse model of POI, our group previously reported an increase in oxidative stress levels, measured as malondialdehyde (MDA; a by-product of lipid peroxidation) in both mucosa and muscularis of small intestine starting shortly after intestinal manipulation; the increase at 1 h after manipulation was more pronounced in the mucosa than in the muscular layer (De Backer *et al.*, 2009).

I.2.3.2 Sepsis and septic ileus

Sepsis is defined as a systemic inflammatory response to infection (systemic inflammatory response syndrome; SIRS), which can progress to severe sepsis with multiple organ failure (MOF) and further to septic shock with acute circulatory failure and refractory hypotension. It is a frequent cause of mortality in intensive care. Sepsis is driven by a complex cascade of events, initiated by bacteria-derived molecules such as LPS or endotoxins with subsequent formation of inflammatory cytokines, ROS and RNS, I/R and mitochondrial dysfunction (Cinel & Opal, 2009). The intestine is very vulnerable during systemic inflammation and can trigger and perpetuate sepsis (Clark & Coopersmith, 2007). Conditions such as major trauma, extensive burns and hypovolemia lead to I/R of the intestine, triggering an intestinal inflammatory reaction and intestinal epithelial barrier dysfunction (Magnotti *et al.*, 1998; de Haan *et al.*, 2009; Flessas *et al.*, 2011). Pro-inflammatory mediators produced in the intestine also reach the systemic circulation, promoting systemic inflammation. Dysfunction of the epithelial barrier allows translocation of live bacteria and/or their components such as LPS through the intestinal mucosa, further reaching the circulation via the intestinal lymph nodes. The intestinal events are accompanied by severe impairment of intestinal motility (septic ileus), promoting bacterial colonization of the normally sterile small intestine and stomach; this will facilitate bacterial translocation and predisposes to pneumonia by aspiration of gastric content (Hassoun *et al.*, 2001; Deitch, 2002; Balzan *et al.*, 2007). Animal models of sepsis consist of administration of LPS or bacteria, or cecal ligation and puncture (CLP) (De Winter & De Man, 2010). The mechanism of sepsis-induced ileus, as assessed by injecting LPS, shows similarity with that of the inflammatory phase of POI (Eskandari *et al.*, 1997), although differences in the degree of particular responses were observed when comparing animals with a similar degree of transit

retardation, induced either by surgical intestinal manipulation or by intraperitoneal injection of LPS. The POI model induced a greater inflammatory response and a greater degree of leukocyte infiltration (Schmidt *et al.*, 2012). IEC apoptosis is reported to increase following sepsis and overexpression of the anti-apoptotic protein Bcl-2 improved survival in multiple animal models of sepsis by prevention of intestinal apoptosis (Coopersmith *et al.*, 2002a; Coopersmith *et al.*, 2002b).

I.2.3.3 Acute I/R injury of the gut

I/R injury occurs due to the re-entry of the blood flow after interrupted blood supply for a time period, where the delivery of oxygen to the tissue was insufficient to support its metabolic demand. The reintroduction of blood flow with simultaneous re-oxygenation of the tissue after an ischemic episode initiates a cascade of events that can potentially worsen the original injury. The intestinal mucosa is extremely sensitive to I/R resulting in tissue edema and fluid movement into the intestinal lumen. Intestinal oxygen delivery can be impaired by both systemic and local vascular conditions. I/R injury of the gut is a significant problem in a variety of clinical conditions such as SIRS and MOF, small bowel transplantation, abdominal aortic aneurysm surgery, mesenteric artery occlusion, cardiopulmonary bypass, trauma and hemorrhagic shock (Collard & Gelman, 2001); this is associated with substantial morbidity and mortality (Grootjans *et al.*, 2010). Intestinal I/R injury is a complex, multifactorial pathophysiological process; primary microcirculatory flow disturbances, caused by ROS production, lead to a subsequent inflammatory cascade. Tissue ischemia (leading to hypoxia) and oxidative stress increase expression of inflammatory genes like cytokines (e.g. TNF-α, IL-1β, IL-6), iNOS, prostaglandins and adhesion molecules [e.g. ICAM-1, vascular cell adhesion molecule (VCAM)-1, E-selectin], initiating local inflammation. The recruitment of circulating neutrophils at this initial site further amplifies the intensity of inflammation and neutrophil infiltration is one of the characteristic microvascular alterations noted with I/R injury. In addition, the widespread endothelial cell apoptosis and the loss of endothelial cells in the vessels supplying the intestine result in thrombosis directly in the intestine (Shah *et al.*, 1997). This injury can further trigger a systemic inflammatory response in distant organs resulting in MOF (Turnage *et al.*, 1994; Cuzzocrea *et al.*, 2002; Ceppa *et al.*, 2003). I/R injury of the gut is associated with the breakdown of intestinal barrier function, which facilitates increased intestinal permeability and bacterial translocation into the portal

and systemic circulation leading to SIRS (Collard & Gelman, 2001; Fink & Delude, 2005). Apoptosis is reported as the major mode of IEC death caused by I/R injury in the small intestine (Ikeda *et al.*, 1998; Liu *et al.*, 2008; Wen *et al.*, 2012). Experimental animal models of intestinal I/R injury suggest that ROS production during the reperfusion period is largely responsible for the injury (Gonzalez *et al.*, 2015). Already in 1986, XO-derived $O_2^{\bullet-}$ was reported to initiate intestinal reperfusion injury (Grisham *et al.*, 1986) (Fig. I.13). The presence of a higher concentration of XO in the small intestine makes it more susceptible to I/R injury than colon (van der Vliet *et al.*, 1989). Recently, rats subjected to intestinal I/R injury were reported to show an increase in gp91phox and p47phox protein expressions in small intestinal mucosa suggesting a possible contribution of NOX-derived ROS during I/R injury (Gan *et al.*, 2013). To the best of our knowledge, to date, no study is available in the literature investigating the involvement of mitochondria-derived ROS in intestinal I/R injury. Supplementation with antioxidants was reported to reduce I/R injury-induced mucosal damage in many animal studies (Mallick *et al.*, 2004).

I. 3   Treatment of POI and sepsis; the intestinal mucosa as treatment target

I.3.1   *Management of POI and sepsis in humans*

Management of POI for humans: Prevention or treatment of POI remains mainly supportive as no single treatment is available. Due to its multifactorial origin, treating POI generally consists of a multimodal approach, also called as fast-track-surgery. This approach includes minimally invasive laparoscopy, epidural local anesthetics, and early enteral feeding and mobilization (Kehlet, 2008). The fast-track approach has shown to reduce complications, accelerate recovery and reduce hospital stay. Other management strategies proposed to reduce POI are use of opioid receptor antagonists, opioid free analgesia (NSAIDs), laxatives, chewing gum, fluid restriction and avoidance of nasogastric tube feeding (Bauer & Boeckxstaens, 2004; Asgeirsson *et al.*, 2010; Vather & Bissett, 2013) (Table I.1).

Management of sepsis for humans: Sepsis is a complex phenomenon characterized by the non-specific nature of signs and symptoms to diagnose it. There are no approved drugs that specifically target sepsis. So, in addition to life supportive measures, other steps should be
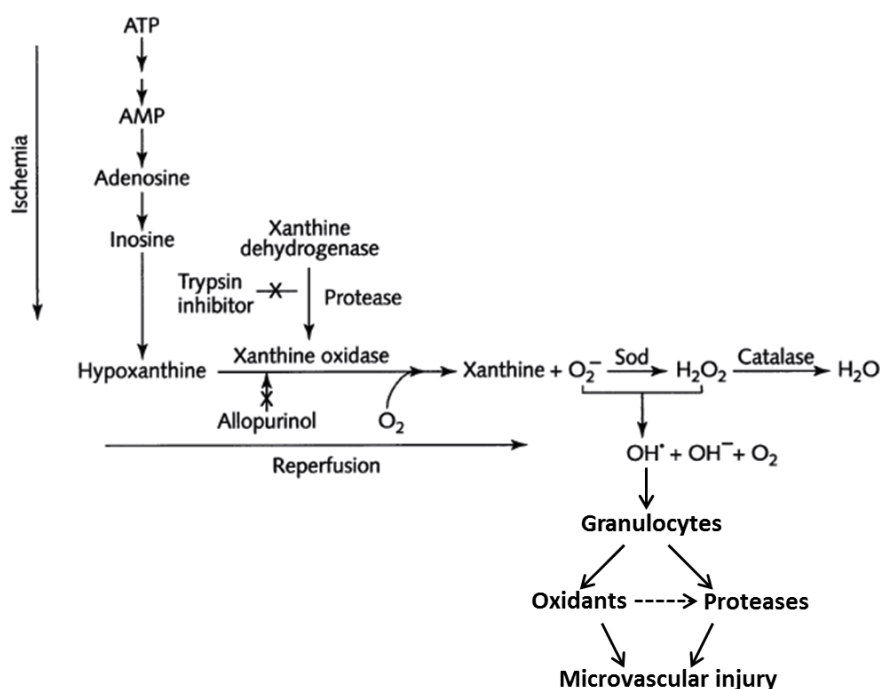
Fig. I.13 Mechanism of XO-mediated free radical injury. During the ischemic episode, ATP is catabolized to hypoxanthine, which accumulates in the tissues. This results in a low energy state leading to an influx of Ca^{2+} into the cells. The intracellular Ca^{2+} then triggers the conversion of xanthine dehydrogenase (XDH) to XO via a calmodulin-regulated protease. Upon reperfusion, O_2 is reintroduced into the tissues and interacts with XO and hypoxanthine to generate a burst of $O_2^{\bullet-}$ and H_2O_2, which, in their turn, interact to produce the more reactive $OH^{\bullet}$. This results in recruitment and activation of granulocytes, which ultimately mediate reperfusion-induced microvascular injury (adapted from Granger *et al.*, 1988).

taken depending upon the severity of the clinical condition. However, the difference between sepsis, severe sepsis and septic shock is not easily detected in clinical practice. The most prominent therapeutic approach for sepsis treatment till date is early goal-directed therapy (EGDT) for sepsis (Daniels, 2011). This approach involves screening patients who are at high risk for developing sepsis by monitoring certain hemodynamic and physiologic parameters intensively (i.e., blood pressure, heart rate and respiratory rate) and administering aggressive treatment (i.e., fluids or vasopressor) within the early hours of potential treatment (called the "golden hours") to maintain or restore the patient's vitals back to optimal functioning before the syndrome progresses to a worsened state (Rivers *et al.*, 2001). In addition, early administration of appropriate antibiotic therapy together with identifying the causative infectious agents (source control) are the other treatment

Table I.1   Management of POI by non-pharmacological and pharmacological treatment options (adapted from Behm & Stollman, 2003; Vather & Bissett, 2013).

Non-pharmacological treatment options

Treatment	*Potential mechanism*
Early enteral nutrition (or gum chewing)	Stimulates GI motility by eliciting reflex response and stimulating release of several hormonal factors
Early mobilization	Possible mechanical stimulation
Laparoscopic surgery	Decreased opiate requirements, decreased pain, less abdominal wall trauma

Pharmacological treatment options

Treatment	*Potential mechanism*
Laxatives/prokinetic agents	Stimulant, prokinetic effects
Opiate antagonists	Block peripheral opiate receptors
Epidural anesthesia	Inhibits sympathetic reflex at cord level, opioid-sparing analgesia
NSAIDs	Opioid-sparing analgesia, inhibits COX-mediated prostaglandin synthesis
Multimodal therapy	Combination therapy may work via multiple mechanisms

approaches upon a patient's presentation to the emergency department (Balk, 2004; Green & Gorman, 2014). Other treatment strategies for the management of sepsis include surgical drainage of infected site, optimizing O_2 delivery to patients with lactic acidosis, use of low dose corticosteroid, targeted immunological therapy, glycemic control, appropriate nutrition and effective supportive therapy (Patel *et al.*, 2003; Skrupky *et al.*, 2011).

I.3.2 *Oxidative stress in the intestinal mucosa as treatment target*

The onset of an earlier oxidative burst in the mucosal layer than in the muscular layer after intestinal manipulation in a murine model of POI, reported by our group (De Backer *et al.*, 2009) suggests that the mucosal layer might not only be a victim but also a (co-)trigger of surgically induced intestinal inflammation. Moreover, during SIRS, increase in gut mucosal permeability and bacterial translocation due to compromised epithelial barrier function can result in further progression of sepsis; this underlines the significance of intestinal mucosal

layer. Given the vital role of the intestinal mucosa in the pathogenesis of both POI and sepsis, strategies targeting towards protection of the mucosal layer could provide effective treatment for these acute GI inflammatory conditions.

As oxidative stress has been implicated in both POI and intestinal dysfunction during sepsis, induction of antioxidant enzymes aimed to increase the antioxidant defense of the intestinal mucosa could be one of the ideal therapeutic strategies to combat such disorders. Among the set of antioxidant genes induced during stress in cells and tissues, heme oxygenase (HO)-1 has been emerging as a novel therapeutic target in the last few decades; it exerts an adaptive response to a wide range of injurious stimuli (Bauer *et al.*, 2008; Agarwal & Bolisetty, 2013) implicated in many disease conditions (Deshane *et al.*, 2005) including GI diseases (Naito *et al.*, 2011). An ever-increasing list of compounds (including natural products and synthetic small molecules) known to induce HO-1 expression show therapeutic benefits during various disease conditions (Li *et al.*, 2007; Abraham & Kappas, 2008; Motterlini & Foresti, 2014). Amongst them, the plant polyphenol resveratrol, in addition to its ability to induce HO-1, has gained much attention due to its diverse therapeutic potential in various diseases attributed to its antioxidant and anti-inflammatory properties (discussed in section I.3.4).

I.3.3   The HO-1/carbon monoxide (CO) system; effects in POI and sepsis

HO is the rate-limiting enzyme in the catabolism of heme resulting in the generation of CO gas, Fe^{2+} and biliverdin, the latter being subsequently reduced to bilirubin by the biliverdin reductase (BVR) enzyme. Originally thought of as a mechanism that only serves to dispose of heme, it is now clear that the products of heme metabolism have important functions under physiological and pathophysiological conditions. Three isoforms of HO have been identified, but there are doubts whether HO-3 has a functional role as it was never convincingly reported at the protein level (Hayashi *et al.*, 2004; Wu & Wang, 2005). HO-1 is the inducible isoform while HO-2 is constitutive. Low levels of HO-1 is expressed in normal GI tract (Coeffier *et al.*, 2002; Barton *et al.*, 2003). HO-2 is present in enteric neurons (Miller *et al.*, 2001; Colpaert *et al.*, 2002), but also in non-neuronal cells in particular interstitial cells of Cajal (Grozdanovic & Gossrau, 1996; Miller *et al.*, 1998).

I.3.3.1 Protective effects of HO-1 induction

HO-1 is induced by a variety of physical and chemical stressors including heme, endotoxin, UV irradiation, heat shock and hemorrhagic shock, all sharing the ability to cause oxidative stress (Maines, 1997). Since the first report showing that HO-1 induction crucially controls inflammation in a model of carrageenan-induced pleurisy in rats (Willis *et al.*, 1996), evidence has accumulated that induction of HO-1 is a fundamental adaptive response to oxidative stress and acute inflammation (Bauer *et al.*, 2008), providing antioxidant, anti-inflammatory and cytoprotective effects. The homeostatic role of HO-1 induction in mitigating the inflammatory response makes sense since ROS are indeed involved in the initiation and progression of inflammation (Mittal *et al.*, 2014). Possible mechanisms include activation of TLRs and the Nacht domain-, Leucine-rich repeat-, and PYD-containing protein (Nalp)-3 inflammasome (Cannizzo *et al.*, 2011) and formation of $ONOO^-$ by rapid combination of $O_2^{\bullet-}$ with $NO^\bullet$ (Mittal *et al.*, 2014). In the GI tract, expression of HO-1 is increased in many experimental models such as intraperitoneal (i.p.) treatment with LPS (Otani *et al.*, 2000), intracolonic administration of trinitrobenzene sulfonic acid (Wang *et al.*, 2001) and surgical intestinal manipulation (De Backer *et al.*, 2009). In patients with IBD, it was found that macrophages and epithelial cells of colonic mucosa exhibit an increased expression of HO-1 although levels of this protein decreased in the case of high inflammatory activity (Paul *et al.*, 2005). Induction of HO-1 by exogenously administered hemin reduces GI inflammation and tissue injury (Attuwaybi *et al.*, 2004; Zhong *et al.*, 2010; Yoriki *et al.*, 2013). HO-1 induction was also shown to mediate the protective effects of the amino acid glutamine in the GI tract (Uehara *et al.*, 2005; Giris *et al.*, 2006; Giris *et al.*, 2007) and to be a mechanism of action of 5-aminosalicylic acid, a classic agent used for the treatment of IBD (Whittle & Varga, 2010). Similar to what has been proposed for the nervous and cardiovascular systems, this opens the possibility of exploiting the HO-1 pathway as a therapeutic target for GI inflammation.

I.3.3.2 Role of the by-products of HO-1

The antioxidant and anti-inflammatory effects of HO-1 induction are related to the breakdown of heme, which is known for its pro-oxidant and cytotoxic properties, and to a concerted action of the three products of heme metabolism namely Fe^{2+}, biliverdin and CO

(Ryter & Choi, 2009). These emerging findings led gradually to the investigation of the biological effects and possible pharmacological application of each single by-product of HO-1. First of all, free Fe^{2+} could be expected to act as a pro-oxidant through the generation of $OH^\bullet$ in the Fenton reaction. However, induction of HO-1 is accompanied by a concomitant up-regulation of ferritin (Nath *et al.*, 1992; Ren *et al.*, 2007), which sequesters Fe^{2+} and has antioxidant properties (Arosio *et al.*, 2009). Additionally, an anti-apoptotic effect of heavy chain ferritin was shown in an I/R model of the liver (Berberat *et al.*, 2003). Biliverdin is quickly reduced by BVR to bilirubin, which has been reported to act as potent intracellular antioxidant against lipid peroxidation (Stocker *et al.*, 1987). Exogenous administration of nanomolar concentrations of bilirubin restored post-ischemic myocardial function and minimized infarct size similarly to induction of HO-1 by hemin, suggesting a primary role of bilirubin in HO-1-mediated tissue protection against reperfusion injury (Clark *et al.*, 2000). Bilirubin also protects against I/R injury in the intestine, an effect that is associated with a decrease in intestinal lipid peroxidation products (Ceran *et al.*, 2001; Hammerman *et al.*, 2002). In a Dutch study, Caucasian patients with Crohn's disease, where oxidative stress is thought to contribute to the pathogenesis, significantly less often beared the uridine 5'-diphospho-glucuronyltransferase (UGT) 1A1*28 homozygous genotype, the latter genotype being associated with Gilbert's syndrome and increased bilirubin levels (de Vries *et al.*, 2012). Correspondingly, patients with Crohn's disease showed significantly lower serum bilirubin levels compared to controls in a study in the Czech republic (Lenicek *et al.*, 2014). Exogenous applications of bilirubin might thus be considered for the treatment of GI conditions where oxidative stress is involved. As biliverdin is rapidly reduced to bilirubin, exogenous administration of biliverdin was also attempted with success. In the GI tract, biliverdin attenuates transplantation-induced injury of the small bowel (Nakao *et al.*, 2004) and ameliorates dextran sodium sulfate-induced colitis (Berberat *et al.*, 2005). CO seems to contribute most significantly to the antioxidant, anti-inflammatory and cytoprotective effects of the HO-1 pathway (Motterlini & Otterbein, 2010) in line with early reports that exogenous CO mimicked the protective effects of HO-1 induction even under inhibition of HO-1 activity (Sato *et al.*, 2001). This explains the recent efforts to exploit the use of CO as a therapeutic agent to mimic the inherent beneficial actions of the HO-1 pathway.

I.3.3.3 Mechanisms of action of CO

The precise molecular mechanisms by which CO exerts its protective effects have not yet been fully elucidated. The major mechanisms of action that have been proposed, mainly on the basis of data in cell lines and non-GI tissue, are described below and each of them might after all be equally important, with one mechanism prevailing over the other(s) depending on the type of cell and/or tissue being considered. CO binds preferentially and with high affinity to transition metals, in particular to the reduced form of heme iron (Fe^{2+}) present in hemoproteins like hemoglobin, soluble guanylate cyclase (sGC), COX, cytochrome p450, cytochrome c oxidase, NOS, and NOX (Estabrook *et al.*, 1970; Dioum *et al.*, 2002; Akamatsu *et al.*, 2004; Roberts *et al.*, 2004; Ryter & Otterbein, 2004; Boczkowski *et al.*, 2006).

Activation of sGC/p38 mitogen-activated protein kinase (MAPK) by CO: CO is believed to act via activation of sGC, leading to an increase in intracellular cyclic guanosine monophosphate (cGMP). The inhibitory effect of CO on leukocyte adhesion in mesenteric venules and on neutrophil migration into the peritoneal cavity induced by carrageenan is counteracted by the sGC inhibitor 1H[1,2,4,]oxadiazolo[4,3-a]quinoxalin-1-one (ODQ) (Freitas *et al.*, 2006). CO seems to modulate MAPK-related pathways (Ryter *et al.*, 2006; Kim *et al.*, 2007). Accordingly, the inhibitory effect of CO on LPS-stimulated macrophages was related to further enhancement of p38 MAPK expression (Otterbein *et al.*, 2000) and the involvement of p38 MAPK activation in the beneficial effects of CO has since been reported in many models *in vivo* (Otterbein *et al.*, 2003; Zhang *et al.*, 2003; Kohmotoa *et al.*, 2007). However, CO is unlikely to activate p38 MAPK directly as it lacks a transition metal centre in the protein structure that would function as a binding site for the gaseous molecule. Thus, the p38 MAPK activation by CO might be the result of another upstream target.

Interaction of the HO-1/CO pathway with iNOS: In LPS-stimulated macrophages, CO decreased nitrite (marker of NO production) levels without changing iNOS protein expression (Sawle *et al.*, 2005) suggesting that CO might inhibit iNOS activity. However, in the same model, Tsoyi *et al.*, (2009) reported that CO is able to reduce iNOS expression, and this was also observed in LPS-treated human umbilical vein endothelial cells (Sun *et al.*, 2008).

Anti-/pro-oxidant effect of CO: Inhibition of NOX by CO, probably by binding to the heme-containing gp91phox/NOX2 unit, was shown to be involved in the anti-inflammatory actions of CO in LPS-stimulated macrophages (Nakahira *et al.*, 2006) and its anti-proliferative actions in human airway smooth muscle cells (Taille *et al.*, 2005). The inhibitory effect of CO on vascular smooth muscle cell migration has been related to inhibition of NOX1 (Rodriguez *et al.*, 2010). In contrast, binding of CO to cytochrome c oxidase (complex IV of the mitochondrial respiratory chain) was reported to result in a significant burst of mitochondrial ROS production and a concomitant conditioning of the cell with up-regulation of antioxidant and cytoprotective genes, which protects it upon subsequent stress stimulation (Bilban *et al.*, 2008). Moreover, in a CLP model, CO induced a mild mitochondrial oxidative stress response in the heart which stimulated mitochondrial biogenesis and improved bioenergetics in association with a reduced inflammatory response (Lancel *et al.*, 2009). This was confirmed in a recent study performed in isolated rat heart mitochondria (Lo Iacono *et al.*, 2011) showing that low micromolar concentrations of CO, probably by binding to cytochrome c oxidase and/or other unidentified targets in the respiratory chain, increase oxygen consumption and mitochondrial H_2O_2 production when physiologically stimulating the electron transfer chain with pyruvate/malate, but significantly decrease the burst of ROS induced by stimulating the reverse electron flow in mitochondria, a phenomenon that appears to typify oxidative and inflammatory disease states (Chen *et al.*, 2007). The latter effect of CO limiting excessive mitochondrial ROS production was attributed to mild "uncoupling" of respiration from ATP synthesis by CO, with a drop in Ψm due to movement of protons from the intermembrane space to the mitochondrial matrix (Lo Iacono *et al.*, 2011).

Induction of HO-1 by CO: The beneficial effects of CO might also be related, at least in some circumstances, to induction of HO-1 providing a positive feedback loop (CO→ induction of HO-1→ more CO→ further induction of HO-1) and allowing the ROS scavenging properties of biliverdin/bilirubin to come into play (Rodella *et al.*, 2006). In human endothelial cells, CO induces HO-1 expression through a mechanism involving Nrf2 activation. This has been shown to be associated with upstream activation of PERK (protein kinase R-like endoplasmic reticulum kinase), one of the three endoplasmic reticulum stress sensors; this correlated with protection against endoplasmic reticulum stress-induced endothelial cell apoptosis (Kim *et al.*, 2007).

I.3.3.4 Administration of CO as therapeutic agent

CO gas: The recognition that HO-1-derived CO functions as a signaling and cytoprotective intracellular mediator prompted scientists to devise strategies to deliver CO safely for therapeutic purposes. CO administered as gas at doses that do not compromise the oxygen carrying capacity of hemoglobin (Hb) was firstly used *in vivo* to show that it protects against hyperoxic injury in rat lung (Otterbein *et al.*, 1999). Since then, inhalation of CO gas at doses of 250 ppm (i.e., particles per million) for a short period of time has shown efficacy in many animal models of disease and devices for applying CO gas by inhalation in man have been developed (Motterlini & Otterbein, 2010). Recently, the distribution of CO upon CO inhalation was reported to be tissue-specific, with the increase in CO levels versus basal, immediately after inhalation of 250 ppm CO for 1 h in rats, ranging from 32-fold in spleen to 2-fold in intestine (Vanova *et al.*, 2014). Despite the fact that these recent findings emphasizing the potential use of CO gas as a therapeutic agent in pathophysiological states, the undesired effect of CO gas inhalation on the oxygen-carrying capacity of Hb is a crucial aspect that needs to be addressed before CO gas can be approved as a therapeutic agent.

CO in preservation solution: In transplantation surgery, CO has also been proposed to be used *ex vivo* as an adjuvant to preservation solution in which organs are normally stored prior to grafting. Indeed, cold storage of rat intestinal grafts in University of Wisconsin solution vigorously bubbled with 5% CO for 5 min before transplantation in recipient animals has been reported to markedly reduce the up-regulation of inflammatory mediators and improve graft blood flow and mucosal barrier function (Nakao *et al.*, 2006b). Similar data have been obtained for rat kidney and lung grafts (Kohmoto *et al.*, 2008; Nakao *et al.*, 2008) and for renal transplantation in pigs (Yoshida *et al.*, 2010). In contact with air, the CO-bubbled storage solution quickly loses CO by release into air, so that the CO-bubbled solution must be kept in a tightly sealed container without an air layer to keep the CO concentration constant (Kohmoto *et al.*, 2008).

CO-releasing molecules (CO-RMs): For this and other reasons, CO-RMs were developed to create the opportunity to deliver CO in a more practical, controllable and accurate way to the target site in comparison to CO gas inhalation. The most extensively studied CO-RMs today consist of two classes: 1) metal carbonyl complexes containing ruthenium, manganese

or molybdenum which carry CO bound to metals and 2) boranocarbonates, which do not contain transition metals and release CO spontaneously based on pH changes (Fig. I.14). While the original CO-RMs (CORM-1 and CORM-2) had to be dissolved in organic solvents like dimethyl sulfoxide (DMSO) (Motterlini *et al.*, 2002), water-soluble CO-RMs such as CORM-A1 and CORM-3 have been subsequently developed with different CO release kinetics (Clark *et al.*, 2003; Motterlini *et al.*, 2005).

In many animal models of inflammation, I/R injury and oxidative stress, these and other similar CO-RMs were shown to have beneficial effects similar to CO gas (Motterlini, 2007; Motterlini & Otterbein, 2010). In the context of organ preservation, and similarly to what has been described with CO gas above, addition of CORM-A1 and CORM-3 during kidney cold storage markedly increased glomerular filtration rate, vascular activity and energy metabolism at reperfusion (Sandouka *et al.*, 2006). Despite these agents need to be optimized and one has to keep in mind the possible toxicity originating from the molecule after release of CO especially when used chronically, CO-RMs offer a great opportunity in drug discovery as they diverge from classical organic drugs and represent one of the few examples where transition metals are used as scaffolds to deliver the active principle. For instance, a metal within the CO-RMs scaffold can be viewed as the "Achilles heel" in the development of these molecules to drugs, due to the common perception that transition metals *per se* can catalyze cytotoxic reactions. However, a great portion of structural and enzymatic proteins in cells contain transition metals, and several metal-handling proteins that protect cells against potentially toxic metal-based reactions are known, suggesting that biological tissues may be able to tolerate low levels of metal carbonyls (Foresti & Motterlini, 2013). Interestingly, we are gradually learning that the transition metal in CO-RMs appears to be influential in transferring efficiently CO into the cells and limiting the potential toxic effects of free CO gas (Foresti & Motterlini, 2010; Michel *et al.*, 2012).

I.3.3.5 Toxicity of exogenous CO

The interaction of CO with transition metals is central to the dichotomous nature (toxicity vs. beneficial effects) of this gaseous molecule. CO binds to Hb with a 200 to 250 times higher affinity than O_2 forming carbon monoxide-hemoglobin (COHb), that decreases the capacity of blood to deliver O_2 to the tissues. The basal COHb level in man is 0.1 to 1%
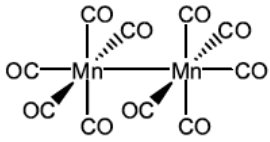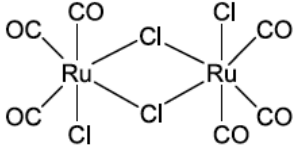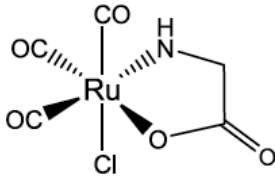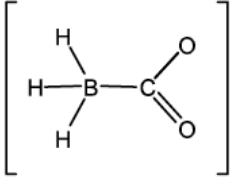
Compound	Chemical structure	CO release kinetic and properties
CORM-1		Fast ($t_{1/2} < 1$ min) CO release is light-dependent Soluble in ethanol and DMSO
CORM-2		Fast ($t_{1/2} \approx 1$ min) CO release induced by ligand substitution Soluble in ethanol and DMSO
CORM-3		Fast ($t_{1/2} \approx 1$ min at pH = 7.4, 37 °C) CO release induced by ligand substitution Water-soluble
CORM-A1		Slow ($t_{1/2} \approx 21$ min at pH = 7.4, 37 °C) CO release is strictly pH-dependent; Water-soluble

Fig. I.14 Chemical structures and features of the first generation of CO-RMs (adapted from Foresti *et al.*, 2008).

in the absence of environmental contamination or smoking (Ryter & Choi, 2013). Toxicity symptoms can occur by COHb levels from 10% on (Von Burg, 1999). Using COHb levels as a marker, it was shown that the systemic amounts of CO upon exogenous CO administration must be of a much higher order than when stimulating endogenous CO production by HO-1 induction (Foresti *et al.*, 2008). In experimental studies with CO or CO-RMs, one thus usually attempts to keep COHb levels below 10%, levels that are also occasionally encountered in heavy smokers. Still, one can be reluctant to apply chronically CO or CO-RMs e.g. for treatment of IBD, in doses inducing COHb levels of 5-10%. Deleterious effects to the heart were indeed shown for chronic ambient CO levels as low as 30 ppm with peaks of 100 ppm (Andre *et al.*, 2010; Reboul *et al.*, 2012). Short term CO therapy should be devoid of such effects and can be expected to be easier acceptable for application in man.

I.3.3.6 Effect of CO in POI

The preclinical studies investigating the influence of CO on the inflammatory phase of POI by manipulating the small intestine after laparotomy and measuring transit 24 h after surgery, are summarized in Table I.2.

CO gas: Moore *et al.*, (2003) reported that inhaled CO (250 ppm for 1 h before and for 24 h after surgery) in mice significantly improved the prolongation of transit induced by surgery, corresponding with improvement of the surgery-induced suppression of spontaneous and betanechol-induced activity in small intestinal circular muscle strips obtained 24 h after surgery. CO is known to relax GI smooth muscle *in vitro*, and might retard GI transit *in vivo* by this effect, but CO inhalation in control non-operated animals did not significantly influence transit. Surgery increased iNOS mRNA expression in the small intestinal muscular layer at 3 and 6 h, and nitrite release in the culture medium of muscular material obtained 24 h after surgery; these effects were suppressed by CO inhalation, suggesting that CO might act by inhibiting iNOS gene expression as well as iNOS activity. Surgery also increased the mRNA expression of pro-inflammatory IL-1β, IL-6 and COX-2, and of anti-inflammatory IL-10 and HO-1; CO reduced IL-1β expression and further enhanced IL-10 and HO-1. This supports that the beneficial effects of CO are at least partially due to increased HO-1 expression. Interestingly, the increase in muscular leukocyte infiltration by surgery was not suppressed by CO.

The same group (Moore *et al.*, 2005) showed in rats that inhaling 250 ppm CO for 3 h before surgery was sufficient to fully reverse surgery-induced retardation in transit, even 75 ppm being sufficient; this certainly means a more feasible schedule for testing in humans than prolonged inhalation. They also showed that 250 ppm for 3 h before surgery is effective in pigs that received repetitive opioid analgesia after surgery to mimic the human condition where the GI inhibitory effects of opioid analgesics also contribute to ileus. Blood COHb levels reached 6% just before surgery and progressively declined thereafter. Although CO inhalation suppressed the increase in total blood white cell count at 4 h after surgery, it did not suppress muscular leukocyte infiltration at 24 h, again suggesting that CO by inhalation is not able to inhibit additional leukocyte recruitment during the pathogenesis of POI.

Table I.2 Effects of CO on GI motility and on inflammatory parameters in the muscular layer in preclinical models of postoperative ileus.

Reference	Moore et al., 2003		Moore et al., 2005		Moore et al., 2005		Nakao et al., 2006a		De Backer et al., 2009	
Species	Mouse		Rat		Pig		Mouse		Mouse	
CO source	Inhalation 250 ppm 1h before to 24h after surgery		Inhalation 250 ppm 3h before surgery		Inhalation 250 ppm 3h before surgery		Intraperitoneal Ringer's lactate, 100% CO bubbled, at end of surgery		Intraperitoneal CORM-3 40 mg.kg^{-1} 3h and 1h before surgery	
Blood carboxyhemoglobin	-		-		6%		8%		2.3%	
	POI	+CO	POI	+CO	POI	+CO	POI	+CO	POI	+CO
GI transit (24h)	↓	↑	↓	↑		↑	↓	↑	↓	↑
In vitro muscle activity	↓	↑	-		-		-		↓	↑
In vitro betanechol	↓	↑	-		↓	↑	-		-	
sGC involvement in CO effect	-		-		-		Yes		-	
p38 MAPK phosphorylation	-		-		-		↑	=	↑	↑
ERK MAPK phosphorylation	-		-		-		↑	↓	↑	↓
JNK MAPK phosphorylation	-		-		-		↑	↓	↑	=
iNOS mRNA	↑	↓	-		-		↑	↓	-	
activity	-		-		-		-		↑	↓
ROS	-		-		-		-		↑	↓
HO-1 mRNA	↑	↑	-		-		↑	=	-	
protein	-		-		-		-		↑	↑
HO total activity	-		-		-		-		↑	↑
MPO (infiltrating leucocytes)	↑	=	-		↑	=	↑	↓	↑	↓
IL-1 β mRNA	↑	↓	-		-		↑	↓	-	
IL-6 mRNA (protein in 4)	↑	=	-		-		↑	=	↑	↓
IL-10 mRNA (protein in 4)	↑	↑	-		-		↑	↑	↑	↑
COX-2 mRNA	↑	=	-		-		↑	↓	-	
ICAM-1 mRNA (protein in 4)	-		-		-		↑	↓	↑	↓
MCP-1 mRNA (protein in 4)	-		-		-		↑	=	↑	↓
NF-κB DNA binding activity	-		-		-		↑	↓	-	

-: not determined.

CO in i.p. solution: Following the report that intestinal grafts performance is enhanced by preserving them in organ preservation solutions saturated with CO (Nakao *et al.*, 2006b), Nakao *et al.*, (2006a) showed that an i.p. injection of Ringer's lactate solution bubbled with 100% CO for 15 min just before closure of the abdomen prevented postsurgical ileus in mice. COHb levels attained almost 8% at 5 min after administration of CO but decreased to less than 4% within 30 min. This very elaborated study showed that treatment with solutions containing CO affects surgery-induced mRNA expression of pro- and anti-inflammatory parameters as reported for inhaled CO, except that the induction of HO-1 mRNA was not further enhanced by CO (Moore *et al.*, 2003). Importantly, CO by i.p. injection suppressed muscular leukocyte infiltration. The study further showed that surgery induced activation of the MAPK p38, extracellular signal-regulated kinase (ERK) and c-Jun amino-terminal kinases (JNK), and of the transcription factor NF-κB; except for p38, these effects were suppressed by CO. The majority of the effects of CO were diminished by pretreatment with the sGC inhibitor ODQ, suggesting activation of sGC by CO early in its protective pathway.

CO-RMs: An i.p. injection of the "fast" CO-releaser CORM-3 (40 mg/kg at 3 and 1 h before surgery), inducing maximal blood COHb levels of 2.3% at 10 min after injection, provided partial protection against retarded transit by surgery in mice, while the inactive compound i-CORM-3 was not effective (De Backer *et al.*, 2009). A similar effect was obtained with equimolecular amounts of the "slow" CO releaser CORM-A1 but COHb levels increased to 8.4% at 20 min after injection. Similar to data obtained with CO in i.p. solution, i.p. administration of CORM-3 suppressed muscular leukocyte infiltration at 6 and 24 h after surgery, and decreased ERK activation, but it increased MAPK p38 activation. Surgery induced a progressive increase in protein expression of HO-1 and in total HO activity; this was further enhanced by CORM-3 at 1 to 6 h after surgery in a p38 MAPK dependent way, as prevented by a p38 MAPK inhibitor. Finally, the study showed that CORM-3 suppresses the progressive increase in muscular oxidative stress levels induced by surgery, illustrating that also anti-oxidative effects of CO might contribute to its beneficial effect in POI. In contrast to previous studies, De Backer *et al.*, (2009) also investigated the role of the mucosal layer. Surgery did not induce pronounced expression of pro-inflammatory cytokines in the mucosa, but it led to an early mucosal oxidative stress burst at 1 h after surgery, which might co-trigger the intestinal epithelial barrier dysfunction during POI (Snoek *et al.*, 2012). CORM-3 reduced this early mucosal oxidative burst in a fully HO-1-dependent way, as shown with the

HO inhibitor chromium mesoporphyrin, while the anti-inflammatory/anti-oxidative effects of CORM-3 in the muscularis are only partially HO-1 dependent.

I.3.3.7 Effect of CO on the intestine in sepsis

In different animal models of sepsis, CO either inhaled as a gas or supplied as CO-RMs was shown to increase survival and to decrease inflammation and tissue damage in critical organs involved in septic MOF, i.e. lung, liver, heart and kidney (Sarady *et al.*, 2004; Hoetzel *et al.*, 2007; Cepinskas *et al.*, 2008; Lancel *et al.*, 2009; Mizuguchi *et al.*, 2009; Lee *et al.*, 2014). In most studies, CO is applied before or just after administering the septic stimulus, which is clinically irrelevant in patients with established sepsis, but a recent study showed that inhalation of CO in a therapeutic way (i.e. 2.5 h after starting the LPS infusion) still provides some degree of protection (Koulouras *et al.*, 2011).

Studies concentrating on the effect of CO in the intestine during experimental sepsis are summarized in Table I.3. The intestinal readouts involve whole tissue homogenates of small intestinal fragments without separation of mucosal or muscular layers. (Liu *et al.*, 2007) reported that CO inhalation at 250 ppm from 1 to 4 h after intravenous (i.v.) injection of LPS in rats ameliorated intestinal injury measured at 4 h after LPS. This corresponded with significant suppression of the LPS-induced intestinal cell apoptosis. Although inhalation of CO gas induced an increase in arterial COHb levels to 6.9%, no significant differences in the partial arterial oxygen pressure and arterial oxygen saturation were observed. Injection of LPS increased intestinal HO-1 mRNA expression, which was further augmented following CO inhalation. CO inhalation reduced the LPS-induced increase in intestinal ICAM-1 and platelet activating factor (PAF) expression as well as leukocyte infiltration and lipid peroxidation so that CO might exert its protective effect via anti-inflammatory, anti-oxidative and anti-apoptotic actions. Similar protective effects were obtained when continuously perfusing 2 l/min of 250 ppm CO (from CO gas compressed at 250 ppm with balanced air in a cylinder) into the peritoneal cavity (through an inlet in the hypogastric right region with an outlet in the epigastric left section) from 1 to 7 h after i.v. administration of LPS (Liu *et al.*, 2010a). Parameters were measured after 1, 3 and 6 h of CO treatment and illustrated that the beneficial effect of CO was maintained for the whole perfusion period. As measured at 3 h after LPS challenge, p38 MAPK phosphorylation was increased by LPS and further enhanced by CO treatment. The group of Liu *et al.*, (2010b) then also investigated the effect of a single

Table I.3   Effects of CO on intestinal tissue integrity and on inflammatory parameters in preclinical models of sepsis.

Reference	Liu *et al.*, 2007		Liu *et al.*, 2010a		Liu *et al.*, 2010b		Wang *et al.*, 2012	
Species	Rat		Rat		Rat		Mouse	
Model	LPS injection i.v.		LPS injection i.v.		LPS injection i.v.		Cecal ligation and puncture (CLP)	
CO source	Inhalation 250 ppm from 1 to 4 h after LPS challenge		Intraperiton. perfusion 2 l/min 250 ppm CO from 1 to 7 h after LPS challenge		Intraperiton. bolus 2 ml/kg 250 ppm CO 1 h after LPS challenge		i.v. CORM-2 8 mg/kg immediately after CLP	
Blood carboxyhemoglobin	6.9%		7.0%		2.6%		-	
	LPS	+CO	LPS	+CO	LPS	+CO	CLP	+CO
Intestinal tissue damage	↑	↓	↑	↓	↑	↓	↑	=
Intestinal cell apoptosis	↑	↓	↑	↓	↑	↓	-	
p38 MAPK phosphorylation	-		↑	↑	↑	↑	-	
iNOS protein	-		-		-		↑	↓
NO production	-		-		-		↑	↓
ROS	↑	↓	↑	↓	↑	↓	↑	↓
SOD activity	-		-		↓	↑	-	
HO-1 mRNA	↑	↑	-		-		-	
MPO (infiltrating leucocytes)	↑	↓	↑	↓	↑	↓	↑	↓
TNF-α protein	-		-		-		↑	↓
IL-1β protein	-		-		-		↑	↓
IL-10 protein	-		-		↓	↑	-	
ICAM-1 protein	↑	↓	↑	↓	↑	↓	↑	↓
PAF-1 protein	↑	↓	↑	↓	↑	↓	-	

-: not determined.

i.p. injection of 2 ml/kg of 250 ppm CO, 1 h after LPS treatment. At 1 and 3 h after injection of CO, the LPS-changed parameters were beneficially influenced by CO but no longer at 6 h. In addition to their previous studies, intestinal levels of SOD activity and IL-10 protein were measured; both markers were suppressed by LPS but partially reversed by CO, with IL-10 being still elevated at 6 h after CO treatment. Although not studying intestinal tissue *per se*, Dal-Secco *et al.*, (2010) confirmed in mice the importance of ICAM-1 for LPS-induced neutrophil migration. The increased expression of ICAM-1 on mesenteric venular endothelium observed 2 h after intraperitoneal injection with LPS was significantly reduced by treating the animals with the CO donor dimanganese decacarbonyl (3 mg/kg subcutaneously) 30 min before LPS challenge. The effect of the CO donor was prevented by ODQ, illustrating that it depends on sGC activation. Recently, Wang *et al.*, (2012) studied the mouse small intestine 24 h after CLP. The intestine showed increased lipid peroxidation, leukocyte infiltration (MPO activity), and TNF-α, IL-1β, ICAM-1 and iNOS protein levels, the latter corresponding with increased NO production. All these effects were attenuated by CORM-2 (8 mg/kg) injected i.v. immediately after the cecal ligation procedure. Histological analysis revealed hydropic degeneration and granulocyte infiltration by the septic procedure; while CORM-2 decreased granulocyte infiltration, it did not improve the hydropic degeneration.

These studies clearly support the idea that the beneficial effect of CO in sepsis might be due, at least in part, to prevention or recovery of intestinal inflammation and tissue damage, therefore avoiding the triggering role of the intestine in sepsis. Although none of the studies in Tables I.3 measured gut barrier function, it can be expected that the anti-inflammatory and antioxidant effects of CO in the intestine will also decrease the intestinal barrier dysfunction in sepsis. Additionally, the enhancement of host bacterial clearance (Chung *et al.*, 2008; Onyiah *et al.*, 2013) and direct bacteriostatic/bactericidal effects by CO and CO-RMs (Desmard *et al.*, 2012) might contribute to the beneficial effect in sepsis.

I.3.4   *Resveratrol; effects in POI and sepsis*

I.3.4.1 *Resveratrol*

Human health is greatly affected by environmental factors including bioactive molecules found in food. Plants produce a wide spectrum of diverse metabolites that are

being investigated for their potential utility in the prevention and treatment of human disease. Phytoalexins are one such group of molecules that are produced by plants in response to exogenous stressors or pathogen attack and have potent antimicrobial activity (Ahuja *et al.*, 2012). Phytoalexins are chemically diverse and show biological activity towards a variety of pathogens; they help in disease resistance as plant antibiotics. "Polyphenols" are the plant derived chemical products that are characterized by the presence of two or more phenolic groups in their structure. They are capable of reducing ROS and thus could serve as antioxidants. Many phytoalexin molecules are polyphenolic in nature. The phytoalexins produced by *Vitis vinifera* (grape) and found abundantly in red wines became a popular subject of biomedical research following the discovery of the "French Paradox", an observation of low incidence of cardiovascular disease in populations in France that regularly consume red wine, in spite of other risk factors including a high-fat diet (Renaud & de Lorgeril, 1992). Red wines are a rich source of phytoalexins and polyphenols (Quideau *et al.*, 2011). Of the many polyphenolic phytoalexins found in red wines, resveratrol (3,4',5-trihydroxy-stilbene) is perhaps the most extensively studied to date. Resveratrol exists in both *cis* and *trans* forms (Fig. I.15). The *trans*-isomeric form displays greater stability than the *cis* form when protected from high pH and light; hence the beneficial effects so far known from the majority of studies are based on investigations with *trans*-resveratrol (Leiro *et al.*, 2004). The concentrations and thus the ratio of *cis* and *trans* isomers of resveratrol vary in different wines depending upon the variety of grapes used in wine preparation. Resveratrol is insoluble in water but soluble in organic solvents like DMSO and ethanol; thus a diet high in fat might actually enhance the uptake of lipid-soluble resveratrol to account for its beneficial effect reported with the "French Paradox". Resveratrol is produced by at least 72 different plant species, some of which are a part of the human diet such as grape skins, soy, peanuts and mulberries; these are thus important dietary sources of this polyphenol (Soleas *et al.*, 1997).

In vivo studies using experimental animals (mice, rats and dog models) suggest that resveratrol is absorbed satisfactorily in the GI tract, with significant concentrations being found in the blood and a number of internal organs (Bertelli *et al.*, 2001).
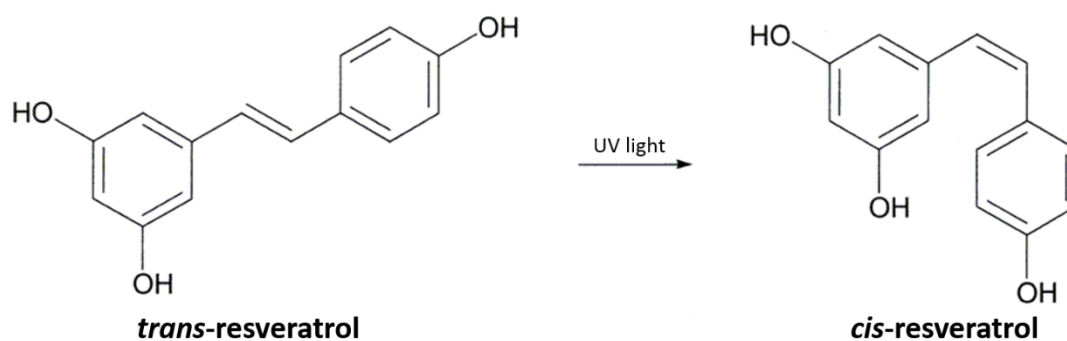
Fig. I.15 Chemical structures of resveratrol isomers showing conversion to *cis*-resveratrol after the irradiation of *trans*-resveratrol with UV light

I.3.4.2 Mechanisms of action of resveratrol

As an isolated compound resveratrol has gained attention in both the scientific community and general public for its plethora of beneficial effects against neurodegenerative disease, cardiovascular disease, obesity, diabetes and cancer, and its lifespan extension (Smoliga *et al.*, 2012). These beneficial effects of resveratrol are due to its anti-inflammatory, anti-oxidative, anti-proliferative and anti-cancer properties. Resveratrol appears to influence the activity of a vast number of enzymes, and the list of downstream targets and affected signaling pathways is continuously growing.

Anti-/pro-oxidant effect of resveratrol: Many of resveratrol's beneficial effects are consistent with a reduction in intracellular oxidative stress. Resveratrol has an inherent antioxidant activity related to its chemical structure. At the level of ROS, resveratrol has H_2O_2 and $OH^\bullet$ scavenging activity (Leonard *et al.*, 2003; Ungvari *et al.*, 2007). Moreover, being a lipid antioxidant, resveratrol has the ability to prevent lipid peroxidation by scavenging peroxyl radicals ($ROO^\bullet$ where R denotes an organic group) within the membrane (Tadolini *et al.*, 2000). Correspondingly, resveratrol has been reported to reduce the copper catalyzed oxidation of human low-density lipoprotein (LDL), a crucial step in the pathogenesis of atherosclerosis and thus could exert cardioprotection (Frankel *et al.*, 1993). Resveratrol was also reported to decrease ROS by reducing the NOX expression in murine aortic walls after vascular injury (Sarr *et al.*, 2006; Vecchione *et al.*, 2009) and NOX activity in angiotensin II or oxidized LDL-treated cultured human endothelial cells (Chow *et al.*, 2007). One advantage of resveratrol as compared to other polyphenols is that this compound does not chelate iron, hence it does not affect iron absorption (Brune *et al.*, 1989). However, resveratrol has a potential to chelate copper (Belguendouz *et al.*, 1997).

Polyphenols, in general, can act either as anti- or pro-oxidants, i.e. inhibitors or enhancers of oxidative and radical chain processes (Halliwell, 2008). Besides the redox potential of the polyphenol, whether an anti- or a pro-oxidant effect predominates, depends on the abundance of metal ions sustaining a redox cycle (Fe^{2+}/Fe^{3+}, Cu^{+}/Cu^{2+}) and/or of oxidizing enzymes, the ion-chelating properties of the molecule, pH, the concentration of the polyphenol, and the subcellular compartment (Babich *et al.*, 2011). Being a polyphenol, resveratrol also exhibits some pro-oxidant activities under certain conditions. E.g. in the presence of Cu^{2+}, resveratrol was shown to catalyze the reduction of Cu^{2+} to Cu^{+} with the resulting oxidized resveratrol products exhibiting pro-oxidative behavior (Ahmad *et al.*, 2000).

Resveratrol also decreases oxidative stress by activating the molecular pathways to increase the level and activity of cellular antioxidant enzymes (Kovacic & Somanathan, 2010). In cultured human lung fibroblasts treated with micromolar concentrations of resveratrol for 48 h or two weeks, a significant increase in MnSOD protein level and activity is observed, an effect that reaches nearly 5-fold at the two week time point (Robb *et al.*, 2008a). This increase in MnSOD is accompanied by a slight increase in the activity of Gpx, but is not accompanied by a general increase in antioxidant enzyme activity, as Cu/Zn SOD and catalase activity are unaffected by resveratrol. The observation of increase in MnSOD protein level and activity by resveratrol was subsequently reported in murine skeletal muscle (Ryan *et al.*, 2010), murine neuronal (Fukui *et al.*, 2010; Kairisalo *et al.*, 2011) and human coronary endothelial (Ungvari *et al.*, 2009) cells. These reports suggest that increase in MnSOD is a common mechanism of antioxidant activity by resveratrol. Resveratrol also increases the expression of detoxification enzymes like NAD(P)H: quinone oxidoreductase (Rubiolo *et al.*, 2008) and of Nrf2, which ultimately leads to upregulation of HO-1 (Chen *et al.*, 2005). Additionally, resveratrol can also increase mitochondrial biogenesis (Csiszar *et al.*, 2009).

***Activation of sirtuins*:** The biological activities of resveratrol have been hypothesized to arise from its interaction with numerous substrates; sirtuins attracted most attention. Sirtuins are a family of highly conserved protein deacetylase enzymes named after the founding member, the *Saccharomyces cerevisiae* silent information regulator 2 (Sir2) protein. In yeast, Sir2 was identified as a putative longevity protein following an observation that its overexpression extends lifespan in *Caenorhabditis elegans* (Tissenbaum & Guarente, 2001).

Mammalian silent mating type information regulator 2 homolog 1 (SIRT1) is closely related to the *C. elegans* protein Sir2. Resveratrol has been identified to be a potent activator of SIRT1 and hence is implicated in increasing lifespan (Howitz *et al.*, 2003) SIRT1 being a key regulator of cellular defenses and cell survival in response to stress. Resveratrol attenuates mitochondrial ROS production via a pathway that involves the activation of SIRT1 and the upregulation of antioxidant defense mechanisms (Ungvari *et al.*, 2009). Activating SIRT1 has been proposed to be a possible strategy of resveratrol to inhibit NF-κB and/or activator protein (AP)-1 signaling pathways during inflammation and oxidative stress, respectively (Chung *et al.*, 2010).

Estrogen like effects of resveratrol: Resveratrol is capable of binding to estrogen receptors to stimulate transcriptional responses (Gehm *et al.*, 1997). Moreover, resveratrol can act as a phytoestrogen, plant derived compounds that mimic the activity of 17-β-estradiol (E2), the primary female sex hormone. Owing to these facts, there is remarkable overlap between the health effects of resveratrol and those of estrogen. Similar to resveratrol, estrogen is neuroprotective, and prevents neurodegeneration in models of Parkinson's disease, Alzheimer's disease and ischemia reperfusion (Wise *et al.*, 2001; Brinton, 2008; Robb & Stuart, 2010). Similarly, resveratrol and estrogen both have beneficial effects on metabolism and cardioprotection (Nikolic *et al.*, 2007; Wu & Hsieh, 2011; Faulds *et al.*, 2012; Voloshyna *et al.*, 2012). Although resveratrol does not dramatically affect reproductive physiology, many of its *in vivo* effects, such as its positive effects on bone health in ovariectomized rodents, are very similar to observations made with estrogen treatment (Lin *et al.*, 2005). Resveratrol stimulates the transcription of an estrogen controlled luciferase reporter gene in a dose-dependent manner in a human breast cancer cell line (MCF-7). Estrogen antagonists inhibit the activation of the reporter gene by resveratrol, and in a competition assay resveratrol successfully prevented the binding of radiolabeled estradiol to estrogen receptors, demonstrating that resveratrol is an estrogen receptor agonist *in vitro* (Gehm *et al.*, 1997). Resveratrol is an agonist for both estrogen receptor-α and estrogen receptor-β (Bowers *et al.*, 2000). Interestingly, both mitochondria and MnSOD are major downstream targets of E2 signaling (Borras *et al.*, 2005) and it is plausible that resveratrol could exert its effect at the mitochondrial level through E2 signaling.

Inhibition of NF-kB: The exact mechanisms through which resveratrol exerts anti-inflammatory effects remain unclear, but mounting evidence supports that resveratrol

seems to affect a wide range of inflammatory parameters. NF-κB is likely to be the major molecular target for the anti-inflammatory effects of resveratrol. The presence of resveratrol prevented the activation of NF-κB triggered by exposure of varied cell types (myeloid, lymphoid and epithelial) to diverse inflammatory triggers like TNF-α, phorbol 12-myristate 13-acetate (PMA), H_2O_2, LPS, okadaic acid and ceramide (Manna *et al.*, 2000b). Thus, treatment with resveratrol suppressed NF-κB-regulated gene products involved in inflammation like TNF-α, IL-6, IL-1β, IL-8, COX-2, iNOS, etc (Csaki *et al.*, 2009). Still, activation of NF-κB by resveratrol has also been reported in IECs (see section *1.4.2*).

I.3.4.3 Administration of resveratrol as therapeutic agent

In animal studies investigating the beneficial effects of resveratrol, it has been administered by i.v., i.p., and oral routes (Shigematsu *et al.*, 2003; Alfaras *et al.*, 2010; Larrosa *et al.*, 2011; Petrat & de Groot, 2011). For a substance present in the human diet obviously one thinks of oral administration in humans. The bioavailability and pharmacokinetics of resveratrol have been studied in experimental animals and humans. Resveratrol supplementation has been demonstrated to be safe for humans based on a phase I study where healthy volunteers were provided with up to 5 g of resveratrol orally, with no major adverse events (Boocock *et al.*, 2007). An enterohepatic cycle has been proposed for resveratrol in both rats and humans. Upon oral administration, resveratrol is rapidly metabolized by extensive first-pass glucuronidation and sulfation both in the intestine by IECs and in the liver; the metabolized forms then circulate to other organs (Goldberg *et al.*, 1995; Bertelli *et al.*, 2001; Soleas *et al.*, 2001; Vitrac *et al.*, 2003; Yu *et al.*, 2009). The glucuronide and sulfate conjugates are also secreted back to the intestine where they may be deconjugated and the resulting resveratrol reabsorbed, or excreted in the feces (Marier *et al.*, 2002; Walle *et al.*, 2004). Thus, the enterohepatic cycle, along with rapid metabolism in the liver, likely explains the low concentration of unchanged resveratrol in the blood stream. Both in humans and rats, unchanged resveratrol reaches a maximum plasma concentration of 1.9% within an hour following oral administration of *trans*-resveratrol (Goldberg *et al.*, 2003; Walle *et al.*, 2004; Boocock *et al.*, 2007). In humans, resveratrol administered intravenously, avoiding first-pass metabolism, was found to be converted into a sulfate conjugate within 30 min (Walle *et al.*, 2004). In the same study, most of the resveratrol following a single 25 mg oral dose was recovered in urine as its glucuronide and

sulfate conjugated metabolites, with only trace amounts of unchanged resveratrol (<5 ng/ml) detected in plasma. Similarly, in rodents also, oral intake of resveratrol in the hundreds of milligrams range yields only low nanomolar plasma levels of unmetabolized resveratrol (Marier *et al.*, 2002; Teng *et al.*, 2012). These results further underline that most of resveratrol taken up orally is eliminated from the body leaving only a small fraction of the parent compound. However, the composition of the food matrix can have an impact on the bioavailability of ingested resveratrol. Correspondingly, significant improvement in energy metabolism and aerobic exercise endurance is observed in mice when resveratrol is added to diets with fat contents equal to or greater than 40%, but not when resveratrol is added to a standard composition diet (Baur *et al.*, 2006; Lagouge *et al.*, 2006). Similarly, resveratrol given in a high-fat diet increases brain antioxidant enzyme activities by approximately 2-fold, while the same dose given in a standard mouse diet does not have a significant effect (Robb *et al.*, 2008b).

Given the low bioavailability and extensive metabolism of oral resveratrol, solutions are sought to increase the bioavailability of resveratrol in order to achieve in plasma the concentrations previously shown to have biological activity in *in vitro* assays (5-100 µmol/L) (Poulsen *et al.*, 2013). New administration strategies are currently under development to help bypass metabolic breakdown of resveratrol and increase its bioavailability. Resveratrol-containing lozenges have been reported to increase buccal absorption of resveratrol (Asensi *et al.*, 2002). Nanoparticles and liposomes are investigated as potential carriers of resveratrol to improve its bioavailability (Teskac & Kristl, 2010; Santos *et al.*, 2011; Gokce *et al.*, 2012). Recently, structural derivatives of resveratrol were shown to have manifold higher antioxidant potential than the native molecule; these derivatives could be of benefit to achieve effective therapeutic concentration of resveratrol *in vivo* (He & Yan, 2013).

I.3.4.4 Effect of resveratrol in POI

In only one study, treatment of rats with resveratrol (10 mg/kg; i.v.) 1 h before operation partly reversed the retarded transit induced by gut manipulation; no inflammatory parameters were studied (Korolkiewicz *et al.*, 2003).

I.3.4.5 Effect of resveratrol on the intestine in sepsis

In experimental models, resveratrol improved sepsis-induced acute organ injury, like lung (Kolgazi *et al.*, 2006) and kidney (Kolgazi *et al.*, 2006; Holthoff *et al.*, 2010), when administered either before or shortly after the septic insult. Similarly, in the GI tract, resveratrol (100 mg/kg, i.p.) treatment immediately after CLP to induce sepsis in rats improved ileal smooth muscle reactivity, as measured by smooth muscle contractile response to KCl and carbachol; this was accompanied by suppression of serum TNF-α and IL-6 levels (Gacar *et al.*, 2012). Oral administration of rats with resveratrol (50 mg/kg) reduced the levels of LPS-induced increase in lipid peroxidation (thiobarbituric acid reactive substances; TBARS) in the small intestine and colon (Larrosa *et al.*, 2011). In this study, resveratrol was administered orally by gastric probe for 3 days; then followed by i.p. injection of LPS with a fourth dose of resveratrol given 45 min after LPS injection. Interestingly, the administration of LPS caused a decrease in resveratrol absorption as assessed from plasma samples; while both glucuronide and sulfate derivatives were found in the resveratrol treated group, LPS-resveratrol treated group showed only glucuronide derivative, with a level 15 fold lower than the resveratrol treated group.

I.4   IECs as model to study mucosal injury

Many studies investigating intestinal pathologies using mouse models suggest that apoptosis of IECs triggers intestinal inflammation (Nenci *et al.*, 2007; Kajino-Sakamoto *et al.*, 2008; Roulis *et al.*, 2011). Enterocytes are the most abundant cell type in the intestinal epithelial cell layer; however, the cellular and molecular mechanisms regulating the cell death of enterocytes and their role in maintenance of mucosal homeostasis are still poorly understood. As *in vivo* studies using experimental animals involve multiple cell components, investigations with isolated cells could be a possible alternative to understand how IECs could individually respond to various inflammatory and oxidative triggers. However, given the low viability of primary IECs after isolation and when grown in culture (Schwerk *et al.*, 2013), i*n vitro* studies involving immortalized epithelial cell lines are frequently used to understand how inflammatory mediators or cells can alter epithelial cell ion transport, permeability and barrier defects, triggering inflammation (Sambruy *et al.*, 2001). Human colon epithelial cell lines like Caco-2, DLD-1, T84, HT-29, HCA-7, LS174T, HCT-8, and I-407 are

often used in scientific investigations. Indeed, the Caco-2 cell line with characteristics of enterocyte-like phenotype, forming confluent cell monolayers bearing properties of transporting epithelia has been internationally recognized as a gold standard model in many pharmaceutical studies to determine intestinal permeability and oral drug uptake (Sambuy *et al.*, 2005; Araujo & Sarmento, 2013). However, all the aforementioned cell lines are colonic and carcinogenic in origin. IEC lines from rodent origin like IEC-4.1, IEC-6 and IEC-18 (from rat), and m-ICc12, MODE-K and YAMC (from mouse) have been used as mammalian surrogates of non-cancerous nature. They are derived from small intestine (with the exception of the murine YAMC cell line). Notably, all the rat derived IEC lines retain many of the characteristics of crypt cells (Podolsky, 2000). However, the murine MODE-K cells exhibit morphological and phenotypic characteristics of normal enterocytes, including intercellular junctions, and expression of cytokeratin and villin (Vidal *et al.*, 1993). The murine m-ICc12 cell line is derived from the bases of small intestinal villi and hence maintains a crypt phenotype (Bens *et al.*, 1996). Thus, the MODE-K cell line represents a suitable model for the analysis of IEC function in mucosal immunity (Vidal *et al.*, 1993). Recently, the development of three-dimensional (3D) intestinal epithelial organoids (also called "epithelial mini-guts") has been proposed as a possible means of maintaining primary IECs in continuous culture (Sato & Clevers, 2013). However, organoid cultures are time-consuming and expensive, obviously making them impractical for large-scale analyses (Schwerk *et al.*, 2013).

TNF-α is a pleiotropic cytokine that has a key role in inflammation induced by infection or tissue injury. TNF-α signaling is primarily executed through TNF-α receptor 1 (TNFR1) which induces direct pro-inflammatory signaling with increased expression of many genes that regulate inflammation (without cytotoxicity in many cell types). However, in cultured cells (of both normal and cancerous nature), TNF-α can induce cell death upon sensitizing the cells by treatment with a protein kinase (staurosporine), transcription (actinomycin-D) or translation (cycloheximide; CHX) inhibitor (Beyaert *et al.*, 1993). In such sensitized cells, binding of TNF-α to TNFR1 can induce apoptosis or necrosis depending upon the availability of death regulatory and execution factors (Jones *et al.*, 2000; Pasparakis & Vandenabeele, 2015). The signaling complex formed by TNFR1 activates initiator caspases (like caspase-8) which then results in activation of executioner caspases (like caspase-3 and caspase-7) to mediate apoptotic cell death (Van Herreweghe *et al.*, 2010).

I.4.1 CO in IEC lines

Publications on the protective effect of CO in IEC lines are summarized in Table I.4. The IEC lines studied are from murine, rat and human origin; the rodent cell lines (MODE-K, YAMC and IEC-6) are derived from non-cancerous GI tissues while the human cell lines (Caco-2, HT-29 and DLD-1) are from tumorous tissue sources. TNF-α is also an important inflammatory mediator in GI inflammation (Holtmann *et al.*, 2002) explaining why studies so far investigating the effect of CO or CO-RMs involved exposing monolayers of IECs to either TNF-α alone or in combination with other pro-inflammatory cytokines such as IL-1β and interferon (IFN)-*γ* (cytokine mix). All these studies involve acute measurements where the cells were exposed to TNF-α or cytokine mix from 30 min to maximally 24 h followed by cellular and transcriptional readouts.

CO treatment protects against IEC death induced by inflammatory cytokines as shown with CO gas in rat IEC-6 cells (Zuckerbraun *et al.*, 2005). With regard to the mechanism of its protective effect, none of the studies have investigated the involvement of sGC and only the study by Megias *et al.*, (2007) examined a possible contribution of p38 MAPK. In fact, CORM-2 treatment reduced the cytokine-induced increase in phosphorylation of MAPK p38, similar to its effect on ERK 1/2 and JNK 1/2 phosphorylation. This is in contrast with many *in vivo* studies on acute GI inflammation reporting that CO further enhances inflammation-induced p38 MAPK phosphorylation (see Tables I.2 and I.3). CO treatment reduced the cytokine-induced expression of iNOS at the mRNA or protein level, correlating with suppression of nitrite production (Dijkstra *et al.*, 2004; Zuckerbraun *et al.*, 2005; Megias *et al.*, 2007). No evidence for a selective effect of CO on iNOS activity as previously reported (Sawle *et al.*, 2005) has been obtained. In a study with rat IEC-6 cells, CO also inhibited LPS- and/or hypoxia (1% O_2)-induced increase in iNOS protein expression which was corroborated by the decrease in the transcriptional activation of the iNOS promoter (Zuckerbraun *et al.*, 2005). The effect of CO on iNOS in IECs might be related to its upstream influence on transcription factors involved in inflammation-induced iNOS expression. CORM-2 reduced the transcriptional activation of NF-κB triggered by a cytokine mixture with reduction of the increased expression of IL-8 in Caco-2 cells (Megias *et al.*, 2007). CORM-2 also inhibited gene expression and protein production of keratinocyte chemoattractant (KC), a functionally related homologue of IL-8 in humans, along with inhibition of NF-κB transcriptional

Table I.4   Effects of CO on IEC lines.

Cell type	Inflammatory trigger	CO source	Effect of inflammatory markers/overall outcome	Reference
Human colonic epithelial cell line, DLD-1	CM*	250–400 ppm CO	↓ iNOS mRNA expression	Dijkstra *et al.*, 2004
Rat small intestinal epithelial cell line, IEC-6	CM	250 ppm CO	↓ iNOS protein expression ↓ nitrite production	Zuckerbraun *et al.*, 2005
	TNF-α plus actinomycin-D	250 ppm CO	↓ cell death (apoptosis)	
	LPS/hypoxia	250 ppm CO	↓ cell death ↓ iNOS protein expression ↓ transcriptional activation of iNOS promoter	
Human colonic epithelial cell line, HT-29	TNF-α	CORM-2 (5-20 µM)	↓ IL-8 mRNA expression ↓ ICAM-1 and COX-2 protein expression	Lee *et al.*, 2007
Human colonic epithelial cell line, Caco-2	CM	CORM-2 (50-150 µM)	↓ nitrite production ↓ iNOS mRNA expression ↓ IL-8 protein expression ↓ transcriptional activation of NF-kB ↓ IκBα phosphorylation ↓ MAPK (p38, ERK 1/2 and JNK 1/2) phosphorylation	Megias *et al.*, 2007
Young adult mouse colonic epithelial cell line, YAMC	No trigger**	CORM-2 (1-10 µM)	↑ wound repair of cell monolayer	Uchiyama *et al.*, 2010
Young adult mouse colonic epithelial cell line, YAMC	TNF-α	CORM-2 (10 µM)	↓ KC mRNA expression ↓ KC production ↓ NF-kB activity	Takagi *et al.*, 2011

* CM: cytokine mixture (combination of TNF-α, IL-1β and IFN-γ)
** No inflammatory trigger is used; central manual scraping of monolayer creating a wound

activation in TNF-α stimulated young adult mouse colonic epithelial cells (Takagi *et al.*, 2011). CORM-2 also showed beneficial effect on IEC restitution (Uchiyama *et al.*, 2010).

The anti-inflammatory effects of CO/CO-RMs required HO-1 induction in other isolated cell systems such as hepatocytes (Zuckerbraun *et al.*, 2003), macrophages (Sawle *et al.*, 2005), microglia (Min *et al.*, 2006) and endothelial cells (Kim *et al.*, 2007); however, treatment with CO-RMs does not influence HO-1 protein expression in human Caco-2 cells (Megias *et al.*, 2007) and thus no evidence for a positive feedback loop CO/HO-1/CO was obtained.

In another human colonic epithelial cell line, HT-29, bilirubin *per se* had a similar inhibitory effect as CORM-2 on TNF-α-induced IL-8, ICAM-1 and COX-2 expression, and the effect was additive when CORM and bilirubin were incubated together suggesting that pharmacological induction of HO-1 might lead to more pronounced beneficial effects than exogenous CO (Lee *et al.*, 2007). However, the HO-1 inducer cobalt protoporphyrin decreased TNF-α plus actinomycin D-induced apoptotic cell death of IEC-6 cells only to the same extent as exogenous CO gas (Zuckerbraun *et al.*, 2005).

All studies in IEC lines thus support that CO can reduce acute mucosal inflammation and damage, and even stimulate IEC restitution.

I.4.2   Resveratrol in IEC lines

The publications on the protective effect of resveratrol in IEC lines are summarized in Table I.5. The first study investigating the effect of resveratrol in human HT-29 cells showed that resveratrol tested at the concentrations of 25-50 μM promoted NF-κB activity induced by LPS challenge (Jeong *et al.*, 2004). Subsequently, resveratrol at 50 μM concentration was reported to increase NF-κB activity in Caco-2 cells treated with different inflammatory agents like LPS, IL-1β or TNF-α; moreover, resveratrol also increased IL-8 production after IL-1β stimulation in the same cell system (Romier *et al.*, 2008). These results together suggest that resveratrol promoted NF-κB activation after inflammatory stimuli in human colonic epithelial cells; however, this is in sharp contrast to the inhibition of NF-κB activity observed with resveratrol in non-intestinal cell types like human monocytes (THP-1), macrophages (U-937), lymphoid (Jurkat), hepatic (HeLa) and glioma (H4) cells (Holmes-McNary & Baldwin, 2000; Manna *et al.*, 2000a; Csiszar *et al.*, 2006). Based on their findings with three inflammatory stimuli, Romier *et al.*, speculated that the permanent exposure of the intestinal cells to high levels of resveratrol for decades might have modified their genetic print, compared with cells present in blood and other organs that are exposed only to small levels of resveratrol (Romier *et al.*, 2008). However, the exact mechanisms for the ability of resveratrol to activate NF-κB in intestinal cells are still not clear.

Resveratrol decreased the LPS-induced increase in iNOS gene and protein expression, nitrite production, and IκBα phosphorylation in Caco-2 and SW480 cell lines (Panaro *et al.*, 2012). In the same study, resveratrol also decreased the protein expression of TLR4; this is

Table I.5   Effects of resveratrol on IEC lines.

Cell type	Inflammatory trigger	Concentration of resveratrol	Effect of inflammatory markers/overall outcome	Reference
Human colonic epithelial cell line, HT-29	LPS	25–50 µM	↑ NF-κB activity	Jeong *et al.*, 2004
Human colonic epithelial cell line, Caco-2	LPS, IL-1β or TNF-α	50 µM	↑ NF-κB activity	Romier *et al.*, 2008
	IL-1β		↑ IL-8 production	
Human colonic epithelial cell lines, Caco-2 and SW480	LPS	30–50 µM	↓ iNOS mRNA and protein expression ↓ nitrite production ↓ IκBα phosphorylation ↓ TLR-4 protein expression	Panaro *et al.*, 2012
Human colonic epithelial cell line grown in three dimensional culture system, Caco-2 spheroids	FAEEs	10 µM	↓ ROS production ↓ epithelial permeability ↑ ZO-1 and occludin protein levels	Elamin *et al.*, 2013
Human colonic epithelial cell line, HT-29	CM*	25 µM	↓ iNOS mRNA and protein expression ↓ nitrite production ↓ PGE$_2$ production ↓ COX-2 mRNA and protein expression ↓ ROS production	Serra *et al.*, 2014

* CM: cytokine mixture (combination of TNF-α, IL-1α and IFN-γ)

the best studied member of TLR family, which is involved in the recognition of endotoxins or bacterial LPS (Triantafilou & Triantafilou, 2005).

Ingested ethanol can be non-oxidatively metabolized in humans resulting in the formation of fatty acid ethyl esters (FAEEs) like ethyl oleate and ethyl palmitate. FAEEs might induce intestinal barrier dysfunction. Indeed, they increased epithelial permeability and ROS production, accompanied by decrease in zona occludens-1 (ZO-1) and occludin tight junction protein levels, in a three-dimensional epithelial cell culture model of Caco-2 cells (Caco-2 spheroids). Resveratrol partially attenuated all these effects; this was attributed to its antioxidant effect (Elamin *et al.*, 2013). In HT-29 cells, resveratrol reduced nitrite and PGE$_2$ production, gene and protein expression of iNOS and COX-2, and ROS production induced by a cytokine mix challenge (Serra *et al.*, 2014).

All these studies suggest that resveratrol can reduce mucosal inflammation and such protect the gut from mucosal damage and epithelial barrier dysfunction.

I.5   References

Abraham NG & Kappas A (2008). Pharmacological and clinical aspects of heme oxygenase. *Pharmacological Reviews* **60**, 79-127.

Agarwal A & Bolisetty S (2013). Adaptive responses to tissue injury: role of heme oxygenase-1. *Trans Am Clin Climatol Assoc* **124**, 111-122.

Ahmad A, Farhan Asad S, Singh S, Hadi SM (2000). DNA breakage by resveratrol and Cu(II): reaction mechanism and bacteriophage inactivation. *Cancer Lett* **154**, 29-37.

Ahuja I, Kissen R, Bones AM (2012). Phytoalexins in defense against pathogens. *Trends Plant Sci* **17**, 73-90.

Akamatsu Y, Haga M, Tyagi S, Yamashita K, Graca-Souza AV, Ollinger R *et al.* (2004). Heme oxygenase-1-derived carbon monoxide protects hearts from transplant associated ischemia reperfusion injury. *Faseb Journal* **18**, 771-772.

Alfaras I, Juan ME, Planas JM (2010). trans-Resveratrol reduces precancerous colonic lesions in dimethylhydrazine-treated rats. *J Agric Food Chem* **58**, 8104-8110.

Anderson RC, Dalziel JE, Gopal PK, Bassett S, Ellis A, Roy NC (2012). The Role of Intestinal Barrier Function in Early Life in the Development of Colitis.

Andre L, Boissiere J, Reboul C, Perrier R, Zalvidea S, Meyer G *et al.* (2010). Carbon monoxide pollution promotes cardiac remodeling and ventricular arrhythmia in healthy rats. *Am J Respir Crit Care Med* **181**, 587-595.

Anup R, Aparna V, Pulimood A, Balasubramanian KA (1999). Surgical stress and the small intestine: role of oxygen free radicals. *Surgery* **125**, 560-569.

Araujo F & Sarmento B (2013). Towards the characterization of an in vitro triple co-culture intestine cell model for permeability studies. *Int J Pharm* **458**, 128-134.

Arosio P, Ingrassia R, Cavadini P (2009). Ferritins: A family of molecules for iron storage, antioxidation and more. *Biochimica Et Biophysica Acta-General Subjects* **1790**, 589-599.

Asensi M, Medina I, Ortega A, Carretero J, Bano MC, Obrador E *et al.* (2002). Inhibition of cancer growth by resveratrol is related to its low bioavailability. *Free Radic Biol Med* **33**, 387-398.

Asgeirsson T, El-Badawi KI, Mahmood A, Barletta J, Luchtefeld M, Senagore AJ (2010). Postoperative Ileus: It Costs More Than You Expect. *Journal of the American College of Surgeons* **210**, 228-231.

Asquith M & Powrie F (2010). An innately dangerous balancing act: intestinal homeostasis, inflammation, and colitis-associated cancer. *J Exp Med* **207**, 1573-1577.

Attuwaybi BO, Kozar RA, Moore-Olufemi SD, Sato N, Hassoun HT, Weisbrodt NW *et al.* (2004). Heme oxygenase-1 induction by hemin protects against gut ischemia/reperfusion injury. *J Surg Res* **118**, 53-57.

Azad MB, Chen Y, Gibson SB (2009). Regulation of autophagy by reactive oxygen species (ROS): implications for cancer progression and treatment. *Antioxid Redox Signal* **11**, 777-790.

Babich H, Schuck AG, Weisburg JH, Zuckerbraun HL (2011). Research strategies in the study of the pro-oxidant nature of polyphenol nutraceuticals. *J Toxicol* **2011**, 467305.

Babior BM (2000). Phagocytes and oxidative stress. *Am J Med* **109**, 33-44.

Babior BM, Kipnes RS, Curnutte JT (1973). Biological defense mechanisms. The production by leukocytes of superoxide, a potential bactericidal agent. *J Clin Invest* **52**, 741-744.

Balk RA (2004). Optimum treatment of severe sepsis and septic shock: evidence in support of the recommendations. *Dis Mon* **50**, 168-213.

Balzan S, de Almeida Quadros C, de Cleva R, Zilberstein B, Cecconello I (2007). Bacterial translocation: overview of mechanisms and clinical impact. *J Gastroenterol Hepatol* **22**, 464-471.

Barton SG, Rampton DS, Winrow VR, Domizio P, Feakins RM (2003). Expression of heat shock protein 32 (hemoxygenase-1) in the normal and inflamed human stomach and colon: an immunohistochemical study. *Cell Stress Chaperones* **8**, 329-334.

Bauer AJ & Boeckxstaens GE (2004). Mechanisms of postoperative ileus. *Neurogastroenterol Motil* **16 Suppl 2**, 54-60.

Bauer M, Huse K, Settmacher U, Claus RA (2008). The heme oxygenase-carbon monoxide system: regulation and role in stress response and organ failure. *Intensive Care Med* **34**, 640-648.

Baur JA, Pearson KJ, Price NL, Jamieson HA, Lerin C, Kalra A *et al.* (2006). Resveratrol improves health and survival of mice on a high-calorie diet. *Nature* **444**, 337-342.

Bedard K & Krause KH (2007). The NOX family of ROS-generating NADPH oxidases: physiology and pathophysiology. *Physiol Rev* **87**, 245-313.

Behm B & Stollman N (2003). Postoperative ileus: etiologies and interventions. *Clin Gastroenterol Hepatol* **1**, 71-80.

Belguendouz L, Fremont L, Linard A (1997). Resveratrol inhibits metal ion-dependent and independent peroxidation of porcine low-density lipoproteins. *Biochem Pharmacol* **53**, 1347-1355.

Bens M, Bogdanova A, Cluzeaud F, Miquerol L, Kerneis S, Kraehenbuhl JP *et al.* (1996). Transimmortalized mouse intestinal cells (m-ICc12) that maintain a crypt phenotype. *Am J Physiol* **270**, C1666-1674.

Berberat PO, A-Rahim YI, Yamashita K, Warny MM, Csizmadia E, Robson SC *et al.* (2005). Heme oxygenase-1-generated biliverdin ameliorates experimental murine colitis. *Inflamm Bowel Dis* **11**, 350-359.

Berberat PO, Katori M, Kaczmarek E, Anselmo D, Lassman C, Ke B *et al.* (2003). Heavy chain ferritin acts as an anti-apoptotic gene that protects livers from ischemia-reperfusion injury. *Faseb Journal* **17**, 1724-+.

Bertelli AA, Baccalini R, Battaglia E, Falchi M, Ferrero ME (2001). Resveratrol inhibits TNF alpha-induced endothelial cell activation. *Therapie* **56**, 613-616.

Beyaert R, Vanhaesebroeck B, Heyninck K, Boone E, De Valck D, Schulze-Osthoff K *et al.* (1993). Sensitization of tumor cells to tumor necrosis factor action by the protein kinase inhibitor staurosporine. *Cancer Res* **53**, 2623-2630.

Bilban M, Haschemi A, Wegiel B, Chin BY, Wagner O, Otterbein LE (2008). Heme oxygenase and carbon monoxide initiate homeostatic signaling. *J Mol Med (Berl)* **86**, 267-279.

Boczkowski J, Poderoso JJ, Motterlini R (2006). CO-metal interaction: Vital signaling from a lethal gas. *Trends Biochem Sci* **31**, 614-621.

Boeckxstaens GE & de Jonge WJ (2009). Neuroimmune mechanisms in postoperative ileus. *Gut* **58**, 1300-1311.

Boocock DJ, Faust GE, Patel KR, Schinas AM, Brown VA, Ducharme MP *et al.* (2007). Phase I dose escalation pharmacokinetic study in healthy volunteers of resveratrol, a potential cancer chemopreventive agent. *Cancer Epidemiol Biomarkers Prev* **16**, 1246-1252.

Boron & Boulpaep (2009). Medical Physiology (Second Edition). *The gastrointestinal system*: 881-1006.

Borras C, Gambini J, Gomez-Cabrera MC, Sastre J, Pallardo FV, Mann GE *et al.* (2005). 17beta-oestradiol up-regulates longevity-related, antioxidant enzyme expression via the ERK1 and ERK2[MAPK]/NFkappaB cascade. *Aging Cell* **4**, 113-118.

Bowers JL, Tyulmenkov VV, Jernigan SC, Klinge CM (2000). Resveratrol acts as a mixed agonist/antagonist for estrogen receptors alpha and beta. *Endocrinology* **141**, 3657-3667.

Brand MD (2010). The sites and topology of mitochondrial superoxide production. *Exp Gerontol* **45**, 466-472.

Brinton RD (2008). Estrogen regulation of glucose metabolism and mitochondrial function: Therapeutic implications for prevention of Alzheimer's disease. *Advanced Drug Delivery Reviews* **60**, 1504-1511.

Brune M, Rossander L, Hallberg L (1989). Iron-Absorption and Phenolic-Compounds - Importance of Different Phenolic Structures. *European Journal of Clinical Nutrition* **43**, 547-558.

Bullen TF, Forrest S, Campbell F, Dodson AR, Hershman MJ, Pritchard DM *et al.* (2006). Characterization of epithelial cell shedding from human small intestine. *Lab Invest* **86**, 1052-1063.

Cannizzo ES, Clement CC, Sahu R, Follo C, Santambrogio L (2011). Oxidative stress, inflamm-aging and immunosenescence. *Journal of Proteomics* **74**, 2313-2323.

Cepinskas G, Katada K, Bihari A, Potter RF (2008). Carbon monoxide liberated from carbon monoxide-releasing molecule CORM-2 attenuates inflammation in the liver of septic mice. *Am J Physiol Gastrointest Liver Physiol* **294**, G184-191.

Ceppa EP, Fuh KC, Bulkley GB (2003). Mesenteric hemodynamic response to circulatory shock. *Curr Opin Crit Care* **9**, 127-132.

Ceran C, Sonmez K, Turkyilmaz Z, Demirogullari B, Dursun A, Duzgun E *et al.* (2001). Effect of bilirubin in ischemia/reperfusion injury on rat small intestine. *J Pediatr Surg* **36**, 1764-1767.

Cheeseman KH & Slater TF (1993). An introduction to free radical biochemistry. *Br Med Bull* **49**, 481-493.

Chen CY, Jang JH, Li MH, Surh YJ (2005). Resveratrol upregulates heme oxygenase-1 expression via activation of NF-E2-related factor 2 in PC12 cells. *Biochem Biophys Res Commun* **331**, 993-1000.

Chen YR, Chen CL, Pfeiffer DR, Zweier JL (2007). Mitochondrial complex II in the post-ischemic heart: oxidative injury and the role of protein S-glutathionylation. *J Biol Chem* **282**, 32640-32654.

Chow SE, Hshu YC, Wang JS, Chen JK (2007). Resveratrol attenuates oxLDL-stimulated NADPH oxidase activity and protects endothelial cells from oxidative functional damages. *J Appl Physiol (1985)* **102**, 1520-1527.

Chung S, Yao H, Caito S, Hwang JW, Arunachalam G, Rahman I (2010). Regulation of SIRT1 in cellular functions: role of polyphenols. *Arch Biochem Biophys* **501**, 79-90.

Chung SW, Liu X, Macias AA, Baron RM, Perrella MA (2008). Heme oxygenase-1-derived carbon monoxide enhances the host defense response to microbial sepsis in mice. *J Clin Invest* **118**, 239-247.

Cinel I & Opal SM (2009). Molecular biology of inflammation and sepsis: a primer. *Crit Care Med* **37**, 291-304.

Clark JA & Coopersmith CM (2007). Intestinal crosstalk: a new paradigm for understanding the gut as the "motor" of critical illness. *Shock* **28**, 384-393.

Clark JE, Foresti R, Sarathchandra P, Kaur H, Green CJ, Motterlini R (2000). Heme oxygenase-1-derived bilirubin ameliorates postischemic myocardial dysfunction. *American Journal of Physiology-Heart and Circulatory Physiology* **278**, H643-H651.

Clark JE, Naughton P, Shurey S, Green CJ, Johnson TR, Mann BE *et al.* (2003). Cardioprotective actions by a water-soluble carbon monoxide-releasing molecule. *Circulation Research* **93**, e2-8.

Coeffier M, Le Pessot F, Leplingard A, Marion R, Lerebours E, Ducrotte P *et al.* (2002). Acute enteral glutamine infusion enhances heme oxygenase-1 expression in human duodenal mucosa. *J Nutr* **132**, 2570-2573.

Collard CD & Gelman S (2001). Pathophysiology, clinical manifestations, and prevention of ischemia-reperfusion injury. *Anesthesiology* **94**, 1133-1138.

Colpaert EE, Timmermans JP, Lefebvre RA (2002). Immunohistochemical localization of the antioxidant enzymes biliverdin reductase and heme oxygenase-2 in human and pig gastric fundus. *Free Radic Biol Med* **32**, 630-637.

Coopersmith CM, Chang KC, Swanson PE, Tinsley KW, Stromberg PE, Buchman TG *et al.* (2002a). Overexpression of Bcl-2 in the intestinal epithelium improves survival in septic mice. *Crit Care Med* **30**, 195-201.

Coopersmith CM, Stromberg PE, Dunne WM, Davis CG, Amiot DM, 2nd, Buchman TG *et al.* (2002b). Inhibition of intestinal epithelial apoptosis and survival in a murine model of pneumonia-induced sepsis. *JAMA* **287**, 1716-1721.

Copple IM (2012). The Keap1-Nrf2 cell defense pathway--a promising therapeutic target? *Adv Pharmacol* **63**, 43-79.

Coskun M (2014). Intestinal epithelium in inflammatory bowel disease. *Front Med (Lausanne)* **1**, 24.

Csaki C, Mobasheri A, Shakibaei M (2009). Synergistic chondroprotective effects of curcumin and resveratrol in human articular chondrocytes: inhibition of IL-1beta-induced NF-kappaB-mediated inflammation and apoptosis. *Arthritis Res Ther* **11**, R165.

Csiszar A, Labinskyy N, Pinto JT, Ballabh P, Zhang H, Losonczy G *et al.* (2009). Resveratrol induces mitochondrial biogenesis in endothelial cells. *Am J Physiol Heart Circ Physiol* **297**, H13-20.

Csiszar A, Smith K, Labinskyy N, Orosz Z, Rivera A, Ungvari Z (2006). Resveratrol attenuates TNF-alpha-induced activation of coronary arterial endothelial cells: role of NF-kappaB inhibition. *Am J Physiol Heart Circ Physiol* **291**, H1694-1699.

Cuzzocrea S, Chatterjee PK, Mazzon E, Dugo L, De Sarro A, Van de Loo FA *et al.* (2002). Role of induced nitric oxide in the initiation of the inflammatory response after postischemic injury. *Shock* **18**, 169-176.

Dagenais M, Douglas T, Saleh M (2014). Role of programmed necrosis and cell death in intestinal inflammation. *Curr Opin Gastroenterol* **30**, 566-575.

Daiber A (2010). Redox signaling (cross-talk) from and to mitochondria involves mitochondrial pores and reactive oxygen species. *Biochim Biophys Acta* **1797**, 897-906.

Dal-Secco D, Freitas A, Abreu MA, Garlet TP, Rossi MA, Ferreira SH *et al.* (2010). Reduction of ICAM-1 expression by carbon monoxide via soluble guanylate cyclase activation accounts for modulation of neutrophil migration. *Naunyn Schmiedebergs Arch Pharmacol* **381**, 483-493.

Daniels R (2011). Surviving the first hours in sepsis: getting the basics right (an intensivist's perspective). *Journal of Antimicrobial Chemotherapy* **66**, Ii11-Ii23.

De Backer O, Elinck E, Blanckaert B, Leybaert L, Motterlini R, Lefebvre RA (2009). Water-soluble CO-releasing molecules reduce the development of postoperative ileus via modulation of MAPK/HO-1 signalling and reduction of oxidative stress. *Gut* **58**, 347-356.

de Haan JJ, Lubbers T, Derikx JP, Relja B, Henrich D, Greve JW *et al.* (2009). Rapid development of intestinal cell damage following severe trauma: a prospective observational cohort study. *Crit Care* **13**, R86.

de Vries HS, te Morsche RHM, Jenniskens K, Peters WHM, de Jong DJ (2012). A functional polymorphism in UGT1A1 related to hyperbilirubinemia is associated with a decreased risk for Crohn's disease. *Journal of Crohns & Colitis* **6**, 597-602.

De Winter BY & De Man JG (2010). Interplay between inflammation, immune system and neuronal pathways: Effect on gastrointestinal motility. *World Journal of Gastroenterology* **16**, 5523-5535.

Deitch EA (2002). Bacterial translocation or lymphatic drainage of toxic products from the gut: what is important in human beings? *Surgery* **131**, 241-244.

Deshane J, Wright M, Agarwal A (2005). Heme oxygenase-1 expression in disease states. *Acta Biochim Pol* **52**, 273-284.

Desmard M, Foresti R, Morin D, Dagouassat M, Berdeaux A, Denamur E *et al.* (2012). Differential antibacterial activity against Pseudomonas aeruginosa by carbon monoxide-releasing molecules. *Antioxid Redox Signal* **16**, 153-163.

Dijkstra G, Blokzijl H, Bok L, Homan M, van Goor H, Faber KN *et al.* (2004). Opposite effect of oxidative stress on inducible nitric oxide synthase and haem oxygenase-1 expression in intestinal inflammation: anti-inflammatory effect of carbon monoxide. *J Pathol* **204**, 296-303.

Dikalov S (2011). Cross talk between mitochondria and NADPH oxidases. *Free Radical Biology and Medicine* **51**, 1289-1301.

Dikalov S, Bikineyeva A, Budzyn K, Nazarewicz R, Lewis W, Harrison DG *et al.* (2010). Therapeutic targeting of mitochondrial superoxide in hypertension. *Faseb Journal* **24**.

Dioum EM, Rutter J, Tuckerman JR, Gonzalez G, Gilles-Gonzalez MA, McKnight SL (2002). NPAS2: a gas-responsive transcription factor. *Science* **298**, 2385-2387.

Doorly MG & Senagore AJ (2012). Pathogenesis and clinical and economic consequences of postoperative ileus. *Surg Clin North Am* **92**, 259-272, viii.

Doughan AK, Harrison DG, Dikalov SI (2008). Molecular mechanisms of angiotensin II-mediated mitochondrial dysfunction - Linking mitochondrial oxidative damage and vascular endothelial dysfunction. *Circulation Research* **102**, 488-496.

Drose S (2013). Differential effects of complex II on mitochondrial ROS production and their relation to cardioprotective pre- and postconditioning. *Biochim Biophys Acta* **1827**, 578-587.

Elamin E, Masclee A, Juuti-Uusitalo K, van Ijzendoorn S, Troost F, Pieters HJ *et al.* (2013). Fatty acid ethyl esters induce intestinal epithelial barrier dysfunction via a reactive oxygen species-dependent mechanism in a three-dimensional cell culture model. *Plos One* **8**, e58561.

Elewaut D, DiDonato JA, Kim JM, Truong F, Eckmann L, Kagnoff MF (1999). NF-kappa B is a central regulator of the intestinal epithelial cell innate immune response induced by infection with enteroinvasive bacteria. *J Immunol* **163**, 1457-1466.

Eskandari MK, Kalff JC, Billiar TR, Lee KKW, Bauer AJ (1997). Lipopolysaccharide activates the muscularis macrophage network and suppresses circular smooth muscle activity. *American Journal of Physiology-Gastrointestinal and Liver Physiology* **273**, G727-G734.

Estabrook RW, Franklin MR, Hildebrandt AG (1970). Factors influencing the inhibitory effect of carbon monoxide on cytochrome P-450-catalyzed mixed function oxidation reactions. *Ann N Y Acad Sci* **174**, 218-232.

Faulds MH, Zhao C, Dahlman-Wright K, Gustafsson JA (2012). The diversity of sex steroid action: regulation of metabolism by estrogen signaling. *J Endocrinol* **212**, 3-12.

Fink MP & Delude RL (2005). Epithelial barrier dysfunction: a unifying theme to explain the pathogenesis of multiple organ dysfunction at the cellular level. *Crit Care Clin* **21**, 177-196.

Fiocchi C (2003). The normal intestinal mucosa: a state of "controlled inflammation." In: TarganSR, ShanahanF, eds. *Inflammatory Bowel Disease From Bench to Bedside*. 2nd ed. Dordrecht: Kluwer Academic, 101-120.

Flessas, II, Papalois AE, Toutouzas K, Zagouri F, Zografos GC (2011). Effects of lazaroids on intestinal ischemia and reperfusion injury in experimental models. *J Surg Res* **166**, 265-274.

Foresti R, Bani-Hani MG, Motterlini R (2008). Use of carbon monoxide as a therapeutic agent: promises and challenges. *Intensive Care Med* **34**, 649-658.

Foresti R & Motterlini R (2010). Interaction of carbon monoxide with transition metals: evolutionary insights into drug target discovery. *Curr Drug Targets* **11**, 1595-1604.

Foresti R & Motterlini R (2013). CO-releasing molecules: avoiding toxicity and exploiting the beneficial effects of CO for the treatment of cardiovascular disorders. *Future Medicinal Chemistry* **5**, 367-369.

Forman HJ, Maiorino M, Ursini F (2010). Signaling functions of reactive oxygen species. *Biochemistry* **49**, 835-842.

Frankel EN, Waterhouse AL, Kinsella JE (1993). Inhibition of Human Ldl Oxidation by Resveratrol. *Lancet* **341**, 1103-1104.

Freitas A, Alves-Filho JC, Secco DD, Neto AF, Ferreira SH, Barja-Fidalgo C *et al.* (2006). Heme oxygenase/carbon monoxide-biliverdin pathway down regulates neutrophil rolling, adhesion and migration in acute inflammation. *Br J Pharmacol* **149**, 345-354.

Freitas M, Lima JLFC, Fernandes E (2009). Optical probes for detection and quantification of neutrophils' oxidative burst. A review. *Analytica Chimica Acta* **649**, 8-23.

Fukui M, Choi HJ, Zhu BT (2010). Mechanism for the protective effect of resveratrol against oxidative stress-induced neuronal death. *Free Radic Biol Med* **49**, 800-813.

Gacar N, Gocmez S, Utkan T, Gacar G, Komsuoglu I, Tugay M *et al.* (2012). Effects of Resveratrol on Ileal Smooth Muscle Reactivity in Polymicrobial Sepsis Model. *Journal of Surgical Research* **174**, 339-343.

Gan X, Su G, Zhao W, Huang P, Luo G, Hei Z (2013). The mechanism of sevoflurane preconditioning-induced protections against small intestinal ischemia reperfusion injury is independent of mast cell in rats. *Mediators Inflamm* **2013**, 378703.

Garrett WS, Gordon JI, Glimcher LH (2010). Homeostasis and inflammation in the intestine. *Cell* **140**, 859-870.

Gehm BD, McAndrews JM, Chien PY, Jameson JL (1997). Resveratrol, a polyphenolic compound found in grapes and wine, is an agonist for the estrogen receptor. *Proceedings of the National Academy of Sciences of the United States of America* **94**, 14138-14143.

Giris M, Erbil Y, Dogru-Abbasoglu S, Yanik BT, Ahs H, Olgac V *et al.* (2007). The effect of heme oxygenase-1 induction by glutamine on TNBS-induced colitis - The effect of glutamine on TNBS colitis. *International Journal of Colorectal Disease* **22**, 591-599.

Giris M, Erbil Y, Oztezcan S, Olgac V, Barbaros U, Deveci U *et al.* (2006). The effect of heme oxygenase-1 induction by glutamine on radiation-induced intestinal damage: the effect of heme oxygenase-1 on radiation enteritis. *American Journal of Surgery* **191**, 503-509.

Gokce EH, Korkmaz E, Dellera E, Sandri G, Bonferoni MC, Ozer O (2012). Resveratrol-loaded solid lipid nanoparticles versus nanostructured lipid carriers: evaluation of antioxidant potential for dermal applications. *Int J Nanomedicine* **7**, 1841-1850.

Goldberg DM, Ng E, Karumanchiri A, Yan J, Diamandis EP, Soleas GJ (1995). Assay of Resveratrol Glucosides and Isomers in Wine by Direct-Injection High-Performance Liquid-Chromatography. *Journal of Chromatography A* **708**, 89-98.

Goldberg DM, Yan J, Soleas GJ (2003). Absorption of three wine-related polyphenols in three different matrices by healthy subjects. *Clinical Biochemistry* **36**, 79-87.

Gonzalez LM, Moeser AJ, Blikslager AT (2015). Animal models of ischemia-reperfusion-induced intestinal injury: progress and promise for translational research. *Am J Physiol Gastrointest Liver Physiol* **308**, G63-75.

Granger DN, Zimmerman BJ, Sekizuka E, Grisham MB (1988). Intestinal Microvascular Exchange in the Rat during Luminal Perfusion with Formyl-Methionyl-Leucyl-Phenylalanine. *Gastroenterology* **94**, 673-681.

Green RS & Gorman SK (2014). Emergency department antimicrobial considerations in severe sepsis. *Emerg Med Clin North Am* **32**, 835-849.

Grisham MB, Hernandez LA, Granger DN (1986). Xanthine oxidase and neutrophil infiltration in intestinal ischemia. *Am J Physiol* **251**, G567-574.

Grootjans J, Lenaerts K, Derikx JP, Matthijsen RA, de Bruine AP, van Bijnen AA *et al.* (2010). Human intestinal ischemia-reperfusion-induced inflammation characterized: experiences from a new translational model. *Am J Pathol* **176**, 2283-2291.

Grossmann J, Walther K, Artinger M, Rummele P, Woenckhaus M, Scholmerich J (2002). Induction of apoptosis before shedding of human intestinal epithelial cells. *American Journal of Gastroenterology* **97**, 1421-1428.

Grozdanovic Z & Gossrau R (1996). Expression of heme oxygenase-2 (HO-2)-like immunoreactivity in rat tissues. *Acta Histochem* **98**, 203-214.

Hall PA, Coates PJ, Ansari B, Hopwood D (1994). Regulation of cell number in the mammalian gastrointestinal tract: the importance of apoptosis. *J Cell Sci* **107 (Pt 12)**, 3569-3577.

Halliwell B (2008). Are polyphenols antioxidants or pro-oxidants? What do we learn from cell culture and in vivo studies? *Arch Biochem Biophys* **476**, 107-112.

Hammerman C, Goldschmidt D, Caplan MS, Kaplan M, Bromiker R, Eidelman AI *et al.* (2002). Protective effect of bilirubin in ischemia-reperfusion injury in the rat intestine. *J Pediatr Gastroenterol Nutr* **35**, 344-349.

Hampton MB, Kettle AJ, Winterbourn CC (1998). Inside the neutrophil phagosome: oxidants, myeloperoxidase, and bacterial killing. *Blood* **92**, 3007-3017.

Hassoun HT, Kone BC, Mercer DW, Moody FG, Weisbrodt NW, Moore FA (2001). Post-injury multiple organ failure: the role of the gut. *Shock* **15**, 1-10.

Hayashi S, Omata Y, Sakamoto H, Higashimoto Y, Hara T, Sagara Y *et al.* (2004). Characterization of rat heme oxygenase-3 gene. Implication of processed pseudogenes derived from heme oxygenase-2 gene. *Gene* **336**, 241-250.

He S & Yan X (2013). From resveratrol to its derivatives: new sources of natural antioxidant. *Current Medicinal Chemistry* **20**, 1005-1017.

Henson PM & Bratton DL (2013). Antiinflammatory effects of apoptotic cells. *J Clin Invest* **123**, 2773-2774.

Hoetzel A, Dolinay T, Schmidt R, Choi AM, Ryter SW (2007). Carbon monoxide in sepsis. *Antioxid Redox Signal* **9**, 2013-2026.

Holmes-McNary M & Baldwin AS, Jr. (2000). Chemopreventive properties of trans-resveratrol are associated with inhibition of activation of the IkappaB kinase. *Cancer Res* **60**, 3477-3483.

Holthoff JH, Woodling KA, Doerge DR, Burns ST, Hinson JA, Mayeux PR (2010). Resveratrol, a dietary polyphenolic phytoalexin, is a functional scavenger of peroxynitrite. *Biochem Pharmacol* **80**, 1260-1265.

Holtmann MH, Schutz M, Galle PR, Neurath MF (2002). Functional relevance of soluble TNF-alpha, transmembrane TNF-alpha and TNF-signal transduction in gastrointestinal diseases with special reference to inflammatory bowel diseases. *Z Gastroenterol* **40**, 587-600.

Howitz KT, Bitterman KJ, Cohen HY, Lamming DW, Lavu S, Wood JG *et al.* (2003). Small molecule activators of sirtuins extend Saccharomyces cerevisiae lifespan. *Nature* **425**, 191-196.

Ikeda H, Suzuki Y, Suzuki M, Koike M, Tamura J, Tong J *et al.* (1998). Apoptosis is a major mode of cell death caused by ischaemia and ischaemia/reperfusion injury to the rat intestinal epithelium. *Gut* **42**, 530-537.

Jeong WS, Kim IW, Hu R, Kong ANT (2004). Modulatory properties of various natural chemopreventive agents on the activation of NF-kappa B signaling pathway. *Pharm Res* **21**, 661-670.

Jones BE, Lo CR, Liu H, Srinivasan A, Streetz K, Valentino KL *et al.* (2000). Hepatocytes sensitized to tumor necrosis factor-alpha cytotoxicity undergo apoptosis through caspase-dependent and caspase-independent pathways. *J Biol Chem* **275**, 705-712.

Kairisalo M, Bonomo A, Hyrskyluoto A, Mudo G, Belluardo N, Korhonen L *et al.* (2011). Resveratrol reduces oxidative stress and cell death and increases mitochondrial antioxidants and XIAP in PC6.3-cells. *Neurosci Lett* **488**, 263-266.

Kajino-Sakamoto R, Inagaki M, Lippert E, Akira SZ, Robine S, Matsumoto K *et al.* (2008). Enterocyte-derived TAK1 signaling prevents epithelium apoptosis and the development of ileitis and colitis. *J Immunol* **181**, 1143-1152.

Kalff JC, Buchholz BM, Eskandari MK, Hierholzer C, Schraut WH, Simmons RL *et al.* (1999). Biphasic response to gut manipulation and temporal correlation of cellular infiltrates and muscle dysfunction in rat. *Surgery* **126**, 498-509.

Karrasch T & Jobin C (2009). Wound healing responses at the gastrointestinal epithelium: a close look at novel regulatory factors and investigative approaches. *Z Gastroenterol* **47**, 1221-1229.

Kehlet H (2008). Fast-track colorectal surgery. *Lancet* **371**, 791-793.

Kim KM, Pae HO, Zheng M, Park R, Kim YM, Chung HT (2007). Carbon monoxide induces heme oxygenase-1 via activation of protein kinase R-like endoplasmic reticulum kinase and inhibits endothelial cell apoptosis triggered by endoplasmic reticulum stress. *Circulation Research* **101**, 919-927.

Kimura S, Zhang GX, Nishiyama A, Shokoji T, Yao L, Fan YY *et al.* (2005). Role of NAD(P)H oxidase- and mitochondria-derived reactive oxygen species in cardioprotection of ischemic reperfusion injury by angiotensin II. *Hypertension* **45**, 860-866.

Klebanoff SJ (1967). Iodination of bacteria: a bactericidal mechanism. *J Exp Med* **126**, 1063-1078.

Klebanoff SJ & Rosen H (1978). Ethylene formation by polymorphonuclear leukocytes. Role of myeloperoxidase. *J Exp Med* **148**, 490-506.

Kohmoto J, Nakao A, Sugimoto R, Wang Y, Zhan J, Ueda H *et al.* (2008). Carbon monoxide-saturated preservation solution protects lung grafts from ischemia-reperfusion injury. *J Thorac Cardiovasc Surg* **136**, 1067-1075.

Kohmotoa J, Nakao A, Stolz DB, Kaizu T, Tsung A, Ikeda A *et al.* (2007). Carbon monoxide protects rat lung transplants from ischemia-reperfusion injury via a mechanism involving p38 MAPK pathway. *American Journal of Transplantation* **7**, 2279-2290.

Kolgazi M, Sener G, Cetinel S, Gedik N, Alican I (2006). Resveratrol reduces renal and lung injury caused by sepsis in rats. *J Surg Res* **134**, 315-321.

Korolkiewicz RP, Ujda M, Dabkowski J, Ruczynski J, Rekowski P, Petrusewicz J (2003). Differential salutary effects of nonselective and selective COX-2 inhibitors in postoperative ileus in rats. *J Surg Res* **109**, 161-169.

Koulouras VP, Li R, Chen L, Hedenstierna GG (2011). Effects of inhaled carbon monoxide and glucocorticoids in porcine endotoxin sepsis. *Int J Clin Exp Med* **4**, 53-66.

Kovacic P & Somanathan R (2010). Multifaceted approach to resveratrol bioactivity: Focus on antioxidant action, cell signaling and safety. *Oxidative Medicine and Cellular Longevity* **3**, 86-100.

Kudin AP, Malinska D, Kunz WS (2008). Sites of generation of reactive oxygen species in homogenates of brain tissue determined with the use of respiratory substrates and inhibitors. *Biochim Biophys Acta* **1777**, 689-695.

Lagouge M, Argmann C, Gerhart-Hines Z, Meziane H, Lerin C, Daussin F *et al.* (2006). Resveratrol improves mitochondrial function and protects against metabolic disease by activating SIRT1 and PGC-1alpha. *Cell* **127**, 1109-1122.

Lambeth JD (2004). NOX enzymes and the biology of reactive oxygen. *Nat Rev Immunol* **4**, 181-189.

Lancel S, Hassoun SM, Favory R, Decoster B, Motterlini R, Neviere R (2009). Carbon monoxide rescues mice from lethal sepsis by supporting mitochondrial energetic metabolism and activating mitochondrial biogenesis. *J Pharmacol Exp Ther* **329**, 641-648.

Larrosa M, Azorin-Ortuno M, Yanez-Gascon MJ, Garcia-Conesa MT, Tomas-Barberan F, Espin JC (2011). Lack of effect of oral administration of resveratrol in LPS-induced systemic inflammation. *Eur J Nutr* **50**, 673-680.

Lee S, Lee SJ, Coronata AA, Fredenburgh LE, Chung SW, Perrella MA *et al.* (2014). Carbon monoxide confers protection in sepsis by enhancing beclin 1-dependent autophagy and phagocytosis. *Antioxid Redox Signal* **20**, 432-442.

Lee SB, Bae IH, Bae YS, Um HD (2006). Link between mitochondria and NADPH oxidase 1 isozyme for the sustained production of reactive oxygen species and cell death. *Journal of Biological Chemistry* **281**, 36228-36235.

Lee SH, Sohn DH, Jin XY, Kim SW, Choi SC, Seo GS (2007). 2',4',6'-tris(methoxymethoxy) chalcone protects against trinitrobenzene sulfonic acid-induced colitis and blocks tumor necrosis factor-alpha-induced intestinal epithelial inflammation via heme oxygenase 1-dependent and independent pathways. *Biochem Pharmacol* **74**, 870-880.

Leedham SJ, Schier S, Thliveris AT, Halberg RB, Newton MA, Wright NA (2005). From gene mutations to tumours--stem cells in gastrointestinal carcinogenesis. *Cell Prolif* **38**, 387-405.

Leiro J, Alvarez E, Arranz JA, Laguna R, Uriarte E, Orallo F (2004). Effects of cis-resveratrol on inflammatory murine macrophages: antioxidant activity and down-regulation of inflammatory genes. *J Leukoc Biol* **75**, 1156-1165.

Lenicek M, Duricova D, Hradsky O, Dusatkova P, Jiraskova A, Lukas M *et al.* (2014). The Relationship Between Serum Bilirubin and Crohn's Disease. *Inflamm Bowel Dis* **20**, 481-487.

Leonard SS, Xia C, Jiang BH, Stinefelt B, Klandorf H, Harris GK *et al.* (2003). Resveratrol scavenges reactive oxygen species and effects radical-induced cellular responses. *Biochem Biophys Res Commun* **309**, 1017-1026.

Leser TD & Molbak L (2009). Better living through microbial action: the benefits of the mammalian gastrointestinal microbiota on the host. *Environ Microbiol* **11**, 2194-2206.

Li C, Hossieny P, Wu BJ, Qawasmeh A, Beck K, Stocker R (2007). Pharmacologic induction of heme oxygenase-1. *Antioxid Redox Signal* **9**, 2227-2239.

Lin Q, Huang YM, Xiao BX, Ren GF (2005). Effects of resveratrol on bone mineral density in ovarectomized rats. *Int J Biomed Sci* **1**, 76-81.

Liu KX, Chen SQ, Huang WQ, Li YS, Irwin MG, Xia ZY (2008). Propofol Pretreatment Reduces Ceramide Production and Attenuates Intestinal Mucosal Apoptosis Induced by Intestinal Ischemia/Reperfusion in Rats. *Anesth Analg* **107**, 1884-1891.

Liu SH, Ma K, Xu B, Xu XR (2010a). Protection of carbon monoxide intraperitoneal administration from rat intestine injury induced by lipopolysaccharide. *Chin Med J (Engl)* **123**, 1039-1046.

Liu SH, Ma K, Xu XR, Xu B (2010b). A single dose of carbon monoxide intraperitoneal administration protects rat intestine from injury induced by lipopolysaccharide. *Cell Stress Chaperones* **15**, 717-727.

Liu SH, Xu XR, Ma K, Xu B (2007). Protection of carbon monoxide inhalation on lipopolysaccharide-induced multiple organ injury in rats. *Chin Med Sci J* **22**, 169-176.

Lo Iacono L, Boczkowski J, Zini R, Salouage I, Berdeaux A, Motterlini R *et al.* (2011). A carbon monoxide-releasing molecule (CORM-3) uncouples mitochondrial respiration and modulates the production of reactive oxygen species. *Free Radic Biol Med* **50**, 1556-1564.

Magnotti LJ, Upperman JS, Xu DZ, Lu Q, Deitch EA (1998). Gut-derived mesenteric lymph but not portal blood increases endothelial cell permeability and promotes lung injury after hemorrhagic shock. *Ann Surg* **228**, 518-527.

Maines MD (1997). The heme oxygenase system: A regulator of second messenger gases. *Annual Review of Pharmacology and Toxicology* **37**, 517-554.

Mallick IH, Yang W, Winslet MC, Seifalian AM (2004). Ischemia-reperfusion injury of the intestine and protective strategies against injury. *Dig Dis Sci* **49**, 1359-1377.

Maloy KJ & Powrie F (2011). Intestinal homeostasis and its breakdown in inflammatory bowel disease. *Nature* **474**, 298-306.

Manna SK, Mukhopadhyay A, Aggarwal BB (2000a). IFN-alpha suppresses activation of nuclear transcription factors NF-kappa B and activator protein 1 and potentiates TNF-induced apoptosis. *J Immunol* **165**, 4927-4934.

Manna SK, Mukhopadhyay A, Aggarwal BB (2000b). Resveratrol suppresses TNF-induced activation of nuclear transcription factors NF-kappa B, activator protein-1, and apoptosis: potential role of reactive oxygen intermediates and lipid peroxidation. *J Immunol* **164**, 6509-6519.

Marieb E, Mallat J, Wilhelm P (2004). Human anatomy (Fourth edition). *The digestive system*: 609-646.

Marier JF, Vachon P, Gritsas A, Zhang J, Moreau JP, Ducharme MP (2002). Metabolism and disposition of resveratrol in rats: extent of absorption, glucuronidation, and enterohepatic recirculation evidenced by a linked-rat model. *J Pharmacol Exp Ther* **302**, 369-373.

Maynard CL, Elson CO, Hatton RD, Weaver CT (2012). Reciprocal interactions of the intestinal microbiota and immune system. *Nature* **489**, 231-241.

McCann SK & Roulston CL (2013). NADPH Oxidase as a Therapeutic Target for Neuroprotection against Ischaemic Stroke: Future Perspectives. *Brain Sci* **3**, 561-598.

Medzhitov R, Preston-Hurlburt P, Janeway CA, Jr. (1997). A human homologue of the Drosophila Toll protein signals activation of adaptive immunity. *Nature* **388**, 394-397.

Megias J, Busserolles J, Alcaraz MJ (2007). The carbon monoxide-releasing molecule CORM-2 inhibits the inflammatory response induced by cytokines in Caco-2 cells. *Br J Pharmacol* **150**, 977-986.

Mehlen P & Puisieux A (2006). Metastasis: a question of life or death. *Nat Rev Cancer* **6**, 449-458.

Michel BW, Lippert AR, Chang CJ (2012). A reaction-based fluorescent probe for selective imaging of carbon monoxide in living cells using a palladium-mediated carbonylation. *J Am Chem Soc* **134**, 15668-15671.

Miller SM, Farrugia G, Schmalz PF, Ermilov LG, Maines MD, Szurszewski JH (1998). Heme oxygenase 2 is present in interstitial cell networks of the mouse small intestine. *Gastroenterology* **114**, 239-244.

Miller SM, Reed D, Sarr MG, Farrugia G, Szurszewski JH (2001). Haem oxygenase in enteric nervous system of human stomach and jejunum and co-localization with nitric oxide synthase. *Neurogastroenterol Motil* **13**, 121-131.

Min KJ, Yang MS, Kim SU, Jou I, Joe EH (2006). Astrocytes induce hemeoxygenase-1 expression in microglia: A feasible mechanism for preventing excessive brain inflammation. *Journal of Neuroscience* **26**, 1880-1887.

Mittal M, Siddiqui MR, Tran K, Reddy SP, Malik AB (2014). Reactive Oxygen Species in Inflammation and Tissue Injury. *Antioxid Redox Signal* **20**, 1126-1167.

Mizuguchi S, Stephen J, Bihari R, Markovic N, Suehiro S, Capretta A *et al.* (2009). CORM-3-derived CO modulates polymorphonuclear leukocyte migration across the vascular endothelium by reducing levels of cell surface-bound elastase. *Am J Physiol Heart Circ Physiol* **297**, H920-929.

Moore BA, Otterbein LE, Turler A, Choi AM, Bauer AJ (2003). Inhaled carbon monoxide suppresses the development of postoperative ileus in the murine small intestine. *Gastroenterology* **124**, 377-391.

Moore BA, Overhaus M, Whitcomb J, Ifedigbo E, Choi AM, Otterbein LE *et al.* (2005). Brief inhalation of low-dose carbon monoxide protects rodents and swine from postoperative ileus. *Crit Care Med* **33**, 1317-1326.

Motterlini R (2007). Carbon monoxide-releasing molecules (CO-RMs): vasodilatory, anti-ischaemic and anti-inflammatory activities. *Biochemical Society Transactions* **35**, 1142-1146.

Motterlini R, Clark JE, Foresti R, Sarathchandra P, Mann BE, Green CJ (2002). Carbon monoxide-releasing molecules: characterization of biochemical and vascular activities. *Circulation Research* **90**, E17-24.

Motterlini R & Foresti R (2014). Heme Oxygenase-1 As a Target for Drug Discovery. *Antioxid Redox Signal* **20**, 1810-1826.

Motterlini R & Otterbein LE (2010). The therapeutic potential of carbon monoxide. *Nature Reviews Drug Discovery* **9**, 728-U724.

Motterlini R, Sawle P, Hammad J, Bains S, Alberto R, Foresti R *et al.* (2005). CORM-A1: a new pharmacologically active carbon monoxide-releasing molecule. *Faseb Journal* **19**, 284-286.

Naito Y, Takagi T, Uchiyama K, Yoshikawa T (2011). Heme oxygenase-1: a novel therapeutic target for gastrointestinal diseases. *J Clin Biochem Nutr* **48**, 126-133.

Nakahira K, Kim HP, Geng XH, Nakao A, Wang X, Murase N *et al.* (2006). Carbon monoxide differentially inhibits TLR signaling pathways by regulating ROS-induced trafficking of TLRs to lipid rafts. *J Exp Med* **203**, 2377-2389.

Nakao A, Faleo G, Shimizu H, Nakahira K, Kohmoto J, Sugimoto R *et al.* (2008). Ex vivo carbon monoxide prevents cytochrome P450 degradation and ischemia/reperfusion injury of kidney grafts. *Kidney Int* **74**, 1009-1016.

Nakao A, Otterbein LE, Overhaus M, Sarady JK, Tsung A, Kimizuka K *et al.* (2004). Biliverdin protects the functional integrity of a transplanted syngeneic small bowel. *Gastroenterology* **127**, 595-606.

Nakao A, Schmidt J, Harada T, Tsung A, Stoffels B, Cruz RJ, Jr. *et al.* (2006a). A single intraperitoneal dose of carbon monoxide-saturated ringer's lactate solution ameliorates postoperative ileus in mice. *J Pharmacol Exp Ther* **319**, 1265-1275.

Nakao A, Toyokawa H, Tsung A, Nalesnik MA, Stolz DB, Kohmoto J *et al.* (2006b). Ex vivo application of carbon monoxide in University of Wisconsin solution to prevent intestinal cold ischemia/reperfusion injury. *American Journal of Transplantation* **6**, 2243-2255.

Nath KA, Balla G, Vercellotti GM, Balla J, Jacob HS, Levitt MD *et al.* (1992). Induction of Heme Oxygenase Is a Rapid, Protective Response in Rhabdomyolysis in the Rat. *Journal of Clinical Investigation* **90**, 267-270.

Nauseef WM (2007). How human neutrophils kill and degrade microbes: an integrated view. *Immunological Reviews* **219**, 88-102.

Nenci A, Becker C, Wullaert A, Gareus R, van Loo G, Danese S *et al.* (2007). Epithelial NEMO links innate immunity to chronic intestinal inflammation. *Nature* **446**, 557-561.

Nikolic I, Liu D, Bell JA, Collins J, Steenbergen C, Murphy E (2007). Treatment with an estrogen receptor-beta-selective agonist is cardioprotective. *J Mol Cell Cardiol* **42**, 769-780.

Onyiah JC, Sheikh SZ, Maharshak N, Steinbach EC, Russo SM, Kobayashi T *et al.* (2013). Carbon monoxide and heme oxygenase-1 prevent intestinal inflammation in mice by promoting bacterial clearance. *Gastroenterology* **144**, 789-798.

Otani K, Shimizu S, Chijiiwa K, Morisaki T, Yamaguchi T, Yamaguchi K *et al.* (2000). Administration of bacterial lipopolysaccharide to rats induces heme oxygenase-1 and formation of antioxidant bilirubin in the intestinal mucosa. *Dig Dis Sci* **45**, 2313-2319.

Otterbein LE, Bach FH, Alam J, Soares M, Lu HT, Wysk M *et al.* (2000). Carbon monoxide has anti-inflammatory effects involving the mitogen-activated protein kinase pathway. *Nature Medicine* **6**, 422-428.

Otterbein LE, Mantell LL, Choi AM (1999). Carbon monoxide provides protection against hyperoxic lung injury. *Am J Physiol* **276**, L688-694.

Otterbein LE, Otterbein SL, Ifedigbo E, Liu F, Morse DE, Fearns C *et al.* (2003). MKK3 mitogen-activated protein kinase pathway mediates carbon monoxide-induced protection against oxidant-induced lung injury. *American Journal of Pathology* **163**, 2555-2563.

Panaro MA, Carofiglio V, Acquafredda A, Cavallo P, Cianciulli A (2012). Anti-inflammatory effects of resveratrol occur via inhibition of lipopolysaccharide-induced NF-kappaB activation in Caco-2 and SW480 human colon cancer cells. *Br J Nutr* **108**, 1623-1632.

Pasparakis M & Vandenabeele P (2015). Necroptosis and its role in inflammation. *Nature* **517**, 311-320.

Patel GP, Gurka DP, Balk RA (2003). New treatment strategies for severe sepsis and septic shock. *Curr Opin Crit Care* **9**, 390-396.

Paul G, Bataille F, Obermeier F, Bock J, Klebl F, Strauch U *et al.* (2005). Analysis of intestinal haem-oxygenase-1 (HO-1) in clinical and experimental colitis. *Clin Exp Immunol* **140**, 547-555.

Peterson LW & Artis D (2014). Intestinal epithelial cells: regulators of barrier function and immune homeostasis. *Nat Rev Immunol* **14**, 141-153.

Petrat F & de Groot H (2011). Protection against severe intestinal ischemia/reperfusion injury in rats by intravenous resveratrol. *J Surg Res* **167**, e145-155.

Podolsky DK (2000). Review article: healing after inflammatory injury--coordination of a regulatory peptide network. *Aliment Pharmacol Ther* **14 Suppl 1**, 87-93.

Poulsen MM, Jorgensen JO, Jessen N, Richelsen B, Pedersen SB (2013). Resveratrol in metabolic health: an overview of the current evidence and perspectives. *Ann N Y Acad Sci* **1290**, 74-82.

Quideau S, Deffieux D, Douat-Casassus C, Pouysegu L (2011). Plant polyphenols: chemical properties, biological activities, and synthesis. *Angew Chem Int Ed Engl* **50**, 586-621.

Radtke F & Clevers H (2005). Self-renewal and cancer of the gut: two sides of a coin. *Science* **307**, 1904-1909.

Ramachandran A, Madesh M, Balasubramanian KA (2000). Apoptosis in the intestinal epithelium: its relevance in normal and pathophysiological conditions. *J Gastroenterol Hepatol* **15**, 109-120.

Reboul C, Thireau J, Meyer G, Andre L, Obert P, Cazorla O *et al.* (2012). Carbon monoxide exposure in the urban environment: an insidious foe for the heart? *Respir Physiol Neurobiol* **184**, 204-212.

Reczek CR & Chandel NS (2015). ROS-dependent signal transduction. *Curr Opin Cell Biol* **33**, 8-13.

Ren H, Leib SL, Ferriero DM, Tauber MG, Christen S (2007). Induction of haem oxygenase-1 causes cortical non-haem iron increase in experimental pneumococcal meningitis: evidence that concomitant ferritin up-regulation prevents iron-induced oxidative damage. *Journal of Neurochemistry* **100**, 532-544.

Renaud S & de Lorgeril M (1992). Wine, alcohol, platelets, and the French paradox for coronary heart disease. *Lancet* **339**, 1523-1526.

Rivers E, Nguyen B, Havstad S, Ressler J, Muzzin A, Knoblich B *et al.* (2001). Early goal-directed therapy in the treatment of severe sepsis and septic shock. *N Engl J Med* **345**, 1368-1377.

Robb EL, Page MM, Wiens BE, Stuart JA (2008a). Molecular mechanisms of oxidative stress resistance induced by resveratrol: Specific and progressive induction of MnSOD. *Biochem Biophys Res Commun* **367**, 406-412.

Robb EL & Stuart JA (2010). trans-Resveratrol as A Neuroprotectant. *Molecules* **15**, 1196-1212.

Robb EL, Winkelmolen L, Visanji N, Brotchie J, Stuart JA (2008b). Dietary resveratrol administration increases MnSOD expression and activity in mouse brain. *Biochem Biophys Res Commun* **372**, 254-259.

Roberts GP, Youn H, Kerby RL (2004). CO-sensing mechanisms. *Microbiol Mol Biol Rev* **68**, 453-473, table of contents.

Rodella L, Lamon BD, Rezzani R, Sangras B, Goodman AI, Falck JR *et al.* (2006). Carbon monoxide and biliverdin prevent endothelial cell sloughing in rats with type I diabetes. *Free Radic Biol Med* **40**, 2198-2205.

Rodriguez AI, Gangopadhyay A, Kelley EE, Pagano PJ, Zuckerbraun BS, Bauer PM (2010). HO-1 and CO decrease platelet-derived growth factor-induced vascular smooth muscle cell migration via inhibition of Nox1. *Arterioscler Thromb Vasc Biol* **30**, 98-104.

Romier B, Van De Walle J, During A, Larondelle Y, Schneider YJ (2008). Modulation of signalling nuclear factor-kappaB activation pathway by polyphenols in human intestinal Caco-2 cells. *Br J Nutr* **100**, 542-551.

Roulis M, Armaka M, Manoloukos M, Apostolaki M, Kollias G (2011). Intestinal epithelial cells as producers but not targets of chronic TNF suffice to cause murine Crohn-like pathology. *Proceedings of the National Academy of Sciences of the United States of America* **108**, 5396-5401.

Rubiolo JA, Mithieux G, Vega FV (2008). Resveratrol protects primary rat hepatocytes against oxidative stress damage: activation of the Nrf2 transcription factor and augmented activities of antioxidant enzymes. *European Journal of Pharmacology* **591**, 66-72.

Ryan MJ, Jackson JR, Hao Y, Williamson CL, Dabkowski ER, Hollander JM *et al.* (2010). Suppression of oxidative stress by resveratrol after isometric contractions in gastrocnemius muscles of aged mice. *J Gerontol A Biol Sci Med Sci* **65**, 815-831.

Ryter SW, Alam J, Choi AM (2006). Heme oxygenase-1/carbon monoxide: from basic science to therapeutic applications. *Physiol Rev* **86**, 583-650.

Ryter SW & Choi AM (2013). Carbon monoxide: present and future indications for a medical gas. *Korean J Intern Med* **28**, 123-140.

Ryter SW & Choi AMK (2009). Heme Oxygenase-1/Carbon Monoxide From Metabolism to Molecular Therapy. *American Journal of Respiratory Cell and Molecular Biology* **41**, 251-260.

Ryter SW & Otterbein LE (2004). Carbon monoxide in biology and medicine. *Bioessays* **26**, 270-280.

Sambruy Y, Ferruzza S, Ranaldi G, De Angelis I (2001). Intestinal cell culture models: Applications in toxicology and pharmacology. *Cell Biology and Toxicology* **17**, 301-317.

Sambuy Y, De Angelis I, Ranaldi G, Scarino ML, Stammati A, Zucco F (2005). The Caco-2 cell line as a model of the intestinal barrier: influence of cell and culture-related factors on Caco-2 cell functional characteristics. *Cell Biology and Toxicology* **21**, 1-26.

Sancho E, Batlle E, Clevers H (2003). Live and let die in the intestinal epithelium. *Curr Opin Cell Biol* **15**, 763-770.

Sancho E, Batlle E, Clevers H (2004). Signaling pathways in intestinal development and cancer. *Annu Rev Cell Dev Biol* **20**, 695-723.

Sandouka A, Fuller BJ, Mann BE, Green CJ, Foresti R, Motterlini R (2006). Treatment with CO-RMs during cold storage improves renal function at reperfusion. *Kidney Int* **69**, 239-247.

Santos AC, Veiga F, Ribeiro AJ (2011). New delivery systems to improve the bioavailability of resveratrol. *Expert Opin Drug Deliv* **8**, 973-990.

Sarady JK, Zuckerbraun BS, Bilban M, Wagner O, Usheva A, Liu F *et al.* (2004). Carbon monoxide protection against endotoxic shock involves reciprocal effects on iNOS in the lung and liver. *Faseb Journal* **18**, 854-856.

Sarr M, Chataigneau M, Martins S, Schott C, El Bedoui J, Oak MH *et al.* (2006). Red wine polyphenols prevent angiotensin II-induced hypertension and endothelial dysfunction in rats: Role of NADPH oxidase. *Cardiovascular Research* **71**, 794-802.

Sato K, Balla J, Otterbein L, Smith RN, Brouard S, Lin Y *et al.* (2001). Carbon monoxide generated by heme oxygenase-1 suppresses the rejection of mouse-to-rat cardiac transplants. *J Immunol* **166**, 4185-4194.

Sato T & Clevers H (2013). Growing self-organizing mini-guts from a single intestinal stem cell: mechanism and applications. *Science* **340**, 1190-1194.

Sato T, Vries RG, Snippert HJ, van de Wetering M, Barker N, Stange DE *et al.* (2009). Single Lgr5 stem cells build crypt-villus structures in vitro without a mesenchymal niche. *Nature* **459**, 262-U147.

Savkovic SD, Koutsouris A, Hecht G (1997). Activation of NF-kappaB in intestinal epithelial cells by enteropathogenic Escherichia coli. *Am J Physiol* **273**, C1160-1167.

Sawle P, Foresti R, Mann BE, Johnson TR, Green CJ, Motterlini R (2005). Carbon monoxide-releasing molecules (CO-RMs) attenuate the inflammatory response elicited by lipopolysaccharide in RAW264.7 murine macrophages. *Br J Pharmacol* **145**, 800-810.

Schmidt J, Stoffels B, Chanthaphavong RS, Buchholz BM, Nakao A, Bauer AJ (2012). Differential molecular and cellular immune mechanisms of postoperative and LPS-induced ileus in mice and rats. *Cytokine* **59**, 49-58.

Schwerk J, Koster M, Hauser H, Rohde M, Fulde M, Hornef MW *et al.* (2013). Generation of Mouse Small Intestinal Epithelial Cell Lines That Allow the Analysis of Specific Innate Immune Functions. *Plos One* **8**.

Serra D, Rufino AT, Mendes AF, Almeida LM, Dinis TC (2014). Resveratrol modulates cytokine-induced Jak/STAT activation more efficiently than 5-aminosalicylic acid: an in vitro approach. *Plos One* **9**, e109048.

Shah KA, Shurey S, Green CJ (1997). Apoptosis after intestinal ischemia-reperfusion injury: a morphological study. *Transplantation* **64**, 1393-1397.

Shigematsu S, Ishida S, Hara M, Takahashi N, Yoshimatsu H, Sakata T *et al.* (2003). Resveratrol, a red wine constituent polyphenol, prevents superoxide-dependent inflammatory responses induced by ischemia/reperfusion, platelet-activating factor, or oxidants. *Free Radic Biol Med* **34**, 810-817.

Shimizu M (2010). Interaction between Food Substances and the Intestinal Epithelium. *Bioscience Biotechnology and Biochemistry* **74**, 232-241.

Sies H (1997). Oxidative stress: oxidants and antioxidants. *Exp Physiol* **82**, 291-295.

Skrupky LP, Kerby PW, Hotchkiss RS (2011). Advances in the management of sepsis and the understanding of key immunologic defects. *Anesthesiology* **115**, 1349-1362.

Slater TF (1984). Free-radical mechanisms in tissue injury. *Biochem J* **222**, 1-15.

Smoliga JM, Vang O, Baur JA (2012). Challenges of Translating Basic Research Into Therapeutics: Resveratrol as an Example. *Journals of Gerontology Series a-Biological Sciences and Medical Sciences* **67**, 158-167.

Snoek SA, Dhawan S, van Bree SH, Cailotto C, van Diest SA, Duarte JM *et al.* (2012). Mast cells trigger epithelial barrier dysfunction, bacterial translocation and postoperative ileus in a mouse model. *Neurogastroenterol Motil* **24**, 172-184, e191.

Soleas GJ, Angelini M, Grass L, Diamandis EP, Goldberg DM (2001). Absorption of trans-resveratrol in Rats. *Flavonoids and Other Polyphenols* **335**, 145-154.

Soleas GJ, Diamandis EP, Goldberg DM (1997). Resveratrol: A molecule whose time has come? And gone? *Clinical Biochemistry* **30**, 91-113.

Stocker R, Yamamoto Y, Mcdonagh AF, Glazer AN, Ames BN (1987). Bilirubin Is an Antioxidant of Possible Physiological Importance. *Science* **235**, 1043-1046.

Sun B, Zou X, Chen Y, Zhang P, Shi G (2008). Preconditioning of carbon monoxide releasing molecule-derived CO attenuates LPS-induced activation of HUVEC. *Int J Biol Sci* **4**, 270-278.

Suzuki Y & Lehrer RI (1980). NAD(P)H oxidase activity in human neutrophils stimulated by phorbol myristate acetate. *J Clin Invest* **66**, 1409-1418.

Tadolini B, Juliano C, Piu L, Franconi F, Cabrini L (2000). Resveratrol inhibition of lipid peroxidation. *Free Radic Res* **33**, 105-114.

Taille C, El-Benna J, Lanone S, Boczkowski J, Motterlini R (2005). Mitochondrial respiratory chain and NAD(P)H oxidase are targets for the antiproliferative effect of carbon monoxide in human airway smooth muscle. *J Biol Chem* **280**, 25350-25360.

Takagi T, Naito Y, Uchiyama K, Suzuki T, Hirata I, Mizushima K *et al.* (2011). Carbon monoxide liberated from carbon monoxide-releasing molecule exerts an anti-inflammatory effect on dextran sulfate sodium-induced colitis in mice. *Dig Dis Sci* **56**, 1663-1671.

Taniguchi Y, Yoshioka N, Nakata K, Nishizawa T, Inagawa H, Kohchi C *et al.* (2009). Mechanism for maintaining homeostasis in the immune system of the intestine. *Anticancer Res* **29**, 4855-4860.

Teng Z, Yuan C, Zhang F, Huan M, Cao W, Li K *et al.* (2012). Intestinal absorption and first-pass metabolism of polyphenol compounds in rat and their transport dynamics in Caco-2 cells. *Plos One* **7**, e29647.

Teskac K & Kristl J (2010). The evidence for solid lipid nanoparticles mediated cell uptake of resveratrol. *Int J Pharm* **390**, 61-69.

Tissenbaum HA & Guarente L (2001). Increased dosage of a sir-2 gene extends lifespan in Caenorhabditis elegans. *Nature* **410**, 227-230.

Triantafilou M & Triantafilou K (2005). The dynamics of LPS recognition: complex orchestration of multiple receptors. *J Endotoxin Res* **11**, 5-11.

Tsoyi K, Ha YM, Kim YM, Lee YS, Kim HJ, Kim HJ *et al.* (2009). Activation of PPAR-gamma by carbon monoxide from CORM-2 leads to the inhibition of iNOS but not COX-2 expression in LPS-stimulated macrophages. *Inflammation* **32**, 364-371.

Turnage RH, Guice KS, Oldham KT (1994). Pulmonary microvascular injury following intestinal reperfusion. *New Horiz* **2**, 463-475.

Turrens JF & Boveris A (1980). Generation of superoxide anion by the NADH dehydrogenase of bovine heart mitochondria. *Biochem J* **191**, 421-427.

Uchiyama K, Naito Y, Takagi T, Mizushima K, Hayashi N, Harusato A *et al.* (2010). Carbon monoxide enhance colonic epithelial restitution via FGF15 derived from colonic myofibroblasts. *Biochem Biophys Res Commun* **391**, 1122-1126.

Uehara K, Takahashi T, Fujii H, Shimizu H, Omori E, Matsumi M *et al.* (2005). The lower intestinal tract-specific induction of heme oxygenase-1 by glutamine protects against endotoxemic intestinal injury. *Crit Care Med* **33**, 381-390.

Ungvari Z, Labinskyy N, Mukhopadhyay P, Pinto JT, Bagi Z, Ballabh P *et al.* (2009). Resveratrol attenuates mitochondrial oxidative stress in coronary arterial endothelial cells. *Am J Physiol Heart Circ Physiol* **297**, H1876-1881.

Ungvari Z, Orosz Z, Rivera A, Labinskyy N, Xiangmin Z, Olson S *et al.* (2007). Resveratrol increases vascular oxidative stress resistance. *Am J Physiol Heart Circ Physiol* **292**, H2417-2424.

van der Flier LG & Clevers H (2009). Stem cells, self-renewal, and differentiation in the intestinal epithelium. *Annu Rev Physiol* **71**, 241-260.

van der Vliet A, Tuinstra TJ, Bast A (1989). Modulation of oxidative stress in the gastrointestinal tract and effect on rat intestinal motility. *Biochem Pharmacol* **38**, 2807-2818.

Van Herreweghe F, Festjens N, Declercq W, Vandenabeele P (2010). Tumor necrosis factor-mediated cell death: to break or to burst, that's the question. *Cell Mol Life Sci* **67**, 1567-1579.

Vanova K, Suk J, Petr T, Cerny D, Slanar O, Vreman HJ *et al.* (2014). Protective effects of inhaled carbon monoxide in endotoxin-induced cholestasis is dependent on its kinetics. *Biochimie* **97**, 173-180.

Vara D & Pula G (2014). Reactive oxygen species: physiological roles in the regulation of vascular cells. *Curr Mol Med* **14**, 1103-1125.

Vather R & Bissett I (2013). Management of prolonged post-operative ileus: evidence-based recommendations. *ANZ J Surg* **83**, 319-324.

Vecchione C, Frati A, Di Pardo A, Cifelli G, Carnevale D, Gentile MT *et al.* (2009). Tumor Necrosis Factor-alpha Mediates Hemolysis-Induced Vasoconstriction and the Cerebral Vasospasm Evoked by Subarachnoid Hemorrhage. *Hypertension* **54**, 150-156.

Vidal K, Grosjean I, evillard JP, Gespach C, Kaiserlian D (1993). Immortalization of mouse intestinal epithelial cells by the SV40-large T gene. Phenotypic and immune characterization of the MODE-K cell line. *J Immunol Methods* **166**, 63-73.

Vitrac X, Desmouliere A, Brouillaud B, Krisa S, Deffieux G, Barthe N *et al.* (2003). Distribution of [C-14]-trans-resveratrol, a cancer chemopreventive polyphenol, in mouse tissues after oral administration. *Life Sciences* **72**, 2219-2233.

Voloshyna I, Hussaini SM, Reiss AB (2012). Resveratrol in cholesterol metabolism and atherosclerosis. *J Med Food* **15**, 763-773.

Von Burg R (1999). Carbon Monoxide. J Appl Toxicol **19**: 379-386.

Walle T, Hsieh F, DeLegge MH, Oatis JE, Jr., Walle UK (2004). High absorption but very low bioavailability of oral resveratrol in humans. *Drug Metab Dispos* **32**, 1377-1382.

Wang WP, Guo X, Koo MW, Wong BC, Lam SK, Ye YN *et al.* (2001). Protective role of heme oxygenase-1 on trinitrobenzene sulfonic acid-induced colitis in rats. *Am J Physiol Gastrointest Liver Physiol* **281**, G586-594.

Wang X, Cao J, Sun BW, Liu DD, Liang F, Gao L (2012). Exogenous carbon monoxide attenuates inflammatory responses in the small intestine of septic mice. *World J Gastroenterol* **18**, 5719-5728.

Wells JM, Loonen LM, Karczewski JM (2010). The role of innate signaling in the homeostasis of tolerance and immunity in the intestine. *Int J Med Microbiol* **300**, 41-48.

Wen SH, Li Y, Li C, Xia ZQ, Liu WF, Zhang XY *et al.* (2012). Ischemic Postconditioning during Reperfusion Attenuates Intestinal Injury and Mucosal Cell Apoptosis by Inhibiting Jak/Stat Signaling Activation. *Shock* **38**, 411-419.

West AP, Shadel GS, Ghosh S (2011). Mitochondria in innate immune responses. *Nat Rev Immunol* **11**, 389-402.

Whittle BJR & Varga C (2010). New light on the anti-colitic actions of therapeutic aminosalicylates: the role of heme oxygenase. *Pharmacological Reports* **62**, 548-556.

Willis D, Moore AR, Frederick R, Willoughby DA (1996). Heme oxygenase: A novel target for the modulation of the inflammatory response. *Nature Medicine* **2**, 87-90.

Wise PM, Dubal DB, Wilson ME, Rau SW, Bottner M, Rosewell KL (2001). Estradiol is a protective factor in the adult and aging brain: understanding of mechanisms derived from in vivo and in vitro studies. *Brain Research Reviews* **37**, 313-319.

Wu JM & Hsieh TC (2011). Resveratrol: a cardioprotective substance. *Ann N Y Acad Sci* **1215**, 16-21.

Wu LY & Wang R (2005). Carbon monoxide: Endogenous production, physiological functions, and pharmacological applications. *Pharmacological Reviews* **57**, 585-630.

Yoriki H, Naito Y, Takagi T, Mizusima K, Hirai Y, Harusato A *et al.* (2013). Hemin ameliorates indomethacin-induced small intestinal injury in mice through the induction of heme oxygenase-1. *J Gastroenterol Hepatol* **28**, 632-638.

Yoshida J, Ozaki KS, Nalesnik MA, Ueki S, Castillo-Rama M, Faleo G *et al.* (2010). Ex vivo application of carbon monoxide in UW solution prevents transplant-induced renal ischemia/reperfusion injury in pigs. *American Journal of Transplantation* **10**, 763-772.

Yu W, Fu YC, Zhou XH, Chen CJ, Wang X, Lin RB *et al.* (2009). Effects of resveratrol on H(2)O(2)-induced apoptosis and expression of SIRTs in H9c2 cells. *J Cell Biochem* **107**, 741-747.

Zhang XC, Shan PY, Otterbein LE, Alam J, Flavell RA, Davis RJ *et al.* (2003). Carbon monoxide inhibition of apoptosis during ischemia-reperfusion lung injury is dependent on the p38 mitogen-activated protein kinase pathway and involves caspase 3. *Journal of Biological Chemistry* **278**, 1248-1258.

Zhong W, Xia Z, Hinrichs D, Rosenbaum JT, Wegmann KW, Meyrowitz J *et al.* (2010). Hemin exerts multiple protective mechanisms and attenuates dextran sulfate sodium-induced colitis. *J Pediatr Gastroenterol Nutr* **50**, 132-139.

Zuckerbraun BS, Billiar TR, Otterbein SL, Kim PKM, Liu F, Choi AMK *et al.* (2003). Carbon monoxide protects against liver failure through nitric oxide-induced heme oxygenase 1. *Journal of Experimental Medicine* **198**, 1707-1716.

Zuckerbraun BS, Otterbein LE, Boyle P, Jaffe R, Upperman J, Zamora R *et al.* (2005). Carbon monoxide protects against the development of experimental necrotizing enterocolitis. *Am J Physiol Gastrointest Liver Physiol* **289**, G607-613.

Chapter II

AIMS

Chapter II   Aims

The IEC layer plays a crucial role in acute GI inflammation. Among the myriad of signaling agents, TNF-α is one of the pro-inflammatory cytokines well known to initiate inflammation in the GI mucosa (Guy-Grand *et al.*, 1998; Ruemmele *et al.*, 1999). TNF-α is known to induce both apoptosis and cell shedding (Piguet *et al.*, 1999) involving TNFR1 (Roulis *et al.*, 2011), increase gap formation with associated cell loss (Kiesslich *et al.*, 2007), and decrease the intestinal permeability barrier (Watson *et al.*, 2009) in mouse models. However, TNF-α alone does not induce apoptosis of isolated IEC lines but requires the inhibition of protein translation with CHX (Bhattacharya *et al.*, 2003; Pajak *et al.*, 2005).

HO-1 confers protection against oxidative stress and inflammation *in vitro* and *in vivo* (Ryter & Choi, 2002). Although the mechanisms of HO-1-dependent cytoprotection remain incompletely understood, accumulating evidence has implicated contributory roles for the products generated from HO activity in particular CO. HO-1 is upregulated by numerous stimuli including oxidative stress and pro-inflammatory cytokines like TNF-α. Recently, the water soluble CO-RMs, CORM-3 and CORM-A1 have facilitated examination of the therapeutic potential of CO in disease models including GI ones and open prospects for practical clinical delivery of CO.

Oxidative stress has been a common denominator in several acute GI disorders. In a previous study in our laboratory, the possible protective effect of CORM-3 on POI was studied in a mouse model (De Backer *et al.*, 2009). Surgical manipulation of the small intestine induces intestinal dysmotility and retarded GI transit, driven by a muscular inflammatory process; TNF-α is one of the early inflammatory mediators involved (Lubbers *et al.*, 2009; Schmidt *et al.*, 2012). Already 1 h after intestinal manipulation, both the mucosal layer and the muscular layer of the small intestine showed a clear cut increase in oxidative stress, the increase in the mucosal layer being most pronounced. In the muscular layer, the increase was maintained for 24 h, but in the mucosal layer the increase at 1 h formed a peak. CORM-3 clearly reduced the surgery-induced intestinal dysmotility and also significantly reduced this oxidative stress. This suggests that oxidative stress through the production of ROS in the intestinal wall might contribute to the pathogenesis of POI. These

results led to the hypothesis that early oxidative stress in the small intestinal epithelial cell layer might lead to cell damage and increased intestinal permeability, contributing to or triggering muscular inflammation. In this thesis, in order to further investigate the *in vivo* observation in an *in vitro* setting, a murine small IEC line MODE-K was selected with TNF-α as an inflammatory stimulus.

Although the expression of HO-1 in most tissues is low, it can be strongly up-regulated endogenously by a wide variety of stimuli including heme but also non-heme stimuli like cytokines, ROS and hypoxia (Pae *et al.*, 2008). A large number of pharmacologic compounds have been demonstrated to induce HO-1 and this induction of HO-1 provides potent cytoprotective effects (Li *et al.*, 2007). Thus, targeted induction of HO-1 can be used as a therapeutic strategy to combat oxidative stress conditions, which may facilitate the development of novel drugs. Among the search for naturally occurring HO-1 inducers, resveratrol, a plant polyphenol with anti-oxidative and anti-inflammatory effects, has recently gained much interest as a potent HO-1 inducer (Son *et al.*, 2013).

Therefore, the aim of this thesis was to establish an *in vitro* IEC model to assess TNF-α-induced oxidative stress, inflammation and cell death, and to investigate the protective effects of CO-RMs and resveratrol versus the TNF-α-induced dysfunction concentrating on their anti-oxidative effect.

In a first project, the murine MODE-K IEC line was established as a model to assess TNF-α/CHX-induced oxidative stress and apoptosis, showing parallel occurrence of ROS and apoptosis. As in the case of many GI cell lines, our preliminary studies showed that TNF-α requires the combination with CHX to initiate apoptosis in MODE-K cells and hence TNF-α/CHX was selected. The influence of the CO-RMs CORM-A1 and CORM-3, and resveratrol on TNF-α/CHX-induced ROS and apoptosis was investigated. In comparison, a series of compounds was tested : the HO-1-derived products biliverdin and bilirubin, the NOX inhibitors apocynin and diphenylene iodonium (DPI), a mitochondrial targeted water-soluble antioxidant Mito-TEMPO, an inhibitor of prolyl hydroxylase dimethyoxallyl glycine (DMOG), and nitrite (as sodium nitrite). For CORM-A1, resveratrol, bilirubin and nitrite, the contribution of HO-1 induction to their protective effects was examined. These results are summarized in **chapter III**.

ROS production from NOXs and mitochondria was implicated in TNF-α-induced apoptosis of rat small IECs (Jin *et al.*, 2008; Baregamian *et al.*, 2009). However, the sources of

TNF-α-induced ROS in mouse small IECs are unknown. Hence, in the second project, we investigated the various sources of ROS production during TNF-α/CHX-induced oxidative stress in MODE-K cells using pharmacological inhibitors of various ROS-generating systems (NOX, ETC complexes and xanthine/xanthine oxidase), ROS scavengers and antioxidants. Given the role of mitochondria in ROS production and cell death, the influence of TNF-α/CHX on Ψm, mitochondrial function and cellular respiration was also studied. The results are summarized in **chapter IV**.

Reducing oxidative stress in the GI epithelial cell layer may be a reasonable therapeutic approach to treat acute GI diseases. The slow releasing water soluble CO-RM, CORM-A1, and resveratrol were the two agents which effectively reduced TNF-α/CHX-induced oxidative stress and cell death of MODE-K cells suggesting a correlation between the antioxidant and cytoprotective effects of these agents (**chapter III**). The aim of our last project was therefore to investigate the influence of CORM-A1 and resveratrol on the different sources of TNF-α/CHX-induced ROS production in MODE-K cells in comparison with their effect versus H_2O_2-, rotenone- or antimycin-A-induced ROS-generating systems. The influence on TNF-α/CHX-induced changes in Ψm, mitochondrial function and cellular respiration was also studied. The results are summarized in **chapter V**.

II.1 References

Baregamian N, Song J, Bailey CE, Papaconstantinou J, Evers BM, Chung DH (2009). Tumor necrosis factor-alpha and apoptosis signal-regulating kinase 1 control reactive oxygen species release, mitochondrial autophagy, and c-Jun N-terminal kinase/p38 phosphorylation during necrotizing enterocolitis. *Oxidative Medicine and Cellular Longevity* **2**, 297-306.

Bhattacharya S, Ray RM, Viar MJ, Johnson LR (2003). Polyamines are required for activation of c-Jun NH2-terminal kinase and apoptosis in response to TNF-alpha in IEC-6 cells. *Am J Physiol Gastrointest Liver Physiol* **285**, G980-991.

De Backer O, Elinck E, Blanckaert B, Leybaert L, Motterlini R, Lefebvre RA (2009). Water-soluble CO-releasing molecules reduce the development of postoperative ileus via modulation of MAPK/HO-1 signalling and reduction of oxidative stress. *Gut* **58**, 347-356.

Guy-Grand D, DiSanto JP, Henchoz P, Malassis-Seris M, Vassalli P (1998). Small bowel enteropathy: role of intraepithelial lymphocytes and of cytokines (IL-12, IFN-gamma, TNF) in the induction of epithelial cell death and renewal. *Eur J Immunol* **28**, 730-744.

Jin S, Ray RM, Johnson LR (2008). TNF-alpha/cycloheximide-induced apoptosis in intestinal epithelial cells requires Rac1-regulated reactive oxygen species. *Am J Physiol Gastrointest Liver Physiol* **294**, G928-937.

Kiesslich R, Goetz M, Angus EM, Hu Q, Guan Y, Potten C *et al.* (2007). Identification of epithelial gaps in human small and large intestine by confocal endomicroscopy. *Gastroenterology* **133**, 1769-1778.

Li C, Hossieny P, Wu BJ, Qawasmeh A, Beck K, Stocker R (2007). Pharmacologic induction of heme oxygenase-1. *Antioxid Redox Signal* **9**, 2227-2239.

Lubbers T, Luyer MD, de Haan JJ, Hadfoune M, Buurman WA, Greve JW (2009). Lipid-rich enteral nutrition reduces postoperative ileus in rats via activation of cholecystokinin-receptors. *Ann Surg* **249**, 481-487.

Pae HO, Lee YC, Chung HT (2008). Heme oxygenase-1 and carbon monoxide: emerging therapeutic targets in inflammation and allergy. *Recent Pat Inflamm Allergy Drug Discov* **2**, 159-165.

Pajak B, Gajkowska B, Orzechowski A (2005). Cycloheximide-mediated sensitization to TNF-alpha-induced apoptosis in human colorectal cancer cell line COLO 205; role of FLIP and metabolic inhibitors. *J Physiol Pharmacol* **56 Suppl 3**, 101-118.

Piguet PF, Vesin C, Donati Y, Barazzone C (1999). TNF-induced enterocyte apoptosis and detachment in mice: induction of caspases and prevention by a caspase inhibitor, ZVAD-fmk. *Lab Invest* **79**, 495-500.

Roulis M, Armaka M, Manoloukos M, Apostolaki M, Kollias G (2011). Intestinal epithelial cells as producers but not targets of chronic TNF suffice to cause murine Crohn-like pathology. *Proceedings of the National Academy of Sciences of the United States of America* **108**, 5396-5401.

Ruemmele FM, Russo P, Beaulieu J, Dionne S, Levy E, Lentze MJ *et al.* (1999). Susceptibility to FAS-induced apoptosis in human nontumoral enterocytes: role of costimulatory factors. *J Cell Physiol* **181**, 45-54.

Ryter SW & Choi AM (2002). Heme oxygenase-1: molecular mechanisms of gene expression in oxygen-related stress. *Antioxid Redox Signal* **4**, 625-632.

Schmidt J, Stoffels B, Chanthaphavong RS, Buchholz BM, Nakao A, Bauer AJ (2012). Differential molecular and cellular immune mechanisms of postoperative and LPS-induced ileus in mice and rats. *Cytokine* **59**, 49-58.

Son Y, Lee JH, Chung HT, Pae HO (2013). Therapeutic roles of heme oxygenase-1 in metabolic diseases: curcumin and resveratrol analogues as possible inducers of heme oxygenase-1. *Oxidative Medicine and Cellular Longevity* **2013**, 639541.

Watson AJ, Duckworth CA, Guan Y, Montrose MH (2009). Mechanisms of epithelial cell shedding in the Mammalian intestine and maintenance of barrier function. *Ann N Y Acad Sci* **1165**, 135-142.

Chapter III

TNF-α/CYCLOHEXIMIDE-INDUCED OXIDATIVE STRESS AND APOPTOSIS IN MURINE INTESTINAL EPITHELIAL MODE-K CELLS

Dinesh Babu [a], Stefaan J Soenen [b], Koen Raemdonck [b], Georges Leclercq [c], Ole De Backer [a], Roberto Motterlini [d], Romain A. Lefebvre [a]

[a] Heymans Institute of Pharmacology, Faculty of Medicine and Health Sciences, Ghent University, Belgium

[b] Laboratory of General Biochemistry and Physical Pharmacy, Faculty of Pharmaceutical Sciences, Ghent University, Belgium

[c] Department of Clinical Chemistry, Microbiology and Immunology, Faculty of Medicine and Health Sciences, Ghent University, Belgium

[d] INSERM U955, University Paris-Est, France

Chapter III

TNF-α/cycloheximide-induced oxidative stress and apoptosis in murine intestinal epithelial MODE-K cells

III.1   Abstract

Background. In the mouse postoperative ileus model, we have shown an increase in oxidative stress after intestinal manipulation occurring earlier in the mucosa than in the muscular layer, which might contribute to epithelial barrier dysfunction. To address these findings *in vitro*, we assessed TNF-α/cycloheximide (CHX)-induced oxidative stress and apoptosis in a mouse intestinal epithelial cell line, MODE-K.

Methods. The influence of heme oxygenase (HO)-1-related products and agents known to reduce reactive oxygen species (ROS) production on TNF-α/CHX-induced oxidative stress and apoptosis were investigated. MODE-K cells were exposed to different concentrations of TNF-α/CHX in the absence/presence of the test agents. Cell viability, caspase-3/7 activity, apoptosis, reduced glutathione (GSH) level and intracellular ROS production were measured.

Key results. TNF-α/CHX decreased cell viability, increased caspase-3/7 activity, induced apoptosis, reduced the GSH level and increased ROS production in a concentration-dependent manner in MODE-K cells. All these effects of TNF-α/CHX were partially prevented by pretreatment with a carbon monoxide-releasing agent (CORM-A1) and nitrite. The antioxidant resveratrol abolished TNF-α/CHX-induced increase in ROS production and caspase-3/7 activity, but apoptosis was only partially prevented. MODE-K cells are sensitive to TNF-α-induced apoptosis in the presence of CHX, which is associated with increased intracellular ROS production and caspase-3/7 activation. The effects were partially mitigated by CORM-A1, nitrite and resveratrol.

Conclusions. Thus, these agents could be of potential use in protecting the epithelial barrier against oxidative stress during intestinal ischemia/reperfusion injury.

III.2 Introduction

Sepsis is an infection with a systemic inflammatory response syndrome, that can progress to multiple organ failure and septic shock. This complex disorder is triggered by an inflammatory cascade initiated by bacteria-derived molecules such as endotoxin, with subsequent formation of endogenous inflammatory cytokines such as tumor necrosis factor (TNF)-α, leading to ischemia/reperfusion, mitochondrial dysfunction and apoptosis (Cinel & Opal, 2009). The gut is a triggering factor in the progression of sepsis (Hassoun *et al.*, 2001a). Severe stress caused by conditions such as major trauma, burns, hemorrhagia and major surgery leads to intestinal ischemia/reperfusion and local production of pro-inflammatory cytokines, that contribute to the systemic inflammation. In addition, ischemia/reperfusion causes disturbance of the intestinal epithelial barrier and bacterial translocation (Balzan *et al.*, 2007), which is facilitated by impairment of bowel motility (ileus) (Hassoun *et al.*, 2001b). The mechanism of sepsis-induced ileus, assessed by injecting endotoxins in animal models, shows similarity to postoperative ileus occurring after abdominal surgery, as endotoxin exposure or intestinal manipulation results in activation of the resident macrophages in the intestinal muscle, leading to production of pro-inflammatory cytokines such as TNF-α, chemokines and adhesion molecules. The latter are essential for further recruitment of circulatory leukocytes into the intestinal muscularis (De Winter & De Man, 2010). The mucosal layer seems a victim rather than an instigator in the pathogenesis of ileus.

Notably, in a mouse model of postoperative ileus we recently reported an early and transient increase in oxidative stress in the mucosal layer, with a peak value at 1 h after intestinal manipulation, preceding the peak in the muscularis (De Backer *et al.*, 2009). The combination of oxidative stress-induced epithelial cell damage, increased intestinal permeability and translocation of intraluminal endotoxins might trigger the muscular inflammation (Anup *et al.*, 1999); TNF-α may play a role in this epithelial distress. When combined with the protein synthesis inhibitor cycloheximide (CHX), TNF-α was shown to initiate apoptosis in isolated gastrointestinal epithelial cells (Bhattacharya *et al.*, 2003; Pajak *et al.*, 2005). Moreover, TNF-α/CHX-induced oxidative stress has been implicated in intestinal epithelial cell apoptosis (Jin *et al.*, 2008). To our knowledge, no *in vitro* study has yet fully explored TNF-α/CHX-induced apoptosis in a murine epithelial cell line. The murine intestinal epithelial cell line MODE-K is an undifferentiated cell line, which has the advantage

of not being derived from tumor tissue, but from the duodenum-jejunum from normal young mice. Hence, it is considered to be an important model exhibiting phenotypic and functional properties of normal mouse enterocytes (Gopal *et al.*, 2008; Hoffmann *et al.*, 2011). The first aim of our present study was to investigate the relationship between oxidative stress and apoptosis by TNF-α/CHX in MODE-K cells.

Heme oxygenase (HO) is an ubiquitous rate limiting enzyme that catabolizes heme into ferrous iron, carbon monoxide (CO) and biliverdin, which is subsequently reduced to bilirubin. The stress inducible isoform HO-1, which is upregulated by numerous stimuli including oxidative stress and pro-inflammatory cytokines (Abraham & Kappas, 2005), serves as a cytoprotective gene by virtue of its potent antioxidant, anti-apoptotic and anti-inflammatory properties (Ryter *et al.*, 2007). Biliverdin and its end product bilirubin are potent antioxidants and were shown to have cytoprotective effects (Ryter *et al.*, 2006; Ryter & Choi, 2009). Accumulating evidence indicates that also CO can mediate many of the biological functions of HO-1 (Ryter *et al.*, 2006). Accordingly, CO-releasing molecules (CO-RMs) have been developed to deliver CO in a controllable manner under physiological conditions providing an advantage of reduced risk of systemic toxicity (Alberto & Motterlini, 2007; Motterlini, 2007; Motterlini & Otterbein, 2010). The water soluble CO-RMs (CORM-3 and CORM-A1) (Clark *et al.*, 2003; Motterlini *et al.*, 2005) have gained increasing interest recently due to their promising pharmacological properties as carriers of therapeutic doses of CO in models of disease including gastrointestinal disorders (Megias *et al.*, 2007; Sun *et al.*, 2007). Indeed, in a murine model of postoperative ileus, we have shown that the "fast" CO releaser CORM-3 markedly reduced the manipulation-induced inflammation of the muscularis and improved surgically induced intestinal dysmotility. This was accompanied by reduction of the early oxidative burst in the mucosa (De Backer *et al.*, 2009). The second aim of our present study was therefore to investigate the influence of HO-1-related products (bilirubin, biliverdin and CO-RMs) on the oxidative/apoptotic response of the MODE-K cell line to TNF-α/CHX. For comparison, several agents that are known to reduce the excessive production of reactive oxygen species (ROS) were also tested: apocynin and diphenylene iodonium (DPI), which can inhibit nicotinamide adenine dinucleotide phosphate (NADPH) oxidase activity; nitrite, that can inhibit mitochondrial ROS production (Shiva *et al.*, 2007); Mito-TEMPO, a mitochondria-targeted antioxidant; and dimethyloxallyl glycine (DMOG), a prolyl hydroxylase inhibitor, that attenuates hypoxia-induced intestinal mucosal

inflammation (Morote-Garcia *et al.*, 2009) and decreases hypoxia-induced ROS production in a human synovial cell line (Biniecka *et al.*, 2011). Finally, resveratrol, a cytoprotective bioactive polyphenol present in red wine, was tested given its potential to attenuate intestinal ischemia/reperfusion injury (Ozkan *et al.*, 2009) and its HO-1 related neuroprotective action against stroke (Sakata *et al.*, 2010).

III.3   Materials and methods

III.3.1 *Chemicals and reagents*

Bilirubin, biliverdin (biliverdin IX hydrochloride) and cobalt protoporphyrin IX (CoPP) were purchased from Frontier Scientific Europe Ltd. (Carnforth, UK). 2-(2,2,6,6-tetramethylpiperidin-1-oxyl-4-ylamino)-2-oxoethyl triphenylphosphonium chloride monohydrate (Mito-TEMPO) was purchased from Enzo Life Sciences. Apocynin, cycloheximide, DMOG, dimethyl sulfoxide (DMSO), DPI, nitrite (as sodium nitrite), propidium iodide (PI), resveratrol and ribonuclease-A were obtained from Sigma (St. Louis, MO, USA). Recombinant murine TNF-α was purchased from R&D system (Minneapolis, MN, USA). Fetal bovine serum, Dulbecco's modified Eagle's medium (DMEM), penicillin/streptomycin, and glutamax were obtained from Gibco BRL (Grand Island, NY, USA). All other chemicals were reagent grade and obtained from Sigma unless otherwise stated.

III.3.2 *Cell culture*

The mouse small intestinal epithelial cell (IEC) line, MODE-K (a generous gift from Dr. Ingo B. Autenrieth, University of Tübingen, Germany) was used in our study. These are small IECs from C3H/HeJ mice immortalized by simian virus (SV)-40 large T gene transfer, exhibiting morphological and phenotypic characteristics of normal enterocytes (Vidal *et al.*, 1993). MODE-K cells (passage 10–35) were cultured in high-glucose DMEM supplemented with 10% fetal bovine serum, 2 mM L-glutamine, and 5% penicillin/streptomycin. Cultures were maintained in a humidified 5% CO_2 atmosphere at 37°C and experiments were conducted on cells at approximately 80-90% confluence. MODE-K cells were seeded at either 3.5 x 10^5 cells per 2 ml of culture medium containing 10% serum in a six-well plate (for apoptosis assay) or at 1 x 10^4 cells per 200 µl of culture medium in a 96-well microtiter plate

(for all other assays), grown for 36 h and then serum starved overnight. On day 3, cells were treated with various concentrations of TNF-α/CHX for 0-6 h. Test drugs were pre-incubated for 1 h followed by co-incubation of drugs with various concentrations of TNF-α/CHX for 3-6 h, with the exception of CoPP that was incubated for 3 h from 24 h till 21 h before exposure to TNF-α/CHX. The influence of test drugs alone on cell viability was studied on day 3 by incubating MODE-K cells for 12 h.

III.3.3 Determination of cell viability

Cell viability was assessed by luminescent cell viability assay with CellTiter-Glo (Promega, Madison, WI, USA) according to the manufacturer's protocol. This assay determines the number of viable cells in culture based on quantitation of ATP present, an indicator of metabolically active cells. Briefly, MODE-K cells were plated into 96-well plates and treated as described under cell culture. At the end of the incubation period with agents on day 3, an equivolume of the luminescent substrate and lysis buffer mix from the assay kit was added. The mixture was transferred to an opaque 96-well plate and luminescence was recorded using a GloMax Microplate Luminometer (Promega). The index of cellular viability was calculated as percentage of luminescence with respect to untreated control cells.

III.3.4 Measurement of caspase-3/7 activity

Caspase-3/7 activity was determined using the chemiluminescent Caspase-Glo 3/7 Assay (Promega, Madison, WI, USA) according to the manufacturer's instructions. The assay provides a luminogenic caspase-3/7 substrate, which contains the tetrapeptide sequence DEVD, in a reagent optimized for caspase activity, luciferase activity, and cell lysis. Briefly, MODE-K cells were plated into 96-well plates and treated as described under cell culture. After incubation, an equivolume of luminescent caspase-3/7 Glo substrate buffer was then added followed by gentle agitation for 30 min. The mixture was transferred to an opaque 96-well plate and luminescence was recorded using a GloMax Microplate Luminometer (Promega). Relative luminescence units were noted and the results are expressed as percentage of luminescence with respect to untreated control.

III.3.5 Flow cytometry analysis of apoptosis

Cellular DNA content and apoptosis were analyzed by flow cytometry as described previously (Nicoletti *et al.*, 1991). This assays is based on the principle that the apoptotic cells with degraded DNA appear as cells with hypodiploid DNA content and are represented in so-called "sub-G1" peaks on DNA histograms. Briefly, cells were plated into six-well plates and after treatment for the indicated time, the cells were rinsed with PBS, harvested and then fixed by the progressive addition of ice-cold 70% ethanol. The fixed cells were washed twice with PBS before staining with PI at 100 µg/ml and RNase at 50 µg/ml in PBS for 20 min. Cell viability was determined by flow cytometry (FACSCalibur, BD Bioscience, NJ) and CellQuest software (Becton Dickinson, San Jose, CA, USA). Cell debris was excluded from analysis by appropriate raising of the forward scatter threshold. The percentage of cells that had undergone apoptosis was assessed to be the ratio of the fluorescent area smaller than the G_0-G_1 peak to the total area of fluorescence. The average of the results from at least three samples for each experimental condition is presented.

III.3.6 Measurement of intracellular reduced glutathione (GSH) levels

The intracellular content of reduced glutathione (GSH) was quantified using the bioluminescent GSH-Glo Glutathione Assay (Promega, Madison, WI, USA), essentially as recommended by the supplier. In brief, MODE-K cells were plated into 96-well plates and treated with TNF-α/CHX ± test drugs as described above. After incubation, adherent cells were directly lysed in 100 µl GSH-Glo lysis and reaction buffer. After addition of 100 µl GSH-Glo Luciferin detection reagent, the mixture was transferred to an opaque 96-well plate and luminescence was detected using a GloMax Microplate Luminometer (Promega). The GSH levels of treated cells are expressed as percentage of the value in untreated control cells.

III.3.7 Measurement of intracellular reactive oxygen species (ROS) generation

The intracellular ROS level was detected using 5-(and-6)-carboxy-2',7'-dichlorodihydrofluorescein diacetate (carboxy-H₂DCFDA) (Molecular Probes, Eugene, OR, USA) as reported (Wang & Joseph, 1999). Carboxy-H₂DCFDA is a cell-permeable indicator for ROS that is nonfluorescent until the acetate groups are removed by intracellular esterases

and oxidation occurs within the cell. When oxidized by various active oxygen species, it is irreversibly converted to the fluorescent form, DCF. The fluorescence generated by DCF is proportional to the rate of carboxy-H_2DCFDA oxidation, which is in turn indicative of the cellular oxidizing activity and intracellular ROS levels. For ROS measurements, briefly, MODE-K cells were plated into black 96-well plates and treated as described. Cells were washed twice in Hanks' balanced salt solution (HBSS) and then incubated in HBSS containing carboxy-H_2DCFDA (10 μM) for 40 min in the dark at 37°C. Fluorescence was measured using an excitation of 485 nm and emission of 530 nm, in a fluorescence plate reader (Wallac EnVision 2101 multilabel reader, Perkin Elmer, Zaventem, Belgium). Basal ROS generation in the cells treated without the stimulus was used as a control.

III.3.8 Western blotting

Total cell extracts were prepared using RIPA buffer and protein concentrations were measured with the BCA protein assay reagent (Pierce). Equal amounts of protein (20 μg) were loaded onto NuPAGE-Novex 4 to 12% Bis-Tris electrophoresis gels (Invitrogen) and blotted onto nitrocellulose membranes (GE Healthcare, Little Chalfont, Buckinghamshire, UK). Membranes were blocked in Tris-buffered saline/0.1% Tween 20 containing 5% nonfat dry milk and incubated overnight with appropriate antibodies for the detection of HO-1 (cat. no. sc-10789, 1:1000; Santa Cruz Biotechnology, Santa Cruz, CA) and β-tubulin (cat. no. ab6046, 1:1000; Abcam, Cambridge, UK). Horseradish peroxidase-linked secondary antibodies (Cell Signaling Technology Inc., Danvers, MA) were visualized by use of Amersham ECL Prime Substrate (GE Healthcare Life Sciences). Densitometry of the bands was performed using Image J software (National Institutes of Health, Bethesda, MD).

III.3.9 Statistical analysis

All data were expressed as mean ± SEM. Comparison of the means was performed using the Student's t-test for two groups of data and ANOVA followed by Bonferroni's multiple comparison test for comparison of more than two groups. Differences were considered to be significant at $P < 0.05$.

III.4   Results

III.4.1   Influence of TNF-α/CHX on cell viability

The aim of the first set of experiments was to assess the sensitivity of MODE-K cells to the cytotoxic effect of TNF-α by testing its influence on cell viability. TNF-α is a cytokine inducing apoptosis but many cell lines only undergo apoptosis when TNF-α is combined with an agent such as CHX. Previous observations in MODE-K cells showed that TNF-α *per se* in concentrations up to 10 ng/ml and incubated for up to 24 h did not induce cell death (Bharhani *et al.*, 2006). We therefore first tested the apoptotic stimulus used in other intestinal epithelial cell lines (20 ng/ml TNF-α plus 25 μg/ml CHX) (Bhattacharya *et al.*, 2003; Naugler *et al.*, 2008; Greenspon *et al.*, 2009). Incubation of MODE K-cells for 6 h with this combination decreased cell viability to 10% of untreated cells, while neither agent alone influenced cell viability, the latter corresponding to data with the same concentrations of both agents in rat IEC-6 cells (Bhattacharya *et al.*, 2003). As preliminary experiments showed that the very pronounced effect of 20 ng/ml TNF-α plus 25 μg/ml CHX on cell viability was not influenced by any of the HO-1 related products, lower concentrations of TNF-α were investigated, in combination with either 25 or 10 μg/ml CHX, as 10 μg·/ml CHX is also often used in combination with TNF-α in cell lines (Johnson & Boise, 1999; Basuroy *et al.*, 2006; Birbes *et al.*, 2006). This showed a high sensitivity of MODE-K cells to TNF-α/CHX as 0.1-1 ng/ml TNF-α together with 10 μg/ml CHX induced a concentration-dependent decrease in cell viability (to 54 ± 3% at 0.1 ng/ml and 22 ± 1% at 1 ng/ml TNF-α, Fig. III.1A), the effect with 1 ng/ml TNF-α plus 10 μg/ml CHX being close to that of 20 ng/ml TNF-α plus 25 μg/ml CHX. The concentration range of 0.1-1 ng/ml TNF-α was therefore studied in the assays for caspase-3/7 activity, apoptosis and oxidative stress.

III.4.2   Influence of TNF-α/CHX on caspase-3/7 activity and apoptotic cell death

The combination of TNF-α/CHX for 6 h induced an increase in caspase-3/7 activity in a concentration-dependent manner (Fig. III.1B). TNF-α (0.1 ng/ml) plus CHX (10 μg/ml) increased caspase-3/7 activity by 3.6 fold when compared to control while TNF-α (1 ng/ml) plus CHX (10 μg/ml) increased the caspase-3/7 activity by nearly 5 fold. Concomitantly,

Fig. III.1 Influence of 0.1-1 ng/ml TNF-α plus 10 µg/ml CHX and of 20 ng/ml TNF-α plus 25 µg/ml CHX, incubated for 6 h, on cell viability (as % of control; A), caspase-3/7 activity (as % of control; B), and apoptosis (C). Control cells were incubated with serum free medium alone. Mean ± SEM of six independent experiments. *$P < 0.05$ versus control. D: Influence of 1 ng/ml TNF-α plus 10 µg/ml CHX, incubated for 0-6 h, on apoptosis. Mean ± SEM of three independent experiments. *$P < 0.05$ versus untreated (0 h) control group.

flow cytometric analysis of PI-stained cells for apoptosis showed that TNF-α induced a concentration-dependent apoptotic cell death (Fig. III.1C). In both assays, the result with 1 ng/ml TNF-α plus 10 µg/ml CHX approached that obtained with 20 ng/ml TNF-α plus 25 µg/ml CHX studied in comparison. To evaluate the kinetics of TNF-α/CHX-induced apoptosis, MODE-K cells were incubated with 1 ng/ml TNF-α plus 10 µg/ml CHX for 0-6 h.

Induction of apoptosis began after exposure to TNF-α/CHX for 2 h and increased further in a time-dependent manner (Fig. III.1D).

III.4.3 Influence of TNF-α/CHX on reduced glutathione (GSH) and reactive oxygen species (ROS) levels

As a sequential pathway of "*ROS production → caspase-3 activity → apoptosis*" has been proposed for TNF-α/CHX-induced cell death in rat IEC-6 cells (Jin *et al.*, 2008), TNF-α/CHX-induced oxidative stress in MODE-K cells was assessed by measurement of intracellular ROS generation and of the classic antioxidant GSH. Incubation of MODE-K cells with 0.1-1 ng/ml TNF-α plus 10 μg/ml CHX for 3 h did not influence GSH levels, while 20 ng/ml TNF-α plus 25 μg/ml CHX significantly decreased the GSH level to 62 ± 2% of untreated cells (Fig. III.2A). However, after 6 h of exposure, TNF-α/CHX reduced cellular GSH levels in a concentration-dependent manner, with 0.1 and 1 ng/ml TNF-α decreasing GSH levels to 69 ± 3% and 44 ± 2%, respectively. TNF-α (20 ng/ml) plus CHX (25 μg/ml) added for 6 h decreased the GSH level to 21 ± 1%.

Incubation of cells with TNF-α/CHX for 3 h also induced a concentration-dependent increase in ROS production (Fig. III.2B). When co-incubated with 10 μg/ml CHX, 0.1 and 1 ng/ml TNF-α increased ROS production to 2.73 fold and 4.52 fold, respectively, compared to control. A time-course experiment with 1 ng/ml TNF-α plus 10 μg/ml CHX showed an increase in ROS production starting at 2 h (Fig. III.2C) illustrating that the increase in ROS production paralleled the induction of apoptosis.

III.4.4 Effects of HO-1 and antioxidant-related products on TNF-α/CHX-induced decrease in cell viability

To determine the highest concentration of the HO-1 and antioxidant-related products that was not cytotoxic *per se*, MODE-K cells were incubated with increasing concentrations of each compound for 12 h (n = 3 for each compound, data not shown). This concentration was then tested on the decrease in cell viability by 0.1-1 ng/ml TNF-α plus 10 μg/ml CHX to screen for the protective effects versus the cytotoxic action of TNF-α/CHX.
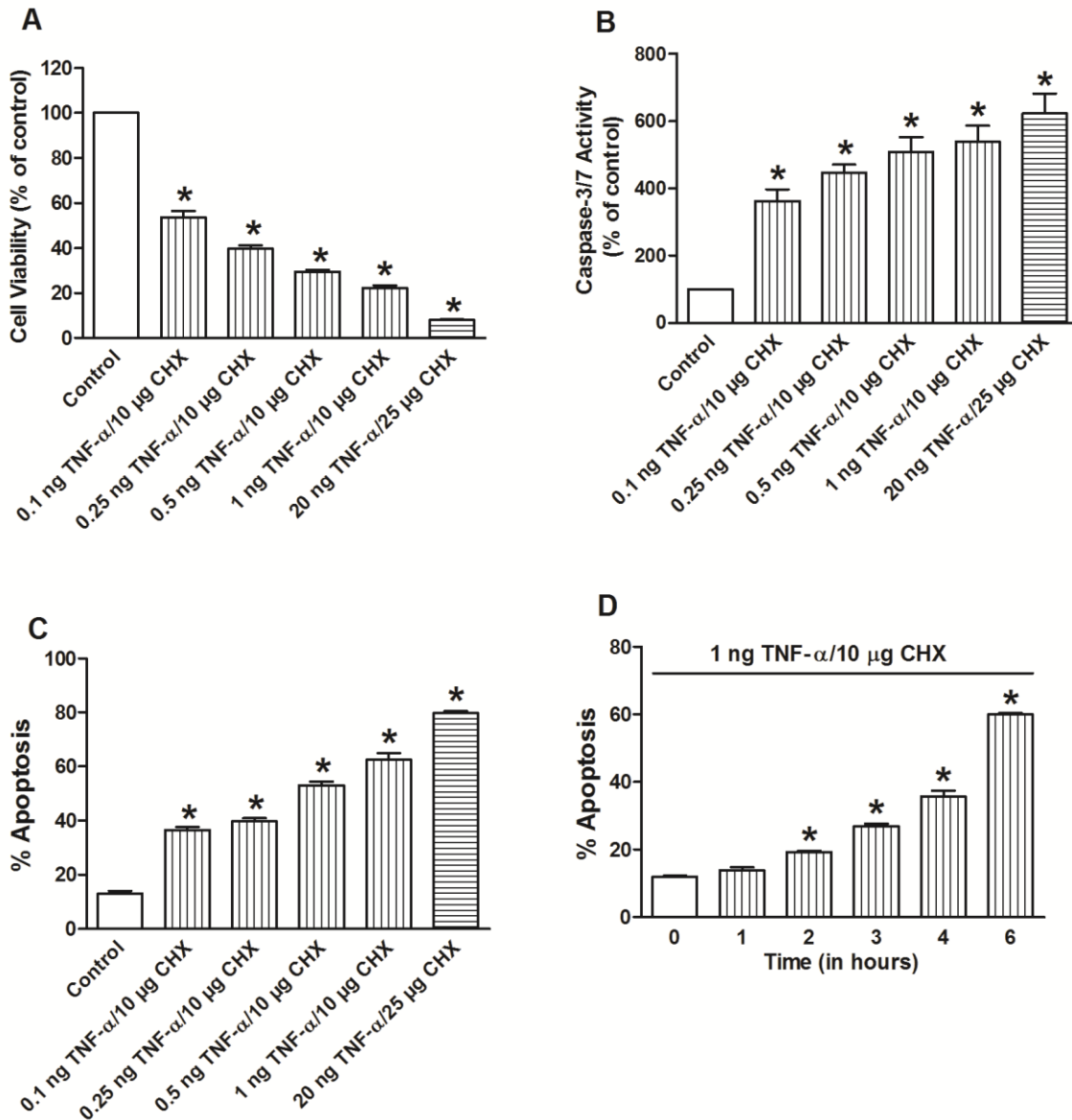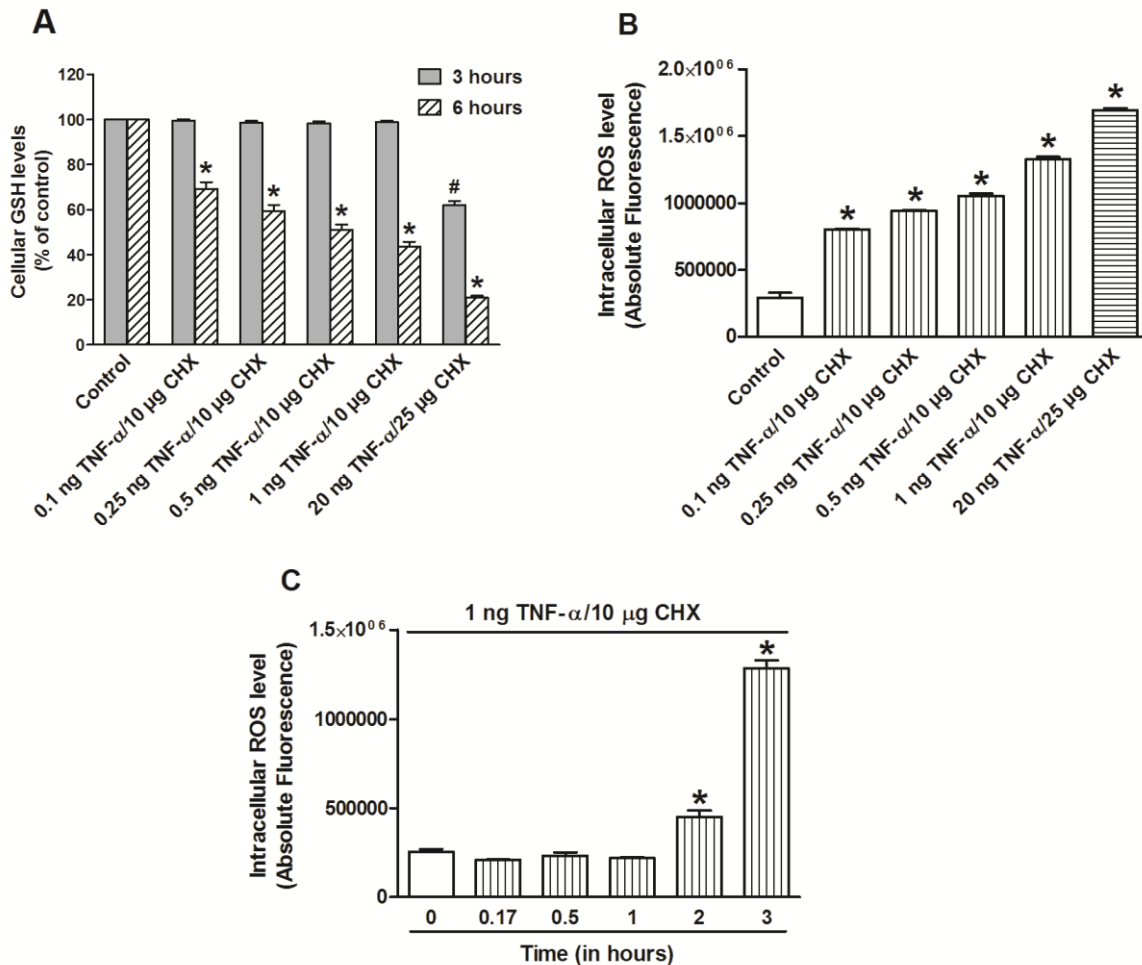
Fig. III.2   Influence of 0.1-1 ng/ml TNF-α plus 10 μg/ml CHX and of 20 ng/ml TNF-α plus 25 μg/ml CHX, incubated for 3 h (A, B) or 6 h (A), on cellular glutathione (GSH; as % of control; A) and intracellular ROS levels (B). Control cells were incubated with serum free medium alone. Mean ± SEM of six (A) or two (B) independent experiments. [#]P < 0.05 versus control (for 3 h). *P < 0.05 versus control (for 6 h). C: Influence of 1 ng/ml TNF-α plus 10 μg/ml CHX, incubated for 0-3 h, on intracellular ROS levels. Mean ± SEM of two independent experiments. *P < 0.05 versus untreated (0 h) control group.

As for the HO-1 related products, 100 μM of bilirubin and 3 μM of biliverdin did not influence TNF-α/CHX-induced decrease in cell viability (data not shown), but 1 μM of bilirubin partially protected against 0.1 and 0.25 ng/ml TNF-α/CHX (Fig. III.3A). CORM-A1 (100 μM) and CORM-3 (100 μM) induced significant partial protection from cell death at all concentrations of TNF-α/CHX tested (Fig. III.3B and C). The most effective CORM (CORM-A1) and the low concentration of bilirubin were selected for further study.

With regard to the antioxidant-related products, apocynin (250 μM), Mito-TEMPO (1 μM) and DMOG (500 μM) did not influence the decrease in cell viability by TNF-α/CHX (data not shown). However, DPI (100 μM) showed prevention from TNF-α-induced

cytotoxicity at 0.1-0.5 ng/ml TNF-α/CHX, while nitrite (10 mM) showed cytoprotection at all tested concentrations of TNF-α/CHX (Fig. III.3D and E). The most effective agent was resveratrol (75 µM), which completely prevented cell death by 0.1 ng/ml TNF-α/CHX and restored cell viability in the presence of 1 ng/ml TNF-α/CHX from 22 ± 1% to 65 ± 3% (Fig. III.3F). On the basis of these results, nitrite (10 mM) and resveratrol (75 µM) were selected to further examine the relation between their influence on TNF-α/CHX-induced oxidative stress and on TNF-α/CHX-induced apoptosis.

III.4.5 Effects of bilirubin, CORM-A1, nitrite and resveratrol on TNF-α/CHX-induced changes in caspase-3/7 activity and apoptosis

Treatment with 1 µM bilirubin, 100 µM CORM-A1, 10 mM nitrite or 75 µM resveratrol significantly attenuated the TNF-α/CHX-induced increase in caspase-3/7 activity at all tested concentrations of TNF-α (Fig. III.4A-D). Among these agents, nitrite and resveratrol showed a more pronounced decrease of the induced caspase activities compared to bilirubin or CORM-A1.

The anti-apoptotic effect was tested versus 0.1 and 1 ng/ml TNF-α/CHX. Bilirubin was not effective in preventing the apoptotic cell death at both tested TNF-α concentrations, while CORM-A1, nitrite and resveratrol partially prevented the apoptotic cell death induced by the two tested concentrations of stimulus (Fig. III.5A-D). The results with bilirubin illustrate that inhibition of TNF-α/CHX-induced caspase-3/7 activity does not necessarily result in a reduction of TNF-α/CHX-induced apoptosis.

III.4.6 Effects of bilirubin, CORM-A1, nitrite and resveratrol on TNF-α/CHX-induced changes in GSH levels and ROS production

The effect of the various agents on cellular levels of GSH were measured in the presence of TNF-α/CHX for 6 h. TNF-α (0.1-1 ng/ml) plus CHX significantly reduced cellular GSH levels while pretreatment with 1 µM bilirubin, 100 µM CORM-A1, 10 mM nitrite or 75 µM resveratrol partially prevented this effect (Fig. III.6A-D). We next investigated whether any of these agents could suppress TNF-α/CHX-induced ROS production by direct measurement of carboxy-H$_2$DCFDA-derived fluorescence. TNF-α (1 ng/ml) plus CHX increased the ROS
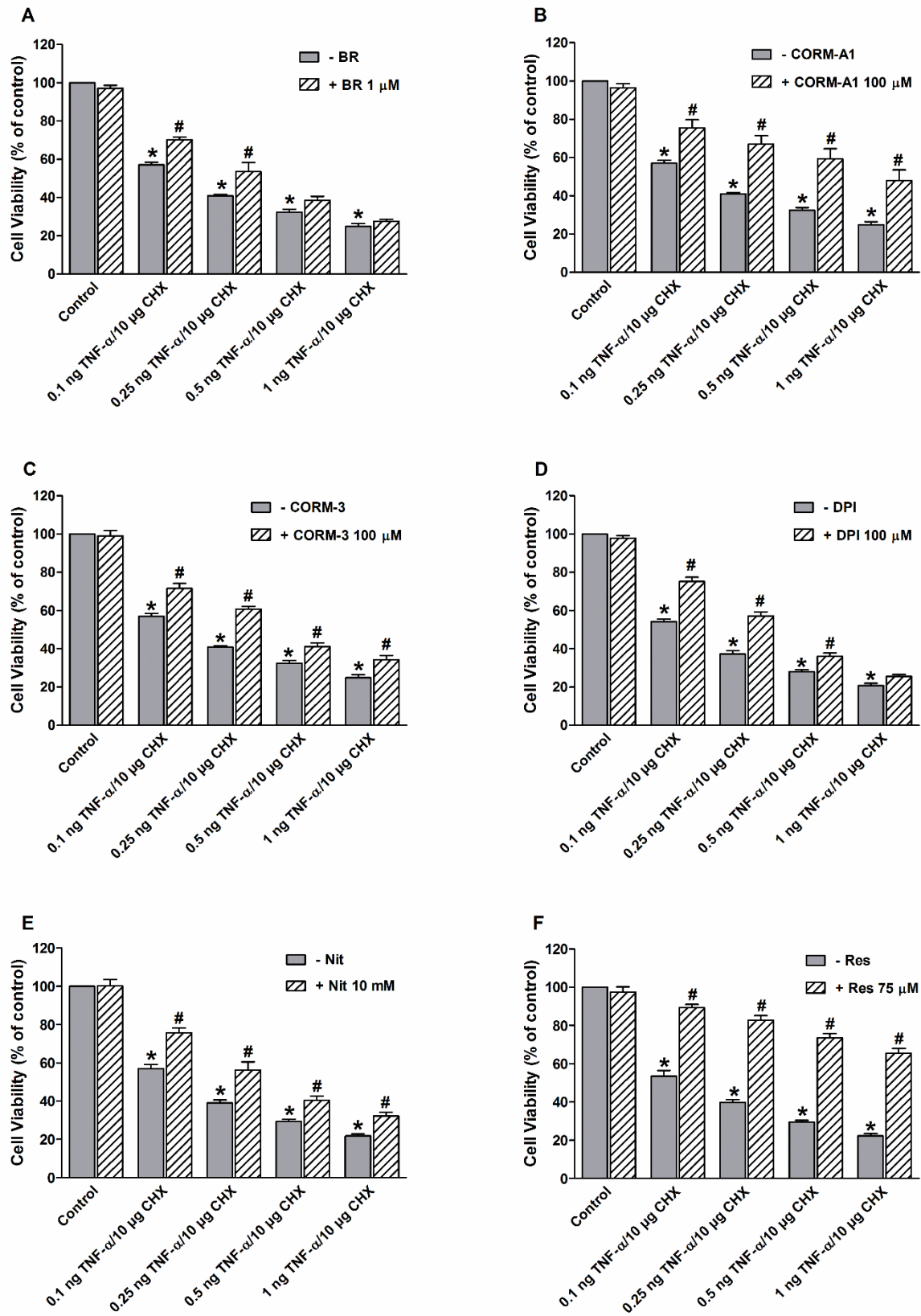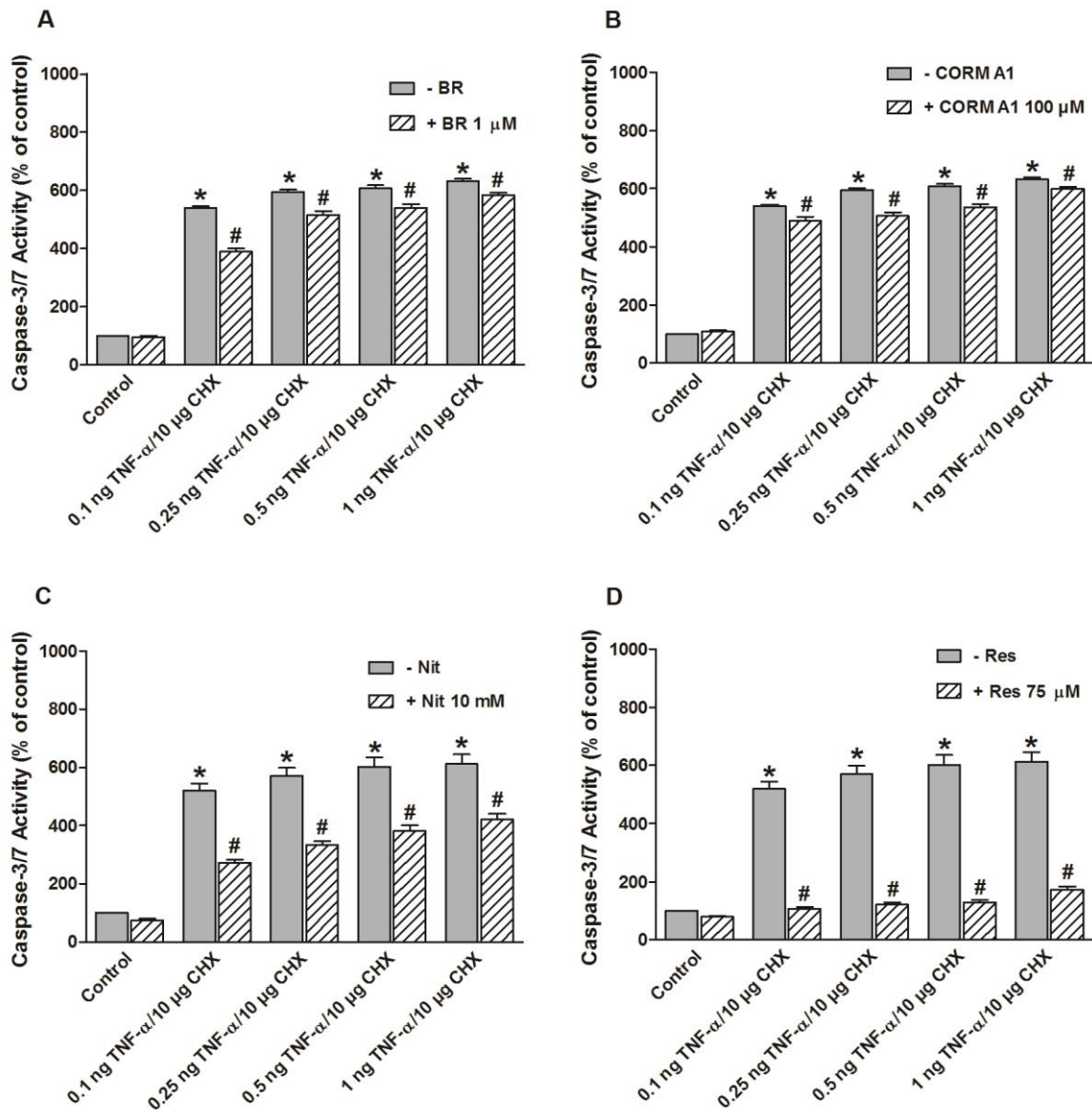
Fig. III.4 Influence of 0.1-1 ng/ml TNF-α plus 10 μg/ml CHX, incubated for 6 h, on caspase-3/7 activity (as % of control) in the absence and presence of 1 μM bilirubin (BR, A), 100 μM CORM-A1 (B), 10 mM nitrite (Nit, C) or 75 μM resveratrol (Res, D). Control cells were incubated with serum free medium alone. Mean ± SEM of six independent experiments. *$P < 0.05$ versus control. [#]$P < 0.05$ versus corresponding group with TNF-α/CHX alone.

Fig. III.3 Influence of 0.1-1 ng/ml TNF-α plus 10 μg/ml CHX, incubated for 6 h, on cell viability (as % of control) in the absence and presence of 1 μM bilirubin (BR, A), 100 μM CORM-A1 (B), 100 μM CORM-3 (C), 100 μM diphenylene iodonium (DPI, D), 10 mM nitrite (Nit, E) or 75 μM resveratrol (Res, F). Control cells were incubated with serum free medium alone. Mean ± SEM of six independent experiments. *$P < 0.05$ versus control. [#]$P < 0.05$ versus corresponding group with TNF-α/CHX alone.

production by 4.63 fold compared to control, which was reduced to 3.51 fold by bilirubin, 2.93 fold by CORM-A1, and 3.57 fold by nitrite (Fig. III.7). On the other hand, resveratrol completely abolished the TNF-α/CHX-induced increase in ROS production. The results with CORM-A1, nitrite and resveratrol suggest that inhibition of TNF-α/CHX-induced ROS production can contribute to the anti-apoptotic effects of these compounds in MODE-K cells.

III.4.7 Effects of bilirubin, CORM-A1, nitrite and resveratrol on TNF-α/CHX-induced changes in HO-1 protein expression

As induction of the expression of endogenous HO-1 has been suggested to contribute to the cytoprotective effects of CO-RMs and resveratrol (Kim *et al.*, 2007; Sakata *et al.*, 2010), the expression of HO-1 was assessed by Western blotting. In MODE-K cells, the baseline HO-1 protein level was significantly decreased by 1 ng/ml TNF-α/CHX (Fig. III.8). The HO-1 inducer CoPP (10 μM) (Tsoyi *et al.*, 2009), used as a positive control, increased HO-1 expression markedly both in the absence and presence of TNF-α/CHX. Treatment with 1 μM bilirubin, 100 μM CORM-A1 or 10 mM nitrite did not affect basal HO-1 expression; in co-presence with TNF-α/CHX, the HO-1 level was not significantly different from that with TNF-α/CHX alone. Notably, 75 μM resveratrol *per se* induced HO-1 expression significantly to 1.63 fold as compared to the basal level. However, pretreatment of 75 μM resveratrol did not prevent the TNF-α/CHX-induced decrease in HO-1 protein expression. The results illustrate that HO-1 expression does not contribute to the cytoprotective effect of CORM-A1, nitrite and resveratrol in MODE-K cells.

III.5   Discussion

The aim of this study was 1) to investigate the oxidative and apoptotic effects of TNF-α/CHX in the murine MODE-K epithelial cell line and 2) to evaluate the influence of HO-1 and antioxidant-related products on the oxidative/apoptotic response to TNF-α/CHX in MODE-K cells.
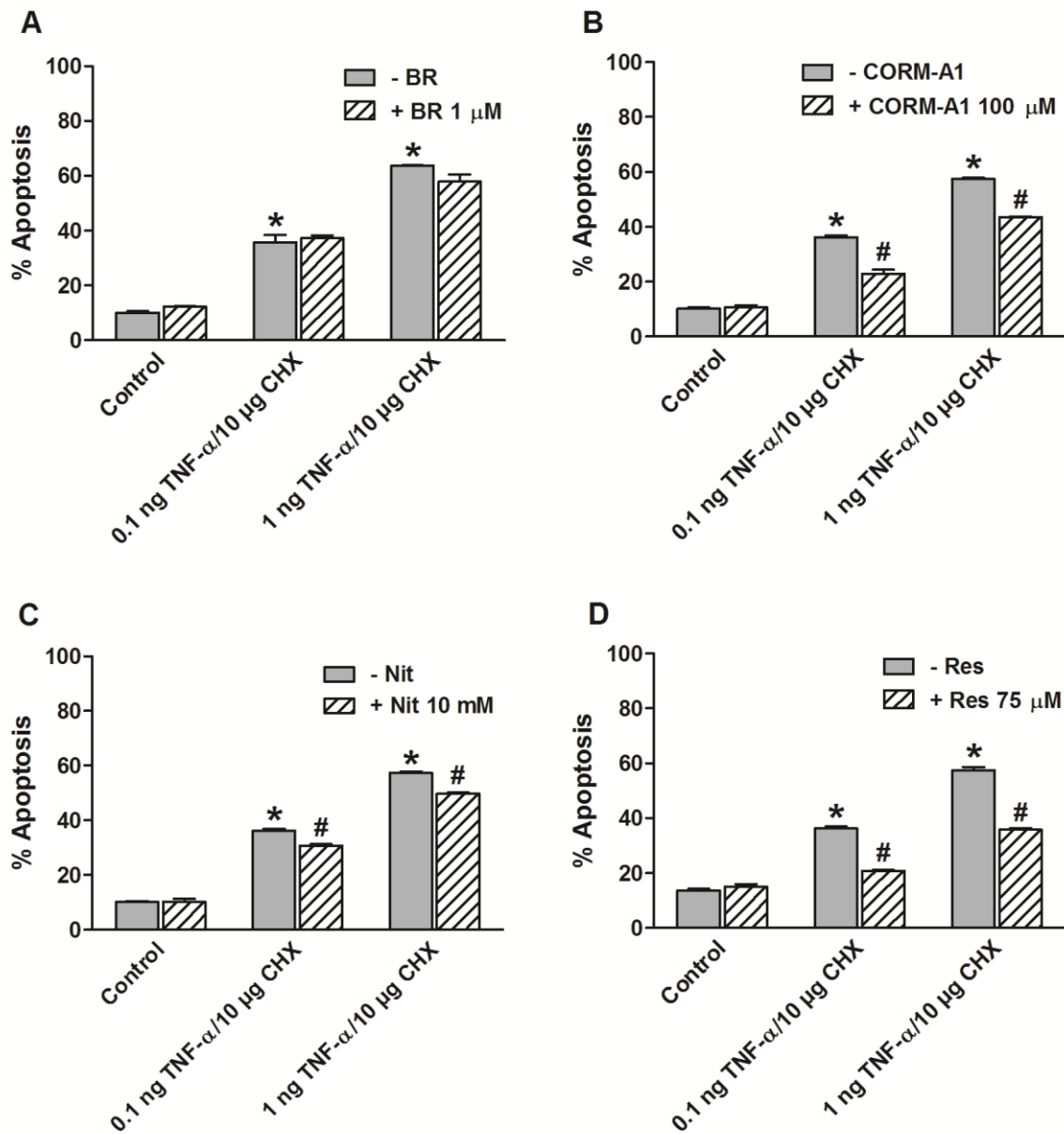
Fig. III.5 Influence of 0.1 and 1 ng/ml TNF-α plus 10 µg/ml CHX, incubated for 6 h, on apoptosis in the absence and presence of 1 µM bilirubin (BR, A), 100 µM CORM-A1 (B), 10 mM nitrite (Nit, C) or 75 µM resveratrol (Res, D). Control cells were incubated with serum free medium alone. Mean ± SEM of three independent experiments. *$P < 0.05$ versus control. #$P < 0.05$ versus corresponding group with TNF-α/CHX alone.

III.5.1 Induction of oxidative stress and cell death in MODE-K cells by TNF-α

The study showed that the MODE-K IEC line is highly sensitive to the cytotoxic effects of TNF-α with CHX, 0.1 ng/ml TNF-α plus 10 µg/ml CHX halving cell viability and 1 ng/ml TNF-α
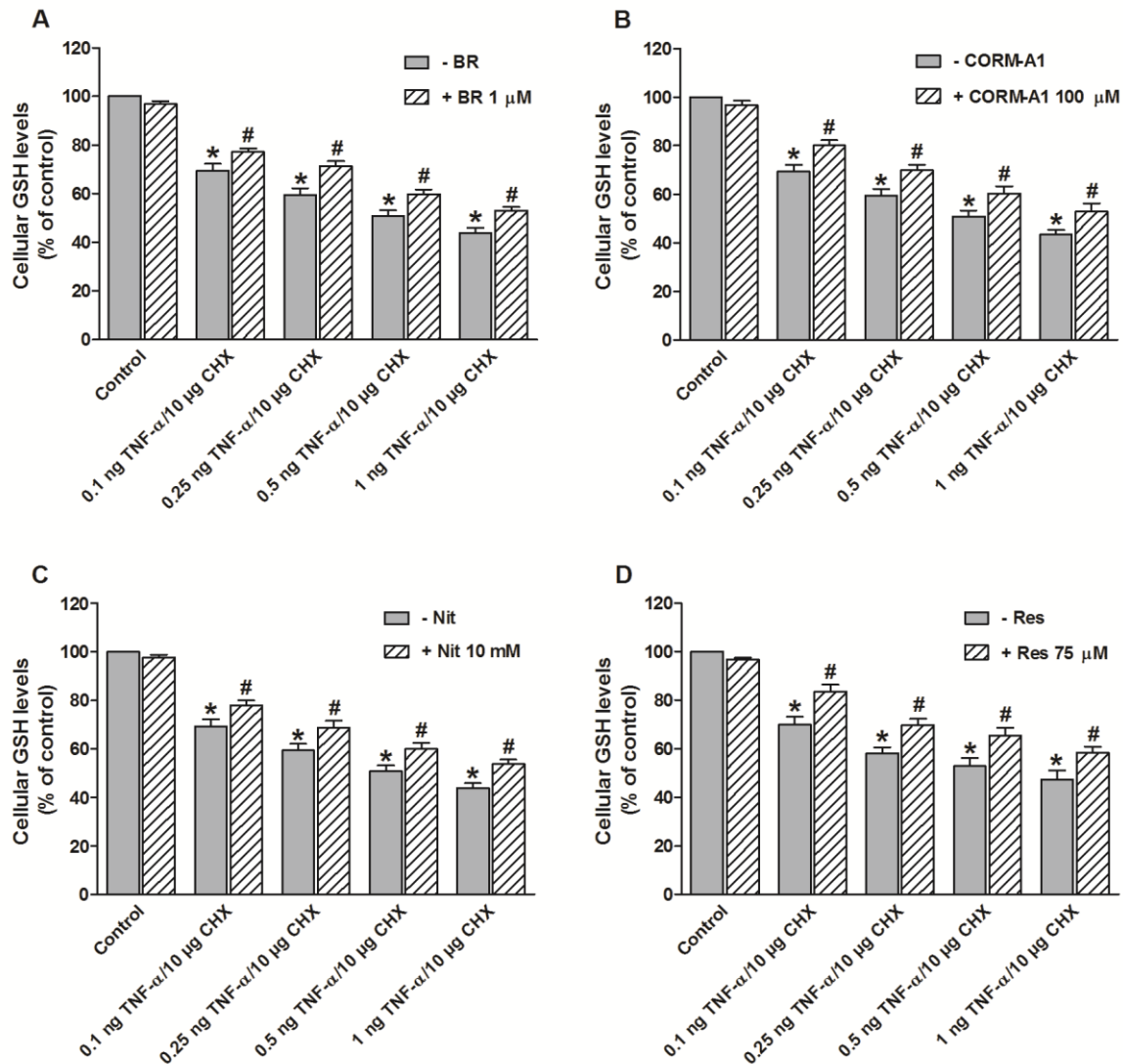
Fig. III.6 Influence of 0.1-1 ng/ml TNF-α plus 10 μg/ml CHX, incubated for 6 h, on cellular glutathione (GSH; as % of control) in the absence and presence of 1 μM bilirubin (BR, A), 100 μM CORM-A1 (B), 10 mM nitrite (Nit, C) or 75 μM resveratrol (Res, D). Control cells were incubated with serum free medium alone. Mean ± SEM of six independent experiments. *$P < 0.05$ versus control. #$P < 0.05$ versus corresponding group with TNF-α/CHX alone.

plus 10 μg/ml CHX reducing cell viability to values close to that by 20 ng/ml TNF-α plus 25 μg/ml CHX. The concentration range 0.1-1 ng/ml corresponds to TNF-α concentrations observed in mice under pathophysiological conditions of sepsis or postoperative ileus. After injection of endotoxin, circulatory peak levels of 0.78 and 2.11 ng/ml TNF-α have been reported (Copeland *et al.*, 2005; Königsrainer *et al.*, 2011); in mesenteric lymph derived from the gastrointestinal tract, still higher and more sustained TNF-α levels of approximately 3 ng/ml were observed (Königsrainer *et al.*, 2011). After intestinal manipulation, a TNF-α level
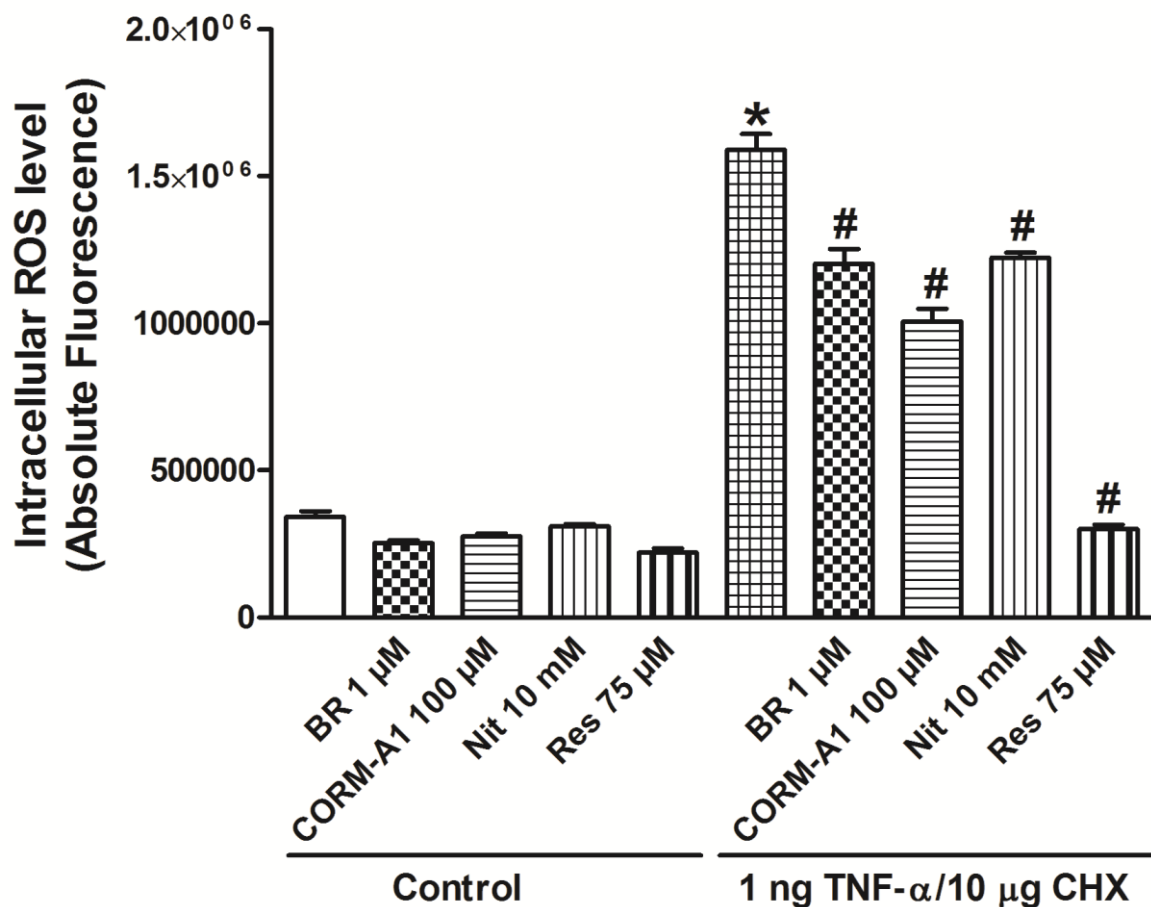
Fig. III.7 Influence of 1 ng/ml TNF-α plus 10 μg/ml CHX, incubated for 3 h, on intracellular ROS levels (as measured by DCF fluorescence) in the absence and presence of 1 μM bilirubin (BR), 100 μM CORM-A1, 10 mM nitrite (Nit) or 75 μM resveratrol (Res). Control cells were incubated with serum free medium alone. Mean ± SEM of four independent experiments. *$P < 0.05$ versus control. [#]$P < 0.05$ versus 1 ng/ml TNF-α plus 10 μg/ml CHX alone.

of 0.08 ng/ml was obtained in peritoneal lavage fluid (Lubbers *et al.*, 2009) and of 2 ng/ml/mg in the supernatant of exteriorized and cultured muscularis layer (Schmidt *et al.*, 2012).

TNF-α/CHX-induced apoptosis occurred in parallel with ROS production. TNF-α (0.1-1 ng/ml) plus CHX treatment for 6 h induced concentration-dependent apoptosis correlating with its influence on cell viability. When studying the time-dependency of 1 ng/ml TNF-α, apoptosis started from 2 h of TNF-α incubation on, and this corresponded with the occurrence of ROS production. The concentration-dependent induction of apoptosis by TNF-α at 6 h was accompanied by a corresponding increase in caspase-3/7 activity, so that the sequence "*ROS production → caspase-3/7 activity → apoptosis*" as reported in rat IEC-6
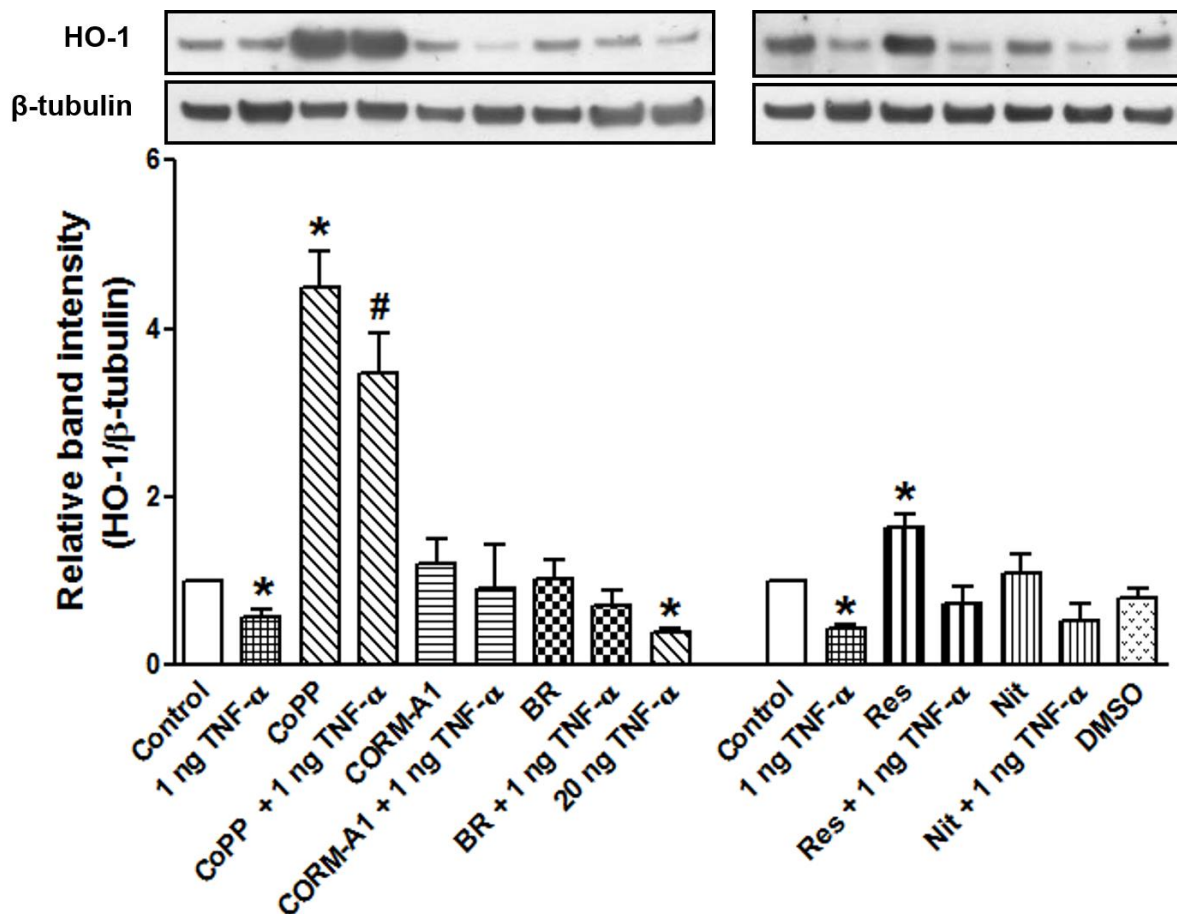
Fig. III.8 Influence of 1 ng/ml TNF-α plus 10 µg/ml CHX, incubated for 3 h, on HO-1 protein expression (relative to β-tubulin) in the absence and presence of 10 µM cobalt protoporphyrin (CoPP), 100 µM CORM-A1, 1 µM bilirubin (BR), 75 µM resveratrol (Res) or 10 mM nitrite (Nit). Control cells were incubated with serum free medium alone. The influence of 20 ng/ml TNF-α plus 25 µg/ml CHX and DMSO, the solvent of Res was also studied. Mean ± SEM of three independent experiments. *$P < 0.05$ versus control. #$P < 0.05$ versus 1 ng·mL^{-1} TNF-α/10 µg·mL^{-1} CHX alone. Representative immunoblots are shown at the top of the figure.

cells (Jin *et al.*, 2008) might also occur in MODE-K cells. The concentration-dependent induction of ROS by TNF-α at 3 h was not paralleled by a decrease in GSH, which only occurred at 6 h. GSH is a potent intracellular antioxidant that attenuates oxidative stress, while cytochrome c is a protein located in the mitochondrial intermembrane space which becomes pro-apoptotic when triggered by increased and sustained ROS production (Yang *et al.*, 1997). Oxidative stress, due to ROS, can cause depletion of GSH levels in the mitochondria leading to the release and oxidation of cytochrome c to the cytosol and subsequent caspase activation. Since reduced GSH in mitochondria is the only defense provided to metabolize peroxides generated from the electron transport chain through the GSH redox cycle (Fernandez-Checa *et al.*, 1998), from our observation, it seems that the

production of ROS in the form of peroxides starts at a later time point (after 3 h) during TNF-α/CHX exposure, while other forms of ROS (hydroxyl radical and superoxide anion) might play a role in earlier apoptosis induction from 2 h of TNF-α/CHX exposure in MODE-K cells.

III.5.2 Influence of HO-1 related products on TNF-α/CHX-induced oxidative stress and apoptosis

At the highest non-cytotoxic concentration used, CORM-3 and more effectively CORM-A1 reduced the decrease of cell viability by TNF-α, while 100 µM bilirubin or 3 µM biliverdin had no effect. However, at much lower concentration (1 µM), bilirubin has been shown to elicit antioxidant effects with significant reduction in ROS production and cell proliferation in human airway smooth muscle cells (Taille *et al.*, 2003). At this concentration, our studies revealed that bilirubin partially prevented cell death induced by the two lower concentrations of TNF-α tested; although partially preventing the 1 ng/ml TNF-α/CHX-induced increase in ROS production and caspase-3/7 activity, bilirubin failed to show any prevention of TNF-α/CHX-induced apoptosis. This is in agreement with a study by Basuroy *et al*. (2006) showing that bilirubin had only a mild effect on TNF-α/CHX-induced apoptosis although it reduced caspase-3 expression in a pronounced way. The mild effect of bilirubin on TNF-α/CHX-induced ROS-production is thus not sufficient to reduce TNF-α/CHX-induced apoptosis; neither is its mild effect on caspase-3/7 activity. The latter can be related to caspase-independent pathways of TNF-α-induced apoptosis as TNF-α has been reported to also induce caspase-independent cell death in a variety of cells like macrophages (Tran *et al.*, 2009), neutrophils (Maianski *et al.*, 2003) and, in particular, HT-29 human adenocarcinoma cells (Wilson & Browning, 2002).

The reduction of TNF-α/CHX-induced caspase-3/7 activity by CORM-A1 was also very mild, but in contrast to bilirubin, CORM-A1 was able to clearly reduce TNF-α/CHX-induced apoptosis. This dissociation can be attributed again to caspase-independent pathways of TNF-α-induced apoptosis. The exact mechanism of the anti-apoptotic effect of CORM-A1 in MODE-K cells remains to be clarified, but our study shows that its anti-apoptotic effect correlates with a reduction in ROS production, which was more pronounced than that observed with bilirubin, as well as an increase in GSH levels. Indeed, caspase-independent

induction of apoptosis by ROS has been reported in PC12 pheochromocytoma cells so that inhibition of ROS production *per se* can be expected to reduce apoptosis (Yuyama *et al.*, 2003). The finding that CORM-A1 exerts significant protection against both TNF-α/CHX-induced oxidative stress and apoptosis supports the notion that CO can mediate the well-known anti-apoptotic effect of HO-1.

CO-RMs were shown to induce HO-1 expression in different types of cells (Sawle *et al.*, 2005; Lee *et al.*, 2006) and this was suggested to contribute to their anti-apoptotic effect (Kim *et al.*, 2007). In thyroid carcinoma cells, HO-1 induction by hemin was shown to protect against TNF-α/CHX-induced apoptosis (Chen *et al.*, 2004). In MODE-K cells in the actual study, basal HO-1 levels were decreased by 3 h exposure to TNF-α plus the protein synthesis inhibitor CHX, although TNF-α alone can reduce endogenous HO-1 expression in some cells (Chae *et al.*, 2006). CoPP, a well-known HO-1 inducer as also confirmed in control MODE-K cells, still clearly induced HO-1 when cells were also incubated with TNF-α/CHX. However, this was not the case with CORM-A1, excluding the possibility that endogenous HO-1 induction contributes to the anti-apoptotic effect of CORM-A1 in MODE-K cells. Correspondingly, exogenous CO protected pancreatic β-cells against TNF-α-induced apoptosis even when HO-1 activity was blocked (Gunther *et al.*, 2002).

III.5.3 Influence of antioxidant related products on TNF-α/CHX-induced oxidative stress and apoptosis

Apocynin is widely used as an NADPH oxidase inhibitor (Stolk *et al.*, 1994) and in Caco-2 cells, it was shown to inhibit polychlorinated biphenyls-induced NADPH oxidase activation and disruption of epithelial integrity (Choi *et al.*, 2010). However, in the present study we found that apocynin did not protect at all MODE-K cells from TNF-α/CHX-induced cytotoxicity. This does not discard the possibility that NADPH oxidase is participating to TNF-α/CHX-induced ROS production in MODE-K cells since the inhibitory effect of apocynin on NADPH oxidase activity has been questioned (Heumüller *et al.*, 2008). Another NADPH oxidase inhibitor, DPI (O'Donnell *et al.*, 1993), partially protected MODE-K cells from TNF-α/CHX-induced cell death at lower concentrations of TNF-α, but not at 1 ng/ml TNF-α.

Mitochondrial ROS has also been implicated in TNF-α-induced cytotoxicity (Schulze-Osthoff *et al.*, 1993). In our study, nitrite but not the mitochondrial-targeted antioxidant

Mito-TEMPO influenced TNF-α/CHX-induced decrease in cell viability of MODE-K cells. The concentration of nitrite (10 mM) used was shown to provide complete rescue of UVA-induced apoptotic cell death in rat aortic endothelial cells (Suschek *et al.*, 2003). We also found that nitrite reduced TNF-α/CHX-induced caspase-3/7 activation. It had a similar influence on TNF-α/CHX-induced ROS production as bilirubin, but in contrast to bilirubin, it also reduced TNF-α/CHX-induced apoptosis. In ischemia/reperfusion injury, nitrite has been shown to act by decreasing mitochondrial ROS generation through inhibition of complex I activity (Shiva *et al.*, 2007). The fluorescent probe, carboxy-H$_2$DCFDA, used in this study as an indicator of generalized oxidative stress is not specific for a single type of ROS like H$_2$O$_2$, peroxynitrite and peroxides (Possel *et al.*, 1997; Afri *et al.*, 2004). Consequently, this probe can detect different ROS types from mitochondria, lipid oxidation and other sources, and the similar degree of ROS reduction by nitrite and bilirubin does not necessarily mean that the same source of ROS is influenced by both agents. A more important role of mitochondrial ROS, rather than ROS from other sources, in the induction of apoptosis, might then explain why nitrite, preferentially reducing mitochondrial ROS production, is able to reduce apoptosis while bilirubin is not.

Despite the fact that hydroxylase inhibitor DMOG has been reported to protect intestinal epithelial cells against TNF-α-induced apoptosis *in vitro* (Cummins *et al.*, 2008) and to decrease hypoxia-induced ROS production in human synovial cells (Biniecka *et al.*, 2011), it failed to prevent TNF-α/CHX-induced cell death in MODE-K cells. Resveratrol, a bioactive polyphenol from red wine, has shown cytoprotection in many models related to interaction with multiple targets, such as, for example, induction of silent mating type information regulator 2 homolog 1 (SIRT-1) (Petrovski *et al.*, 2011). Its attenuating effect on dextran sulfate sodium-induced colitis was also related to SIRT-1 induction (Singh *et al.*, 2010). Recently, induction of HO-1 was implied in the neuroprotective effect of resveratrol against stroke (Sakata *et al.*, 2010). In our study, resveratrol *per se* increased basal HO-1 protein expression in MODE-K cells, but it did not prevent the decrease by TNF-α/CHX excluding HO-1 induction as the mechanism of action for its protective effect versus TNF-α/CHX. In MODE-K cells, resveratrol was by far the most effective cytoprotective agent as it fully abolished TNF-α/CHX-induced ROS production and caspase-3/7 activation; surprisingly, it only reduced apoptosis by approximately 50%. This suggests that TNF-α/CHX-induced apoptosis of MODE-K cells can occur in a ROS- and caspase-3/7-independent way.

In conclusion, these data indicate that mouse intestinal epithelial MODE-K cells are highly sensitive to TNF-α-induced apoptosis in the presence of CHX. TNF-α/CHX-induced apoptosis was accompanied by increased intracellular ROS generation and caspase-3/7 activation. CORM-A1, nitrite and most importantly resveratrol attenuated TNF-α/CHX-induced ROS production, caspase-3/7 activation and apoptosis. These agents might therefore be useful to prevent epithelial damage during ischemia/reperfusion injury.

III.6   References

Abraham NG & Kappas A (2005). Heme oxygenase and the cardiovascular-renal system. *Free Radic Biol Med* **39**, 1-25.

Afri M, Frimer AA, Cohen Y (2004). Active oxygen chemistry within the liposomal bilayer Part IV: Locating 2 ',7 '-dichlorofluorescein (DCF), 2 ',7 '-dichlorodihydrofluorescein (DCFH) and 2 ',7 '-dichlorodihydrofluorescein diacetate (DCFH-DA) in the lipid bilayer. *Chemistry and Physics of Lipids* **131**, 123-133.

Alberto R & Motterlini R (2007). Chemistry and biological activities of CO-releasing molecules (CORMs) and transition metal complexes. *Dalton Trans*, 1651-1660.

Anup R, Aparna V, Pulimood A, Balasubramanian KA (1999). Surgical stress and the small intestine: role of oxygen free radicals. *Surgery* **125**, 560-569.

Balzan S, de Almeida Quadros C, de Cleva R, Zilberstein B, Cecconello I (2007). Bacterial translocation: overview of mechanisms and clinical impact. *J Gastroenterol Hepatol* **22**, 464-471.

Basuroy S, Bhattacharya S, Tcheranova D, Qu Y, Regan RF, Leffler CW *et al.* (2006). HO-2 provides endogenous protection against oxidative stress and apoptosis caused by TNF-alpha in cerebral vascular endothelial cells. *Am J Physiol Cell Physiol* **291**, C897-908.

Bharhani MS, Borojevic R, Basak S, Ho E, Zhou P, Croitoru K (2006). IL-10 protects mouse intestinal epithelial cells from Fas-induced apoptosis via modulating Fas expression and altering caspase-8 and FLIP expression. *Am J Physiol Gastrointest Liver Physiol* **291**, G820-829.

Bhattacharya S, Ray RM, Viar MJ, Johnson LR (2003). Polyamines are required for activation of c-Jun NH2-terminal kinase and apoptosis in response to TNF-alpha in IEC-6 cells. *Am J Physiol Gastrointest Liver Physiol* **285**, G980-991.

Biniecka M, Fox E, Gao W, Ng CT, Veale DJ, Fearon U *et al.* (2011). Hypoxia induces mitochondrial mutagenesis and dysfunction in inflammatory arthritis. *Arthritis Rheum* **63**, 2172-2182.

Birbes H, Zeiller C, Komati H, Nemoz G, Lagarde M, Prigent AF (2006). Phospholipase D protects ECV304 cells against TNFalpha-induced apoptosis. *FEBS Lett* **580**, 6224-6232.

Chae HJ, Chin HY, Lee GY, Park HR, Yang SK, Chung HT *et al.* (2006). Carbon monoxide and nitric oxide protect against tumor necrosis factor-alpha-induced apoptosis in osteoblasts: HO-1 is necessary to mediate the protection. *Clinica Chimica Acta* **365**, 270-278.

Chen GG, Liu ZM, Vlantis AC, Tse GM, Leung BC, van Hasselt CA (2004). Heme oxygenase-1 protects against apoptosis induced by tumor necrosis factor-alpha and cycloheximide in papillary thyroid carcinoma cells. *J Cell Biochem* **92**, 1246-1256.

Choi YJ, Seelbach MJ, Pu H, Eum SY, Chen L, Zhang B *et al.* (2010). Polychlorinated biphenyls disrupt intestinal integrity via NADPH oxidase-induced alterations of tight junction protein expression. *Environ Health Perspect* **118**, 976-981.

Cinel I & Opal SM (2009). Molecular biology of inflammation and sepsis: a primer. *Crit Care Med* **37**, 291-304.

Clark JE, Naughton P, Shurey S, Green CJ, Johnson TR, Mann BE *et al.* (2003). Cardioprotective actions by a water-soluble carbon monoxide-releasing molecule. *Circulation Research* **93**, e2-8.

Copeland S, Warren HS, Lowry SF, Calvano SE, Remick D, Inflammation *et al.* (2005). Acute inflammatory response to endotoxin in mice and humans. *Clin Diagn Lab Immunol* **12**, 60-67.

Cummins EP, Seeballuck F, Keely SJ, Mangan NE, Callanan JJ, Fallon PG *et al.* (2008). The hydroxylase inhibitor dimethyloxalylglycine is protective in a murine model of colitis. *Gastroenterology* **134**, 156-165.

De Backer O, Elinck E, Blanckaert B, Leybaert L, Motterlini R, Lefebvre RA (2009). Water-soluble CO-releasing molecules reduce the development of postoperative ileus via modulation of MAPK/HO-1 signalling and reduction of oxidative stress. *Gut* **58**, 347-356.

De Winter BY & De Man JG (2010). Interplay between inflammation, immune system and neuronal pathways: Effect on gastrointestinal motility. *World Journal of Gastroenterology* **16**, 5523-5535.

Fernandez-Checa JC, Garcia-Ruiz C, Colell A, Morales A, Mari M, Miranda M *et al.* (1998). Oxidative stress: role of mitochondria and protection by glutathione. *Biofactors* **8**, 7-11.

Gopal R, Birdsell D, Monroy FP (2008). Regulation of toll-like receptors in intestinal epithelial cells by stress and Toxoplasma gondii infection. *Parasite Immunol* **30**, 563-576.

Greenspon J, Li RY, Xiao L, Rao JN, Marasa BS, Strauch ED *et al.* (2009). Sphingosine-1-Phosphate Protects Intestinal Epithelial Cells from Apoptosis Through the Akt Signaling Pathway. *Digestive Diseases and Sciences* **54**, 499-510.

Gunther L, Berberat PO, Haga M, Brouard S, Smith RN, Soares MP *et al.* (2002). Carbon monoxide protects pancreatic beta-cells from apoptosis and improves islet function/survival after transplantation. *Diabetes* **51**, 994-999.

Hassoun HT, Kone BC, Mercer DW, Moody FG, Weisbrodt NW, Moore FA (2001a). Post-injury multiple organ failure: the role of the gut. *Shock* **15**, 1-10.

Hassoun HT, Weisbrodt NW, Mercer DW, Kozar RA, Moody FG, Moore FA (2001b). Inducible nitric oxide synthase mediates gut ischemia/reperfusion-induced ileus only after severe insults. *J Surg Res* **97**, 150-154.

Heumüller S, Wind S, Barbosa-Sicard E, Schmidt H, Busse R, Schröder K *et al.* (2008). Apocynin is not an inhibitor of vascular NADPH oxidases but an antioxidant. *Hypertension* **51**, 211-217.

Hoffmann M, Messlik A, Kim SC, Sartor RB, Haller D (2011). Impact of a probiotic Enterococcus faecalis in a gnotobiotic mouse model of experimental colitis. *Mol Nutr Food Res* **55**, 703-713.

Jin S, Ray RM, Johnson LR (2008). TNF-alpha/cycloheximide-induced apoptosis in intestinal epithelial cells requires Rac1-regulated reactive oxygen species. *Am J Physiol Gastrointest Liver Physiol* **294**, G928-937.

Johnson BW & Boise LH (1999). Bcl-2 and caspase inhibition cooperate to inhibit tumor necrosis factor-alpha-induced cell death in a Bcl-2 cleavage-independent fashion. *J Biol Chem* **274**, 18552-18558.

Kim KM, Pae HO, Zheng M, Park R, Kim YM, Chung HT (2007). Carbon monoxide induces heme oxygenase-1 via activation of protein kinase R-like endoplasmic reticulum kinase and inhibits endothelial cell apoptosis triggered by endoplasmic reticulum stress. *Circulation Research* **101**, 919-927.

Königsrainer I, Türck M, Eisner F, Meile T, Hoffmann J, Küper M *et al.* (2011). The gut is not only the target but a source of inflammatory mediators inhibiting gastrointestinal motility during sepsis. *Cell Physiol Biochem.* **28**, 753-760.

Lee BS, Heo J, Kim YM, Shim SM, Pae HO, Kim YM *et al.* (2006). Carbon monoxide mediates heme oxygenase 1 induction via Nrf2 activation in hepatoma cells. *Biochem Biophys Res Commun* **343**, 965-972.

Lubbers T, Luyer MD, de Haan JJ, Hadfoune M, Buurman WA, Greve JW (2009). Lipid-rich enteral nutrition reduces postoperative ileus in rats via activation of cholecystokinin-receptors. *Ann Surg* **249**, 481-487.

Maianski NA, Roos D, Kuijpers TW (2003). Tumor necrosis factor alpha induces a caspase-independent death pathway in human neutrophils. *Blood* **101**, 1987-1995.

Megias J, Busserolles J, Alcaraz MJ (2007). The carbon monoxide-releasing molecule CORM-2 inhibits the inflammatory response induced by cytokines in Caco-2 cells. *Br J Pharmacol* **150**, 977-986.

Morote-Garcia JC, Rosenberger P, Nivillac NM, Coe IR, Eltzschig HK (2009). Hypoxia-inducible factor-dependent repression of equilibrative nucleoside transporter 2 attenuates mucosal inflammation during intestinal hypoxia. *Gastroenterology* **136**, 607-618.

Motterlini R (2007). Carbon monoxide-releasing molecules (CO-RMs): vasodilatory, anti-ischaemic and anti-inflammatory activities. *Biochem Soc Trans* **35**, 1142-1146.

Motterlini R & Otterbein LE (2010). The therapeutic potential of carbon monoxide. *Nat Rev Drug Discov* **9**, 728-743.

Motterlini R, Sawle P, Hammad J, Bains S, Alberto R, Foresti R *et al.* (2005). CORM-A1: a new pharmacologically active carbon monoxide-releasing molecule. *Faseb Journal* **19**, 284-286.

Naugler KM, Baer KA, Ropeleski MJ (2008). Interleukin-11 antagonizes Fas ligand-mediated apoptosis in IEC-18 intestinal epithelial crypt cells: role of MEK and Akt-dependent signaling. *Am J Physiol Gastrointest Liver Physiol* **294**, G728-737.

Nicoletti I, Migliorati G, Pagliacci MC, Grignani F, Riccardi C (1991). A rapid and simple method for measuring thymocyte apoptosis by propidium iodide staining and flow cytometry. *J Immunol Methods* **139**, 271-279.

O'Donnell BV, Tew DG, Jones OT, England PJ (1993). Studies on the inhibitory mechanism of iodonium compounds with special reference to neutrophil NADPH oxidase. *Biochem J* **290 (Pt 1)**, 41-49.

Ozkan OV, Yuzbasioglu MF, Ciralik H, Kurutas EB, Yonden Z, Aydin M *et al.* (2009). Resveratrol, a natural antioxidant, attenuates intestinal ischemia/reperfusion injury in rats. *Tohoku J Exp Med* **218**, 251-258.

Pajak B, Gajkowska B, Orzechowski A (2005). Cycloheximide-mediated sensitization to TNF-alpha-induced apoptosis in human colorectal cancer cell line COLO 205; role of FLIP and metabolic inhibitors. *J Physiol Pharmacol* **56 Suppl 3**, 101-118.

Petrovski G, Gurusamy N, Das DK (2011). Resveratrol in cardiovascular health and disease. *Resveratrol and Health* **1215**, 22-33.

Possel H, Noack H, Augustin W, Keilhoff G, Wolf G (1997). 2,7-Dihydrodichlorofluorescein diacetate as a fluorescent marker for peroxynitrite formation. *FEBS Lett* **416**, 175-178.

Ryter SW, Alam J, Choi AM (2006). Heme oxygenase-1/carbon monoxide: from basic science to therapeutic applications. *Physiol Rev* **86**, 583-650.

Ryter SW & Choi AM (2009). Heme oxygenase-1/carbon monoxide: from metabolism to molecular therapy. *Am J Respir Cell Mol Biol* **41**, 251-260.

Ryter SW, Kim HP, Nakahira K, Zuckerbraun BS, Morse D, Choi AM (2007). Protective functions of heme oxygenase-1 and carbon monoxide in the respiratory system. *Antioxid Redox Signal* **9**, 2157-2173.

Sakata Y, Zhuang H, Kwansa H, Koehler RC, Dore S (2010). Resveratrol protects against experimental stroke: putative neuroprotective role of heme oxygenase 1. *Exp Neurol* **224**, 325-329.

Sawle P, Foresti R, Mann BE, Johnson TR, Green CJ, Motterlini R (2005). Carbon monoxide-releasing molecules (CO-RMs) attenuate the inflammatory response elicited by lipopolysaccharide in RAW264.7 murine macrophages. *Br J Pharmacol* **145**, 800-810.

Schmidt J, Stoffels B, Chanthaphavong RS, Buchholz BM, Nakao A, Bauer AJ (2012). Differential molecular and cellular immune mechanisms of postoperative and LPS-induced ileus in mice and rats. *Cytokine* **59**, 49-58.

Schulze-Osthoff K, Beyaert R, Vandevoorde V, Haegeman G, Fiers W (1993). Depletion of the mitochondrial electron transport abrogates the cytotoxic and gene-inductive effects of TNF. *EMBO J* **12**, 3095-3104.

Shiva S, Sack MN, Greer JJ, Duranski M, Ringwood LA, Burwell L *et al.* (2007). Nitrite augments tolerance to ischemia/reperfusion injury via the modulation of mitochondrial electron transfer. *J Exp Med* **204**, 2089-2102.

Singh UP, Singh NP, Singh B, Hofseth LJ, Price RL, Nagarkatti M *et al.* (2010). Resveratrol (trans-3,5,4'-trihydroxystilbene) induces silent mating type information regulation-1 and down-regulates nuclear transcription factor-kappaB activation to abrogate dextran sulfate sodium-induced colitis. *J Pharmacol Exp Ther* **332**, 829-839.

Stolk J, Hiltermann TJ, Dijkman JH, Verhoeven AJ (1994). Characteristics of the inhibition of NADPH oxidase activation in neutrophils by apocynin, a methoxy-substituted catechol. *Am J Respir Cell Mol Biol* **11**, 95-102.

Sun BW, Jin Q, Sun Y, Sun ZW, Chen X, Chen ZY *et al.* (2007). Carbon liberated from CO-releasing molecules attenuates leukocyte infiltration in the small intestine of thermally injured mice. *World J Gastroenterol* **13**, 6183-6190.

Suschek CV, Schroeder P, Aust O, Sies H, Mahotka C, Horstjann M *et al.* (2003). The presence of nitrite during UVA irradiation protects from apoptosis. *FASEB J* **17**, 2342-2344.

Taille C, Almolki A, Benhamed M, Zedda C, Megret J, Berger P *et al.* (2003). Heme oxygenase inhibits human airway smooth muscle proliferation via a bilirubin-dependent modulation of ERK1/2 phosphorylation. *J Biol Chem* **278**, 27160-27168.

Tran TM, Temkin V, Shi B, Pagliari L, Daniel S, Ferran C *et al.* (2009). TNFalpha-induced macrophage death via caspase-dependent and independent pathways. *Apoptosis* **14**, 320-332.

Tsoyi K, Lee TY, Lee YS, Kim HJ, Seo HG, Lee JH *et al.* (2009). Heme-oxygenase-1 induction and carbon monoxide-releasing molecule inhibit lipopolysaccharide (LPS)-induced high-mobility group box 1 release in vitro and improve survival of mice in LPS- and cecal ligation and puncture-induced sepsis model in vivo. *Mol Pharmacol* **76**, 173-182.

Vidal K, Grosjean I, evillard JP, Gespach C, Kaiserlian D (1993). Immortalization of mouse intestinal epithelial cells by the SV40-large T gene. Phenotypic and immune characterization of the MODE-K cell line. *J Immunol Methods* **166**, 63-73.

Wang H & Joseph JA (1999). Quantifying cellular oxidative stress by dichlorofluorescein assay using microplate reader. *Free Radical Biology and Medicine* **27**, 612-616.

Wilson CA & Browning JL (2002). Death of HT29 adenocarcinoma cells induced by TNF family receptor activation is caspase-independent and displays features of both apoptosis and necrosis. *Cell Death and Differentiation* **9**, 1321-1333.

Yang J, Liu X, Bhalla K, Kim CN, Ibrado AM, Cai J *et al.* (1997). Prevention of apoptosis by Bcl-2: release of cytochrome c from mitochondria blocked. *Science* **275**, 1129-1132.

Yuyama K, Yamamoto H, Nishizaki I, Kato T, Sora I, Yamamoto T (2003). Caspase-independent cell death by low concentrations of nitric oxide in PC12 cells: involvement of cytochrome C oxidase inhibition and the production of reactive oxygen species in mitochondria. *J Neurosci Res* **73**, 351-363.

Chapter IV

MITOCHONDRIA AND NADPH OXIDASES ARE THE MAJOR SOURCES OF TNF-α/CYCLOHEXIMIDE-INDUCED OXIDATIVE STRESS IN MURINE INTESTINAL EPITHELIAL MODE-K CELLS

Dinesh Babu [a], Georges Leclercq [b], Vera Goossens [c,d], Tom Vanden Berghe [c,d], Evelien Van Hamme [c,d], Peter Vandenabeele [c,d], Romain A Lefebvre [a]

[a] Heymans Institute of Pharmacology, Faculty of Medicine and Health Sciences, Ghent University, Belgium

[b] Department of Clinical Chemistry, Microbiology and Immunology, Faculty of Medicine and Health Sciences, Ghent University, Belgium

[c] Inflammation Research Center, Molecular Signaling and Cell Death Unit, VIB, Ghent, Belgium

[d] Department of Biomedical Molecular Biology, Molecular Signaling and Cell Death Unit, Ghent University, Ghent, Belgium

Chapter IV

Mitochondria and NADPH oxidases are the major sources of

TNF-α/cycloheximide-induced oxidative stress in murine intestinal epithelial

MODE-K cells

IV.1   Abstract

Background. TNF-α/cycloheximide (CHX)-induced apoptosis of the mouse intestinal epithelial cell line MODE-K corresponds with the production of reactive oxygen species (ROS). The aim of the study is to investigate the sources of ROS production contributing to apoptotic cell death during TNF-α/CHX-induced oxidative stress in MODE-K cells.

Methods. Total ROS or mitochondrial superoxide anion production was measured simultaneously with cell death in the absence or presence of pharmacological inhibitors of various ROS-producing systems, and of ROS scavengers/antioxidants. The influence of TNF-α/CHX on mitochondrial membrane potential (Ψ_m) and cellular oxygen consumption was also studied.

Key results. TNF-α/CHX time-dependently increased intracellular total ROS and mitochondrial superoxide anion production in MODE-K cells, starting from 2 h. Inhibition of nicotinamide adenine dinucleotide phosphate (NADPH) oxidase (NOX) by a pan-NOX inhibitor (VAS-2870) and a specific inhibitor of Rac1 (NSC23766) significantly reduced TNF-α/CHX-induced total ROS and cell death levels. The mitochondrial electron transport chain inhibitors, amytal (I_Q site of complex I) and TTFA (Q_P site of complex II) showed a pronounced decrease in TNF-α/CHX-induced total ROS, mitochondrial superoxide anion and cell death levels. TNF-α/CHX treatment caused an immediate decrease in mitochondrial respiration, and a loss of Ψ_m and increase in mitochondrial dysfunction from 1 h on.

Conclusions. The results suggest that mitochondria and NOX are the two major sources of ROS overproduction during TNF-α/CHX-induced cell death in MODE-K cells, with superoxide anions being the major ROS species. Particularly, the quinone-binding sites of

mitochondrial complex I (site I_Q) and complex II (site Q_P) seem to be the major sites of mitochondrial ROS production.

IV.2   Introduction

Several acute and chronic intestinal inflammatory conditions such as necrotizing enterocolitis, postoperative ileus and inflammatory bowel disease (IBD) are accompanied with impairment of the intestinal epithelial barrier (Sharma & Tepas, 2010; Snoek *et al.*, 2012; Pastorelli *et al.*, 2013). Upon the systemic inflammatory reaction during sepsis, disruption of the intestinal epithelial barrier can promote the progression towards multiple organ failure (Deitch, 2002). Amongst the pro-inflammatory cytokines produced in the inflamed intestine, tumor necrosis factor (TNF)-α is considered to play an important role in disrupting the intestinal epithelial barrier by induction of intestinal epithelial cell (IEC) apoptosis and shedding. Already in 1998, Piguet *et al*. showed in mice that acute intravenous administration of exogenous TNF-α leads to apoptosis of the IEC layer in a TNF type I receptor (TNFR1)-dependent manner and TNF was recently shown to be the crucial mediator of IEC apoptosis and shedding upon intraperitoneal injection of lipopolysaccharide in mice (Piguet *et al.*, 1998; Williams *et al.*, 2013). Apoptosis and IEC shedding in mouse is histologically analogous to that in humans (Bullen *et al.*, 2006).

Reactive oxygen species (ROS) have been implicated as second messengers during TNF-α-induced cell death in various cell systems (for review, see (Shen & Pervaiz, 2006)). The major ROS-producing enzyme systems are the nicotinamide adenine dinucleotide phosphate (NADPH) oxidase family, the mitochondrial electron transport chain (ETC) with complex I and III as major superoxide producers, xanthine oxidase and dysfunctional uncoupled endothelial nitric oxide (NO) synthase (eNOS) (Li *et al.*, 2013a). The contribution of ROS to TNF-α-induced IEC apoptosis has been mainly investigated in rat IECs. ROS production from NADPH oxidase (NOX) was implicated in TNF-α-induced apoptosis of the rat IEC line IEC-6 (Jin *et al.*, 2008), while mitochondrial dysfunction including enhanced mitochondrial ROS production was proposed for TNF-α-induced apoptosis in rat IEC line RIE-1 (Baregamian *et al.*, 2009). Additionally, in rat enterocytes isolated 1 h after opening of the abdominal wall and intestinal handling, a condition inducing postoperative ileus where TNF-α is one of the inflammatory cytokines involved (Kalff *et al.*, 2003), xanthine oxidase activity was significantly increased (Anup *et al.*, 1999) and correspondingly, exposure of a human IEC monolayer to xanthine/xanthine oxidase significantly increased permeability (Mukojima *et al.*, 2009). eNOS is not expressed in IECs (Chen *et al.*, 2002; Konig *et al.*, 2002) so that

uncoupled eNOS is unlikely as a ROS source in IECs. For the mouse IEC line MODE-K, we have previously reported that TNF-α/cycloheximide (CHX)-induced apoptosis corresponds with the production of ROS (Babu *et al.*, 2012). The aim of the actual study was therefore to investigate the intracellular sources of TNF-α-induced ROS production in this model with particular attention for the mitochondrial sites of ROS production. Mitochondrial ROS are primarily superoxide anions and at least seven distinct sites of mitochondrial superoxide production have been described (Brand, 2010). A basal level of mitochondrial superoxide anions is present during normal respiration and its generation from complex I and III of the ETC is accepted to occur under physiologic conditions (Chen *et al.*, 2003; Muller *et al.*, 2004). Additionally, emerging evidence shows that complex II could also contribute to significant ROS production during pathological conditions like ischemia/reperfusion (Drose, 2013). In this study in MODE-K cells, total or mitochondrial ROS production by TNF-α/CHX was measured in parallel with induced cell death via flow cytometry in the absence or presence of pharmacological inhibitors of the various ROS-producing systems. Additionally, the influence of TNF-α/CHX on mitochondrial membrane potential (Ψ_m) and cellular oxygen consumption was studied.

IV.3 Materials and methods

IV.3.1 Chemicals and reagents

Recombinant murine TNF-α was purchased from R&D system (Minneapolis, MN, USA). Reagents for cell culture, including Dulbecco's modified Eagle's medium (DMEM), penicillin/streptomycin, glutamax and fetal bovine serum were obtained from Gibco BRL (Grand Island, NY, USA). 2-(2,2,6,6-tetramethylpiperidin-1-oxyl-4-ylamino)-2-oxoethyl) triphenylphosphonium chloride monohydrate (Mito-TEMPO) and JC-10 were purchased from Enzo Life Sciences (Zandhoven, Belgium). APC Annexin V, carboxylated (carboxy-H_2DCFDA) and chloromethyl (CM-H_2DCFDA) analogues of 2'7'-dichlorodihydrofluorescein diacetate acetyl ester (H_2DCFDA), Hoechst blue 33342, MitoTracker Deep Red FM, MitoTracker Green FM, MitoSOX Red, Sytox Red, Sytox Green and tetramethyl rhodamine methyl ester (TMRM) were purchased from Molecular Probes – Invitrogen (Carlsbad, CA, USA). The cell permeable lipophilic iron chelator, salicylaldehyde isonicotinoyl hydrazone

(SIH) was a kind gift from Prof. Dr. U Brunk. All other chemicals were obtained from Sigma (St. Louis, MO, USA).

IV.3.2 Cell culture

The mouse small IEC line, MODE-K (a generous gift from Dr. Ingo B. Autenrieth, University of Tübingen, Germany) was used in our study. This is a cell line derived from the duodenum-jejunum from normal young C3H/HeJ mouse immortalized by simian virus (SV)-40 large T gene transfer. The cells are undifferentiated but still exhibit morphological and phenotypic characteristics of normal enterocytes (Vidal *et al.*, 1993). MODE-K cells (passage 10–35) were cultured in high-glucose DMEM supplemented with 10% fetal bovine serum, 2 mM L-glutamine, and 5% penicillin/streptomycin. Cultures were maintained in a humidified 5% CO_2 atmosphere at 37°C and experiments were conducted on cells at approximately 80-90% confluence. MODE-K cells were seeded at specified cell density in various experiments, grown for 36 h and then serum starved overnight (except when used for the cellular oxygen consumption assay). On day 3, cells were treated with various concentrations of TNF-α/CHX for 0-6 h. All the drugs tested for possible interference with TNF-α/CHX-induced effects were pre-incubated from 1 h before exposure to TNF-α/CHX, followed by co-incubation of drugs with various concentrations of TNF-α/CHX for 6 h, with the exception of the hydrophilic iron chelator desferrioxamine (DFO), which needs 3 h pre-incubation before exposure to TNF-α/CHX. The influence of drugs *per se* on cell viability was studied on day 3 by incubating MODE-K cells with a concentration dilution series for 12 h. The drugs were tested for possible interference with TNF-α/CHX-induced effects at the highest possible concentration without an effect *per se* on cell viability based on quantitation of ATP in MODE-K cells.

IV.3.3 Cellular ATP measurement and determination of cell viability

Cell viability was assessed using the CellTiter-Glo Luminescent Cell Viability Assay (Promega, Madison, WI, USA) according to the manufacturer's protocol. This assay determines the number of viable cells in culture based on quantitation of ATP present, an indicator of metabolically active cells. Briefly, MODE-K cells were plated at 1 x 10^4 cells per 200 μL of culture medium per well in a 96-well microtiter plate. At the end of the 12 h incubation period with drugs on day 3, an equivolume of the luminescent substrate and lysis buffer mix from the assay kit was added. The mixture was transferred to an opaque 96-well

plate and luminescence was recorded using a GloMax Microplate Luminometer (Promega). The index of cellular viability was calculated as percentage of luminescence with respect to untreated control cells.

IV.3.4 Flow cytometric analysis of mode of cell death

We have previously reported that TNF-α/CHX induces apoptotic cell death in MODE-K cells as evidenced by increase in caspase-3/7 activity and DNA fragmentation (assessed as hypodiploid DNA content by flow cytometry) (Babu *et al.*, 2012). The mode and kinetics of cell death was further characterized by annexin V and propidium iodide (PI) staining by using FITC Annexin V Apoptosis Detection Kit I (BD Pharmingen). One of the earliest events during apoptosis, the exposure of phosphatidylserine to the outer cell surface, is measured by its binding to FITC annexin V. Briefly, 2.5×10^5 cells per well were seeded in 6-well plates. After exposure of cells to TNF-α/CHX for 0-6 h, floating and adherent cells were collected, washed with PBS and then resuspended in 1x annexin V binding buffer at 1×10^6 cells/ml. To 0.1 ml of solution containing 1×10^5 cells, 5 µl of FITC Annexin V and 5 µl PI (10 µg/ml in PBS) were added; the cell suspension was gently vortexed and left incubated for 30 min at RT in the dark. A volume of 400 µl of 1x annexin V binding buffer was then added to each sample. Within 1 h, the cells were analyzed by flow cytometry (FACSCalibur, BD Bioscience, NJ) and quantified using CellQuest software (Becton Dickinson, San Jose, CA, USA). FITC Annexin V fluorescence was measured using a 530/30 nm bandpass filter (FL1) and PI fluorescence using a 670 nm longpass filter (FL3). At least 30,000 cells were acquired from each sample. Quadrant statistics were performed to determine viable (Annexin V$^-$/PI$^-$), early apoptotic (Annexin V$^+$/PI$^-$), late apoptotic/necrotic (Annexin V$^+$/PI$^+$) and dead cells (Annexin V$^-$/PI$^+$).

IV.3.5 Measurement of intracellular ROS generation

IV.3.5.1 Simultaneous determination of intracellular total ROS generation and cell death

The intracellular total ROS production was detected using carboxy-H$_2$DCFDA. Carboxy-H$_2$DCFDA is a cell-permeable indicator for ROS that is nonfluorescent until the acetate groups are removed by intracellular esterases and oxidation occurs within the cell. When oxidized by various active oxygen species, it is irreversibly converted to the fluorescent form, DCF. The fluorescence generated by DCF is proportional to the rate of

carboxy-H$_2$DCFDA oxidation, which is in turn indicative of the cellular oxidizing activity and intracellular ROS levels. For ROS measurements, briefly, 2.5 x 10^5 cells per well were seeded in 6-well plates. Following exposure of cells to TNF-α/CHX for 0-6 h with/without drugs, carboxy-H$_2$DCFDA (10 µM) was loaded to the cells for 40 min before the end of the treatment period in the dark at 37°C. The floating and adherent cells were collected by trypsinization, washed twice with Hanks' balanced salt solution (HBSS) with calcium and magnesium. Sytox Red (2.5 nM) dead cell stain was added to the cell suspension and simultaneous detection of ROS production and cell death was performed in a single experimental setup by flow cytometry using 488 nm excitation wavelength with 530/30 nm (FL1; DCF) and 670/30 (FL4; Sytox Red) emission filters. The green fluorescence of the ROS probes was measured only in the viable (Sytox Red-negative) cell population. Cells treated with hydrogen peroxide (H$_2$O$_2$) for either 40 min or 3 h were used as a positive control.

IV.3.5.2   Simultaneous determination of mitochondrial superoxide anion, apoptosis and cell death

MitoSOX Red was used to detect mitochondrial superoxide production anion. This modified cationic dihydroethidium dye is localized to the mitochondria where it is oxidized by superoxide anion to generate bright red fluorescence. Mitochondrial superoxide anion generation, apoptosis and cell death were determined in a single experimental setup as previously described (Mukhopadhyay *et al.*, 2007). Briefly, the cells were loaded with 5 µM MitoSOX Red and 5 µl APC Annexin V (the latter only for the time kinetic assay) for 30 min before the end of treatment period, collected, washed twice with HBSS and then stained with 2 nM Sytox Green. The samples were run on a flow cytometer with 488 nm excitation to measure oxidized MitoSOX Red in the FL2 channel, APC Annexin V (FL4) and Sytox Green (FL1). Cell debris with low FSC (forward scatter) and SSC (side scatter) was excluded from the analysis. The cells were then analyzed for APC Annexin V (FL4) and Sytox Green (FL1). Cells that exhibited apoptosis (FL4-positive) or were dead (FL1-positive) were excluded from the analysis, and viable cells (Annexin V$^-$/Sytox Green$^-$) were gated and the mean fluorescence intensity (MFI) of MitoSOX Red staining was analyzed. Thus, MitoSOX Red of the cells analyzed excluded any non-specific interferences from apoptotic and dead cells. Cells treated for 30 min with 10 µM antimycin-A, an agent well known to generate superoxide anions by binding to the Qi site of cytochrome c reductase in the mitochondrial complex III, were used as a positive control.

For all ROS experiments, (a) the fluorescence properties of at least 30,000 cells were acquired from each sample, (b) the samples were analyzed immediately and strictly protected from light, (c) basal ROS generation in the cells treated without the stimulus (either medium alone or solvent-treated medium) was used as a control, (d) mean fluorescence intensities (MFIs) were expressed as percentage of control level set as 100%.

IV.3.5.3 Imaging of intracellular total ROS/mitochondrial superoxide anion production and cell death

The ROS production in MODE-K cells was also analyzed by imaging using laser scanning confocal microscopy (LSCM). Imaging of intracellular total ROS and cell death was performed after co-staining with CM-H$_2$DCFDA and Sytox Red while imaging of mitochondrial superoxide anion production and cell death was performed after co-staining with MitoSOX Red and Sytox Green. Additionally, the cell-permeable DNA dye Hoechst 33342 was used in both experiments for nuclear staining. CM-H$_2$DCFDA is a chloromethyl derivative of H$_2$DCFDA, but it is much better retained in live cells than carboxy-H$_2$DCFDA. CM-H$_2$DCFDA passively diffuses into cells, where its acetate groups are cleaved by intracellular esterases and its thiol-reactive chloromethyl group reacts with intracellular glutathione and other thiols. Subsequent oxidation yields fluorescent DCF that is trapped inside the cell, which facilitates long-term studies. In brief, MODE-K cells were grown on 20 mm-culture dishes at a density of 2.3 x 10^5 cells per dish. On day three, the cells were stimulated with TNF-α (1 ng/ml) plus CHX (10 µg/ml) for 1-6 h at 37°C; the combination of dyes (1 µM CM-H$_2$DCFDA and 1 µM Sytox Red or 1.25 µM MitoSOX Red and 2 µM Sytox Green, together with 10 µg/ml Hoechst 33342) was incubated from 40 min before the end of the incubation period. The cells were then washed once and confocal images were captured with a Zeiss LSM780 confocal microscope (Zeiss, Jena, Germany) every hour from 0 to 6 h. Images were taken by using a Plan-Neofluar 25×/0.8 Imm Korr DIC M27 objective (1024 x 1024, pixel size: 332 nm x 332 nm). Hoechst was excited with the Ti:Sa Laser MaiTai at 780 nm (1.2%). DCF and Sytox Green were excited using the 488 nm line of an Argon laser (0.5%). MitoSOX and Sytox Red were excited using a 633 nm diode laser (15%). Hoechst signals were collected from 415 to 499 nm, DCF and Sytox Green from 499 to 569 nm, and MitoSOX and Sytox Red from 605 to 690 nm. Z-sections were made every 2 µm. Image processing was performed using Fiji software.

IV.3.6 Detection of mitochondrial membrane potential (Ψ_m)

IV.3.6.1   Estimation of mitochondrial membrane potential (Ψ_m)

Estimation of mitochondrial membrane potential (Ψ_m) was performed using JC-10, a membrane permeable fluorescent probe. JC-10 is a cationic fluorophore, which is rapidly taken up by cells and mitochondria due to their negative charge. Inside mitochondria, JC-10 forms J-aggregates which emit fluorescence at 590 nm (FL2; red fluorescence). Remaining JC-10 in cytosol maintains the monomeric form and emits fluorescence at 525 nm (FL1; green fluorescence). Uptake levels of JC-10 in mitochondria depend on the polarization state of the mitochondrial membrane. Depolarized mitochondria have lower uptake of JC-10 compared to polarized mitochondria of a normal healthy cell. Briefly, 2.5 x 10^5 cells per well were seeded in 6-well plates. Following the treatment, cells were washed twice with HBSS and then incubated with 5 µM JC-10 solution prepared in DMEM media for 30 min. Subsequently, the cells were quickly washed with HBSS prior to measurement. The fluorescence intensities of JC-10 monomers and aggregates were quantified, respectively, by FL1 (530/30 nm) and FL2 (585/42 nm) detectors of the flow cytometer. The JC-10 aggregate/monomer ratio is directly proportional to mitochondrial membrane potential intensity. This ratiometric method was used with this dye to provide a semi-quantitative measurement of Ψ_m.

IV.3.6.2   Simultaneous determination of mitochondrial membrane potential (Ψ_m), apoptosis and cell death

Determination of the changes in mitochondrial membrane potential (Ψ_m) was also performed using TMRM along with staining of APC Annexin V (for apoptosis, only for the time kinetic assay) and Sytox Green (for cell death). TMRM is a cell-permeant, lipophilic cationic, red-orange fluorescent dye that is readily sequestered by active mitochondria. Unlike JC-10, TMRM is a single wavelength dye that can be combined with a cell death marker to measure fluorescence exclusively in the live cells. Briefly, following the treatment, the cells were washed twice with HBSS and then incubated with 200 nM TMRM solution and 5 µl APC Annexin V (the latter only for time kinetic assay) prepared in DMEM media for 30 min. Subsequently, the cells were quickly washed twice with HBSS and stained with 2 nM Sytox Green prior to measurement. The percentage of TMRM, Annexin V APC and Sytox Green stained cells was calculated from at least 30,000 cells of each sample in comparison to

the control. TMRM was excited at 488 nm, and fluorescence emitted at 588 nm (FL2) was measured only in the viable (Annexin V$^-$/Sytox Green$^-$) cells by flow cytometry. Cells treated for 30 min with 50 μM carbonyl cyanide 3-chlorophenylhydrazone (CCCP), a potent uncoupler of oxidative phosphorylation which causes rapid loss of Ψ_m (loss of TMRM fluorescence), was used as a positive control.

IV.3.7 Measurement of mitochondrial dysfunction

Determination of respiratory chain damage was performed by double staining with two different mitochondria-specific dyes, MitoTracker Green FM and MitoTracker Deep Red FM to distinguish total and respiring mitochondria, respectively. Mitochondria in cells stained with MitoTracker Green FM dye exhibit bright green fluorescein-like fluorescence (FL1; fluorescence emission at 516 nm) as this dye accumulates in the lipid environment of mitochondria and becomes fluorescent. MitoTracker Deep Red FM is a red fluorescence probe (FL4; fluorescence emission at 665 nm) that does not fluoresce until it enters an actively respiring cell, where it is oxidized to the corresponding fluorescent mitochondrion-selective probe and then sequestered in the mitochondria. The treated cells were incubated with 200 nM MitoTracker Green FM and 25 nM MitoTracker Deep Red FM in the dark at 37°C for 30 min before the end of the treatment period. Next, the cells were harvested and the pellets were suspended in 0.5 ml of PBS. The samples were analyzed immediately by flow cytometry. The percentage of MitoTracker Green-positive/MitoTracker Deep Red-negative cells is an important parameter of accumulation of cells with non-respiring (dysfunctional) mitochondria (Zhou *et al.*, 2011).

For ROS, Ψ_m and mitochondrial dysfunction assays, the samples were acquired and analyzed using a FACSCalibur using CellQuest software or with an LSR II using DIVA software (BD Biosciences).

IV.3.8 Mitochondrial respiration

Cellular oxygen consumption in the DMEM XF assay medium containing 1% FCS was measured in a Seahorse XF96 Analyzer (Seahorse Bioscience, Billerica, MA, USA). Oxygen consumption rate (OCR) and extracellular acidification rate (ECAR) were analyzed following the manufacturer's protocols. Measurements are based on oxygen-dependent quenching of

a built-in fluorescent sensor. Briefly, MODE-K cells were seeded at 6.5 x 10^4 cells per well in Seahorse XF96 specialized cell culture plates. Approximately 24 h later, media was replaced with DMEM XF assay medium (unbuffered DMEM supplemented with 25 mM glucose, 2 mM L-glutamax and 1 mM sodium pyruvate) and cells were incubated for 1 h at 37°C without CO_2. Then, basal OCR and ECAR were measured simultaneously in the Seahorse XF96 extracellular flux analyzer for 2 h 30 min. Reagents and chemicals for respiratory stress testing were loaded onto XF96 extracellular flux assay plate. TNF-α/CHX, CCCP or rotenone/antimycin-A were diluted in DMEM running medium and loaded into port-A, port-B and port-C, respectively. Titrations were preliminarily performed to determine the optimal concentration of CCCP. In all cell groups, CCCP (50 μM) was added at 115 min to determine maximal respiration. Then rotenone (2.5 μM) and antimycin-A (5 μM) were added at 130 min to block mitochondrial respiration and non-mitochondrial respiration was determined. To test the influence of TNF-α/CHX, it was added at 30 min after five measurements of basal respiration. After measuring OCR and ECAR for 2 h 30 min, the amount of dead cells in the microchamber of each well was determined on a BD Pathway™ 855 instrument as described previously (Duprez *et al.*, 2011). This allows normalization of the respiratory rates in function of the amount of cells in each microchamber. Cells were plated with at least 5 replicate wells for each treatment group. The OCR and ECAR values were expressed as percentage of control versus basal measurements.

IV.3.9 Statistical analysis

All data were expressed as mean ± SEM. Comparison of the means was performed using the Student's *t*-test for two groups of data and ANOVA followed by Bonferroni's multiple comparison test for comparison of more than two groups. Differences were considered to be significant at *P* < 0.05.

IV.4 Results

IV.4.1 ROS is an important contributor to TNF-α/CHX-induced cell death in MODE-K cells

We previously reported that TNF-α/CHX-induces ROS production in MODE-K cells (Babu *et al.*, 2012). In the current study, simultaneous measurement of intracellular total ROS production and cell death was performed by flow cytometric analysis with carboxy-

H_2DCFDA as ROS indicator and Sytox Red as a marker for dead cells. ROS production measurements were performed exclusively in the live cell population. As shown in Fig. IV.1A (left panel), incubation of the cells with 0.1-1 ng/ml TNF-α plus 10 µg/ml CHX for 6 h induced a concentration-dependent increase in MFI of DCF as compared with the control group, originating from an increasing percentage of DCF-positive live cells (Fig. IV.2A). The increase in ROS production is paralleled by an increase in cell death as measured by Sytox Red positivity (Fig. IV.1A, right panel). The increase in DCF MFI by 1 ng/ml TNF-α plus 10 µg/ml CHX is maximal as higher concentrations of TNF-α (up to 20 ng/ml) in combination with 10 µg/ml CHX induced the same degree of DCF MFI (Fig. IV.2B); the response is close to that by 20 ng/ml TNF-α plus 25 µg/ml CHX, a classic apoptotic stimulus used in other intestinal epithelial cell lines (Bhattacharya *et al.*, 2003; Jin *et al.*, 2008; Naugler *et al.*, 2008; Greenspon *et al.*, 2009). To evaluate the time kinetics of TNF-α/CHX-induced ROS production and cell death, MODE-K cells were incubated with 1 ng/ml TNF-α plus 10 µg/ml CHX for 0.5-6 h. As assessed by flow cytometry, significant induction of both ROS generation and cell death began after 2 h of exposure to TNF-α/CHX and increased further in a time-dependent manner (Fig. IV.1B); this was confirmed by laser scanning confocal microscopy (LSCM) (Fig. IV.3). The cell death modality followed apoptotic cell death kinetics as observed by the onset of annexin positivity at the same time where ROS production started, i.e., 2 h, with further increase upon time (Fig. IV.1C and 2C). Incubation for 40 min with hydrogen peroxide (H_2O_2), a positive control for total ROS production, also increased DCF fluorescence concentration-dependently (0.5-3 mM), only causing a minor increase in cell death at 3 mM (Fig. IV.4A). Increasing the incubation time of H_2O_2 to 3 h increased both total ROS production and cell death in a concentration-dependent manner (Fig. IV.4B).

To understand the role of ROS production in TNF-α/CHX-induced cell death in MODE-K cells, a set of antioxidants and ROS scavengers was tested versus 1 ng/ml TNF-α plus 10 µg/ml CHX (Table IV.1). With regard to the effects of hydrophilic antioxidants, the superoxide anion scavenger tiron completely abolished TNF-α/CHX-induced ROS production with significant partial reduction of cell death (Fig. IV.5A) while N-acetylcysteine (NAC), a precursor of the antioxidant reduced glutathione (GSH), significantly reduced both ROS production and cell death induced by TNF-α/CHX (Fig. IV.5B). The lipophilic antioxidants, butylated hydroxytoluene (BHT) and butylated hydroxyanisole (BHA) both as good as abolished TNF-α/CHX-induced ROS production and cell death, suggesting a possible causal
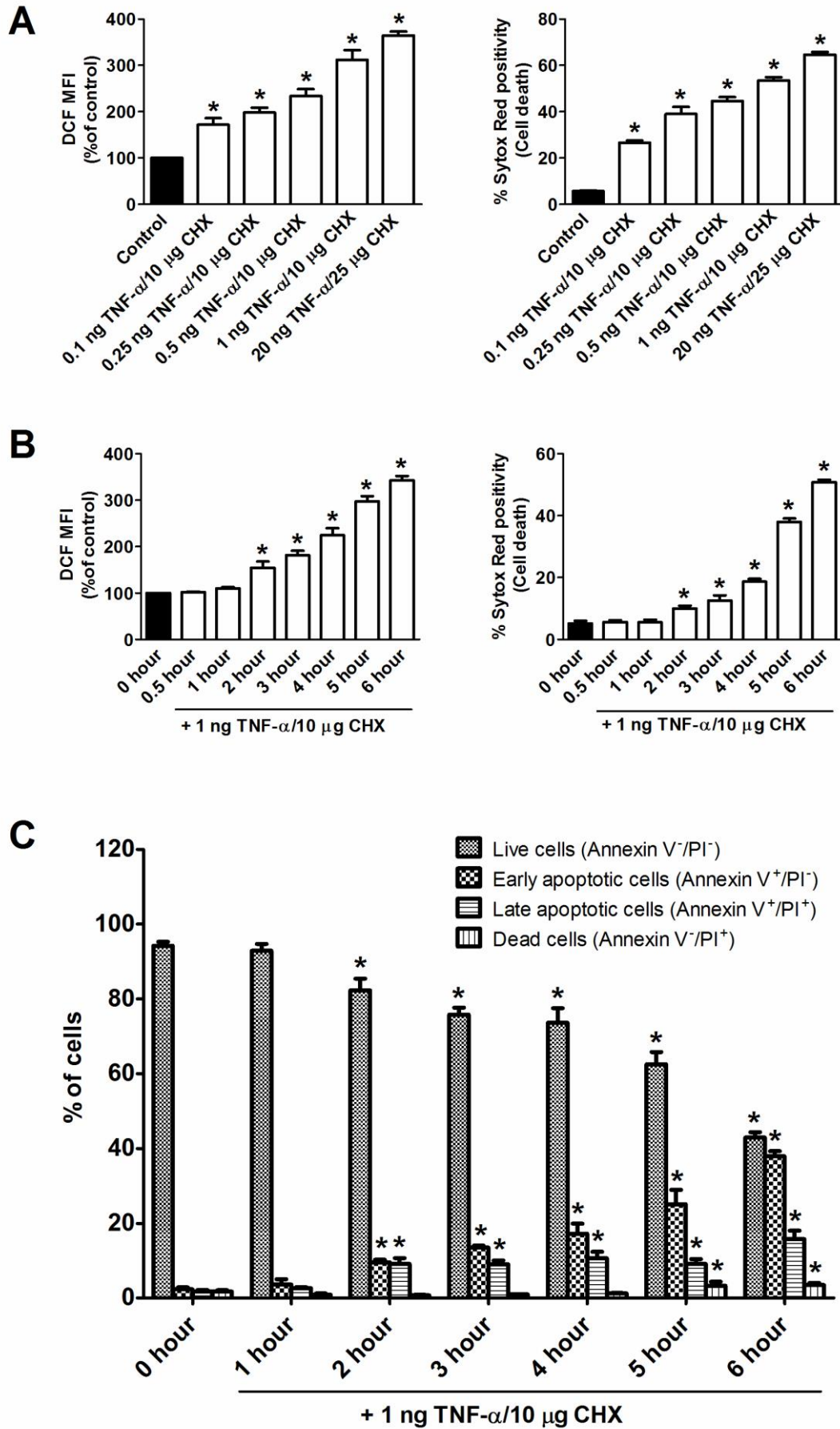
relationship between intracellular ROS generation and cell death in this cell system (Fig. IV.5C and 6A). On the other hand, the iron chelators, desferrioxamine (DFO) and salicylaldehyde isonicotinoyl hydrazone (SIH) also abolished TNF-α/CHX-induced ROS production but without any effect on cell death (Fig. IV.5D and 6B). In contrast, when using DFO or SIH versus 3 mM H_2O_2 (incubated for 3 h), they abolished both H_2O_2-induced total ROS production and cell death (Fig. IV.4C and D).
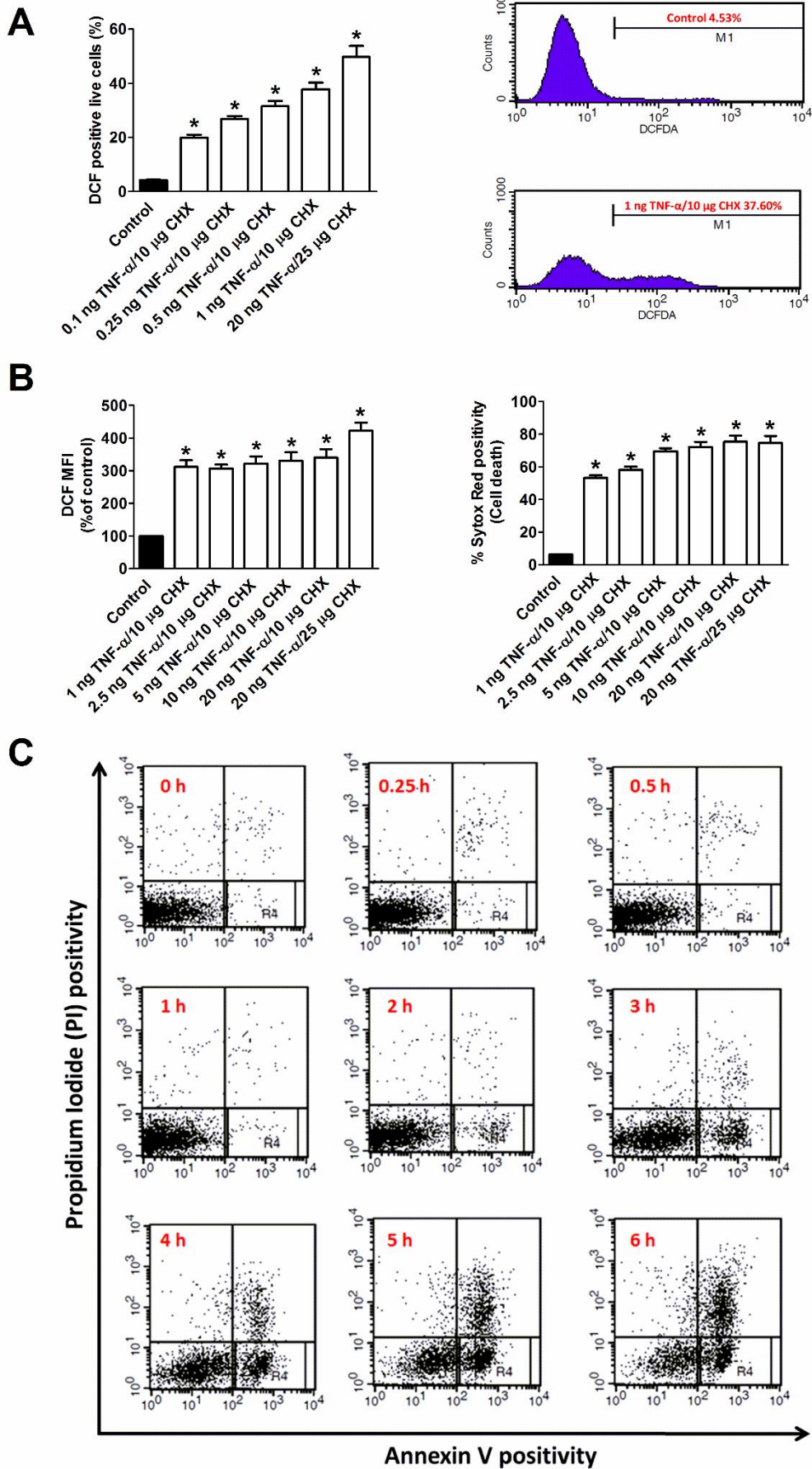
IV.4.2 NOX and mitochondrial ETC complex enzymes, but not xanthine oxidase, contribute to TNF-α/CHX-induced total ROS production and cell death in MODE-K cells

To determine the sources of ROS generation in response to TNF-α/CHX in MODE-K cells, we systematically used pharmacological inhibitors of various ROS producing systems within the IECs. Neither the xanthine oxidase inhibitor allopurinol (Fig. IV.7A) nor diphenylene iodonium (DPI; Fig. IV.7B), the most commonly used NOX inhibitor which acts on flavoproteins, influenced TNF-α/CHX-induced ROS production or cell death. However, a well-validated selective pan-NOX inhibitor, VAS-2870, partially reduced TNF-α/CHX-induced ROS accompanied by partial reduction in cell death suggesting that NOX is a possible source of ROS production in MODE-K cells (Fig. IV.7C). Furthermore, treatment with NSC23766, a Rac1 inhibitor known to block NOX activation, also significantly mitigated the ROS production and cell death to a similar level as VAS-2870 (Fig. IV.7D).

Next, various mitochondrial respiration inhibitors blocking a complex enzyme of the ETC were tested (Fig. IV.8). Amytal, an inhibitor of the downstream quinone-binding site in complex I (I_Q) greatly decreased TNF-α/CHX-induced ROS production with near abolishment of cell death (Fig. IV.9A). The ubiquinone binding (Q_P) site inhibitor of complex II, theonyltrifluoroacetone (TTFA) completely blocked TNF-α/CHX-induced total ROS

Fig. IV.1   ROS production (assessed with carboxy-H_2DCFDA) and cell death (assessed with Sytox Red) in TNF-α/CHX-treated MODE-K cells measured by flow cytometry. (A) Influence of 0.1-1 ng/ml TNF-α plus 10 µg/ml CHX and of 20 ng/ml TNF-α plus 25 µg/ml CHX, incubated for 6 h, on intracellular total ROS levels (expressed as % of control DCF MFI; left panel) and cell death (expressed as % Sytox Red positivity; right panel). Control cells were incubated with serum-free medium alone. Mean ± SEM of six independent experiments. *$P < 0.05$ versus control. (B) Time course study of the influence of 1 ng/ml TNF-α plus 10 µg/ml CHX, incubated for 0.5-6 h, on intracellular total ROS levels (left panel) and cell death (right panel). Mean ± SEM of three independent experiments. *$P < 0.05$ versus untreated (0 h) control group. (C) Influence of 1 ng/ml TNF-α plus 10 µg/ml CHX, incubated for 1-6 h, on FITC-Annexin V/propidium iodide (PI) positivity. Mean ± SEM of three independent experiments. *$P < 0.05$ versus untreated (0 h) control group.

Time-dependent increase in total ROS production (DCF) and cell death (Sytox Red) with 1 ng TNF-α/10 µg CHX for 0-6 hours
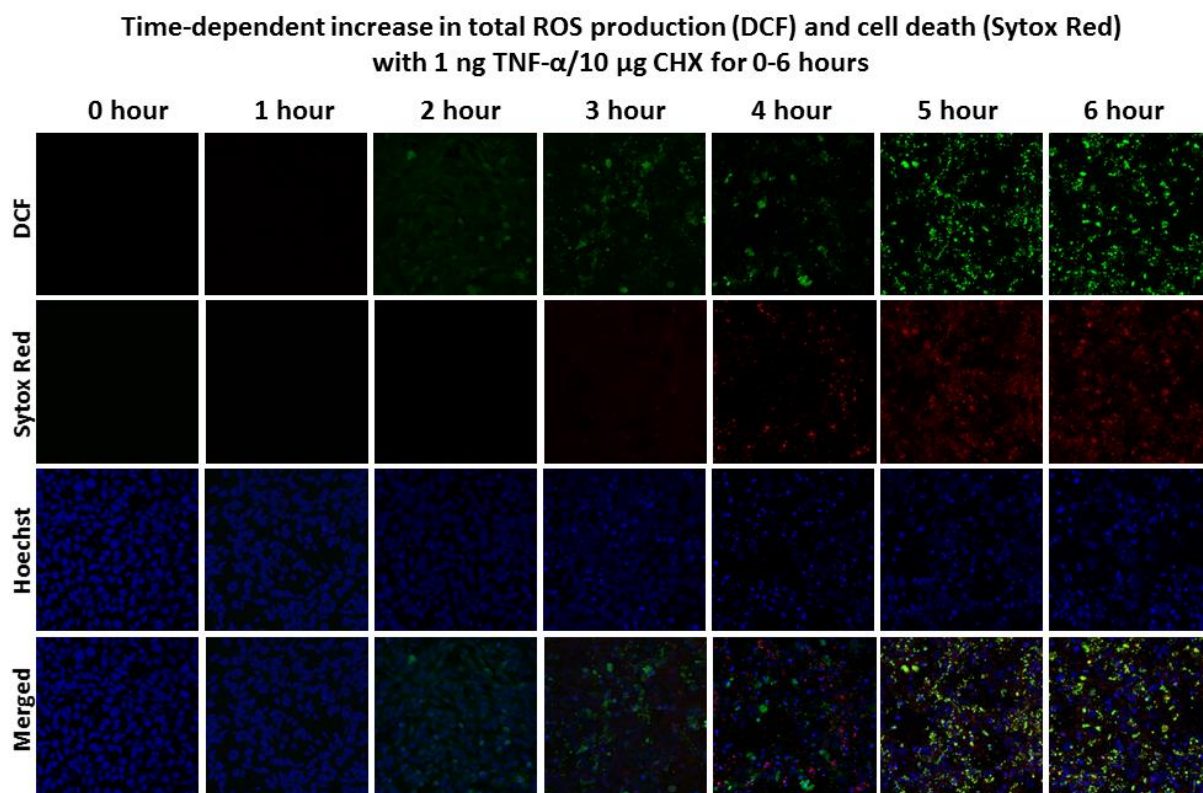
Fig. IV.3 Time-dependent induction of ROS production (assessed with CM-H2DCFDA) and cell death (assessed with Sytox Red) by TNF-α/CHX in MODE-K cells as imaged with laser scanning confocal microscopy. Time course study of influence of 1 ng/ml TNF-α plus 10 µg/ml CHX, incubated for 0-6 h, on intracellular total ROS production and cell death after staining with the ROS probe CM-H2DCFDA (for total ROS production; green, first row), the cell-impermeable DNA dye Sytox Red (cell death; red, second row) and chromatin decondensation using the cell-permeable DNA dye Hoechst 33365 (for nuclei; blue, third row) imaged in separate channels and processed as merged image (fourth row). Results are representative of at least two independent experiments imaged at every one-hour time point.

Fig. IV.2 ROS production (assessed with carboxy-H2DCFDA) and cell death (assessed with Sytox Red) in MODE-K cells. (A) Influence of 0.1-1 ng/ml TNF-α plus 10 µg/ml CHX and of 20 ng/ml TNF-α plus 25 µg/ml CHX, incubated for 6 h, on intracellular total ROS production expressed as the percentage of DCF-positive live cells (left panel). Control cells were incubated with serum-free medium alone. Mean ± SEM of six independent experiments. *P < 0.05 versus untreated control group. Representative histogram of control and 1 ng/ml TNF-α plus 10 µg/ml CHX-treated group after carboxy-H2DCFDA staining in live cell population. The cells in M1 region represents the DCF-positive cells (right panel). (B) Influence of 1-20 ng/ml TNF-α plus 10 µg/ml CHX and of 20 ng/ml TNF-α plus 25 µg/ml CHX, incubated for 6 h, on intracellular total ROS production after carboxy-H2DCFDA staining (expressed as % of control DCF MFI; left panel) and cell death (expressed as % Sytox Red positivity; right panel). Mean ± SEM of six independent experiments. *P < 0.05 versus untreated control group. (C) Time course study of TNF-α/CHX-induced apoptotic cell death in MODE-K cells. Representative dot plots of flow cytometric analysis showing the influence of 1 ng/ml TNF-α plus 10 µg/ml CHX, incubated for 0.25-6 h, on FITC Annexin V/propidium iodide (PI) positivity. Membrane changes leading to phosphatidylserine exposure occurring with the onset of apoptosis is measured by its binding with FITC Annexin V. Viable cells with intact membranes exclude PI, whereas the membranes of dead and damaged cells are permeable to PI. The shift of cells from the lower left quadrant (FITC Annexin V⁻/PI⁻) to the lower right quadrant (FITC Annexin V⁺/PI⁻) is clearly visible from 2 h on, while the shift to the upper right quadrant (FITC annexin V⁺/PI⁺) is visible from 3 h on.

Effect of commonly used antioxidants or inhibitors of ROS-generating enzymes on TNF-α/CHX-induced intracellular total ROS level and cell death		
	Percentage reduction of TNF-α/CHX-induced	
Antioxidants or inhibitors	**ROS level (DCF fluorescence)**	**Cell death (Sytox Red positivity)**
Tiron 2.5 mM	95.2 ± 2.6*	46.6 ± 5.6*
N-acetylcysteine (NAC) 20 mM	66.9 ± 2.7*	44.2 ± 1.2*
Butylated hydroxyanisole (BHA) 200 µM	98.7 ± 0.7*	108.6 ± 2.8*
Butylated hydroxytoluene (BHT) 50 µM	94.6 ± 1.7*	90.1 ± 2.1*
Desferrioxamine (DFO) 1 mM	98.3 ± 1.4*	8.5 ± 2.3
Salicylaldehyde isonicotinoyl hydrazone (SIH) 100 µM	86.7 ± 1.6*	2.9 ± 5.1
Allopurinol 200 µM	3.4 ± 13.3	1.2 ± 4.2
Diphenylene iodonium (DPI) 100 µM	1.3 ± 4.2	0.6 ± 2.1
VAS-2870 10 µM	61.9 ± 2.9*	36.1 ± 3.3*
NSC23766 50 µM	75.4 ± 4.0*	34.7 ± 5.5*
Amytal 5 mM	76.3 ± 2.6*	90.5 ± 1.3*
Theonyltrifluoroacetone (TTFA) 0.25 mM	97.5 ± 0.9*	75.8 ± 5.6*
Malonate 1 mM	60.6 ± 1.1*	-0.4 ± 4.0
Antimycin-A 10 µM	-29.2 ± 34.9	-9.1 ± 12.2
Myxothiazole 1 µM	25.9 ± 1.8*	44.0 ± 2.9*
Potassium cyanide (KCN) 2 mM	90.7 ± 1.1*	81.5 ± 1.2*
Oligomycin 1 µM	38.0 ± 12.0*	42.0 ± 0.8*
Carbonylcyanide m-chlorophenylhydrazone (CCCP) 1 µM	52.2 ± 7.7*	47.0 ± 9.3*
Carbonyl cyanide p-trifluoro methoxyphenylhydrozone (FCCP) 0.5 µM	23.5 ± 1.7*	57.7 ± 1.9*
Mito-TEMPO 5 µM	9.6 ± 4.1	8.0 ± 7.9

Mean ± SEM, n = 3, *: Significant reduction of the increase in intracellular total ROS level or cell death, induced by TNF-α (1 ng/ml)/CHX (10 µg/ml) ($P < 0.05$)

production with concomitant reduction of cell death (Fig. IV.9B). On the other hand, malonate, a competitive carboxylate (succinate) site inhibitor of complex II at the flavin binding domain, significantly reduced the ROS level but without any influence on cell death (Fig. IV.9C). Antimycin-A and myxothiazole, acting at different sites within complex III, are known to increase or decrease ROS, respectively. Accordingly, antimycin-A (Qi site inhibitor) *per se* induced ROS production but did not modulate TNF-α/CHX-induced ROS and cell death levels (Fig. IV.9D). On the other hand, myxothiazole (Qo site inhibitor) at the concentration used *per se* mildly induced ROS production; but it also mildly reduced TNF-α/CHX-induced ROS with pronounced recovery of cell death (Fig. IV.10A). The complex IV inhibitor potassium cyanide (KCN) nearly abolished TNF-α/CHX-induced ROS production and cell death (Fig. IV.10B). The complex V (F0F1-ATP synthase) inhibitor, oligomycin moderately reduced both TNF-α/CHX-induced ROS production and cell death, even though at the used concentration it *per se* mildly induced ROS production without affecting cell death as compared to control (Fig. IV.10C). The proton ionophore uncouplers, CCCP and carbonyl cyanide p-trifluoromethoxyphenylhydrozone (FCCP) both decreased TNF-α/CHX-induced ROS production and cell death partially but with variable effects, where FCCP resulted in less pronounced reduction of ROS levels and in higher cell death prevention as compared to CCCP (Fig. IV.10D and 11A). It should be noted however that FCCP *per se* increased ROS production mildly as compared to control. The mitochondria-targeted antioxidant Mito-TEMPO did not show any effect on ROS generation or cell death induced by TNF-α/CHX (Fig. IV.11B).

These results suggest that NOX and mitochondria, but not xanthine oxidase, contribute to ROS production and cell death after TNF-α/CHX challenge in MODE-K cells.

Table IV.1   Effect of commonly used antioxidants or inhibitors of ROS-generating enzymes on TNF-α (1 ng/ml) plus CHX (10 µg/ml)-induced intracellular total ROS level and cell death in MODE-K cells stained with carboxy-H_2DCFDA and Sytox Red (expressed as % reduction of the increase induced by TNF-α/CHX; a negative value indicates that the response to TNF-α/CHX increased in the presence of the compound). DCF: dichlorofluorescein. Mean ± SEM of three independent experiments. *: Significant reduction of the response to TNF-α/CHX ($P < 0.05$).
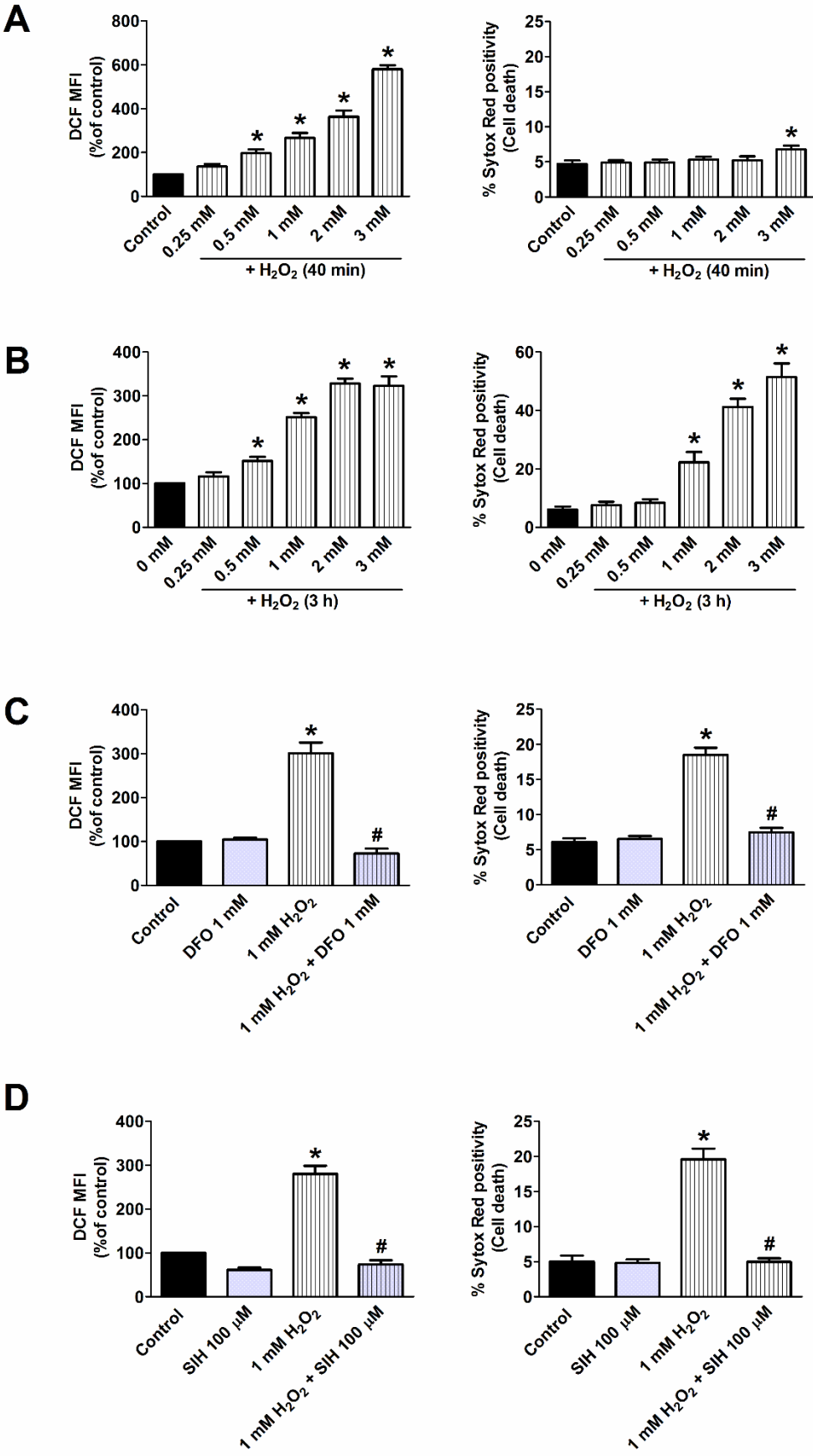
IV.4.3 TNF-α/CHX induces mitochondrial superoxide anion production in MODE-K cells

In mitochondria, superoxide anion is generated as a byproduct during the flow of electrons through the four ETC complexes to molecular oxygen and is considered as the primary ROS originating from mitochondria. MitoSOX Red, a novel sensitive probe for highly selective detection of superoxide anion generated in the mitochondria of live cells (Robinson *et al.*, 2006) was thus tested. Incubation of MODE-K cells with 0.1-1 ng/ml TNF-α plus 10 µg/ml CHX for 6 h increased MitoSOX Red-detectable superoxide levels in a concentration-dependent manner, corresponding with the concentration-dependent increase in cell death (Fig. IV.12A). Moreover, 1 ng/ml TNF-α plus 10 µg/ml CHX for 0.5-6 h induced a time-dependent increase in mitochondrial superoxide anion production (Fig. IV.12B, left panel) starting at 2 h, which was paralleled by apoptosis (annexin positivity; data not shown) and cell death (Sytox Green positivity; Fig. IV. 12B, right panel). The mitochondrial superoxide level induced by 6 h of incubation with 1 ng/ml TNF-α plus 10 µg/ml CHX was nearly 3 fold higher as the control level. Laser scanning confocal microscopic (LSCM) analysis confirmed the time-dependent increase in mitochondrial superoxide level (MitoSOX Red fluorescence) and cell death (Sytox Green fluorescence) by 1 ng/ml TNF-α plus 10 µg/ml CHX (Fig. IV.13). Antimycin-A also increased generation of mitochondrial superoxide in a concentration-dependent manner further confirming the specificity of detection of mitochondrial superoxide generation by MitoSOX Red (data not shown).

The mitochondrial complex I and II inhibitors amytal and TTFA, that nearly abolished total ROS production and cell death by TNF-α/CHX, were then tested on TNF-α/CHX-induced mitochondrial superoxide anion generation. Treatment with amytal significantly decreased TNF-α (1 ng/ml) plus CHX (10 µg/ml)-induced mitochondrial superoxide level by 72.9 ± 3.3% and cell death by 83.6 ± 4.9% (n = 3; Fig. IV.12C). TTFA abolished TNF-α/CHX-induced

Fig. IV.4 ROS production and cell death in H_2O_2-treated MODE-K cells. (A and B) Influence of 0.25-3 mM H_2O_2, incubated for 40 min (A) or 3 h (B), on intracellular total ROS levels (expressed as % of control DCF MFI; left panel) and cell death (expressed as % Sytox Red positivity; right panel). Control cells were incubated with serum-free medium alone. Mean ± SEM of six (A) and three (B) independent experiments are given. *$P < 0.05$ versus control. (C and D) Effect of desferrioxamine (DFO) or salicylaldehyde isonicotinoyl hydrazone (SIH) on H_2O_2-induced intracellular total ROS production and cell death in MODE-K cells measured by flow cytometry. Influence of 1 mM H_2O_2, incubated for 3 h, on intracellular total ROS levels (left panel) and cell death (right panel) in the absence and presence of 1 mM DFO (C) or 100 µM SIH (D). Control cells were incubated with serum-free medium alone; the effect of DFO or SIH *per se* was also tested. Mean ± SEM of three independent experiments. *$P < 0.05$ versus control. #$P < 0.05$ versus 1 mM H_2O_2 alone.
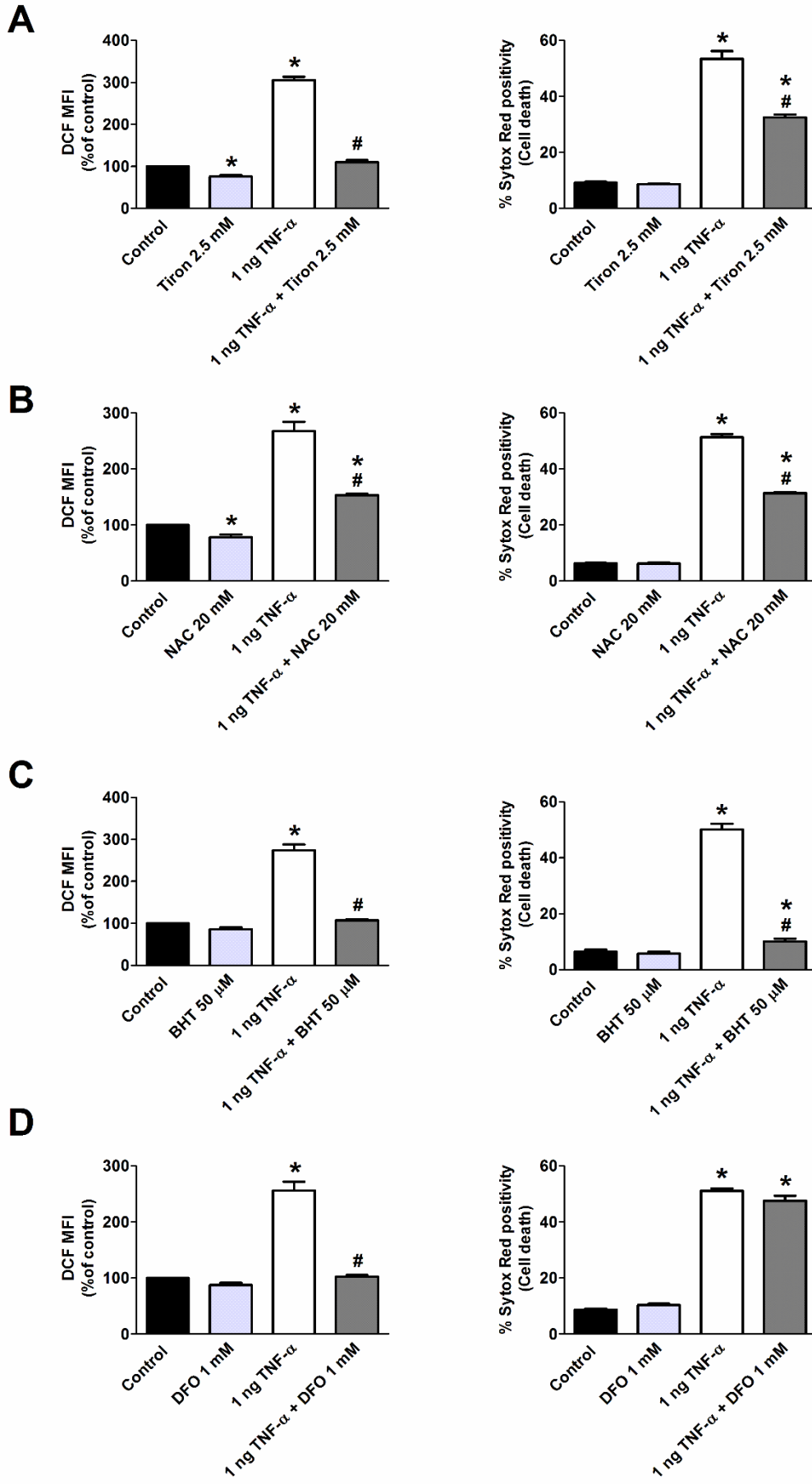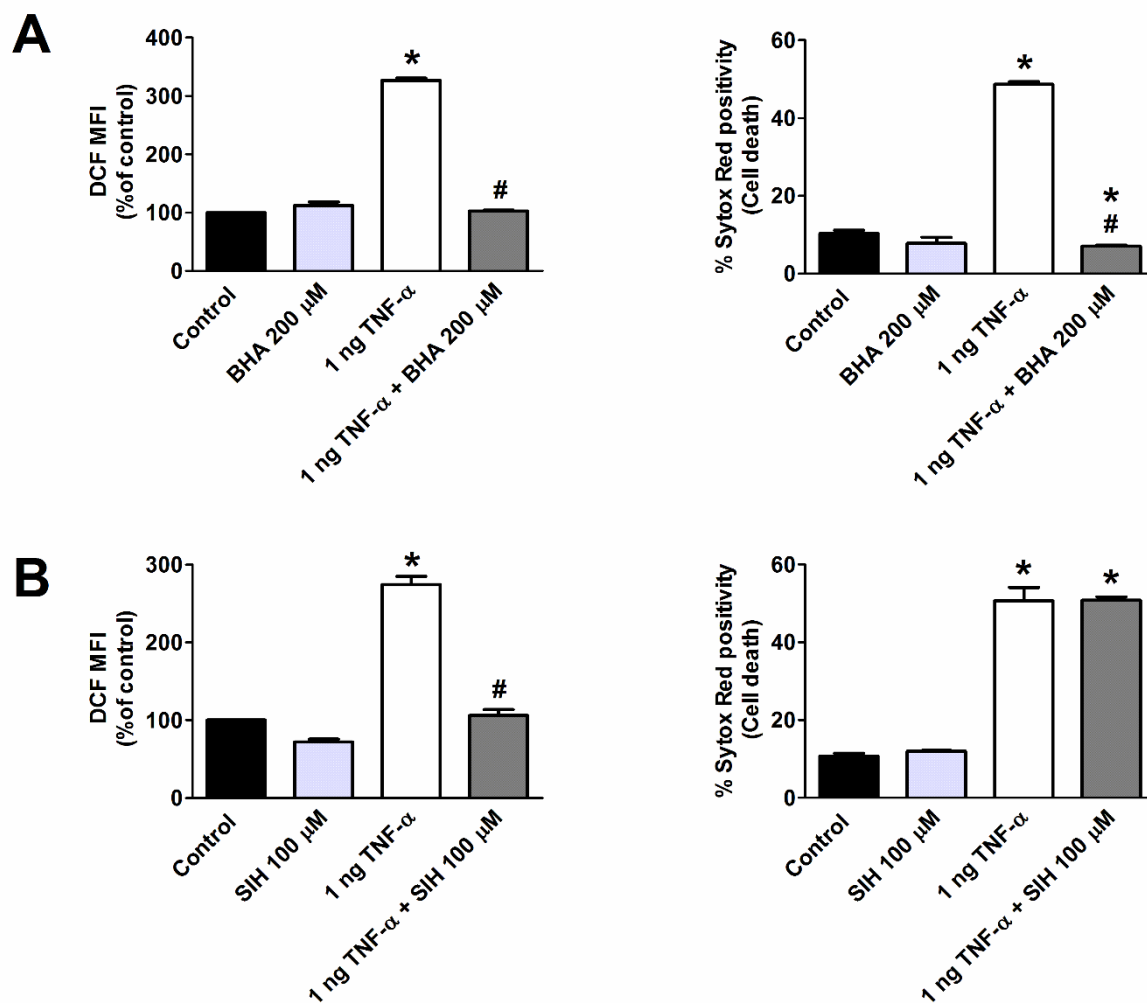
Fig. IV.6 Effect of a lipophilic antioxidant or of an iron chelator on TNF-α/CHX-induced total ROS production (assessed with carboxy-H₂DCFDA) and cell death (assessed with Sytox Red) in MODE-K cells measured by flow cytometry. Influence of 1 ng/ml TNF-α plus 10 µg/ml CHX, incubated for 6 h, on intracellular total ROS levels (left panel) and cell death (right panel) in the absence and presence of 200 µM butylated hydroxyanisole (BHA; A) or 100 µM salicylaldehyde isonicotinoyl hydrazone (SIH; B). Control cells were incubated with serum-free medium alone; the effect of BHT or SIH *per se* was also tested. Mean ± SEM of three independent experiments. *$P < 0.05$ versus control. #$P < 0.05$ versus 1 ng/ml TNF-α plus 10 µg/ml CHX alone.

mitochondrial superoxide production and reduced TNF-α/CHX-induced cell death by 77.5 ± 3.8% (n = 3; Fig. IV.12D). This suggests that complex I (ubiquinone binding I_Q site) and II (Q_P site) might be the major contributors of mitochondrial superoxide production.

Fig. IV.5 Effect of antioxidants on TNF-α/CHX-induced total ROS production and cell death in MODE-K cells. Influence of 1 ng/ml TNF-α plus 10 µg/ml CHX, incubated for 6 h, on intracellular total ROS levels (left panel) and cell death (right panel) in the absence and presence of 2.5 mM tiron (A), 20 mM N-acetylcysteine (NAC; B), 50 µM butylated hydroxytoluene (BHT; C) or 1 mM desferrioxamine (DFO; D). Control cells were incubated with serum-free medium alone; the effect of each antioxidant *per se* was also tested. Mean ± SEM of three independent experiments. *$P < 0.05$ versus control. #$P < 0.05$ versus 1 ng/ml TNF-α plus 10 µg/ml CHX alone.
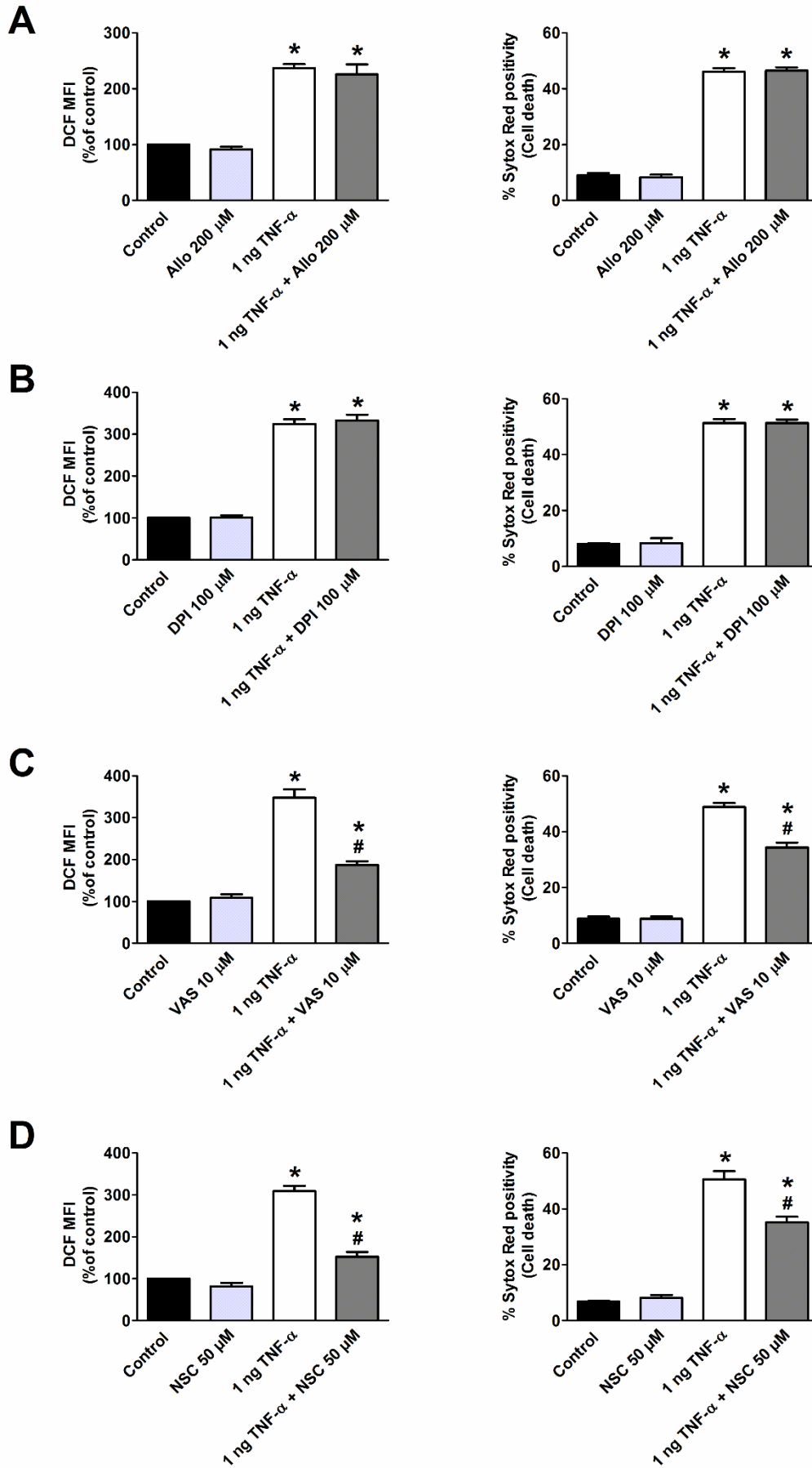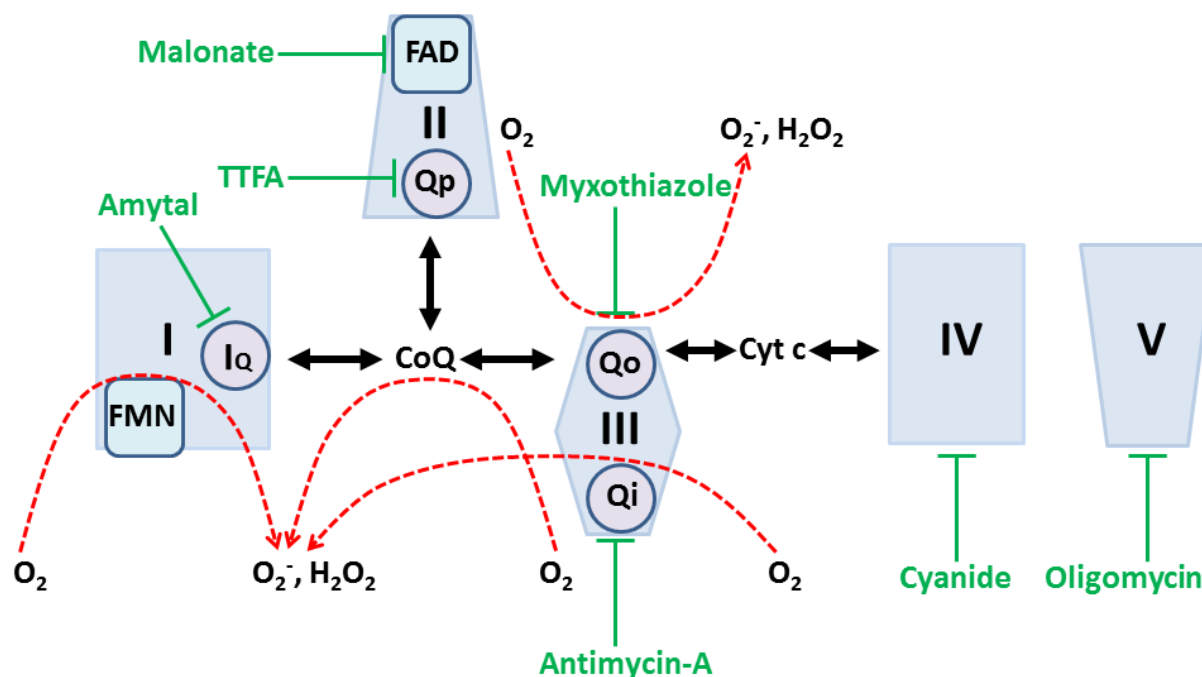
Fig. IV.8 Graphical representation of different ROS producing sites in the mitochondria and the site of action of mitochondrial complex inhibitors. Flavin mononucleotide (FMN); Coenzyme Q (CoQ); Ubiquinone binding site of complex I (I_Q); Flavin adenine dinucleotide (FAD); Proximal ubiquinone binding site of complex II (Q_P); Ubiquinol oxidation site of complex III (Qo site); Ubiquinone reduction site of complex III (Qi site); Cytochrome c (Cyt c).

IV.4.4 Influence of TNF-α/CHX on mitochondrial membrane potential (Ψ_m), mitochondrial dysfunction and respiratory rate of MODE-K cells

As ROS generation and depolarization of mitochondrial membrane potential (Ψ_m) can contribute to apoptosis (Ricci *et al.*, 2003), we next examined the changes in Ψ_m in MODE-K cells. Treatment of MODE-K cells with 0.1-1 ng/ml TNF-α plus 10 µg/ml CHX induced a concentration-dependent increase in cells with depolarized mitochondria (TMRM assay,

Fig. IV.7 Effect of inhibitors of xanthine oxidase, NOX or Rac1 on TNF-α/CHX-induced total ROS production and cell death in MODE-K cells. Influence of 1 ng/ml TNF-α plus 10 µg/ml CHX, incubated for 6 h, on intracellular total ROS levels (left panel) and cell death (right panel) in the absence and presence of 200 µM allopurinol (Allo; A), 100 µM diphenylene iodonium (DPI; B), 10 µM VAS-2870 (VAS; C) or 50 µM NSC23766 (NSC; D). Control cells were incubated with serum-free medium alone; the effect of each inhibitor *per se* was also tested. Mean ± SEM of three independent experiments. *$P < 0.05$ versus control. #$P < 0.05$ versus 1 ng/ml TNF-α plus 10 µg/ml CHX alone.
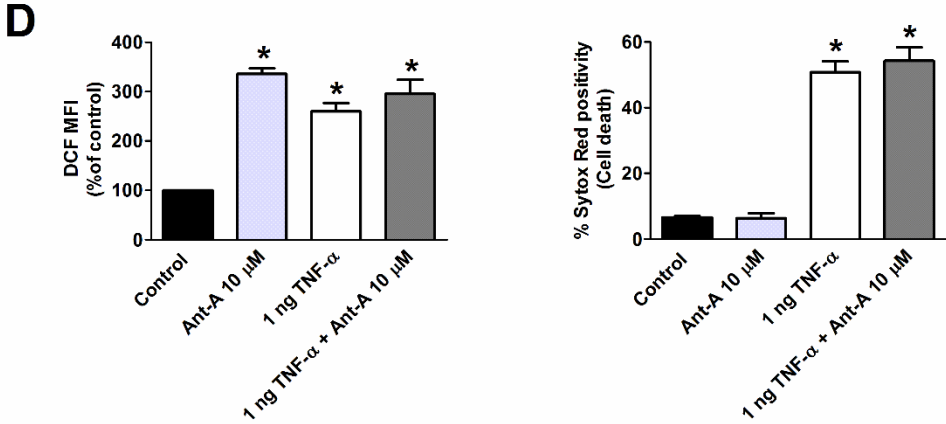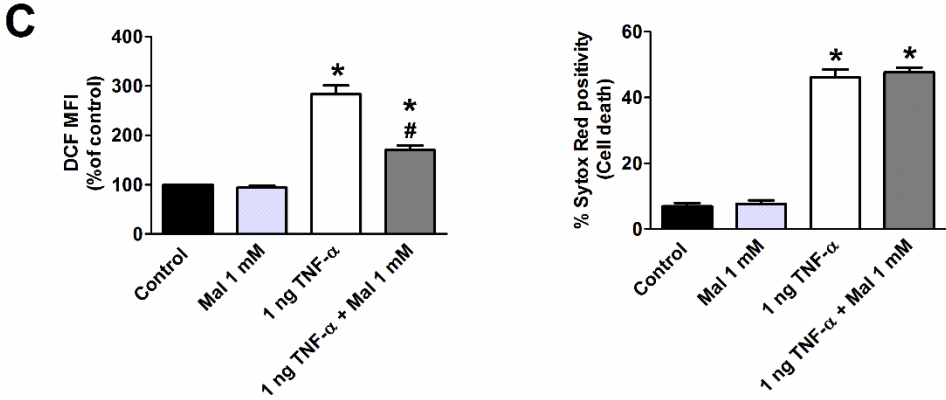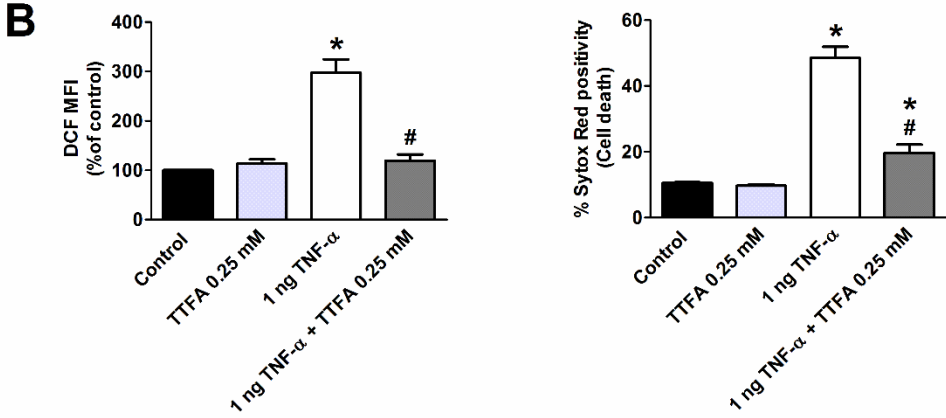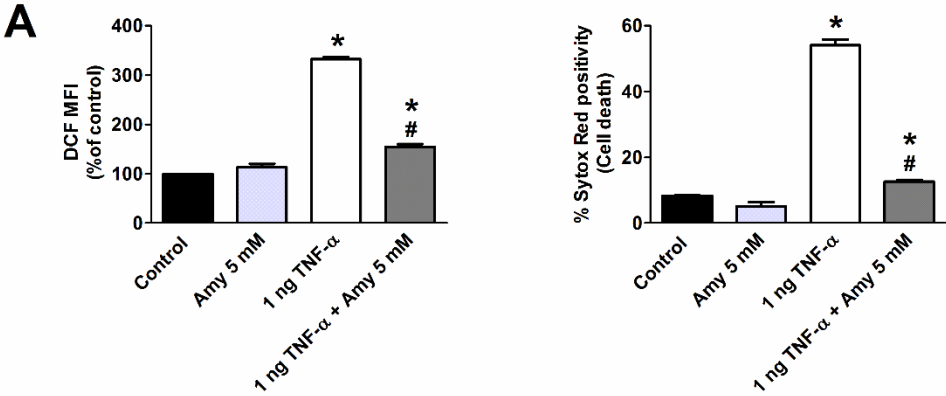
Fig. IV.14A, left panel and JC-10 assay, Fig. IV.15A) with concomitant increase in cell death (as assessed with Sytox Green in combination with the TMRM assay, Fig. IV.14A, right panel). About 60% of the cells treated with TNF-α (1 ng/ml) plus CHX (10 μg/ml) showed a reduction in Ψ_m, suggesting that a decrease in their respiratory chain activity or mitochondrial uncoupling might play an important role in cell death. The positive control CCCP dissipated the mitochondrial membrane potential in a concentration-dependent manner (JC-10 assay, Fig. IV.15B). The time kinetic assay with TNF-α (1 ng/ml) plus CHX (10 μg/ml) for 0.25-6 h showed that the depolarization of mitochondria started as early as 1 h and increased further in a time-dependent manner while annexin positivity and cell death started at 2 h (Fig. IV.14B). This suggests that collapse of the Ψ_m occurred as an early event during TNF-α/CHX-induced apoptotic cell death in MODE-K cells. The most effective tested antioxidant, BHA, nearly abolished TNF-α/CHX-induced mitochondrial depolarization and cell death (Fig. IV.15C) implying that the changes in mitochondrial membrane potential might be a crucial event during cell death in MODE-K cells. Additionally, as an indicator of dysfunction of mitochondria, two types of mitochondria-specific dyes were used to distinguish actively respiring (MitoTracker Deep Red FM-positive) and total (MitoTracker Green FM-positive) mitochondria. TNF-α (0.1-1 ng/ml) plus CHX (10 μg/ml) increased the amount of respiration-interrupted mitochondria in a concentration- and time-dependent (tested with 1 ng/ml; increase starting at 1 h) manner suggesting that mitochondrial dysfunction plays a crucial role in apoptotic cell death of MODE-K cells (Fig. IV.16 and 17). These data together suggest that dysfunctional mitochondria with reduced integrity might allow leakage of ROS from the mitochondria contributing to cell death.

We next investigated whether the observed increase in ROS production and decrease in mitochondrial transmembrane potential could be related to modulation of mitochondrial energy metabolism. To this end, we measured cellular oxygen consumption and glycolysis rate using a Seahorse XF96 analyzer. Addition of TNF-α (1 ng/ml) plus CHX (10 μg/ml)

Fig. IV.9 Effect of inhibitors of mitochondrial electron transport chain complex I, II or III on TNF-α/CHX-induced total ROS production and cell death in MODE-K cells. Influence of 1 ng/ml TNF-α plus 10 μg/ml CHX, incubated for 6 h, on intracellular total ROS levels (left panel) and cell death (right panel) in the absence and presence of 5 mM amytal (Amy; A), 0.25 mM theonyltrifluoroacetone (TTFA; B), 1 mM malonate (Mal; C) or 10 μM antimycin-A (Ant-A; D). Control cells were incubated with serum-free medium alone; the effect of each inhibitor *per se* was also tested. Mean ± SEM of three independent experiments. *$P < 0.05$ versus control. #$P < 0.05$ versus 1 ng/ml TNF-α plus 10 μg/ml CHX alone.
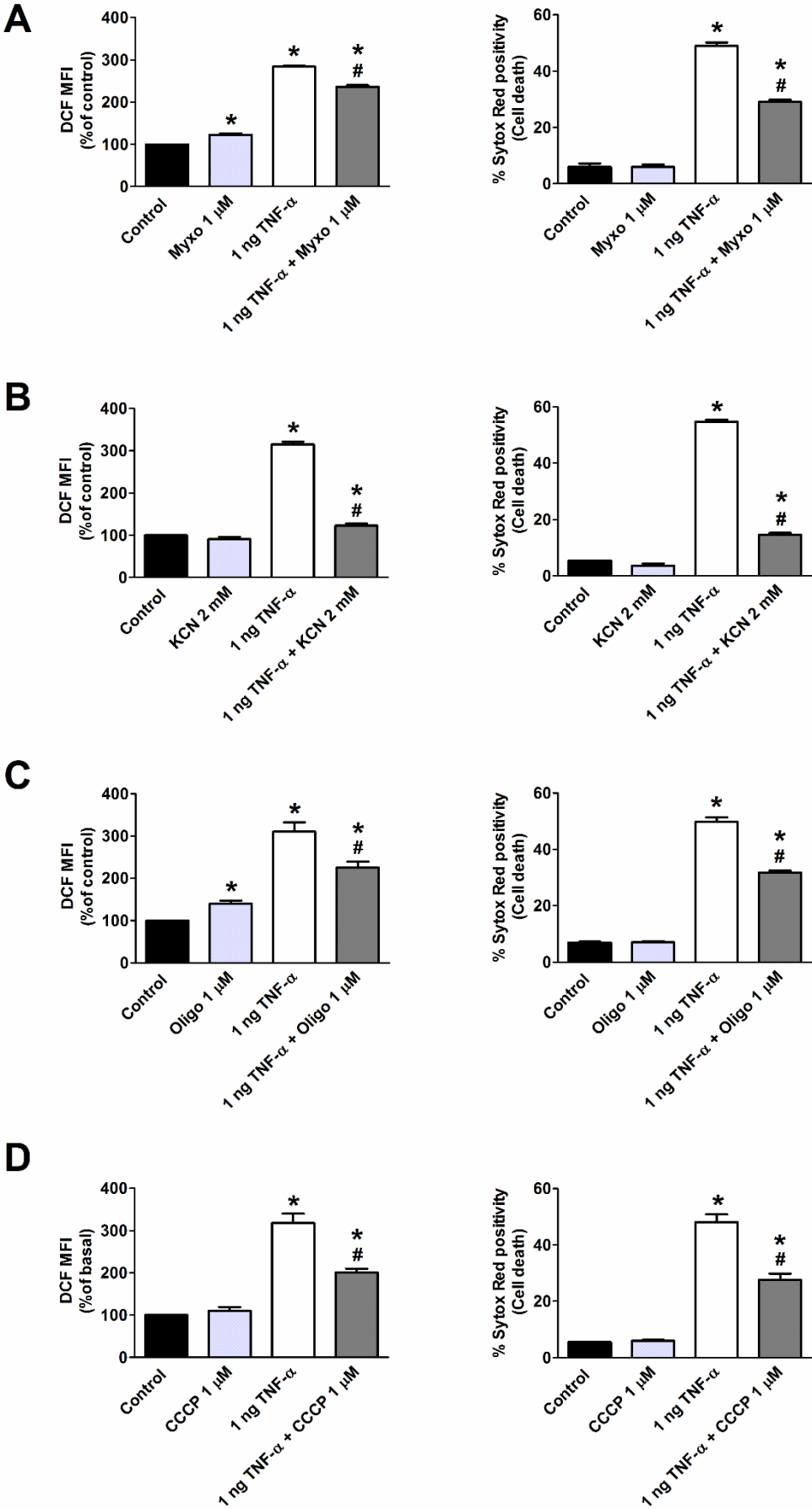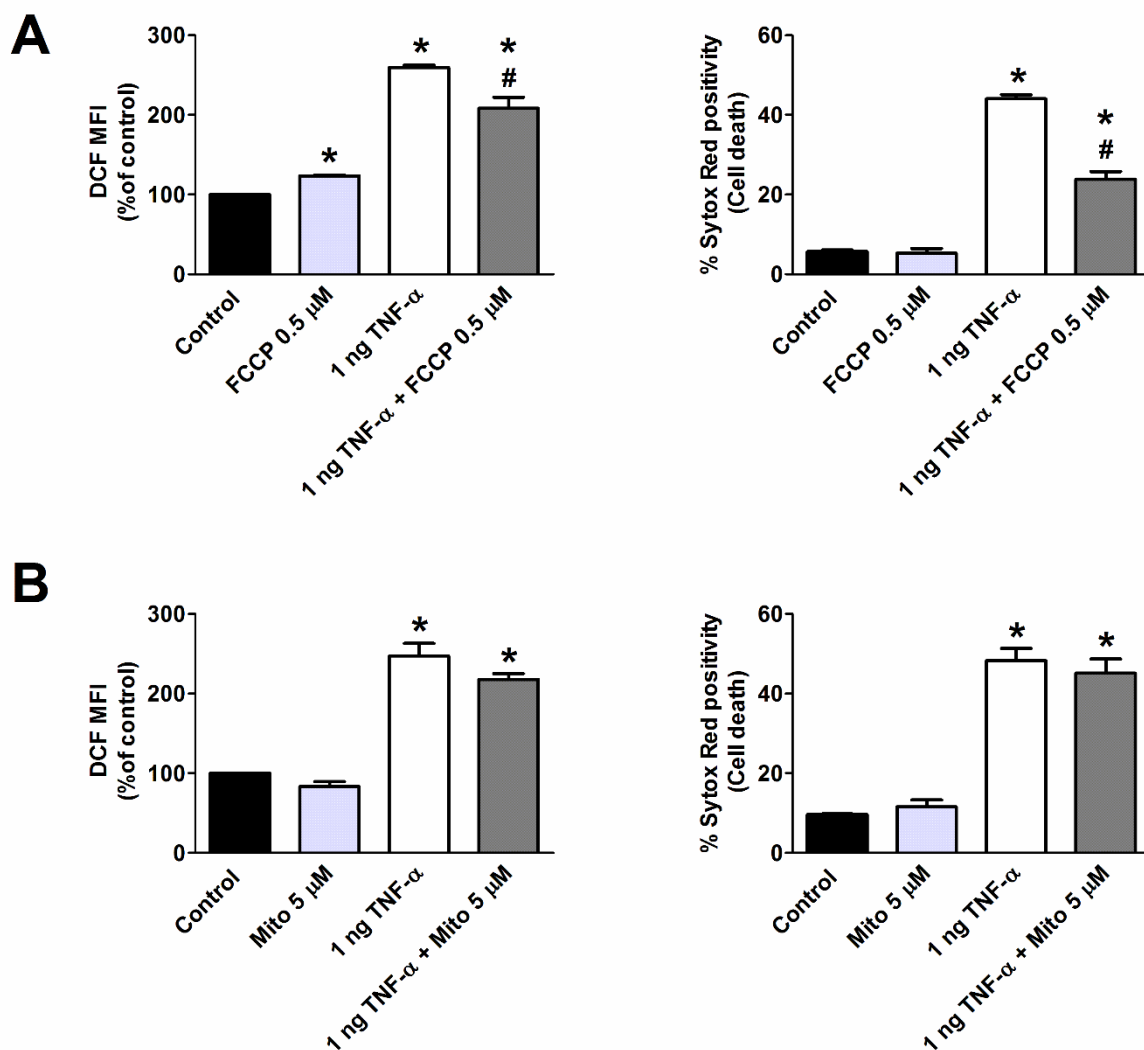
Fig. IV.11   (A and B) Effect of a proton ionophore uncoupler or of a mitochondria-targeted antioxidant on TNF-α/CHX-induced total ROS production and cell death in MODE-K cells. Influence of 1 ng/ml TNF-α plus 10 μg/ml CHX, incubated for 6 h, on intracellular total ROS levels (left panel) and cell death (right panel) in the absence and presence of 0.5 μM carbonyl cyanide p-trifluoromethoxyphenylhydrozone (FCCP; A) or 5 μM Mito-TEMPO (Mito; B). Control cells were incubated with serum-free medium alone; the effect of the compounds *per se* was also tested. Mean ± SEM of three independent experiments. *$P < 0.05$ versus control. #$P < 0.05$ versus 1 ng/ml TNF-α plus 10 μg/ml CHX alone.

Fig. IV.10   Effect of inhibitors of mitochondrial electron transport chain complex III, IV or V or of a proton ionophore uncoupler on TNF-α/CHX-induced total ROS production and cell death in MODE-K cells. Influence of 1 ng/ml TNF-α plus 10 μg/ml CHX, incubated for 6 h, on intracellular total ROS levels (left panel) and cell death (right panel) in the absence and presence of 1 μM myxothiazole (Myxo; A), 2 mM potassium cyanide (KCN; B), 1 μM oligomycin (Oligo; C) or 1 μM carbonylcyanide m-chlorophenylhydrazone (CCCP; D). Control cells were incubated with serum-free medium alone; the effect of each inhibitor *per se* was also tested. Mean ± SEM of three independent experiments. *$P < 0.05$ versus control. #$P < 0.05$ versus 1 ng/ml TNF-α plus 10 μg/ml CHX alone.
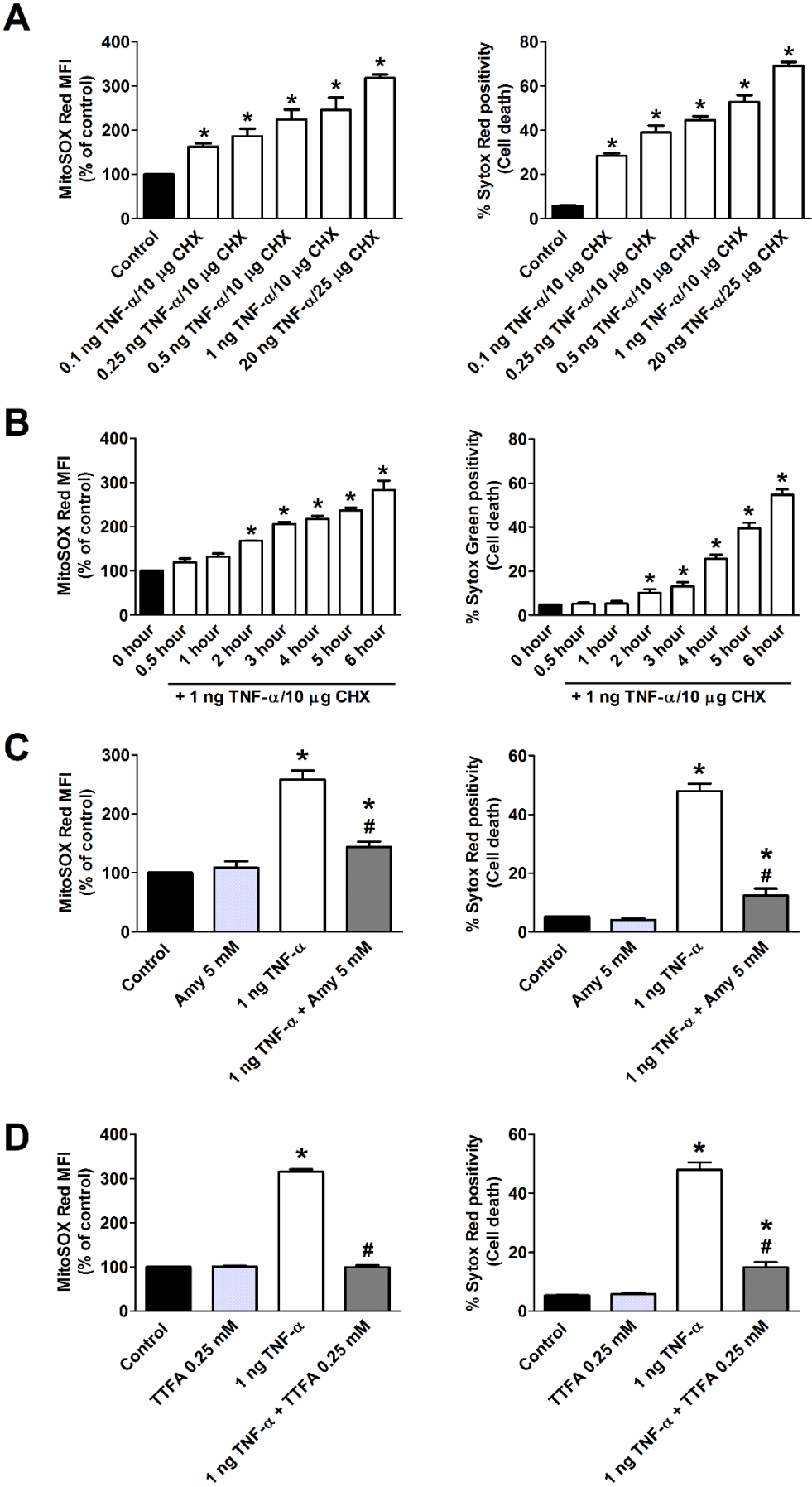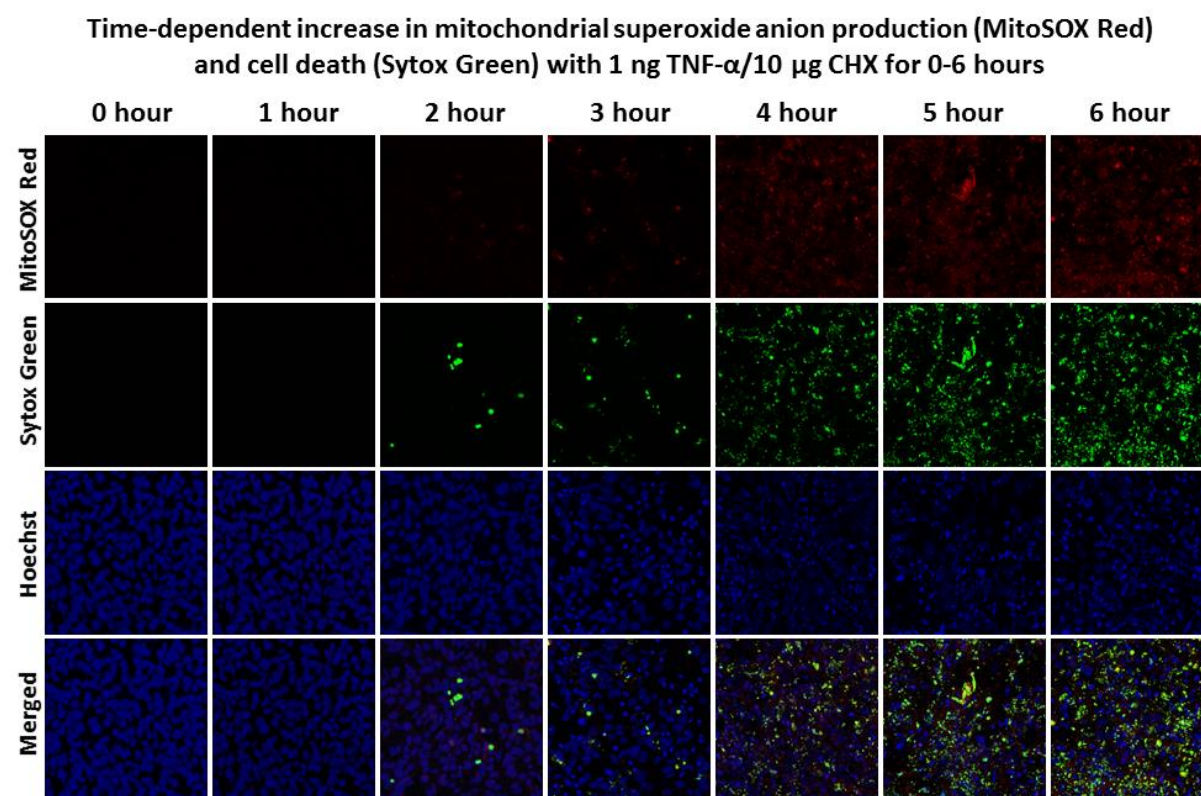
Fig. IV.13 Time-dependent induction of mitochondrial superoxide anion production (assessed with MitoSOX Red) and cell death (assessed with Sytox Green) by TNF-α/CHX in MODE-K cells as imaged with laser scanning confocal microscopy. Time course study of influence of 1 ng/ml TNF-α plus 10 µg/ml CHX, incubated for 0-6 h, on mitochondrial superoxide anion production and cell death after staining with the mitochondrial superoxide probe MitoSOX Red (for superoxide production; red, first row), the cell-impermeable DNA dye Sytox Green (cell death; green, second row) and chromatin decondensation using the cell-permeable DNA dye Hoechst 33365 (for nuclei; blue, third row) imaged in separate channels and processed as merged image (fourth row). Results are representative of at least two independent experiments imaged at every one-hour time point.

Fig. IV.12 TNF-α/CHX-induced mitochondrial superoxide anion production (assessed with MitoSOX Red) and cell death (assessed with Sytox Red) in MODE-K cells measured by flow cytometry. (A) Influence of 0.1-1 ng/ml TNF-α plus 10 µg/ml CHX and of 20 ng/ml TNF-α plus 25 µg/ml CHX, incubated for 6 h, on mitochondrial superoxide anion levels (expressed as % of control MitoSOX Red MFI; left panel) and cell death (expressed as % Sytox Red positivity; right panel). Control cells were incubated with serum-free medium alone. Mean ± SEM of six independent experiments. (B) Time course study of the influence of 1 ng/ml TNF-α plus 10 µg/ml CHX, incubated for 0.5-6 h, with simultaneous determination of mitochondrial superoxide anion production (expressed as % of control MitoSOX Red MFI; left panel), annexin positivity (data not shown) and cell death (expressed as % Sytox Green positivity; right panel). Mean ± SEM of three independent experiments. *$P < 0.05$ versus untreated control group in all panels. (C and D) Effect of inhibitors of mitochondrial electron transport chain complex I or complex II on TNF-α/CHX-induced mitochondrial superoxide anion production and cell death in MODE-K cells measured by flow cytometry. Influence of 1 ng/ml TNF-α plus 10 µg/ml CHX, incubated for 6 h, on mitochondrial superoxide anion levels (left panel) and cell death (right panel) in the absence and presence of 5 mM amytal (Amy; C) or 0.25 mM theonyltrifluoroacetone (TTFA; D). Control cells were incubated with serum-free medium alone; the effect of each inhibitor *per se* was also tested. Mean ± SEM of three independent experiments. *$P < 0.05$ versus control. #$P < 0.05$ versus 1 ng/ml TNF-α plus 10 µg/ml CHX alone.
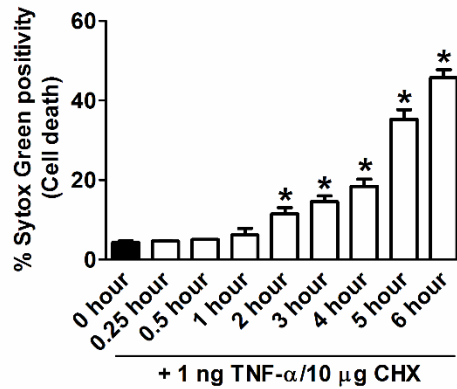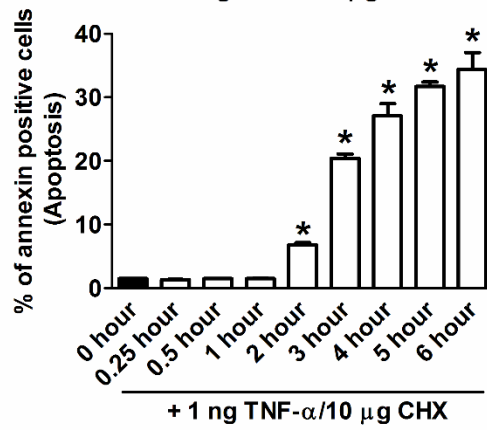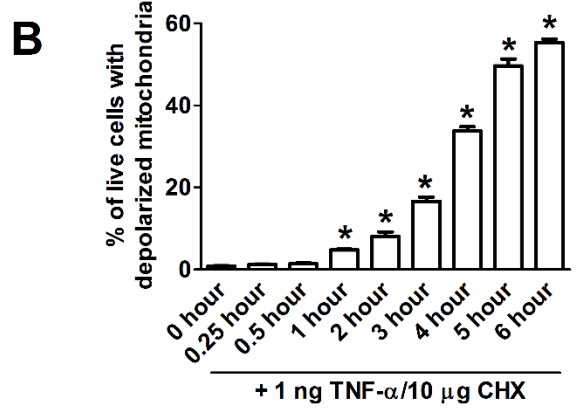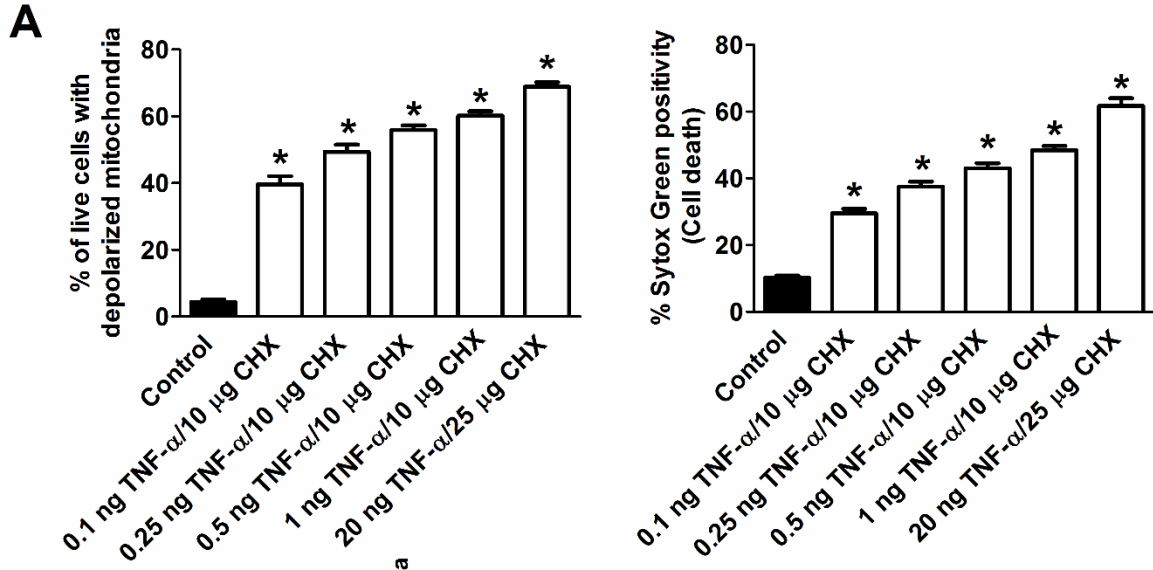
induced a significant decrease in basal oxygen consumption rate (OCR; a measure of mitochondrial respiration) of MODE-K cells within a few minutes of its administration. The first value of OCR in the presence of TNF-α/CHX dropped by 21% compared to the value just before its addition; in the corresponding control group (medium treatment only), the drop was only 4% ($P < 0.05$ versus control). This drop in OCR after TNF-α/CHX addition persisted over the period of observation (until 115 min) with concurrent decrease of the basal extracellular acidification rate (ECAR; a measure of lactate release; data not shown) as compared to control (Fig. IV.18A and B). TNF-α/CHX also increased the maximal respiration induced by CCCP, however without any influence on the minimal non-mitochondrial respiratory rate.

IV.5   Discussion

IV.5.1 ROS overproduction plays a major role in TNF-α/CHX-induced cell death of MODE-K cells

In the present study, we have utilized the well-characterized DCF fluorescence assay for measurement of total ROS production and observed that TNF-α/CHX-induced ROS only appears after 2 h in MODE-K cells. In contrast, TNF-α induced a rapid and transient increase in ROS production (rising as early as 15 min and already again decreasing in the 1 h exposure period) in rat RIE-1 cells (Baregamian *et al.*, 2009), while TNF-α/CHX induced a rapid increase in ROS production from 20 min on (that was maintained for the 2 h exposure period) in rat IEC-6 cells (Jin *et al.*, 2008). Interestingly, MODE-K cells showed a significant increase in DCF fluorescence only upon treatment with a high concentration of exogenous H_2O_2 (0.5 mM) for 40 min while, contrarily, the same concentration of H_2O_2 for 15 min increased DCF fluorescence in the rat IEC-6 cells to the same ROS level as induced by TNF-α (20 ng/ml) plus

Fig. IV.14 TNF-α/CHX-induced depolarization of mitochondrial membrane potential and apoptotic cell death in MODE-K cells measured by flow cytometry. (A) Influence of 0.1-1 ng/ml TNF-α plus 10 µg/ml CHX and of 20 ng/ml TNF-α plus 25 µg/ml CHX, incubated for 6 h, on mitochondrial membrane potential (expressed as % of cells with depolarized mitochondria after TMRM staining; left panel) and cell death (expressed as % Sytox Green positivity; right panel). Control cells were incubated with serum-free medium alone. Mean ± SEM of six independent experiments. *$P < 0.05$ versus control. (B) Time course study of influence of 1 ng/ml TNF-α plus 10 µg/ml CHX, incubated for 0.25-6 h, on mitochondrial membrane potential (% of cells with depolarized mitochondria after TMRM staining), apoptosis (annexin positivity) and cell death (Sytox Green positivity). Mean ± SEM of three independent experiments. *$P < 0.05$ versus untreated (0 h) control group.
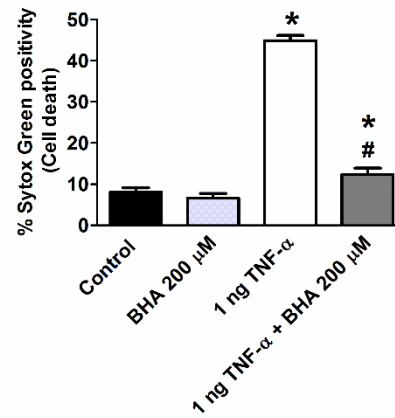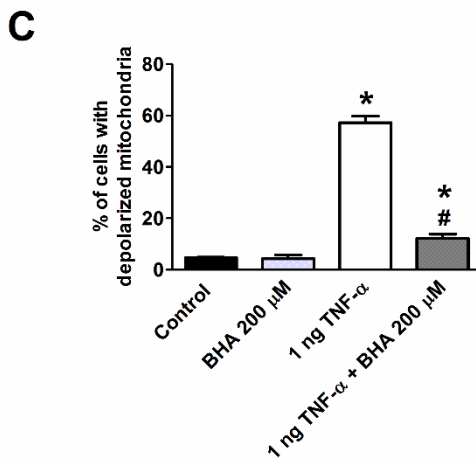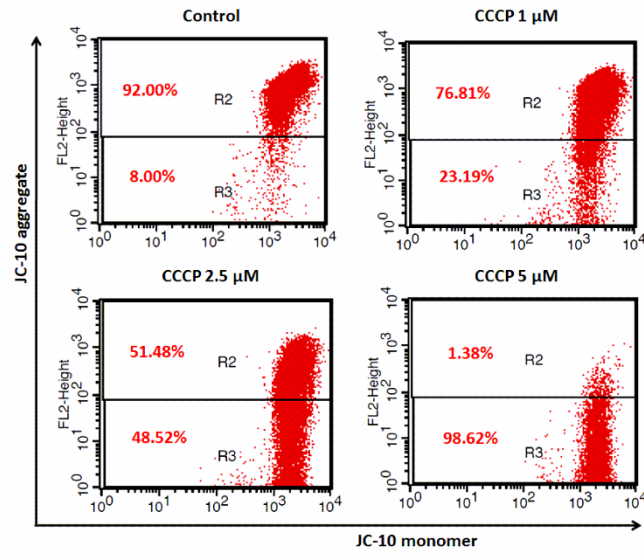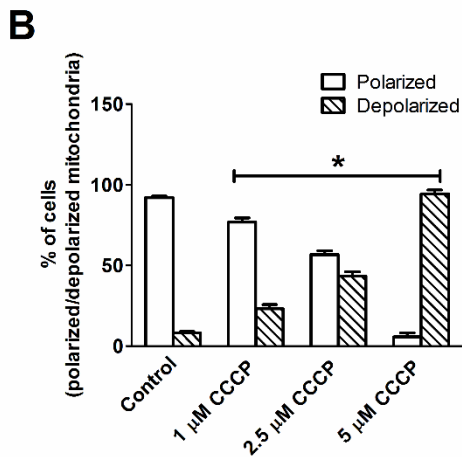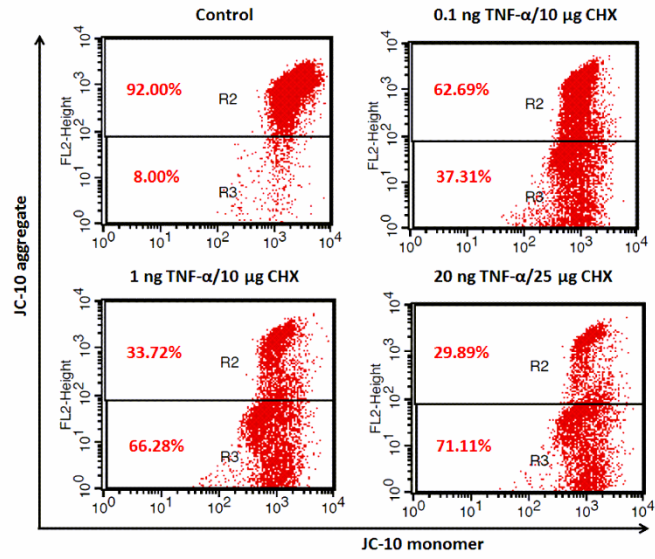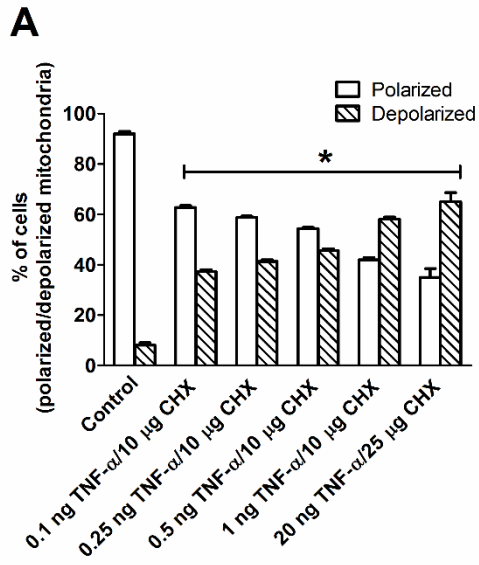
CHX (25 µg/ml) treatment for 30 min (Jin *et al.*, 2008). This suggests that MODE-K cells are highly resistant to the initial burst of oxidative stress by H_2O_2. Moreover, the time-dependent ROS and cell death generation by TNF-α/CHX starting at 2 h suggests that the mouse intestinal epithelial cells are able to counteract the initial burst of oxidative stress up to a certain time point, after which the antioxidant defense can no longer be maintained. From then on, ROS signaling might lead to apoptotic cell death, as evidenced by annexin positivity.

The reduction of both total ROS and cell death by a variety of antioxidants implies that ROS production might contribute to TNF-α/CHX-induced cell death in MODE-K cells. Moreover, the more pronounced effect of lipophilic BHT and BHA as compared to NAC in reducing TNF-α/CHX-induced ROS level and cell death suggests that the cytotoxic ROS produced is less accessible to NAC, which is a hydrophilic antioxidant, and thus might be released predominantly in the hydrophobic domain of the mitochondrial membrane. This is corroborated by the inability of the water-soluble mitochondria-targeted antioxidant mito-TEMPO to suppress ROS generation or cell death. Therefore, we additionally assessed the contribution of mitochondrial ROS by direct measurement of the primary species of intra-mitochondrial ROS, the superoxide anion with MitoSOX Red and we have shown, for the first time, an increase in the levels of mitochondrial superoxide anion with TNF-α/CHX in IECs. Our observation that mitochondria are an important source of ROS generation during TNF-α-induced cell death in mouse MODE-K IECs is in agreement with previous reports in rat IECs, where the involvement of mitochondrial ROS in TNF-α-induced ROS production was studied

Fig. IV.15 Influence of TNF-α/CHX and CCCP on mitochondrial membrane depolarization and effect of the antioxidant butylated hydroxyanisole (BHA) versus TNF-α/CHX in MODE-K cells as assessed by flow cytometry. (A) Influence of 0.1-1 ng/ml TNF-α plus 10 µg/ml CHX and of 20 ng/ml TNF-α plus 25 µg/ml CHX, incubated for 6 h, on mitochondrial membrane potential measured after JC-10 staining by flow cytometry (expressed as % of cells with polarized and depolarized mitochondria; left panel). (B) Influence of 1-5 µM·CCCP, incubated for 6 h, on mitochondrial membrane potential measured after JC-10 staining (expressed as % of cells with polarized and depolarized mitochondria; left panel). Control cells were incubated with serum-free medium alone. Mean ± SEM of three independent experiments. *$P < 0.05$ versus control. In both (A) and (B), the right panels show representative dot plots of the flow cytometric analysis for the different concentrations of TNF-α/CHX or CCCP on the distribution of JC-10 aggregates (cells emitting red fluorescence in the FL-2 channel; R2 gate) and JC-10 monomers (cells emitting green JC-10 detected in the FL-1 channel; R3 gate). (C) Influence of 1 ng/ml TNF-α plus 10 µg/ml CHX, incubated for 6 h, on mitochondrial membrane potential (expressed as % of cells with depolarized mitochondria after TMRM staining; left panel) and cell death (expressed as % Sytox Green positivity; right panel) in the absence and presence of 200 µM butylated hydroxyanisole (BHA). Control cells were incubated with serum-free medium alone; the effect of BHA *per se* was also tested. Mean ± SEM of three independent experiments. *$P < 0.05$ versus control. #$P < 0.05$ versus 1 ng/ml TNF-α plus 10 µg/ml CHX alone.
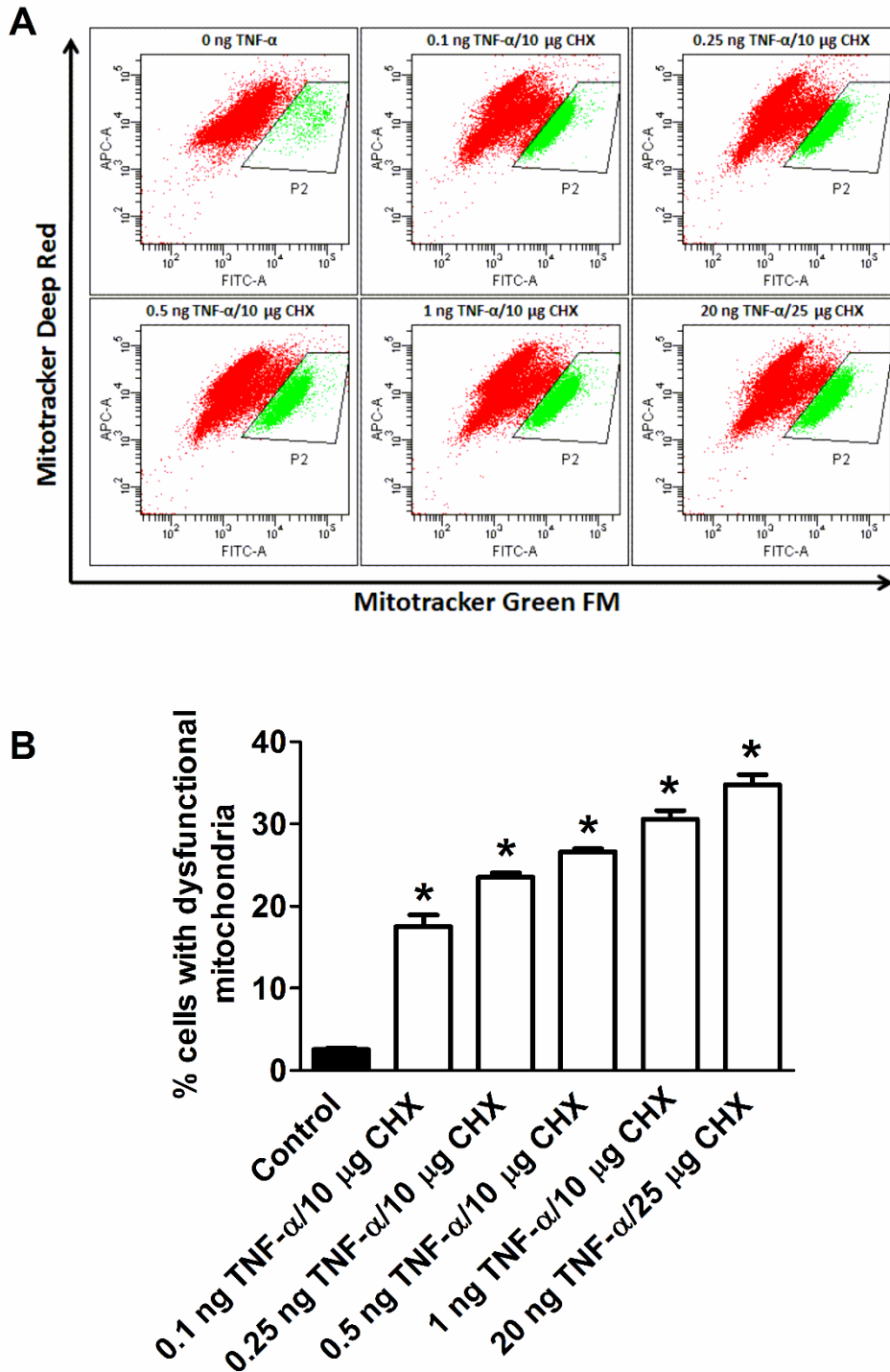
Fig. IV.16 TNF-α/CHX-induced concentration-dependent mitochondrial dysfunction in MODE-K cells. (A) Influence of 0.1-1 ng/ml TNF-α plus 10 µg/ml CHX and of 20 ng/ml TNF-α plus 25 µg/ml CHX, incubated for 6 h, on the amount of respiring mitochondria assessed with Mitotracker Green FM (FL1; FITC) and Mitotracker Deep Red FM (FL4; APC) staining. Representative dot plots of the flow cytometric analysis showing the effect of various concentrations of TNF-α/CHX on the population of cells (gated on live cells) losing mitochondrial potential and with respiration-interrupted mitochondria (shift of cell population towards P2 gated region). (B) Quantification of flow cytometric measurements (expressed as % of cells with dysfunctional mitochondria). Mean ± SEM of three independent experiments. *$P < 0.05$ versus untreated control group.
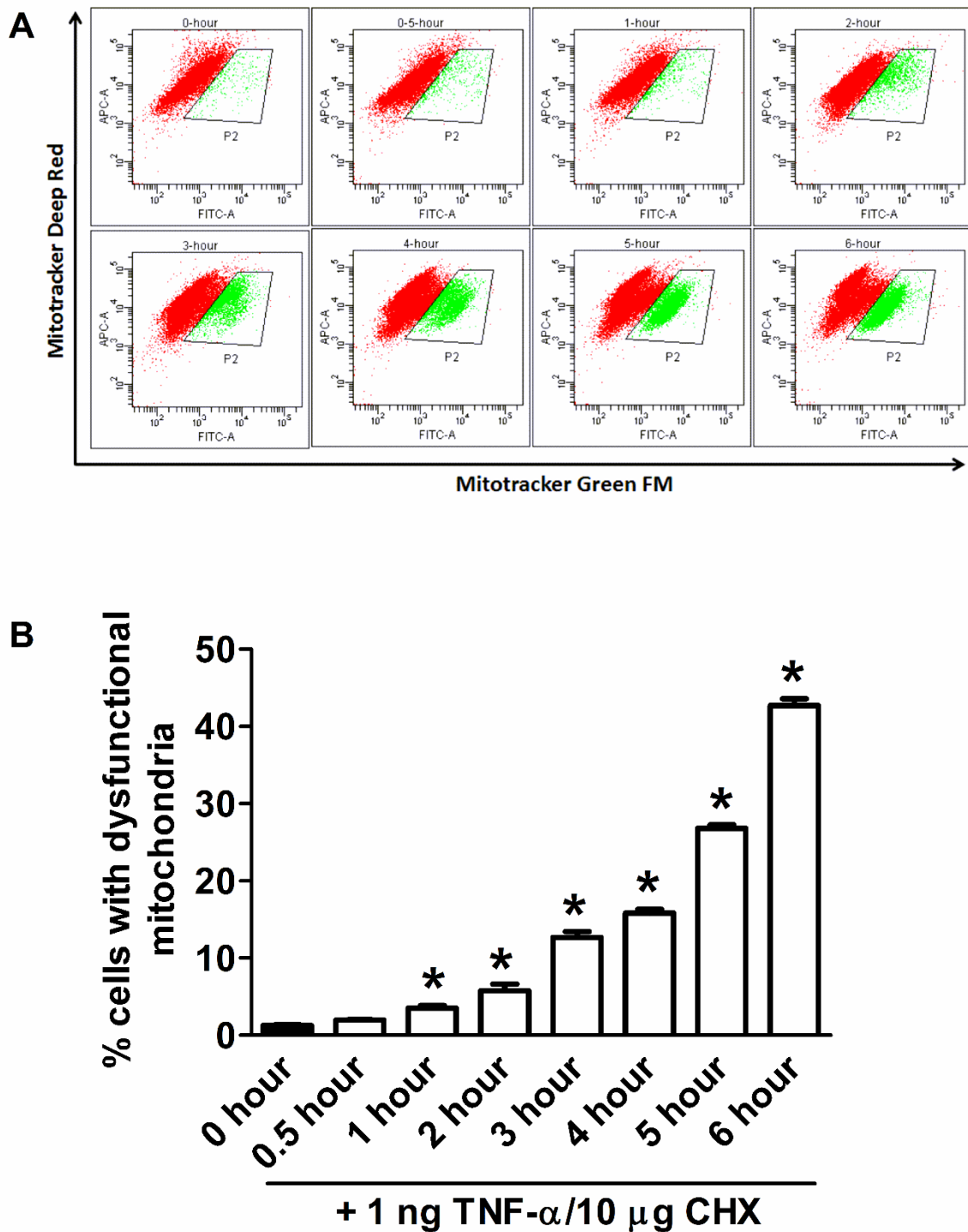
Fig. IV.17 TNF-α/CHX-induced time-dependent mitochondrial dysfunction in MODE-K cells. (A) Time course study of influence of 1 ng/ml TNF-α plus 10 μg/ml CHX, incubated for 0-6 h, on the amount of respiring mitochondria assessed with Mitotracker Green FM (FL1; FITC) and Mitotracker Deep Red FM (FL4; APC) staining. Representative dot plots of the flow cytometric analysis showing the effect of 1 ng/ml TNF-α plus 10 μg/ml CHX upon time on the population of cells (gated on live cells) losing mitochondrial potential and with respiration-interrupted mitochondria (shift of cell population towards P2 gated region). (B) Quantification of flow cytometric measurements (expressed as % of cells with dysfunctional mitochondria). Mean ± SEM of three independent experiments. *$P < 0.05$ versus untreated (0 h) control group.
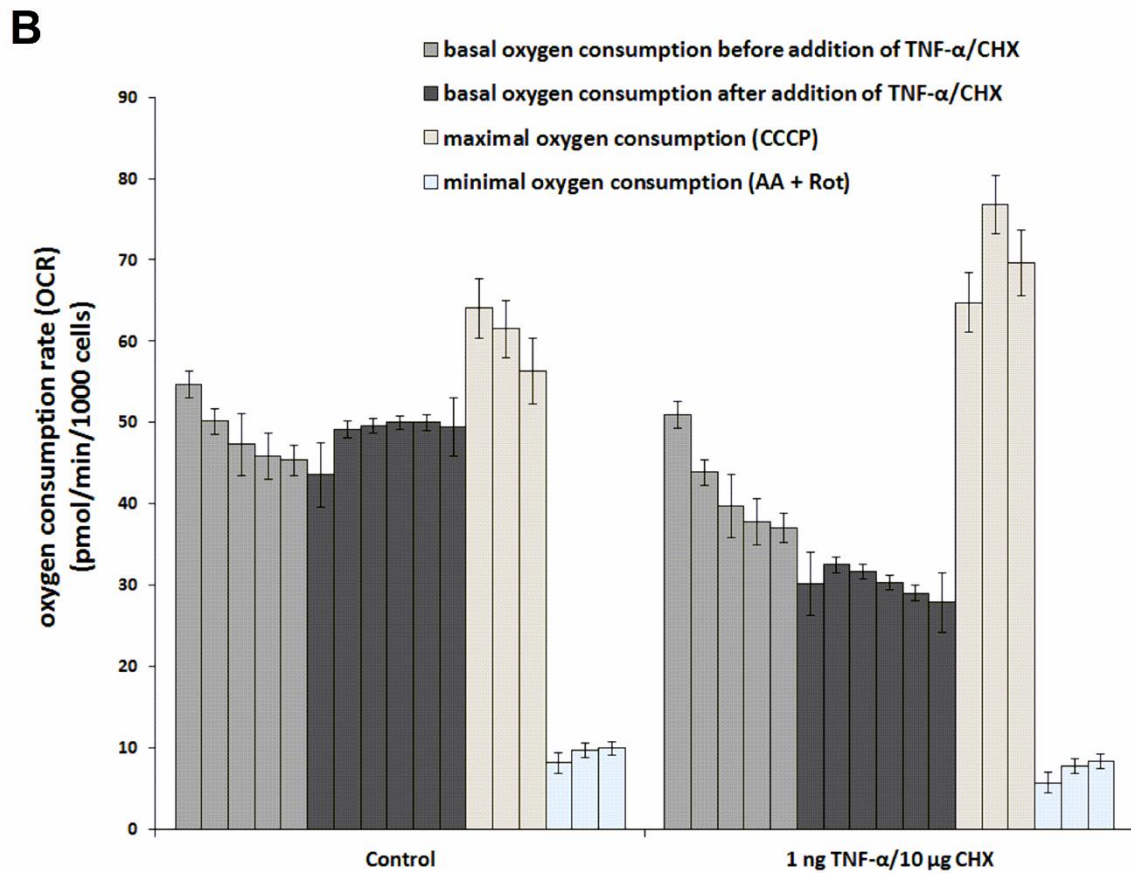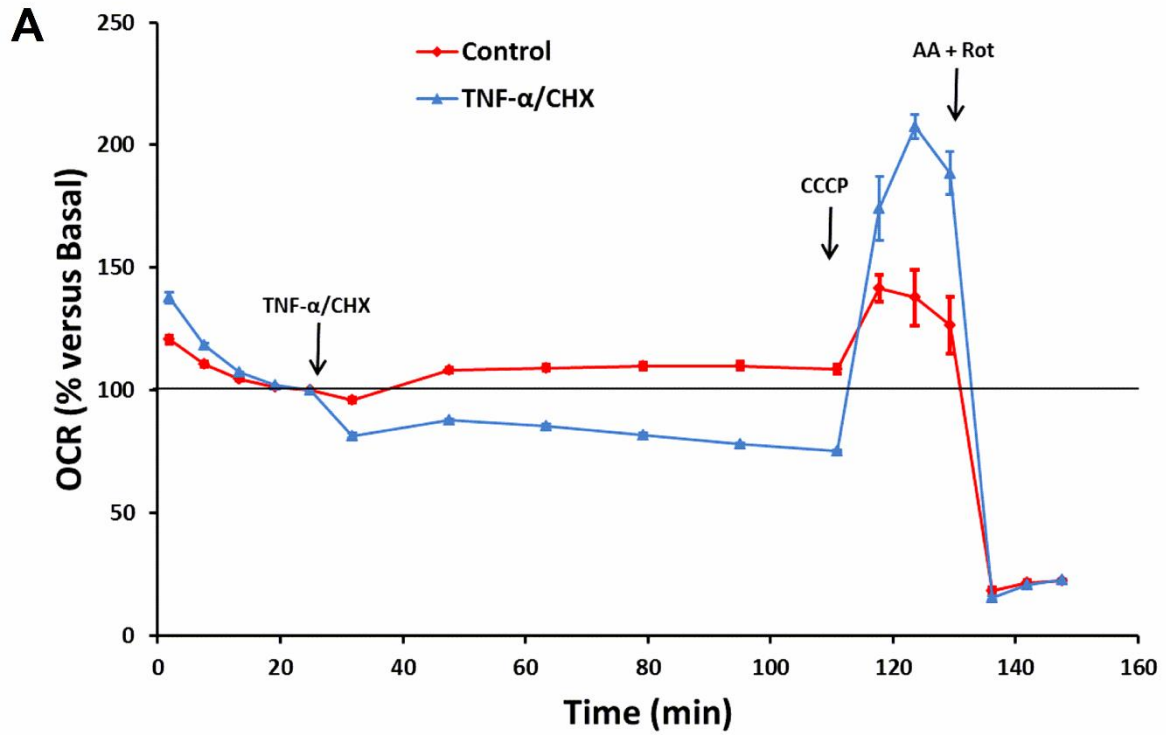
by use of mitochondrial DNA (mtDNA)-depleted rho zero (ρ°) cells (RIE-1 cells) (Baregamian *et al.*, 2009) and using dihydrorhodamine 123 (IEC-6 cells) (Jin *et al.*, 2008). However, our result with the novel fluorogenic probe MitoSOX Red certifies both species (superoxide anion) and organelle specificity (mitochondria) of ROS generation in living cells retaining a functional mitochondrial respiratory chain. The kinetic measurement of mitochondrial superoxide levels indicates the onset of mitochondrial ROS production at 2 h after exposure to TNF-α/CHX, when also apoptotic cell death starts.

The abolishment of TNF-α/CHX-induced total ROS production by iron chelators without any influence on cell death excludes the contribution of iron-mediated oxidative stress in TNF-α/CHX-induced cell death of MODE-K cells. Iron mediates the Fenton reaction, transferring hydrogen peroxide to the highly toxic hydroxyl radical. The latter can thus indeed not contribute to TNF-α/CHX-induced cell death in MODE-K cells in the presence of the iron chelators (Vanden Berghe *et al.*, 2010). Although non-specific and measuring all types of ROS, DCF shows more pronounced reactivity with hydroxyl radical than with hydrogen peroxide (39 fold difference) and superoxide anion (110 fold difference) (Setsukinai *et al.*, 2003). In the presence of iron chelators, other ROS than hydroxyl radical, such as superoxide anion and hydrogen peroxide, might still be generated and contribute to cell death, but not be measurable with DCF. In contrast, the influence of DFO versus a cytotoxic concentration of H_2O_2 illustrates that H_2O_2-induced cytotoxicity is mainly due to the hydroxyl radical. Similar to the iron chelators, tiron abolished TNF-α/CHX-induced ROS production, but in contrast to them, it partially reduced TNF-α/CHX-induced cell death. Tiron is known to exert its antioxidant effect by metal chelation in addition to its superoxide anion

**Fig. IV.18** TNF-α/CHX-induced decrease in mitochondrial respiration in MODE-K cells. (A) Influence of 1 ng/ml TNF-α plus 10 µg/ml CHX, incubated for 2 h, on cellular oxygen consumption rate (OCR, expressed as % of basal). OCR was measured at different time points for 2.5 h. First, five consecutive measurements of baseline respiration during incubation with medium alone for 30 min were done. Then, 1 ng/ml TNF-α plus 10 µg/ml CHX was injected or not (control) followed by six consecutive measurements. Subsequently, the protonophore CCCP was added (50 µM) to measure maximal oxygen consumption for three measurements. Finally, the complex I inhibitor rotenone (2.5 µM) plus the complex III inhibitor antimycin-A (5 µM) were injected, followed by three consecutive measurements to determine the minimal mitochondrial respiration. Finally, the amount of viable cells (HOECHST[+]/PI^{-} cells) in the microchamber of each well was determined by automated imaging. Data are expressed as percentage relative to the basal OCR measured just before TNF-α/CHX injection. The data represent the average of five replicates for each condition. (B) Absolute values for basal, maximal and minimal OCR after addition of medium (control) or TNF-α/CHX in MODE-K cells were analyzed as described above in (A). The data represent the oxygen consumption rate (pmol O_2 per minute) per 1000 cells ± S.E.M (*n*=4).

scavenger and superoxide dismutase mimetic properties (Krishna *et al.*, 1992). Thus, the reduction of TNF-α/CHX-induced cell death by tiron in contrast to the lack of effect of the iron chelators could be attributed to the latter effects at the cytoplasmic level.

IV.5.2 *NOXs contribute to ROS production during TNF-α/CHX-induced cell death in MODE-K cells*

The contribution of mitochondria as a major source of ROS production however does not exclude other ROS sources in the cell. Allopurinol failed to modulate TNF-α/CHX-induced ROS levels and cell death excluding xanthine oxidase as a possible source of ROS production in MODE-K cells. The NOX isozymes present in the mouse small intestinal epithelium are NOX1 and dual oxidase (DUOX)1/2 (Bedard & Krause, 2007; Jones *et al.*, 2013). DPI, the most commonly used classical inhibitor of NOX enzymes, did not modulate the ROS level or the cell death induced by TNF-α/CHX. DPI is a specific flavoprotein inhibitor that not only inhibits the flavin component of NOX, but also inhibits the flavin site in mitochondrial complex I, which leads to increased mitochondrial ROS generation from complex I at a concentration as low as 1 µM (Li *et al.*, 2003; Riganti *et al.*, 2004; Liu & Schubert, 2009). However, in our study DPI at 100 µM *per se* did not induce total ROS generation. These results suggest that the ROS production site of TNF-α/CHX-treated MODE-K cells is not a DPI-inhibitable flavin site. However, the recently developed pan-NOX inhibitor VAS-2870 (Altenhofer *et al.*, 2012) moderately decreased TNF-α/CHX-induced increase in ROS, suggesting that part of ROS generation could be attributed to NOX enzymes. Additionally, a relatively similar effect of NSC23766 to that of VAS-2870 implies that Rac1 mediated activation of NOX isozymes partly contributes to TNF-α/CHX-induced ROS production in MODE-K cells, corresponding to the role of Rac1 regulation in NOX-derived ROS production by TNF-α/CHX treatment of rat IEC-6 cells (Jin *et al.*, 2008). TNF-α has also been reported to lead to NOX-induced ROS production in cell systems other than IECs (Li *et al.*, 2005; Kim *et al.*, 2007; Lai *et al.*, 2012). Moreover, activation of TNFR1 has been shown to lead to recruitment of NOX1, involving riboflavin kinase (Yazdanpanah *et al.*, 2009). Thus, NOX is clearly one of the enzymatic ROS production systems involved during TNF-α/CHX-induced cell death of MODE-K cells.

IV.5.3 Mitochondrial complex I and II are the major contributors of ROS production during TNF-α/CHX-induced cell death in MODE-K cells

Mitochondrial ROS has previously also been implicated in TNF-α-induced cytotoxicity (Jin *et al.*, 2008; Kim *et al.*, 2010). The investigation of the relative contribution of the respiratory chain complexes to TNF-α/CHX-induced ROS production by use of various inhibitors revealed the complex nature of ROS production in living MODE-K cells. Amytal, an inhibitor of the quinone-binding site in complex I (I_Q) reduced TNF-α/CHX-induced ROS by 76% and cell death by 91%. In contrast to malonate that inhibits complex II at the flavin binding domain, the pronounced effect of TTFA in mitigating TNF-α/CHX-induced ROS and cell death strongly suggests that the Qp site of complex II might be a major mitochondrial contributor of ROS production during TNF-α/CHX-induced cell death. The mitochondrial respiratory chain complexes I and III have been suggested to be the major mitochondrial ROS sources in the physiological state with normal oxygen levels (Chen *et al.*, 2003; Turrens, 2003). However, complex II has been implicated in hypoxia-induced ROS generation (Paddenberg *et al.*, 2003) and tissue damage associated with oxidative stress (Ralph *et al.*, 2011). As treatment of MODE-K cells with TNF-α/CHX quickly induces decreased mitochondrial oxygen consumption (based on mitochondrial respiration analysis), mechanisms as occurring during hypoxia could develop so that it is plausible that complex II might also contribute to ROS production. Under such a condition, blockade of complex II at the Qp site by TTFA leads to a reduction of complex I related ROS production, generated by the reverse electron transfer from complex II into complex I. The partial reduction of TNF-α/CHX-induced ROS and cell death by myxothiazole, a Qo site inhibitor of complex III, implies that complex III is also involved in ROS production by TNF-α in MODE-K cells.

Cyanide is a well-known inhibitor of cytochrome c oxidase (complex IV), by binding to heme a3; the effect of potassium cyanide shows that complex IV also in some way participates in ROS production by TNF-α/CHX-treated MODE-K cells. Oligomycin, an inhibitor of the proton-translocating ATP-synthase, also showed a protective effect in MODE-K cells, which is in agreement with a report in Hela cancer cells where oligomycin inhibited TNF-α-induced ROS overproduction and cell death (Shchepina *et al.*, 2002) suggesting a possible involvement of energy-coupled mechanisms in TNF-α-induced effects. Complex IV (involved in the reduction of molecular oxygen to water) and complex V (involved in the production of

ATP) are probably not direct sites of ROS production, but probably indirectly regulate ROS production from the mitochondria. The major sources of TNF-α/CHX-induced ROS production indeed seem complexes I, II and III at their interaction sites with the coenzyme Q (CoQ) in the Q cycle pool : I_Q in complex I, Q_P in complex II and Qo in complex III. Superoxide released from complex III via Qo is released towards the intermembrane space, while complex I and II release superoxide towards the matrix. Superoxide released from complex III towards the matrix via the Qi site does not seem to contribute to TNF-α/CHX-induced ROS production in MODE-K cells, as antimycin-A had no protective influence. The effect of amytal and TTFA in mitigating TNF-α/CHX-induced MitoSOX Red fluorescence further underlines that complexes I (at the I_Q site) and II (at the Q_P site) are major mitochondrial ROS production sites during TNF-α/CHX-induced cell death in MODE-K cells. Indeed, reverse electron transport from complex II to complex I is proposed to be a major pathway for mitochondrial ROS production (Drose, 2013).

As the electrons are passed between the complexes from I to IV, complexes I, III and IV pump protons out of the mitochondrial matrix into the intermembrane space creating an electrochemical gradient across the mitochondrial inner membrane, the proton-motive force, consisting of a transmembrane electric potential and a transmembrane pH gradient. ROS production in the mitochondria is highly sensitive to changes in proton-motive force with slight increases intensifying ROS production and vice versa (Mailloux & Harper, 2012). Mild mitochondrial uncoupling with reduction of the mitochondrial membrane potential could thus effectively limit ROS generation (Produit-Zengaffinen *et al.*, 2007) and this has been implicated as a negative feedback mechanism, counteracting elevated ROS (Papa & Skulachev, 1997; Echtay *et al.*, 2003). Under conditions of oxidative stress, reduction of the proton gradient across the mitochondrial membrane by mild uncoupling is known to reduce mitochondrial ROS production particularly during reverse electron transport (Miwa *et al.*, 2003; Lambert & Brand, 2004; Giardina *et al.*, 2008). In addition to reducing mitochondrial superoxide anion production, "mild" mitochondrial uncoupling has been hypothesized to be a protective mechanism against excessive ROS production by invoking the antioxidant defense system preventing cell death ("uncoupling to survive") (Skulachev, 1996; Brand, 2000; Mailloux & Harper, 2011). The addition of the proton ionophore uncouplers 1 h before exposure of MODE-K cells to TNF-α/CHX lowers the proton-motive force, and can thus be expected to attenuate mitochondrial superoxide production. The proton ionophore-induced

uncoupling might also induce the protective antioxidant defense system, contributing to the reduction of TNF-α/CHX-induced cell death with FCCP and CCCP.

Mitochondrial function is crucial in maintaining the cellular integrity as mitochondria are the main cellular sites controlling energy metabolism and the redox state. Moreover, mitochondrial membrane potential (Ψ_m), metabolic state of mitochondria, and oxygen levels are the major factors regulating ROS production in mitochondria (Li *et al.*, 2013b). The effect of the potent antioxidant BHA in restoring mitochondrial membrane polarization necessary for oxidative phosphorylation with concomitant recovery of cell death further underlines the importance of mitochondrial integrity to prevent TNF-α/CHX-induced cell death. Our observation that treatment of MODE-K cells with TNF-α/CHX causes a rapid decrease in cellular oxygen consumption creating a hypoxic state (within 5 min of addition) and a decrease in Ψ_m (occurring within 60 min) and mitochondrial dysregulation (starting at 60 min) at earlier time points than ROS production and cell death (starting at 2 h), suggests that there could be a sequential link between these events. Taken together, targeted therapies to mitigate mitochondrial ROS could be of potential therapeutic benefit in reducing intestinal epithelial cell death and barrier dysfunction.

IV.5.4 Possible interplay between NOX and mitochondria during TNF-α/CHX-induced cell death in MODE-K cells

More recently, the possible existence of interplay between the NOX and mitochondrial sources of ROS has been proposed, where an increase in mitochondrial ROS can lead to NOX activation and vice versa (Dikalov, 2011). Interestingly, an increase in cellular ROS level originating from mitochondria was observed during serum starvation of human 293T cells; the mitochondrial ROS then trigger NOX1 activation by stimulating phospho-inositide 3-kinase and Rac1 and this pathway maintains ROS production in a later phase. Moreover, mitochondrial ROS are essential to initiate the process leading to cell death, but need the sustained accumulation of ROS by NOX activation to effectively induce cell death, as both inhibition of mitochondrial- or NOX-related ROS production prevented cell death (Lee *et al.*, 2006). In agreement with that, the more pronounced effect in decreasing total cellular ROS and cell death by some of the mitochondrial complex inhibitors as compared to the moderate effect of the NOX inhibitor VAS-2870 in MODE-K cells,

suggests that TNF-α/CHX treatment of serum-starved MODE-K cells might trigger an initial phase of mitochondria-derived ROS production followed by a late phase of ROS production from NOX, whereby Rac1 might mediate the late (but not early) stage of ROS accumulation by interacting with NOX1. Additionally, a report in pulmonary artery smooth muscle cells showed more direct evidence for a role of hypoxia-induced mitochondrial ROS formation in NOX activation and further ROS production mediated via PKCε activation (Rathore *et al.*, 2008). So, it seems plausible that a similar ROS-derived cell death mechanism might occur upon TNF-α/CHX exposure of serum-deprived MODE-K cells, as this results in a state of low oxygen level as observed by the decrease in cellular oxygen consumption. However, this warrants further investigation to better understand the cross-talk between mitochondria and NOX during cellular stress response in IECs.

In summary, this study presents evidence that mitochondria and NOX are the two major sources of ROS overproduction during TNF-α/CHX-induced cell death in MODE-K cells with superoxide anions being the major ROS species. In particular, the quinone-binding sites of mitochondrial complex I (site I_Q) and complex II (site Q_P) seem to be the major sites of mitochondrial ROS production. Moreover, with TNF-α/CHX treatment, the decrease in mitochondrial respiration and loss of Ψ_m occurring as early events followed by subsequent ROS production might lead to apoptotic cell death in MODE-K cells. These findings might advance our understanding of the role of ROS production during cytokine-induced epithelial cell death involved in many acute gastrointestinal inflammatory conditions for the development of selective targeted therapy towards mitigating mitochondrial oxidative stress.

IV.6   References

Altenhofer S, Kleikers PW, Radermacher KA, Scheurer P, Rob Hermans JJ, Schiffers P *et al.* (2012). The NOX toolbox: validating the role of NADPH oxidases in physiology and disease. *Cell Mol Life Sci* **69**, 2327-2343.

Anup R, Aparna V, Pulimood A, Balasubramanian KA (1999). Surgical stress and the small intestine: role of oxygen free radicals. *Surgery* **125**, 560-569.

Babu D, Soenen SJ, Raemdonck K, Leclercq G, De Backer O, Motterlini R *et al.* (2012). TNF-alpha/cycloheximide-induced oxidative stress and apoptosis in murine intestinal epithelial MODE-K cells. *Curr Pharm Des* **18**, 4414-4425.

Baregamian N, Song J, Bailey CE, Papaconstantinou J, Evers BM, Chung DH (2009). Tumor necrosis factor-alpha and apoptosis signal-regulating kinase 1 control reactive oxygen species release, mitochondrial autophagy, and c-Jun N-terminal kinase/p38 phosphorylation during necrotizing enterocolitis. *Oxidative Medicine and Cellular Longevity* **2**, 297-306.

Bedard K & Krause KH (2007). The NOX family of ROS-generating NADPH oxidases: physiology and pathophysiology. *Physiol Rev* **87**, 245-313.

Bhattacharya S, Ray RM, Viar MJ, Johnson LR (2003). Polyamines are required for activation of c-Jun NH2-terminal kinase and apoptosis in response to TNF-alpha in IEC-6 cells. *Am J Physiol Gastrointest Liver Physiol* **285**, G980-991.

Brand MD (2000). Uncoupling to survive? The role of mitochondrial inefficiency in ageing. *Exp Gerontol* **35**, 811-820.

Brand MD (2010). The sites and topology of mitochondrial superoxide production. *Exp Gerontol* **45**, 466-472.

Bullen TF, Forrest S, Campbell F, Dodson AR, Hershman MJ, Pritchard DM *et al.* (2006). Characterization of epithelial cell shedding from human small intestine. *Lab Invest* **86**, 1052-1063.

Chen Q, Vazquez EJ, Moghaddas S, Hoppel CL, Lesnefsky EJ (2003). Production of reactive oxygen species by mitochondria: central role of complex III. *J Biol Chem* **278**, 36027-36031.

Chen YM, Qian ZM, Zhang J, Chang YZ, Duan XL (2002). Distribution of constitutive nitric oxide synthase in the jejunum of adult rat. *World J Gastroenterol* **8**, 537-539.

Deitch EA (2002). Bacterial translocation or lymphatic drainage of toxic products from the gut: what is important in human beings? *Surgery* **131**, 241-244.

Dikalov S (2011). Cross talk between mitochondria and NADPH oxidases. *Free Radic Biol Med* **51**, 1289-1301.

Drose S (2013). Differential effects of complex II on mitochondrial ROS production and their relation to cardioprotective pre- and postconditioning. *Biochimica Et Biophysica Acta-Bioenergetics* **1827**, 578-587.

Duprez L, Takahashi N, Van Hauwermeiren F, Vandendriessche B, Goossens V, Vanden Berghe T *et al.* (2011). RIP kinase-dependent necrosis drives lethal systemic inflammatory response syndrome. *Immunity* **35**, 908-918.

Echtay KS, Esteves TC, Pakay JL, Jekabsons MB, Lambert AJ, Portero-Otin M *et al.* (2003). A signalling role for 4-hydroxy-2-nonenal in regulation of mitochondrial uncoupling. *EMBO J* **22**, 4103-4110.

Giardina TM, Steer JH, Lo SZ, Joyce DA (2008). Uncoupling protein-2 accumulates rapidly in the inner mitochondrial membrane during mitochondrial reactive oxygen stress in macrophages. *Biochim Biophys Acta* **1777**, 118-129.

Greenspon J, Li RY, Xiao L, Rao JN, Marasa BS, Strauch ED *et al.* (2009). Sphingosine-1-Phosphate Protects Intestinal Epithelial Cells from Apoptosis Through the Akt Signaling Pathway. *Dig Dis Sci* **54**, 499-510.

Jin S, Ray RM, Johnson LR (2008). TNF-alpha/cycloheximide-induced apoptosis in intestinal epithelial cells requires Rac1-regulated reactive oxygen species. *Am J Physiol Gastrointest Liver Physiol* **294**, G928-937.

Jones RM, Luo L, Ardita CS, Richardson AN, Kwon YM, Mercante JW *et al.* (2013). Symbiotic lactobacilli stimulate gut epithelial proliferation via Nox-mediated generation of reactive oxygen species. *EMBO J* **32**, 3017-3028.

Kalff JC, Turler A, Schwarz NT, Schraut WH, Lee KKW, Tweardy DJ *et al.* (2003). Intra-abdominal activation of a local inflammatory response within the human muscularis externa during laparotomy. *Annals of Surgery* **237**, 301-315.

Kim JJ, Lee SB, Park JK, Yoo YD (2010). TNF-alpha- induced ROS production triggering apoptosis is directly linked to Romo1 and Bcl-X-L. *Cell Death and Differentiation* **17**, 1420-1434.

Kim YS, Morgan MJ, Choksi S, Liu ZG (2007). TNF-induced activation of the Nox1 NADPH oxidase and its role in the induction of necrotic cell death. *Mol Cell* **26**, 675-687.

Konig P, Dedio J, Muller-Esterl W, Kummer W (2002). Distribution of the novel eNOS-interacting protein NOSIP in the liver, pancreas, and gastrointestinal tract of the rat. *Gastroenterology* **123**, 314-324.

Krishna CM, Liebmann JE, Kaufman D, DeGraff W, Hahn SM, McMurry T *et al.* (1992). The catecholic metal sequestering agent 1,2-dihydroxybenzene-3,5-disulfonate confers protection against oxidative cell damage. *Arch Biochem Biophys* **294**, 98-106.

Lai CF, Shao JS, Behrmann A, Krchma K, Cheng SL, Towler DA (2012). TNFR1-activated reactive oxidative species signals up-regulate osteogenic Msx2 programs in aortic myofibroblasts. *Endocrinology* **153**, 3897-3910.

Lambert AJ & Brand MD (2004). Superoxide production by NADH:ubiquinone oxidoreductase (complex I) depends on the pH gradient across the mitochondrial inner membrane. *Biochem J* **382**, 511-517.

Lee SB, Bae IH, Bae YS, Um HD (2006). Link between mitochondria and NADPH oxidase 1 isozyme for the sustained production of reactive oxygen species and cell death. *J Biol Chem* **281**, 36228-36235.

Li H, Horke S, Forstermann U (2013a). Oxidative stress in vascular disease and its pharmacological prevention. *Trends Pharmacol Sci* **34**, 313-319.

Li JM, Fan LM, Christie MR, Shah AM (2005). Acute tumor necrosis factor alpha signaling via NADPH oxidase in microvascular endothelial cells: role of p47phox phosphorylation and binding to TRAF4. *Mol Cell Biol* **25**, 2320-2330.

Li N, Ragheb K, Lawler G, Sturgis J, Rajwa B, Melendez JA *et al.* (2003). DPI induces mitochondrial superoxide-mediated apoptosis. *Free Radic Biol Med* **34**, 465-477.

Li XY, Fang P, Mai JT, Choi ET, Wang H, Yang XF (2013b). Targeting mitochondrial reactive oxygen species as novel therapy for inflammatory diseases and cancers. *Journal of Hematology & Oncology* **6**.

Liu YB & Schubert DR (2009). The specificity of neuroprotection by antioxidants. *Journal of Biomedical Science* **16**.

Mailloux RJ & Harper ME (2011). Uncoupling proteins and the control of mitochondrial reactive oxygen species production. *Free Radic Biol Med* **51**, 1106-1115.

Mailloux RJ & Harper ME (2012). Mitochondrial proticity and ROS signaling: lessons from the uncoupling proteins. *Trends Endocrinol Metab* **23**, 451-458.

Miwa S, St-Pierre J, Partridge L, Brand MD (2003). Superoxide and hydrogen peroxide production by Drosophila mitochondria. *Free Radic Biol Med* **35**, 938-948.

Mukhopadhyay P, Rajesh M, Hasko G, Hawkins BJ, Madesh M, Pacher P (2007). Simultaneous detection of apoptosis and mitochondrial superoxide production in live cells by flow cytometry and confocal microscopy. *Nat Protoc* **2**, 2295-2301.

Mukojima K, Mishima S, Oda J, Homma H, Sasaki H, Ohta S *et al.* (2009). Protective effects of free radical scavenger edaravone against xanthine oxidase-mediated permeability increases in human intestinal epithelial cell monolayer. *J Burn Care Res* **30**, 335-340.

Muller FL, Liu YH, Van Remmen H (2004). Complex III releases superoxide to both sides of the inner mitochondrial membrane. *J Biol Chem* **279**, 49064-49073.

Naugler KM, Baer KA, Ropeleski MJ (2008). Interleukin-11 antagonizes Fas ligand-mediated apoptosis in IEC-18 intestinal epithelial crypt cells: role of MEK and Akt-dependent signaling. *Am J Physiol Gastrointest Liver Physiol* **294**, G728-737.

Paddenberg R, Ishaq B, Goldenberg A, Faulhammer P, Rose F, Weissmann N *et al.* (2003). Essential role of complex II of the respiratory chain in hypoxia-induced ROS generation in the pulmonary vasculature. *Am J Physiol Lung Cell Mol Physiol* **284**, L710-719.

Papa S & Skulachev VP (1997). Reactive oxygen species, mitochondria, apoptosis and aging. *Mol Cell Biochem* **174**, 305-319.

Pastorelli L, De Salvo C, Mercado JR, Vecchi M, Pizarro TT (2013). Central role of the gut epithelial barrier in the pathogenesis of chronic intestinal inflammation: lessons learned from animal models and human genetics. *Front Immunol* **4**, 280.

Piguet PF, Vesin C, Guo J, Donati Y, Barazzone C (1998). TNF-induced enterocyte apoptosis in mice is mediated by the TNF receptor 1 and does not require p53. *Eur J Immunol* **28**, 3499-3505.

Produit-Zengaffinen N, Davis-Lameloise N, Perreten H, Becard D, Gjinovci A, Keller PA *et al.* (2007). Increasing uncoupling protein-2 in pancreatic beta cells does not alter glucose-induced insulin secretion but decreases production of reactive oxygen species. *Diabetologia* **50**, 84-93.

Ralph SJ, Moreno-Sanchez R, Neuzil J, Rodriguez-Enriquez S (2011). Inhibitors of succinate: quinone reductase/Complex II regulate production of mitochondrial reactive oxygen species and protect normal cells from ischemic damage but induce specific cancer cell death. *Pharm Res* **28**, 2695-2730.

Rathore R, Zheng YM, Niu CF, Liu QH, Korde A, Ho YS *et al.* (2008). Hypoxia activates NADPH oxidase to increase [ROS](i) and [Ca2+](i) through the mitochondrial ROS-PKC epsilon signaling axis in pulmonary artery smooth muscle cells. *Free Radic Biol Med* **45**, 1223-1231.

Ricci JE, Gottlieb RA, Green DR (2003). Caspase-mediated loss of mitochondrial function and generation of reactive oxygen species during apoptosis. *J Cell Biol* **160**, 65-75.

Riganti C, Gazzano E, Polimeni M, Costamagna C, Bosia A, Ghigo D (2004). Diphenyleneiodonium inhibits the cell redox metabolism and induces oxidative stress. *J Biol Chem* **279**, 47726-47731.

Robinson KM, Janes MS, Pehar M, Monette JS, Ross MF, Hagen TM *et al.* (2006). Selective fluorescent imaging of superoxide in vivo using ethidium-based probes. *Proc Natl Acad Sci USA* **103**, 15038-15043.

Setsukinai K, Urano Y, Kakinuma K, Majima HJ, Nagano T (2003). Development of novel fluorescence probes that can reliably detect reactive oxygen species and distinguish specific species. *J Biol Chem* **278**, 3170-3175.

Sharma R & Tepas JJ, 3rd (2010). Microecology, intestinal epithelial barrier and necrotizing enterocolitis. *Pediatr Surg Int* **26**, 11-21.

Shchepina LA, Pletjushkina OY, Avetisyan AV, Bakeeva LE, Fetisova EK, Izyumov DS *et al.* (2002). Oligomycin, inhibitor of the F0 part of H+-ATP-synthase, suppresses the TNF-induced apoptosis. *Oncogene* **21**, 8149-8157.

Shen HM & Pervaiz S (2006). TNF receptor superfamily-induced cell death: redox-dependent execution. *FASEB J* **20**, 1589-1598.

Skulachev VP (1996). Role of uncoupled and non-coupled oxidations in maintenance of safely low levels of oxygen and its one-electron reductants. *Q Rev Biophys* **29**, 169-202.

Snoek SA, Dhawan S, van Bree SH, Cailotto C, van Diest SA, Duarte JM *et al.* (2012). Mast cells trigger epithelial barrier dysfunction, bacterial translocation and postoperative ileus in a mouse model. *Neurogastroenterol Motil* **24**, 172-184, e191.

Turrens JF (2003). Mitochondrial formation of reactive oxygen species. *J Physiol* **552**, 335-344.

Vanden Berghe T, Vanlangenakker N, Parthoens E, Deckers W, Devos M, Festjens N *et al.* (2010). Necroptosis, necrosis and secondary necrosis converge on similar cellular disintegration features. *Cell Death and Differentiation* **17**, 922-930.

Vidal K, Grosjean I, evillard JP, Gespach C, Kaiserlian D (1993). Immortalization of mouse intestinal epithelial cells by the SV40-large T gene. Phenotypic and immune characterization of the MODE-K cell line. *J Immunol Methods* **166**, 63-73.

Williams JM, Duckworth CA, Watson AJ, Frey MR, Miguel JC, Burkitt MD *et al.* (2013). A mouse model of pathological small intestinal epithelial cell apoptosis and shedding induced by systemic administration of lipopolysaccharide. *Dis Model Mech* **6**, 1388-1399.

Yazdanpanah B, Wiegmann K, Tchikov V, Krut O, Pongratz C, Schramm M *et al.* (2009). Riboflavin kinase couples TNF receptor 1 to NADPH oxidase. *Nature* **460**, 1159-1163.

Zhou R, Yazdi AS, Menu P, Tschopp J (2011). A role for mitochondria in NLRP3 inflammasome activation. *Nature* **469**, 221-225.

Chapter V

ANTIOXIDANT POTENTIAL OF CORM-A1 AND RESVERATROL DURING TNF-α/CYCLOHEXIMIDE-INDUCED OXIDATIVE STRESS AND APOPTOSIS IN MURINE INTESTINAL EPITHELIAL MODE-K CELLS

Dinesh Babu [a], Georges Leclercq [b], Vera Goossens [c,d], Quinten Remijsen [c,d], Peter Vandenabeele [c,d], Roberto Motterlini [e], Romain A Lefebvre [a]

[a] Heymans Institute of Pharmacology, Faculty of Medicine and Health Sciences, Ghent University, Belgium

[b] Department of Clinical Chemistry, Microbiology and Immunology, Faculty of Medicine and Health Sciences, Ghent University, Belgium

[c] Inflammation Research Center, Molecular Signaling and Cell Death Unit, VIB, Ghent, Belgium

[d] Department of Biomedical Molecular Biology, Molecular Signaling and Cell Death Unit, Ghent University, Ghent, Belgium

[e] Inserm U955, Equipe 12 and University Paris-Est Créteil, Faculty of Medicine, F-94000, Créteil, France

Chapter V

Antioxidant potential of CORM-A1 and resveratrol during

TNF-α/cycloheximide-induced oxidative stress and apoptosis in murine

intestinal epithelial MODE-K cells

V.1   Abstract

Background. Targeting excessive production of reactive oxygen species (ROS) could be an effective therapeutic strategy to prevent oxidative stress-associated gastrointestinal inflammation. NADPH oxidase (NOX) and mitochondrial complexes (I and II) are the major sources of ROS production contributing to TNF-α/cycloheximide (CHX)-induced apoptosis in the mouse intestinal epithelial cell line, MODE-K.

Methods. In the current study, the influence of a polyphenolic compound (resveratrol) and a water-soluble carbon monoxide (CO)-releasing molecule (CORM-A1) on the different sources of TNF-α/CHX-induced ROS production in MODE-K cells was assessed. This was compared with H_2O_2-, rotenone- or antimycin-A-induced ROS-generating systems. Intracellular total ROS, mitochondrial-derived ROS and mitochondrial superoxide anion ($O_2^{\bullet-}$) production levels were assessed. Additionally, the influence on TNF-α/CHX-induced changes in mitochondrial membrane potential (Ψ_m) and mitochondrial function was studied.

Key results. In basal conditions, CORM-A1 did not affect intracellular total or mitochondrial ROS levels, while resveratrol increased intracellular total ROS but reduced mitochondrial ROS production. TNF-α/CHX- and H_2O_2-mediated increase in intracellular total ROS production was reduced by both resveratrol and CORM-A1, whereas only resveratrol attenuated the increase in mitochondrial ROS triggered by TNF-α/CHX. CORM-A1 decreased antimycin-A-induced mitochondrial $O_2^{\bullet-}$ production without any influence on TNF-α/CHX- and rotenone-induced mitochondrial $O_2^{\bullet-}$ levels, while resveratrol abolished all three effects. Finally, resveratrol greatly reduced and abolished TNF-α/CHX-induced mitochondrial

depolarization and mitochondrial dysfunction, while CORM-A1 only mildly affected these parameters.

Conclusions. These data indicate that the cytoprotective effect of resveratrol is predominantly due to mitigation of mitochondrial ROS, while CORM-A1 acts solely on NOX-derived ROS to protect MODE-K cells from TNF-α/CHX-induced cell death. This might explain the more pronounced cytoprotective effect of resveratrol.

V.2   Introduction

Disturbance of the intestinal epithelial barrier function is observed with the development of mucosal inflammation during acute and chronic enteropathies (Sharma & Tepas, 2010; Snoek *et al.*, 2012; Pastorelli *et al.*, 2013). Reactive oxygen species (ROS) are one of the major key players involved in the initiation and progression of inflammation (Mittal *et al.*, 2014). Oxidative stress-induced epithelial cell damage leading to increased intestinal permeability and translocation of intraluminal endotoxins might trigger muscular inflammation during various conditions involving acute gastrointestinal (GI) inflammation such as postoperative ileus, septic ileus, necrotizing enterocolitis and acute intestinal ischemia/reperfusion (I/R) (Anup *et al.*, 1999; de Winter *et al.*, 2005; Baregamian *et al.*, 2009; De Backer *et al.*, 2009; Guan *et al.*, 2009). Moreover, overproduction of ROS with extensive mucosal injury has also been observed for chronic GI inflammation in animal models of inflammatory bowel disease (IBD) (Ahn *et al.*, 2001; Reifen *et al.*, 2004; Cetinkaya *et al.*, 2005) and in colonic samples of ulcerative colitis patients (Oshitani *et al.*, 1993; Nishikawa *et al.*, 2005). Antioxidant treatment appears to reduce oxidative stress and associated inflammation in animal models of colitis (Millar *et al.*, 1996; Damiani *et al.*, 2007; Vasina *et al.*, 2010) and in patients with ulcerative colitis (Aghdassi *et al.*, 2003; Barbosa *et al.*, 2003; Seidner *et al.*, 2005).

An array of pro-inflammatory cytokines is released within the intestinal mucosa during various GI inflammatory disorders (Kim *et al.*, 2012) and, among others, tumor necrosis factor (TNF)-α is an early inflammatory mediator in inflamed intestine (Holtmann *et al.*, 2002). Induction of intestinal epithelial cell (IEC) apoptosis and cell shedding by TNF-α is thought to play an important role in epithelial barrier dysfunction. We and others have reported that ROS play an important role in TNF-α-induced apoptotic cell death of IECs (Jin *et al.*, 2008; Baregamian *et al.*, 2009; Babu *et al.*, 2012). In rat IEC-6 cells, the nicotinamide adenine dinucleotide phosphate (NADPH) oxidase (NOX) family and the mitochondrial electron transport chain (ETC) are the two major ROS-producing sources involved in TNF-α/cycloheximide (CHX)-induced cell death (Jin *et al.*, 2008). The same accounts for murine MODE-K cells; particularly, in addition to NOX, complexes I and II of the mitochondrial ETC were found to be the main sites of superoxide anion ($O_2^{\bullet-}$) production from the mitochondria, the primary ROS species originating from this organelle (Babu *et al.*,

2015). These data indicate that the endogenous antioxidant defence system might not be sufficient to counteract TNF-α-induced ROS production, suggesting that mitigating excessive ROS production might be of therapeutic value to reduce intestinal barrier dysfunction during GI inflammation.

Among the endogenous intracellular antioxidant pathways, heme oxygenase-1 (HO-1) has a prominent role in the adaptation of tissues against oxidative stress since this redox-sensitive inducible enzyme generates biliverdin, a powerful antioxidant, and carbon monoxide (CO), which acts as a crucial signaling factor mediating a variety of important pharmacological effects (Ryter *et al.*, 2006). CO-releasing molecules (CO-RMs), a class of organometallic compounds liberating CO in biological systems in a controllable manner, have been developed to mimic the antioxidant, anti-inflammatory and cytoprotective effects of CO (Motterlini *et al.*, 2002; Sawle *et al.*, 2005; Motterlini & Otterbein, 2010). The inhibitory effect of CO and CO-RMs on cytokine-induced changes in IECs might contribute to their beneficial effect in acute GI inflammation (Babu *et al.*, 2014). The exact mechanism(s) of action of CO is still under scrutiny but emerging evidence indicates that the beneficial properties of CO may be linked to its ability to bind to heme-containing proteins such as NOX and mitochondrial complexes in different tissues (Taille *et al.*, 2005; Bilban *et al.*, 2008). The cytoprotective properties of CO/CO-RMs in IECs and their effect on cellular targets mediating ROS production in comparison to classical antioxidants have not been investigated so far. Resveratrol, a bioactive polyphenolic antioxidant present in red wine has been extensively studied with regard to cardiovascular and neuronal protection (Foti Cuzzola *et al.*, 2011; Wang *et al.*, 2012). Experimental data show that it also significantly ameliorates acute intestinal inflammation, such as induced by I/R (Ozkan *et al.*, 2009) or by oral infection with Toxoplasma gondii (Bereswill *et al.*, 2010). We previously showed that CORM-A1 as well as resveratrol reduced both TNF-α/CHX-induced ROS production and apoptosis in MODE-K IECs (Babu *et al.*, 2012). The aim of the present study was therefore to investigate the influence of CORM-A1 and resveratrol on the different sources of TNF-α/CHX-induced ROS production in MODE-K cells. We also examined the effects of CORM-A1 and resveratrol on mitochondrial function by assessing TNF-α/CHX-induced changes in mitochondrial membrane potential (Ψ_m) and cellular oxygen consumption.

V.3   Materials and methods

V.3.1   Chemicals and reagents

Reagents for cell culture, including Dulbecco's modified Eagle's medium (DMEM), penicillin/streptomycin, glutamax and fetal bovine serum were obtained from Gibco BRL (Grand Island, NY, USA). JC-10 was purchased from Enzo Life Sciences (Zandhoven, Belgium). Carboxylated analogue of 2'7'-dichlorodihydrofluorescein diacetate acetyl ester (carboxy-H_2DCFDA), dihydrorhodamine 123 (DHR123), Hoechst blue 33342, MitoTracker Deep Red FM, MitoTracker Green FM, MitoSOX Red, Sytox Green, Sytox Red and tetramethylrhodamine methyl ester (TMRM) were purchased from Molecular Probes – Invitrogen (Carlsbad, CA, USA). Recombinant murine TNF-α was purchased from R&D system (Minneapolis, MN, USA). The cell permeable lipophilic iron chelator, salicylaldehyde isonicotinoyl hydrazone (SIH), was a kind gift from Prof. Dr. U Brunk. CORM-A1 was synthesized as previously described (Motterlini *et al.*, 2005). All other chemicals were obtained from Sigma (St. Louis, MO, USA). All chemicals were dissolved in DMSO, except CORM-A1 and desferrioxamine (DFO), that were dissolved in water, and TNF-α, that was dissolved in phosphate buffered saline.

V.3.2   Cell culture

The mouse small IEC line, MODE-K (a generous gift from Dr. Ingo B. Autenrieth, University of Tübingen, Germany) was used in our study. This is a cell line derived from the duodenum-jejunum from normal young C3H/HeJ mouse immortalized by simian virus (SV)-40 large T gene transfer. The cells are undifferentiated but still exhibit morphological and phenotypic characteristics of normal enterocytes (Vidal *et al.*, 1993). MODE-K cells (passage 10–35) were cultured in high-glucose DMEM supplemented with 10% fetal bovine serum, 2 mM L-glutamine, and 5% penicillin (10,000 units/ml)/streptomycin (10 mg/ml). Cultures were maintained in a humidified 5% CO_2 atmosphere at 37°C and experiments were conducted on cells at approximately 80-90% confluence. MODE-K cells were seeded at specified cell density in various experiments, grown for 36 h and then serum starved overnight (except when used for the cellular oxygen consumption assay). On day 3, cells were treated with 1 ng/ml TNF-α plus 10 µg/ml CHX for 6 h. All the drugs tested for possible interference with TNF-α/CHX-induced effects were pre-incubated from 1 h before exposure

to TNF-α/CHX followed by co-incubation of drugs with TNF-α/CHX for 6 h, with the exception of the hydrophilic iron chelator DFO, which needs 3 h pre-incubation before exposure to TNF-α/CHX. Except otherwise indicated, the drugs used in the actual study (allopurinol, CORM-A1, DFO, NSC23766, resveratrol, SIH and VAS-2870) were applied in the highest possible concentration without an effect *per se* on cell viability of MODE-K cells when incubated for 12 h, based on quantitation of ATP (see Babu *et al.*, 2012; Babu *et al.*, 2015).

V.3.3 *Simultaneous determination of intracellular total or mitochondrial ROS generation and cell death*

In our previous study in MODE-K cells, CORM-A1 and resveratrol reduced both TNF-α/CHX-induced ROS production and apoptosis as assessed in two separate assays, i.e. fluorescence measurement of carboxy-H$_2$DCFDA with a microtiter plate reader, and flow cytometric analysis of DNA hypoploidy upon staining with propidium iodide (PI), respectively (Babu *et al.*, 2012). In the actual study, ROS production and cell death were measured simultaneously by flow cytometry, allowing measurement of ROS production in gated viable cells.

Carboxy-H$_2$DCFDA is a cell-permeable indicator for ROS that is nonfluorescent until the acetate groups are removed by intracellular esterases and oxidation occurs within the cell. When oxidized by various active oxygen species, it is irreversibly converted to the fluorescent form, DCF. The fluorescence generated by DCF is proportional to the rate of carboxy-H$_2$DCFDA oxidation, which is in turn indicative of the cellular oxidizing activity and intracellular ROS levels. DHR123 has been reported as a marker for mitochondrial ROS production (Jin *et al.,* 2008; Basu Ball *et al.*, 2011; Tiede *et al.*, 2011). It is an uncharged and non-fluorescent ROS indicator that can passively diffuse across membranes where it is oxidized to cationic rhodamine 123 (R123) which localizes in the mitochondria and exhibits green fluorescence. For ROS measurements, briefly, 2.5 x 10^5 cells per well were seeded in 6-well plates. Following exposure of cells to 1 ng/ml TNF-α plus 10 µg/ml CHX for 6 h with/without drugs, carboxy-H$_2$DCFDA (10 µM) or DHR123 (1 µM) was loaded to the cells for 40 min before the end of the treatment period in the dark at 37°C. The floating and adherent cells were collected by trypsinization and washed twice with Hanks' balanced salt solution (HBSS) with calcium and magnesium. Sytox Red (2.5 nM) dead cell stain was added to the cell suspension and simultaneous detection of ROS production and cell death was performed

in a single experimental setup by flow cytometry using 488 nm excitation wavelength with 530/30 nm (FL1; DCF or R123) and 670/30 (FL4; Sytox Red) emission filters. Viable (Sytox Red-negative) cells were gated and the green fluorescence of the ROS probes was analyzed in these cells. Cells treated with 1 mM hydrogen peroxide (H_2O_2) for 40 min were used as a positive control.

V.3.4   Simultaneous determination of mitochondrial $O_2^{\bullet-}$ and cell death

MitoSOX Red was used to detect mitochondrial $O_2^{\bullet-}$ production. This modified cationic dihydroethidium dye is localized to the mitochondria where it is oxidized by $O_2^{\bullet-}$ to generate bright red fluorescence (Robinson *et al.*, 2006). Mitochondrial $O_2^{\bullet-}$ generation and cell death were determined in a single experimental setup by treating the cell samples with MitoSOX Red and Sytox Red. Briefly, the cells were loaded with 5 µM MitoSOX Red for 30 min before the end of treatment period, collected, washed twice with HBSS and then stained with 2.5 nM Sytox Red. The samples were run on a flow cytometer with 488 nm excitation to measure oxidized MitoSOX Red in the FL2 channel and Sytox Red in the FL4 channel. Cell debris with low FSC (forward scatter) and SSC (side scatter) was excluded from the analysis. Dead cells (FL4-positive) were also excluded from the analysis and the mean fluorescence intensity (MFI) of MitoSOX Red staining was analyzed in the gated viable cell population (Sytox Red-negative). Thus, MitoSOX Red of the cells analyzed excluded any non-specific interferences from dead cells. Cells treated for 30 min with 10 µM antimycin-A, an agent well known to generate $O_2^{\bullet-}$ by binding to the Qi site of cytochrome c reductase in the mitochondrial complex III, were used as a positive control.

For all ROS experiments, (a) the fluorescence properties of at least 30,000 cells were acquired from each sample, (b) the samples were analyzed immediately and strictly protected from light, (c) basal ROS generation in cells not exposed to TNF-α/CHX, in culture medium alone or in medium containing the solvent of the drug to be studied versus TNF-α/CHX, was used as a control, and (d) mean fluorescence intensities (MFIs) were expressed as percentage of control level set as 100%.

V.3.5   Detection of mitochondrial membrane potential (Ψ_m)

Estimation of mitochondrial membrane potential (Ψ_m) was performed using JC-10, a membrane permeable fluorescent probe. JC-10 is a cationic fluorophore, which is rapidly taken up by cells and mitochondria due to their negative charge. Inside mitochondria, JC-10 forms J-aggregates which emit fluorescence at 590 nm (FL2; red fluorescence). Remaining JC-10 in cytosol maintains the monomeric form and emits fluorescence at 525 nm (FL1; green fluorescence). Uptake levels of JC-10 in mitochondria depend on the polarization state of the mitochondrial membrane. Depolarized mitochondria have lower uptake of JC-10 compared to polarized mitochondria of a normal healthy cell. Briefly, 2.5 x 10^5 cells per well were seeded in 6-well plates. Following the treatment, cells were washed twice with HBSS and then incubated with 5 µM JC-10 solution prepared in DMEM media for 30 min. Subsequently, the cells were quickly washed with HBSS prior to measurement. The fluorescence intensities of JC-10 monomers and aggregates were quantified, respectively, by FL1 (530/30 nm) and FL2 (585/42 nm) detectors of the flow cytometer. The JC-10 aggregate/monomer ratio is directly proportional to mitochondrial membrane potential intensity. This ratiometric method was used with this dye to provide a semi-quantitative measurement of Ψ_m.

V.3.6   Simultaneous determination of mitochondrial membrane potential (Ψ_m) and cell death

Determination of the changes in mitochondrial membrane potential (Ψ_m) was also performed using TMRM along with staining of Sytox Green (for cell death). TMRM is a cell-permeant, lipophilic cationic, red-orange fluorescent dye that is readily sequestered by active mitochondria. Unlike JC-10, TMRM is a single wavelength dye that can be combined with a cell death marker to measure fluorescence exclusively in the live cells. Briefly, following the treatment, the cells were washed twice with HBSS and then incubated with 200 nM TMRM solution prepared in DMEM media for 30 min. Subsequently, the cells were quickly washed twice with HBSS and stained with 2 nM Sytox Green prior to measurement. The percentage of TMRM and Sytox Green stained cells was calculated from at least 30,000 cells of each sample in comparison to the control. TMRM was excited at 488 nm, and fluorescence emitted at 588 nm (FL2) was measured in gated viable (Sytox Green-negative)

cells by flow cytometry. Cells treated for 30 min with 50 µM carbonyl cyanide 3-chlorophenylhydrazone (CCCP), a potent uncoupler of oxidative phosphorylation which causes rapid loss of Ψ_m (loss of TMRM fluorescence), were used as a positive control.

V.3.7   Measurement of mitochondrial dysfunction

Determination of respiratory chain damage was performed by double staining with two different mitochondria-specific dyes, MitoTracker Green FM and MitoTracker Deep Red FM to distinguish total and respiring mitochondria, respectively. Mitochondria in cells stained with MitoTracker Green FM dye exhibit bright green fluorescein-like fluorescence (FL1; fluorescence emission at 516 nm) as this dye accumulates in the lipid environment of mitochondria and becomes fluorescent. MitoTracker Deep Red FM is a red fluorescence probe (FL4; fluorescence emission at 665 nm) that does not fluoresce until it enters an actively respiring cell, where it is oxidized to the corresponding fluorescent mitochondrion-selective probe and then sequesters in the mitochondria. The treated cells were incubated with 200 nM MitoTracker Green FM and 25 nM MitoTracker Deep Red FM in the dark at 37°C for 30 min before the end of the treatment period. Next, the cells were harvested and the pellets were suspended in 0.5 mL of PBS. The samples were analyzed immediately by flow cytometry. The percentage of MitoTracker Green-positive/MitoTracker Deep Red-negative cells is an important parameter of accumulation of cells with non-respiring (dysfunctional) mitochondria (Zhou *et al.*, 2011).

For ROS, Ψ_m and mitochondrial dysfunction assays, the samples were acquired and analyzed using a FACSCalibur using CellQuest software or with an LSR II using DIVA software (BD Biosciences).

V.3.8   Mitochondrial respiration

Cellular oxygen consumption in the DMEM XF assay medium containing 1% FCS was measured in a Seahorse XF96 Analyzer (Seahorse Bioscience, Billerica, MA, USA). Oxygen consumption rate (OCR) and extracellular acidification rate (ECAR) were analyzed following the manufacturer's protocols. Measurements are based on oxygen-dependent quenching of a built-in fluorescent sensor. Briefly, MODE-K cells were seeded at 6.5×10^4 cells per well in Seahorse XF96 specialized cell culture plates. Approximately 24 h later, media were replaced

with DMEM XF assay medium (unbuffered DMEM supplemented with 25 mM glucose, 2 mM L-glutamax and 1 mM sodium pyruvate) and cells were incubated at 37°C without CO_2. OCR and ECAR were measured simultaneously in the Seahorse XF96 extracellular flux Analyzer for 2.5 h. Reagents and chemicals for respiratory stress testing were loaded onto XF96 extracellular flux assay plate. TNF-α/CHX, CCCP or rotenone/antimycin-A were diluted in DMEM running medium and loaded into port-A, port-B and port-C, respectively. Titrations were preliminarily performed to determine the optimal concentration of CCCP. In all cell groups, CCCP (50 µM) was added at 115 min to determine maximal respiration, then rotenone (2.5 µM) and antimycin-A (5 µM) were added at 130 min to block mitochondrial respiration, determining non-mitochondrial respiration. To test the influence of TNF-α/CHX, it was added at 30 min after five measurements of basal respiration. Experiments without and with TNF-α/CHX administration, were also performed in the continuous presence of CORM-A1 or resveratrol, starting their incubation at 37°C without CO_2 from 1 h before analysis of OCR and ECAR. After measuring OCR and ECAR for 2.5 h, the number of live and dead cells in the microchamber of each well was determined on a BD Pathway™ 855 imaging instrument as described previously (Duprez *et al.*, 2011). Nuclei of all cells were stained by the nuclear dye Hoechst blue 33342, while nuclei of dead cells were stained by both Hoechst blue 33342 and PI. The number of live cells was used for normalization of the respiratory rate in each microchamber. Cells were plated with at least 5 replicate wells for each treatment group. The OCR and ECAR values were expressed as absolute values of measurements.

V.3.9   Statistical analysis

All data were expressed as mean ± SEM. Comparison of the means was performed using the Student's *t*-test for two groups of data and ANOVA followed by Bonferroni's multiple comparison test for comparison of more than two groups. Differences were considered to be significant at $P < 0.05$.

V.4   Results

V.4.1   Effects of CORM-A1 and resveratrol on TNF-α/CHX-induced changes in intracellular total ROS production and cell death

To determine whether the modulation of ROS production by CORM-A1 and resveratrol could contribute to their corresponding cytoprotective activities, TNF-α/CHX-induced intracellular total ROS production and cell death were simultaneously measured by flow cytometry analysis. Treatment of MODE-K cells with CORM-A1 (100 µM) *per se* was without effect but CORM-A1 significantly reduced both TNF-α/CHX-induced ROS production (Fig. V.1A and C) and dead cells (Fig. V.1D). In contrast, resveratrol (75 µM) *per se* increased total ROS production to similar levels induced by TNF-α/CHX but without affecting cell survival. Interestingly, treatment of cells with resveratrol significantly reduced both TNF-α/CHX-induced ROS production and cell death (Fig. V.1B, E and F). These results together imply that the cytoprotective effects of CORM-A1 and resveratrol in MODE-K cells can be attributed at least in part to their ability to mitigate oxidative stress as evidenced by their direct influence on intracellular ROS production.

V.4.2   Effects of CORM-A1 and resveratrol on H_2O_2-induced changes in intracellular total ROS production

The antioxidant capacity of CORM-A1 and resveratrol was further investigated *in vitro* using the model of H_2O_2-induced oxidative stress in MODE-K cells. For these experiments, incubation of cells with 1 mM H_2O_2 for 40 min was selected as this condition induced a level of intracellular total ROS production similar to that induced by TNF-α/CHX for 6 h, albeit without inducing cell death. H_2O_2 increased ROS production by 170% as compared to control and CORM-A1 significantly attenuated this effect (Fig. V.2A and C). Resveratrol *per se* increased ROS production to similar levels as induced by H_2O_2, but still could abolish H_2O_2-induced increase in total ROS production (Fig. V.2B and E). Treatment with a hydrophilic (DFO) and a lipophilic (SIH) iron chelator abolished H_2O_2-induced ROS production, with SIH also significantly reducing basal ROS production (Fig. V.3A and C).

Fig. V.1 Effects of CORM-A1 or resveratrol on TNF-α/CHX-induced intracellular total ROS production and cell death in MODE-K cells. MODE-K cells were treated with TNF-α (1 ng/ml) plus CHX (10 μg/ml) in the absence or presence of CORM-A1 (100 μM) or resveratrol (75 μM). **A-B** Effect of CORM-A1 (A) or resveratrol (B) on TNF-α/CHX-induced intracellular total ROS levels assessed with carboxy-H_2DCFDA (DCF), and gated on the viable, Sytox Red-negative population. Representative overlay histogram plots of DCF fluorescence are shown. The cells in M1 region represent the DCF-positive cells contributing to the shift in fluorescence. **C-F** Influence of TNF-α/CHX, incubated for 6 h, on intracellular total ROS levels (expressed as % of control DCF MFI) and cell death (expressed as % Sytox Red positivity) in the absence and presence of CORM-A1 (C, D) or resveratrol (Res; E, F). Control cells were incubated with serum free medium alone; the effect of CORM-A1 or resveratrol *per se* was also tested. Mean ± SEM of three independent experiments. *$P < 0.05$ *vs.* control. #$P < 0.05$ *vs.* TNF-α/CHX alone.
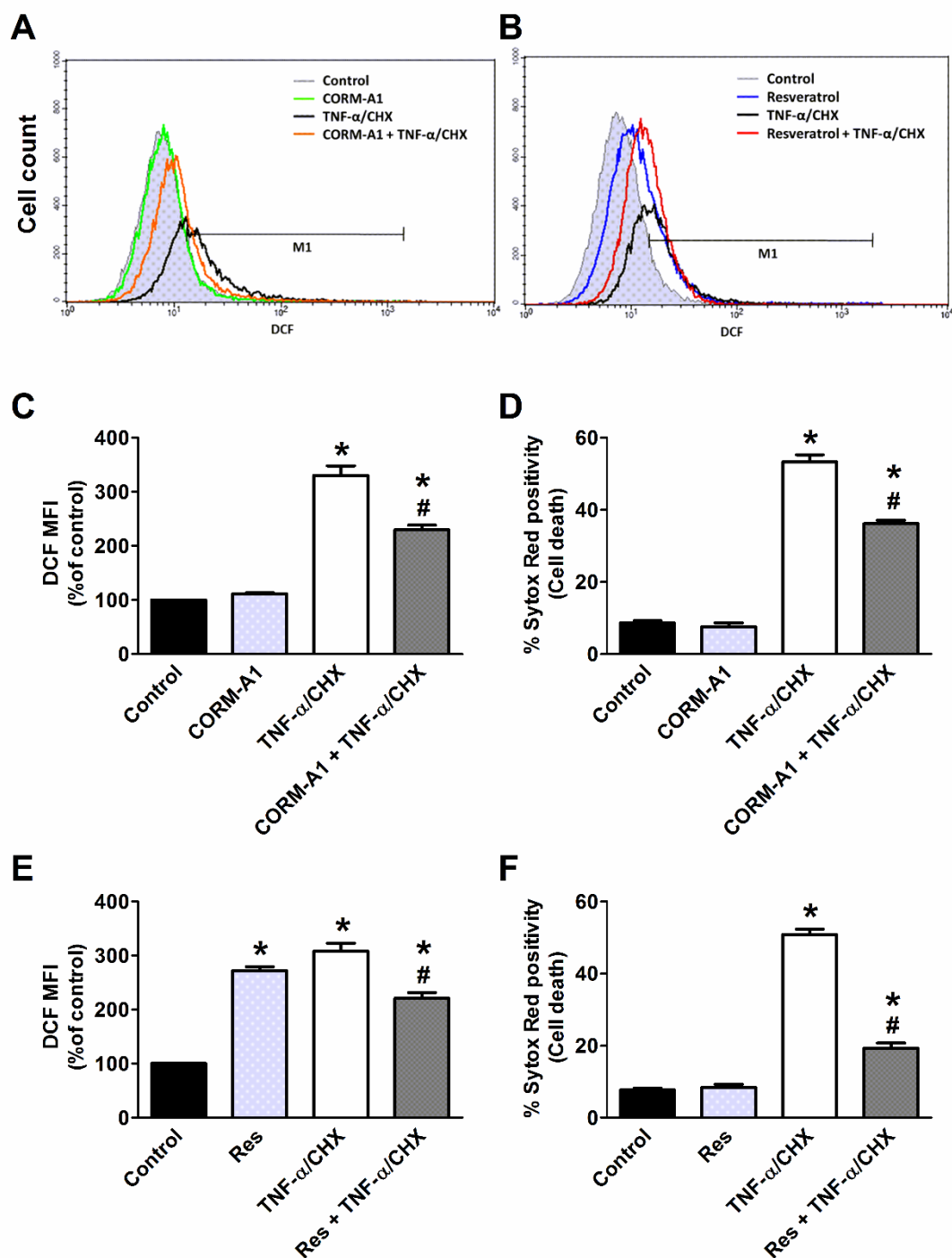
Fig. V.2 Effects of CORM-A1 or resveratrol on H_2O_2-induced intracellular total ROS production and cell death in MODE-K cells. MODE-K cells were treated with H_2O_2 (1 mM) in the absence or presence of CORM-A1 (100 μM) or resveratrol (75 μM). **A-B** Effect of CORM-A1 (A) or resveratrol (B) on H_2O_2-induced intracellular total ROS levels assessed with carboxy-H_2DCFDA (DCF), and gated on the viable, Sytox Red-negative population. Representative overlay histogram plots of DCF fluorescence are shown. The cells in M1 region represent the DCF-positive cells contributing to the shift in fluorescence. **C-F** Influence of H_2O_2, incubated for 40 min, on intracellular total ROS levels (expressed as % of control DCF MFI) and cell death (expressed as % Sytox Red positivity) in the absence and presence of CORM-A1 (C, D) or resveratrol (Res; E, F). Control cells were incubated with serum free medium alone; the effect of CORM-A1 or resveratrol *per se* was also tested (not shown in the histograms of **A** and **B** for clarity). Mean ± SEM of three independent experiments. *$P < 0.05$ *vs.* control. #$P < 0.05$ *vs.* H_2O_2 alone.

Fig. V.3 Effects of the iron chelators desferrioxamine (DFO; 1 mM) and salicylaldehyde isonicotinoyl hydrazone (SIH; 100 µM) on H_2O_2 (1 mM)-induced intracellular total ROS production (assessed with carboxy-H_2DCFDA) and cell death (assessed with Sytox Red) in MODE-K cells measured by flow cytometry. **A-D** Influence of H_2O_2, incubated for 40 min, on intracellular total ROS levels (expressed as % of control DCF MFI) and cell death (expressed as % Sytox Red positivity) in the absence and presence of DFO (A, B) or SIH (C, D). Control cells were incubated with serum free medium alone; the effect of DFO or SIH *per se* was also tested. Mean ± SEM of three independent experiments. *$P < 0.05$ *vs.* control. #$P < 0.05$ *vs.* H_2O_2 alone.

V.4.3 Effects of CORM-A1 and resveratrol on TNF-α/CHX-induced changes in mitochondrial ROS production and cell death

In rat IEC-6 cells, some supporting evidence that DHR123 marks mitochondrial ROS has been reported (Jin *et al.*, 2008). The DHR123 fluorescent probe was therefore used to assess the effects of CORM-A1 and resveratrol on TNF-α/CHX-induced ROS production by mitochondria. Treatment with TNF-α/CHX resulted in a significant increase in mitochondrial ROS production compared to control cells (Fig. V.4A, B, C and E). CORM-A1 did not have any
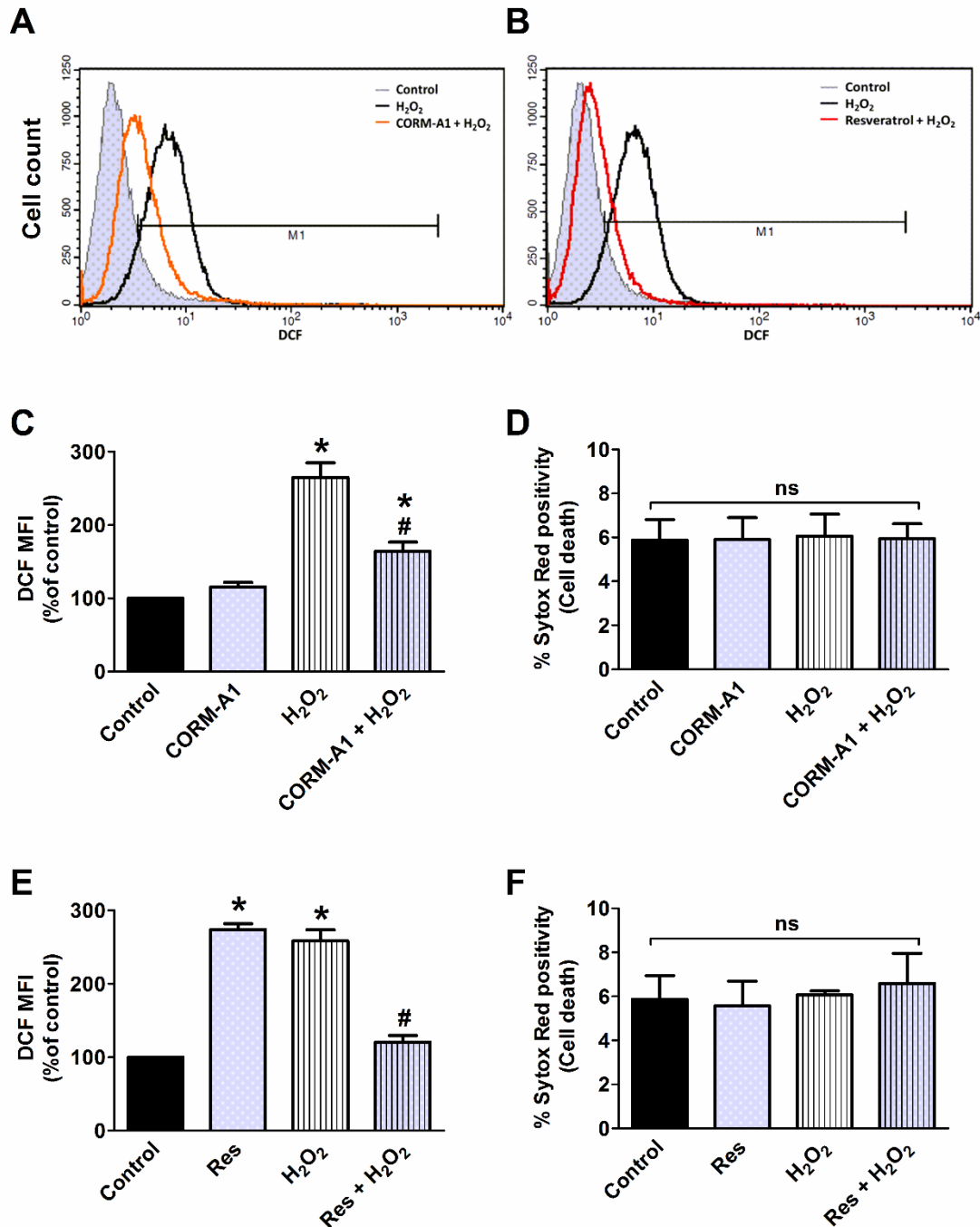
Fig. V.4 Effects of CORM-A1 or resveratrol on TNF-α/CHX-induced mitochondrial ROS production and cell death in MODE-K cells. MODE-K cells were treated with TNF-α (1 ng/ml) plus CHX (10 µg/ml) in the absence or presence of CORM-A1 (100 µM) or resveratrol (75 µM). **A-B** Effect of CORM-A1 (A) or resveratrol (B) on TNF-α/CHX-induced mitochondrial ROS levels assessed with DHR123 (R123), and gated on the viable, Sytox Red-negative population. Representative overlay histogram plots of R123 fluorescence are shown. The cells in M1 region represent the R123-positive cells contributing to the shift in fluorescence. **C-F** Influence of TNF-α/CHX, incubated for 6 h, on mitochondrial ROS levels (expressed as % of control R123 MFI) and cell death (expressed as % Sytox Red positivity) in the absence and presence of CORM-A1 (C, D) or resveratrol (Res; E, F). Control cells were incubated with serum free medium alone; the effect of CORM-A1 or resveratrol *per se* was also tested. Mean ± SEM of three independent experiments. *$P < 0.05$ *vs.* control. #$P < 0.05$ *vs.* TNF-α/CHX alone.

effect on this parameter (Fig. V.4A and C) despite being able to markedly reduce TNF-α/CHX-induced cell death (Fig. V.4D). In contrast, resveratrol reduced basal mitochondrial ROS levels but also abolished TNF-α/CHX-induced increase in mitochondrial ROS production with a concomitant decrease in TNF-α/CHX-induced cell death (Fig. V.4B, E and F).

V.4.4 Effects of CORM-A1 and resveratrol on TNF-α/CHX-induced changes in mitochondrial $O_2^{\bullet-}$ production and cell death

The influence of CORM-A1 and resveratrol on TNF-α/CHX-induced mitochondrial $O_2^{\bullet-}$ production was assessed by using the fluorescent probe MitoSOX Red in conjunction with Sytox Red, to discriminate viable versus dead cells, in a single experimental setup. Treatment with TNF-α/CHX increased mitochondrial $O_2^{\bullet-}$ production by approximately 3 fold as compared to control. Although CORM-A1 significantly reduced TNF-α/CHX-induced cell death (Fig. V.5D), it did not influence TNF-α/CHX-induced mitochondrial $O_2^{\bullet-}$ production (Fig. V.5A and C). In contrast, treatment with resveratrol significantly reduced basal mitochondrial $O_2^{\bullet-}$ levels and prevented the TNF-α/CHX-induced increase in mitochondrial $O_2^{\bullet-}$ levels (Fig. V.5B and E), with concomitant decrease in TNF-α/CHX-induced cell death (Fig. V.5F).

V.4.5 Influence of higher concentrations of CORM-A1 and resveratrol on intracellular total ROS and mitochondrial $O_2^{\bullet-}$ production in MODE-K cells

Results till now showed that in MODE-K cells 100 μM CORM-A1, incubated for 7 h, *per se* did not influence intracellular total ROS or mitochondrial $O_2^{\bullet-}$ levels (Fig. V.1C, 2C and 5C). Similar results were obtained with higher concentrations of CORM-A1 (150 and 200 μM) (Fig. V.6A and C). Treatment of cells with 100 μM CORM-A1 did not change mitochondrial $O_2^{\bullet-}$ production even at earlier time points (0.25 to 3 h) (Fig. V.6E). However, a higher concentration of CORM-A1 (200 μM) promoted a significant increase in mitochondrial $O_2^{\bullet-}$ when incubated for 1 or 2 h (Fig. V.6E). Resveratrol at 75 μM for 7 h was shown to increase intracellular total ROS and decrease mitochondrial $O_2^{\bullet-}$ (Fig. V.1E, 2E and 5E). Higher concentrations of resveratrol (100 μM and 125 μM) induced a concentration-dependent increase in total ROS production (Fig. V.7A) and decrease in mitochondrial $O_2^{\bullet-}$ production (Fig. V.7C) which was accompanied by a significant increase in cell death occurring at 125 μM
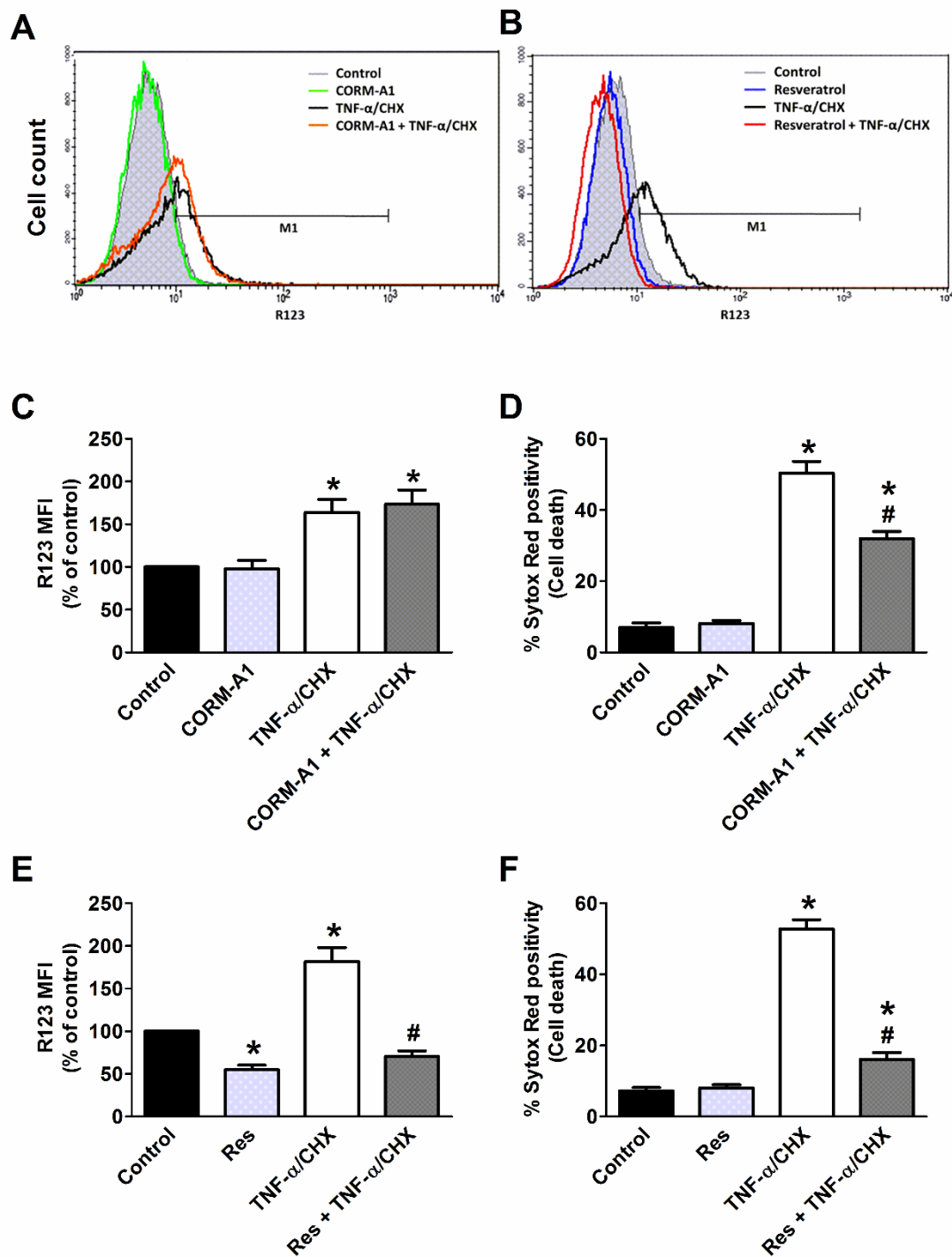
196

Fig. V.5 Effects of CORM-A1 or resveratrol on TNF-α/CHX-induced mitochondrial $O_2^{\bullet-}$ production and cell death in MODE-K cells. MODE-K cells were treated with TNF-α (1 ng/ml) plus CHX (10 μg/ml) in the absence or presence of CORM-A1 (100 μM) or resveratrol (75 μM). **A-B** Effect of CORM-A1 (A) or resveratrol (B) on TNF-α/CHX-induced mitochondrial $O_2^{\bullet-}$ levels assessed with MitoSOX Red, and gated on the viable, Sytox Red-negative population. Representative overlay histogram plots of MitoSOX Red fluorescence are shown. The cells in M1 region represent the MitoSOX Red-positive cells contributing to the shift in fluorescence. **C-F** Influence of TNF-α/CHX, incubated for 6 h, on mitochondrial $O_2^{\bullet-}$ levels (expressed as % of control MitoSOX Red MFI) and cell death (expressed as % Sytox Red positivity) in the absence and presence of CORM-A1 (C, D) or resveratrol (Res; E, F). Control cells were incubated with serum free medium alone; the effect of CORM-A1 or resveratrol *per se* was also tested. Mean ± SEM of three independent experiments. *$P < 0.05$ *vs.* control. #$P < 0.05$ *vs.* TNF-α/CHX alone.

Fig. V.6 Effects of CORM-A1 (100, 150 and 200 μM) on intracellular total ROS production (assessed with carboxy-H$_2$DCFDA), mitochondrial O$_2^{\bullet-}$ production (assessed with MitoSOX Red) and cell death (assessed with Sytox Red) in MODE-K cells measured by flow cytometry. **A-D** Influence of CORM-A1, incubated for 7 h, on intracellular total ROS levels (expressed as % of control DCF MFI; A), mitochondrial O$_2^{\bullet-}$ levels (expressed as % of control MitoSOX Red MFI; C) and cell death (expressed as % Sytox Red positivity; B and D). **E** Influence of CORM-A1 (100 and 200 μM), incubated for 0.25-3 h, on mitochondrial O$_2^{\bullet-}$ levels. Mean ± SEM of three independent experiments. *$P < 0.05$ *vs.* control (0 h).
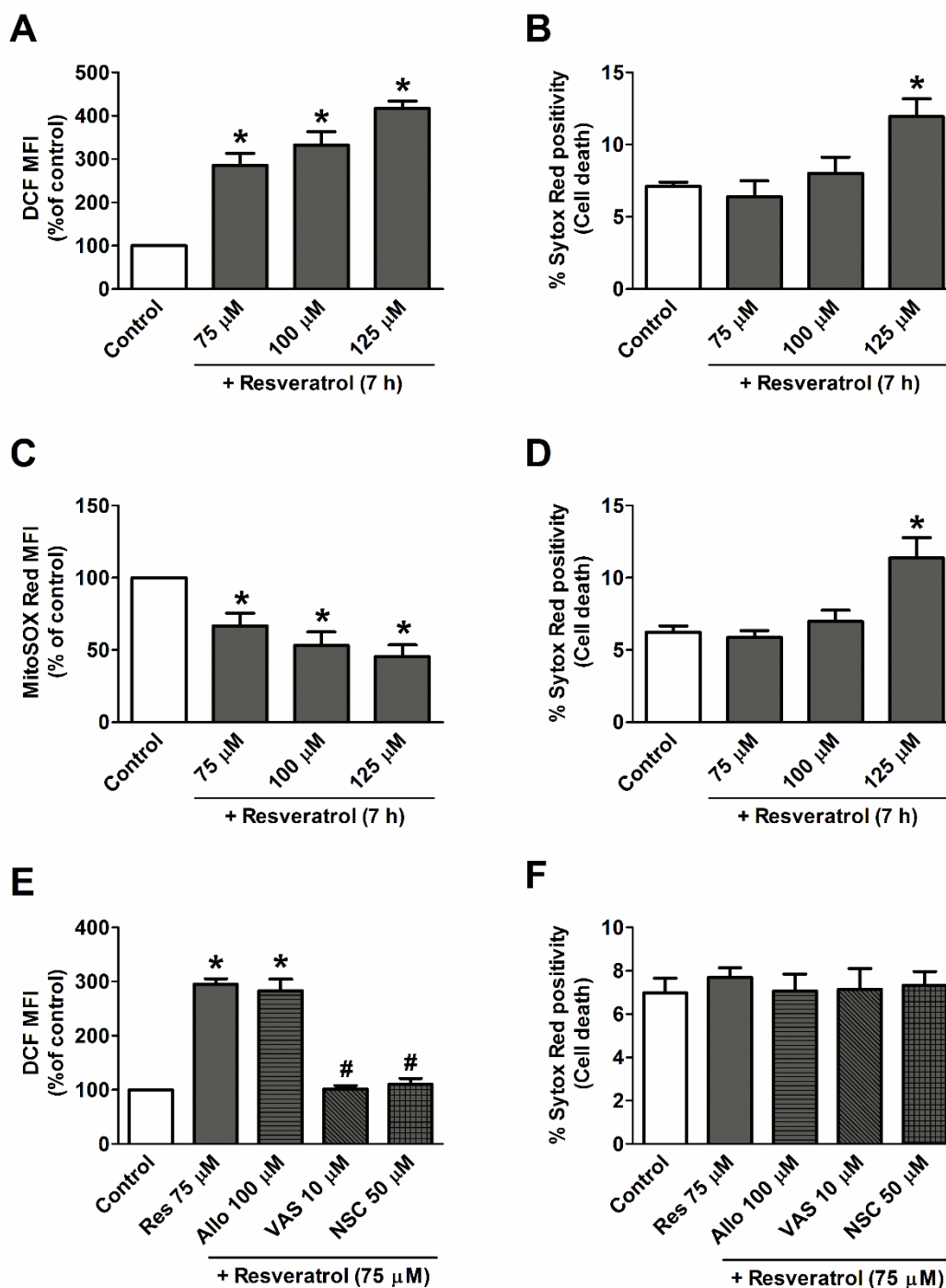
Fig. V.7 Effects of resveratrol (75, 100 and 125 µM) on intracellular total ROS production (assessed with carboxy-H₂DCFDA), mitochondrial O₂$^{•-}$ production (assessed with MitoSOX Red) and cell death (assessed with Sytox Red) in MODE-K cells measured by flow cytometry. **A-D** Influence of resveratrol, incubated for 7 h, on intracellular total ROS levels (expressed as % of control DCF MFI; A), mitochondrial O₂$^{•-}$ levels (expressed as % of control MitoSOX Red MFI; C) and cell death (expressed as % Sytox Red positivity; B and D). **E-F** Effects of inhibitors of xanthine oxidase, NOX or Rac-1 on resveratrol-induced total ROS production in MODE-K cells measured by flow cytometry. Influence of resveratrol (75 µM), incubated for 7 h, on intracellular total ROS levels (E) and cell death (F) in the absence and presence of allopurinol (Allo; 100 µM), VAS-2870 (VAS; 10 µM) or NSC23766 (NSC; 50 µM). Control cells were incubated with serum free medium alone. Mean ± SEM of three independent experiments. *$P < 0.05$ *vs.* control. #$P < 0.05$ *vs.* resveratrol alone.

(Fig. V.7B and D). The increase in intracellular total ROS by 75 μM resveratrol was not influenced by the xanthine/xanthine oxidase inhibitor allopurinol, but was abolished by the pan-NOX inhibitor VAS-2870 and the Rac1 inhibitor NSC23766 (Fig. V.7E).

V.4.6 Effects of CORM-A1 and resveratrol on mitochondrial complex I- and complex III-induced changes in mitochondrial $O_2^{\bullet-}$ and cell death

The effect of CORM-A1 and resveratrol on $O_2^{\bullet-}$ production at the level of mitochondrial complex I and complex III was investigated. Rotenone (7.5 μM), an inhibitor of mitochondrial complex I, induced a robust increase in mitochondrial $O_2^{\bullet-}$ level comparable to that induced by TNF-α/CHX (Fig. V.8A, B, C and E) without affecting cell survival (Fig. V.8D and F). The concentration of 7.5 μM rotenone was selected based on a concentration-response study of the effect of rotenone on mitochondrial $O_2^{\bullet-}$, when incubated for 6 h to mimic the exposure time to TNF-α/CHX (Fig. V.9A). Treatment with CORM-A1 did not affect rotenone-induced mitochondrial $O_2^{\bullet-}$ production while resveratrol completely abolished this effect (Fig. V.8A, B, C and E).

The influence of CORM-A1 and resveratrol on mitochondrial $O_2^{\bullet-}$ production at the level of mitochondrial complex III was investigated by use of the complex III inhibitor antimycin-A, an agent well-known to induce $O_2^{\bullet-}$ production at this site. Antimycin-A was used at 10 μM for 6 h as this concentration did not induce cell death in MODE-K cells, but increased mitochondrial $O_2^{\bullet-}$ production to a level comparable to that induced by TNF-α/CHX (Fig. V.9C and D). Interestingly, CORM-A1 significantly decreased (Fig. V.10A and C) while resveratrol completely abolished (Fig. V.10B and E) antimycin-A-induced mitochondrial $O_2^{\bullet-}$ production.

V.4.7 Effects of CORM-A1 and resveratrol on TNF-α/CHX-induced changes in mitochondrial membrane potential (Ψ_m), mitochondrial dysfunction and cellular oxygen consumption of MODE-K cells

We next studied the influence of CORM-A1 and resveratrol on TNF-α/CHX-induced changes in Ψ_m. Two different potentiometric dyes, TMRM and JC-10, were used. TMRM

Fig. V.8 Effects of CORM-A1 or resveratrol on mitochondrial complex I (rotenone)-induced mitochondrial $O_2^{\bullet-}$ production and cell death in MODE-K cells. MODE-K cells were treated with rotenone (7.5 µM) in the absence or presence of CORM-A1 (100 µM) or resveratrol (75 µM). **A-B** Effect of CORM-A1 (A) or resveratrol (B) on rotenone-induced mitochondrial $O_2^{\bullet-}$ levels assessed with MitoSOX Red, and gated on the viable, Sytox Red-negative population. Representative overlay histogram plots of MitoSOX Red fluorescence are shown. The cells in M1 region represent the MitoSOX Red-positive cells contributing to the shift in fluorescence. **C-F** Influence of rotenone (Rot), incubated for 6 h, on mitochondrial $O_2^{\bullet-}$ levels (expressed as % of control MitoSOX Red MFI) and cell death (expressed as % Sytox Red positivity) in the absence and presence of CORM-A1 (C, D) or resveratrol (Res; E, F). Control cells were incubated with serum free medium alone; the effect of CORM-A1 or resveratrol *per se* was also tested (not shown in the histograms of **A** and **B** for clarity). Mean ± SEM of three independent experiments. *$P < 0.05$ *vs.* control. #$P < 0.05$ *vs.* rotenone alone.
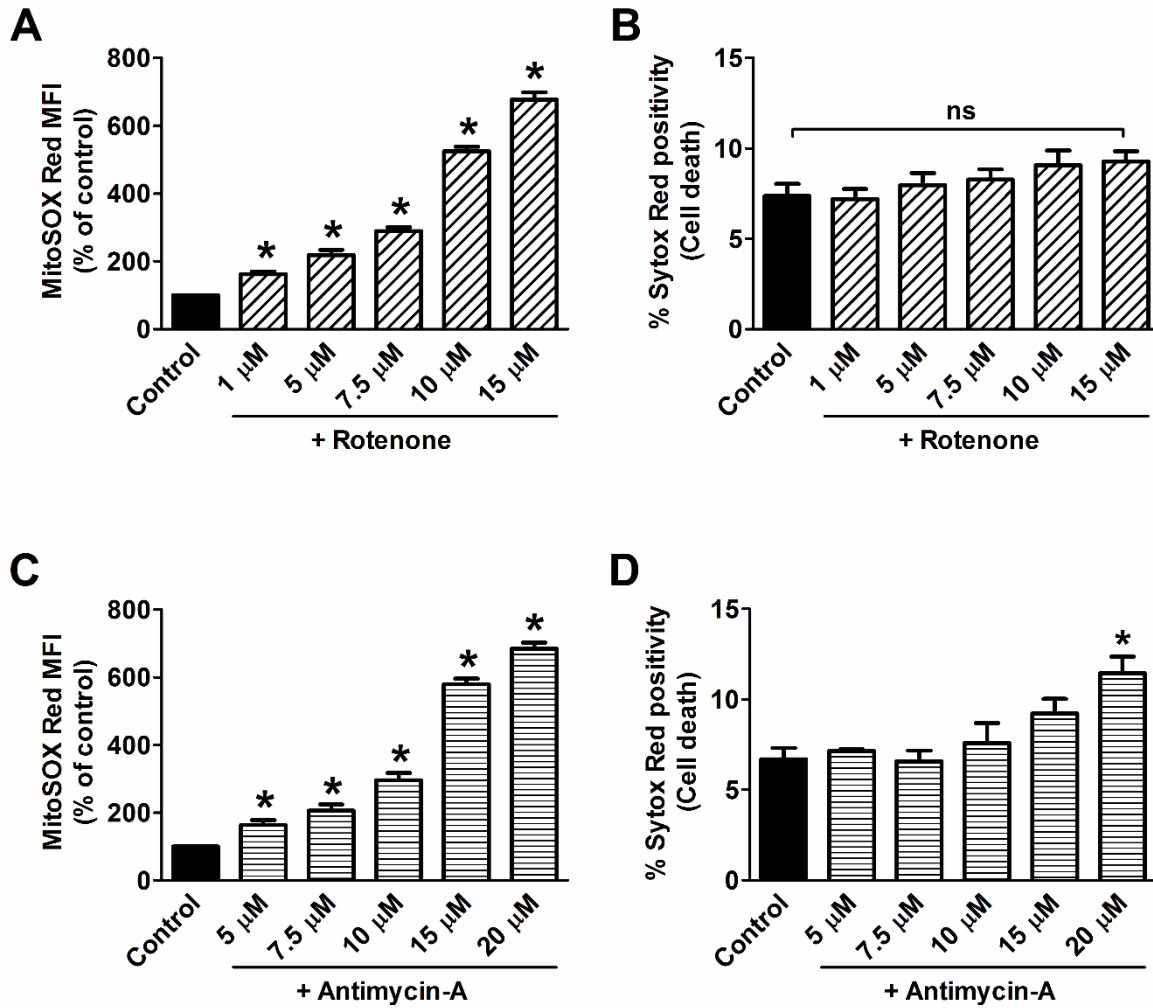
Fig. V.9 Mitochondrial $O_2^{\bullet-}$ production (assessed with MitoSOX Red) and cell death (assessed with Sytox Red) in rotenone (1-15 µM)- and antimycin-A (5-20 µM)-treated MODE-K cells measured by flow cytometry. **A-D** Influence of rotenone (A, B) or antimycin-A (C, D), incubated for 6 h, on mitochondrial $O_2^{\bullet-}$ levels (expressed as % of control MitoSOX Red MFI) and cell death (expressed as % Sytox Red positivity). Control cells were incubated with serum free medium alone. Mean ± SEM of three independent experiments. *$P < 0.05$ *vs.* control.

enables the possibility of analyzing cell death simultaneously in combination with the cell death marker Sytox Green. About 7-8% of control cells showed depolarized mitochondria. Treatment of cells with TNF-α/CHX caused a 60% depolarization of mitochondria as measured with both TMRM (Fig. V.11A and C) and JC-10 staining (Fig. V.12A and B). CORM-A1 decreased the number of depolarized cells to 43% and 48% (Fig. V.11A and 12A) while resveratrol decreased it to 17% and 19% (Fig. V.11C and 12B) for TMRM and JC-10, respectively.
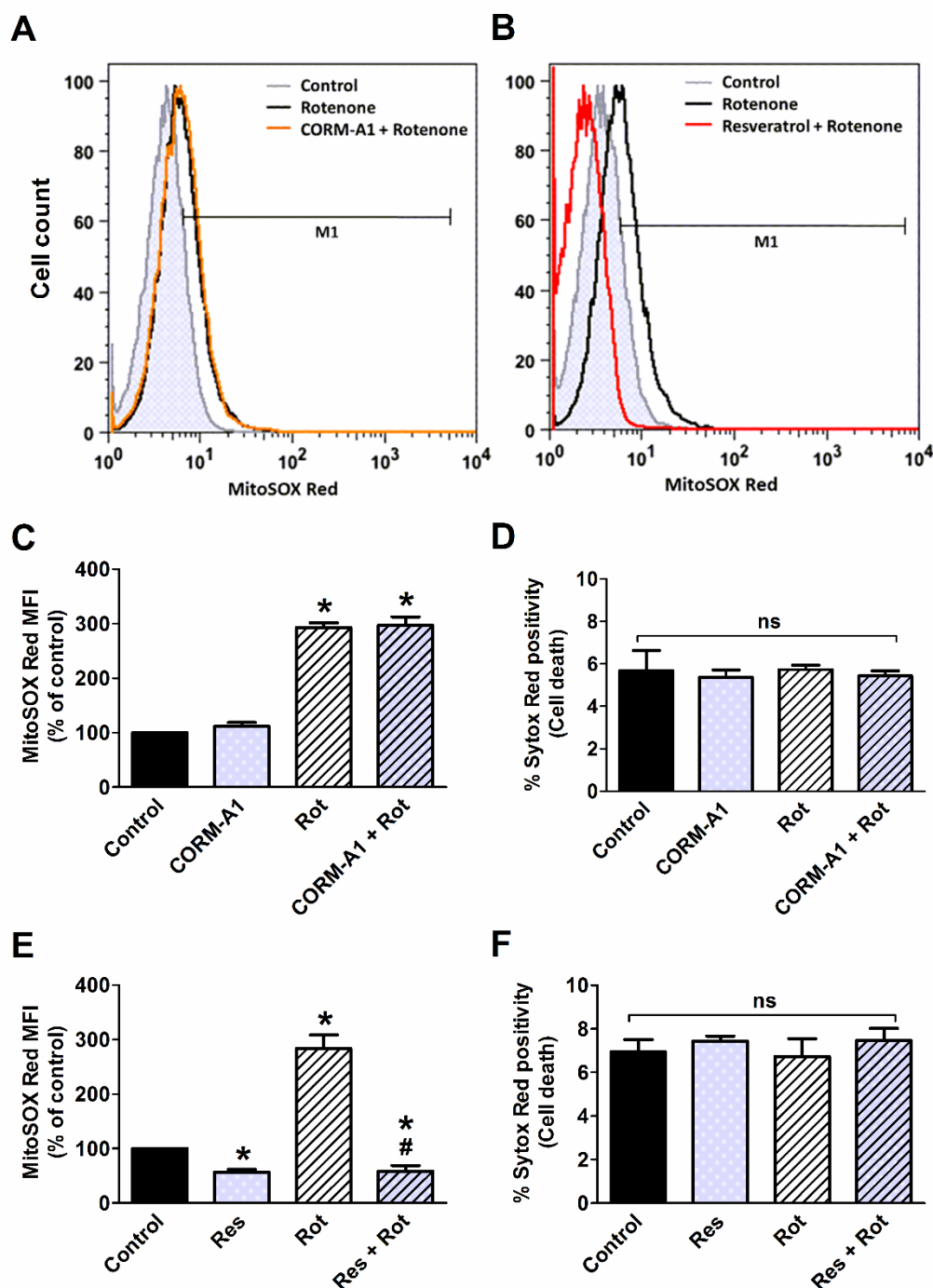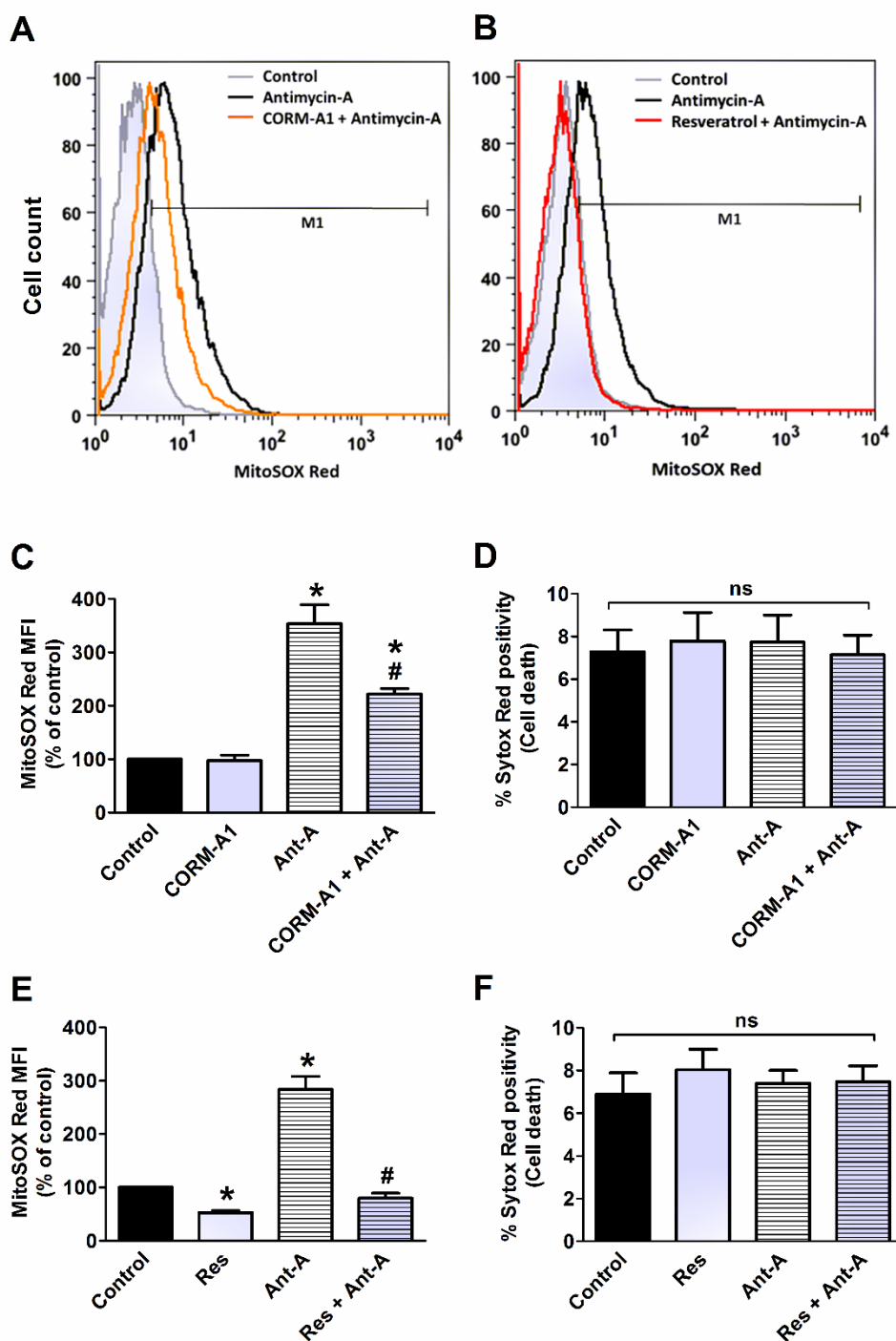
Fig. V.10 Effects of CORM-A1 or resveratrol on mitochondrial complex III (antimycin-A)-induced mitochondrial $O_2^{\bullet-}$ production and cell death in MODE-K cells. MODE-K cells were treated with antimycin-A (10 µM) in the absence or presence of CORM-A1 (100 µM) or resveratrol (75 µM). **A-B** Effect of CORM-A1 (A) or resveratrol (B) on antimycin-A-induced mitochondrial $O_2^{\bullet-}$ levels assessed with MitoSOX Red, and gated on the viable, Sytox Red-negative population. Representative overlay histogram plots of MitoSOX Red fluorescence are shown. The cells in M1 region represent the MitoSOX Red-positive cells contributing to the shift in fluorescence. **C-F** Influence of antimycin-A (Ant-A), incubated for 6 h, on mitochondrial $O_2^{\bullet-}$ levels (expressed as % of control MitoSOX Red MFI) and cell death (expressed as % Sytox Red positivity) in the absence and presence of CORM-A1 (C, D) or resveratrol (Res; E, F). Control cells were incubated with serum free medium alone; the effect of CORM-A1 or resveratrol *per se* was also tested (not shown in the histograms of **A** and **B** for clarity). Mean ± SEM of three independent experiments. *$P < 0.05$ *vs.* control. #$P < 0.05$ *vs.* antimycin-A alone.
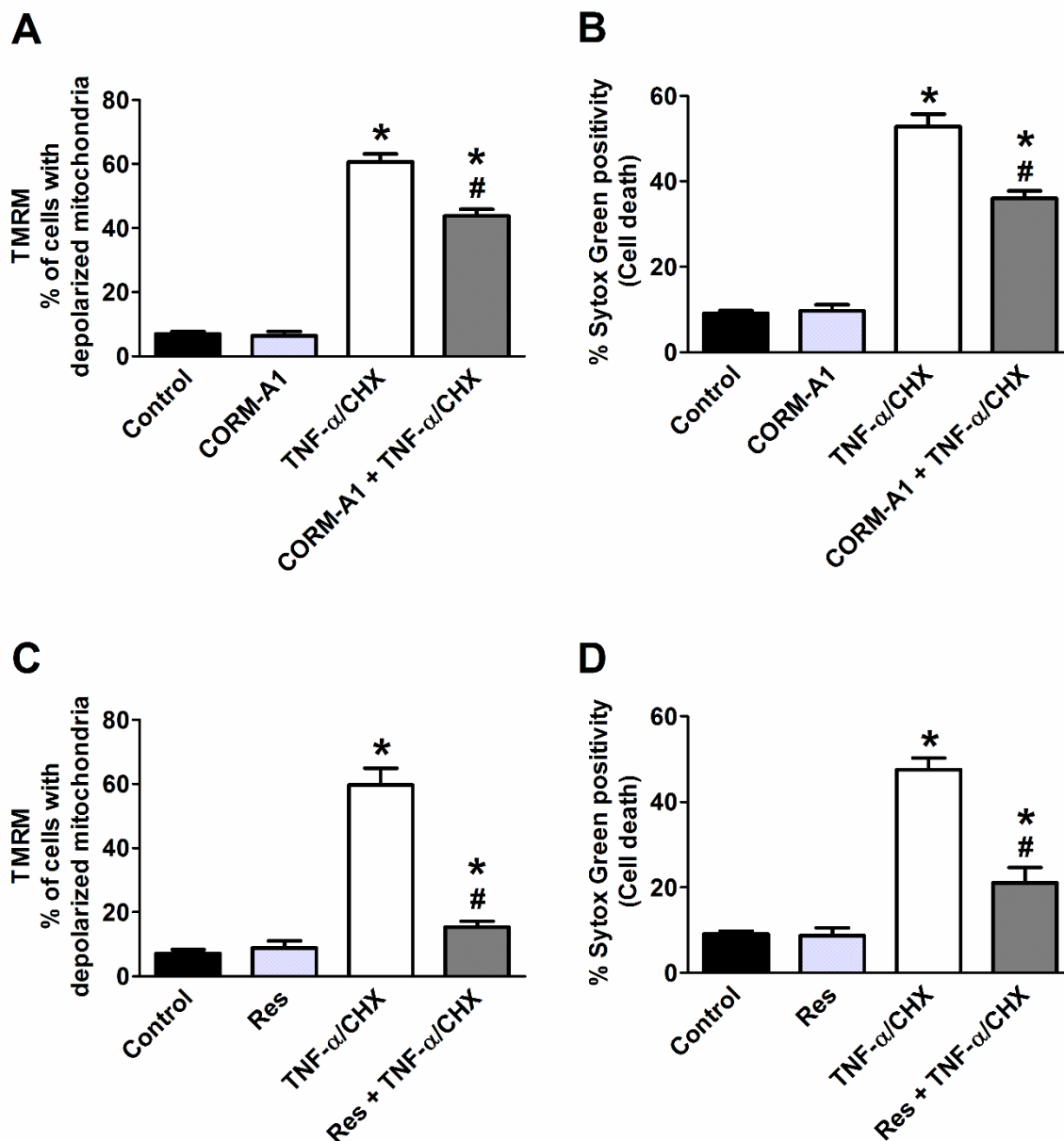
Fig. V.11 Effects of CORM-A1 (100 μM) or resveratrol (75 μM) on TNF-α (1 ng/ml)/CHX (10 μg/ml)-induced changes in mitochondrial membrane potential (assessed with TMRM) and cell death (assessed with Sytox Green) in MODE-K cells measured by flow cytometry. **A-D** Influence of TNF-α/CHX, incubated for 6 h, on mitochondrial membrane potential (expressed as % of cells with depolarized mitochondria after TMRM staining) and cell death (expressed as % Sytox Green positivity) in the absence and presence of CORM-A1 (A, B) or resveratrol (Res; C, D). Control cells were incubated with serum free medium alone; the effect of CORM-A1 or resveratrol *per se* was also tested. Mean ± SEM of three independent experiments. *$P < 0.05$ *vs.* control. #$P < 0.05$ *vs.* TNF-α/CHX alone.

Double staining of MODE-K cells with two different mitochondria-specific dyes to distinguish actively respiring (MitoTracker Deep Red FM-positive) and total (MitoTracker Green FM-positive) mitochondria showed an increase in the amount of respiration-interrupted
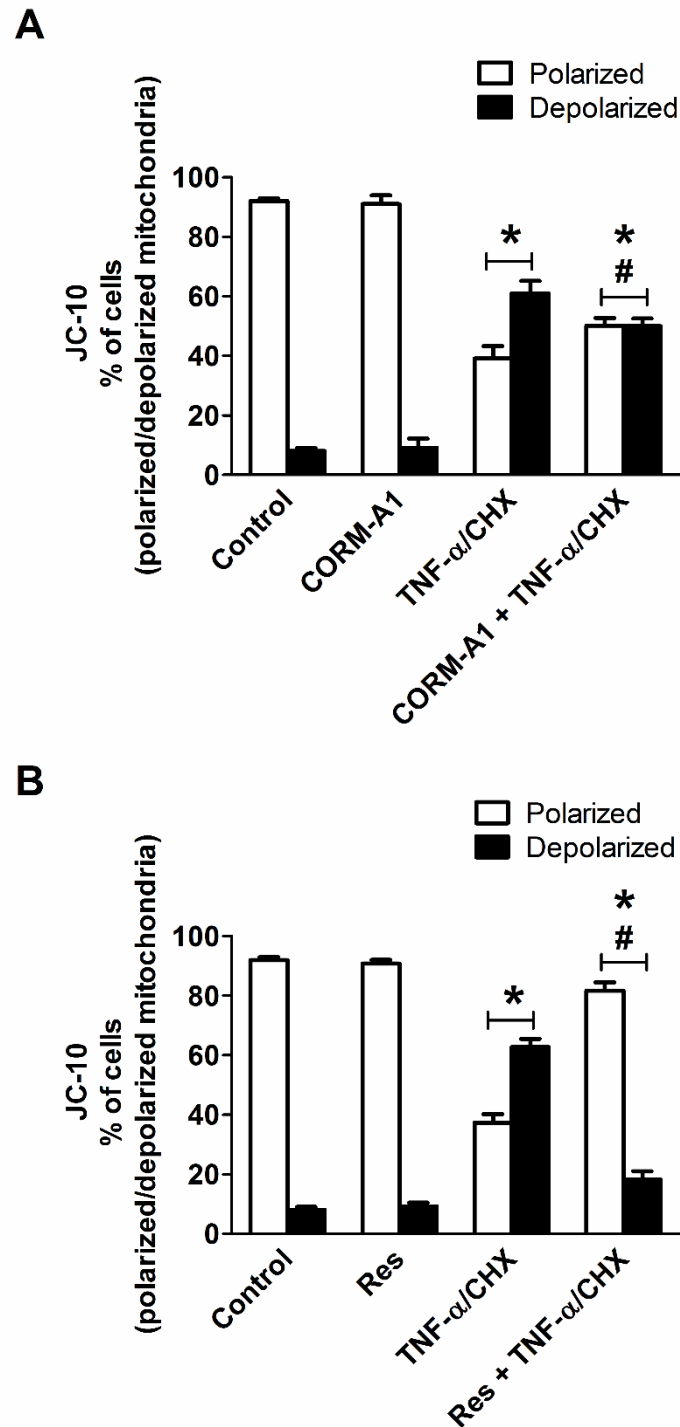
Fig. V.12 Effects of CORM-A1 (100 µM) or resveratrol (75 µM) on TNF-α (1 ng/ml)/CHX (10 µg/ml)-induced mitochondrial membrane depolarization (assessed with JC-10) in MODE-K cells measured by flow cytometry. Influence of TNF-α/CHX, incubated for 6 h, on mitochondrial membrane potential measured by flow cytometry (expressed as % of cells with polarized and depolarized mitochondria after JC-10 staining) in the absence and presence of CORM-A1 (A) or resveratrol (Res; B). Control cells were incubated with serum free medium alone; the effect of CORM-A1 or resveratrol *per se* was also tested. Mean ± SEM of three independent experiments. *$P < 0.05$ *vs.* control. #$P < 0.05$ *vs.* TNF-α/CHX alone.

mitochondria upon treatment of cells with TNF-α/CHX as compared to untreated control cells (46 ± 2% versus 4% ± 1% in P2 gated region; Fig. V.13B and D; third panel in Fig. V.13A and C). Treatment with CORM-A1 (Fig. V.13A and B) significantly decreased, while treatment with resveratrol (Fig. V.13C and D) abolished the TNF-α/CHX-induced increase in dysfunctional mitochondria, the level becoming lower than in control cells.

Cellular oxygen consumption rate (OCR) was measured using a Seahorse XF96 Analyzer to study the influence of CORM-A1 and resveratrol on TNF-α/CHX-treated MODE-K cells. Addition of TNF-α/CHX significantly decreased basal OCR within a few minutes of its administration and this decrease was maintained over time. Moreover, TNF-α/CHX increased the maximal respiration induced by the uncoupling agent CCCP without affecting non-mitochondrial respiratory rate (Fig. V.14A and B; V.15A and B). CORM-A1 *per se* significantly decreased basal OCR but from 1.5 h after its administration OCR slowly recuperated. Just before adding CCCP the OCR was still lower than in control cells; both maximal respiration and non-mitochondrial respiration were decreased compared to control cells. In MODE-K cells, treated with TNF-α/CHX in the presence of CORM-A1, the OCR remained low till administration of CCCP; the maximal respiration was lower than in controls and in cells treated with TNF-α/CHX alone (Fig. V.14A and 15A). Resveratrol *per se* decreased basal OCR to a similar extent as CORM-A1 but this decrease was stable till administration of CCCP; maximal respiration was not influenced by resveratrol but minimal respiration was decreased compared to controls. In MODE-K cells, treated with TNF-α/CHX in the presence of resveratrol, OCR values were similar to those in cells treated with TNF-α/CHX alone, except that maximal respiration was now decreased compared to controls (Fig. V.14B and 15B).

V.5   Discussion

Treatment of MODE-K cells with TNF-α/CHX induces apoptosis, which is associated with increased production of ROS. We previously found that CORM-A1 and resveratrol reduce both these effects (Babu *et al.*, 2012). We have also recently identified that NOX and mitochondrial ETC complexes (I and II) are the major sources of ROS production during TNF-α/CHX-induced apoptosis (Babu *et al.*, 2015). Here, we investigated the influence of
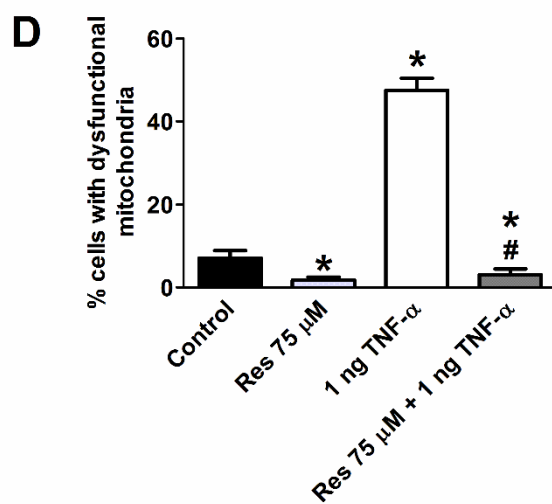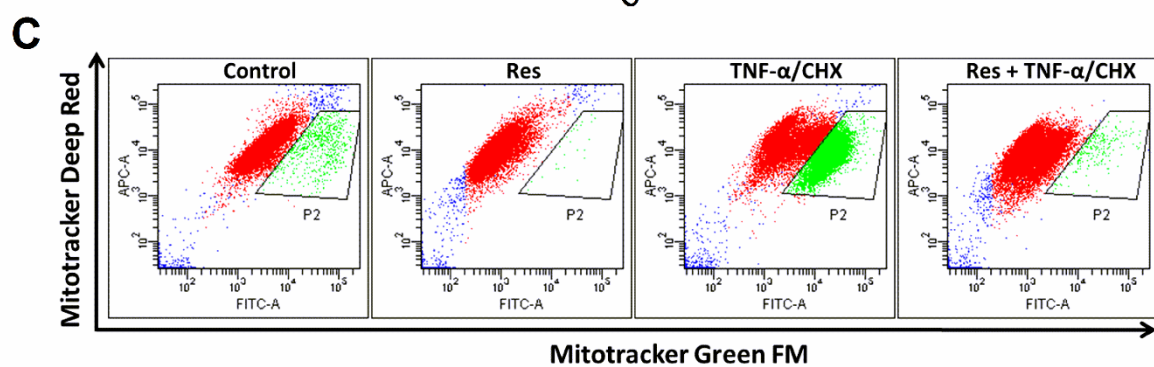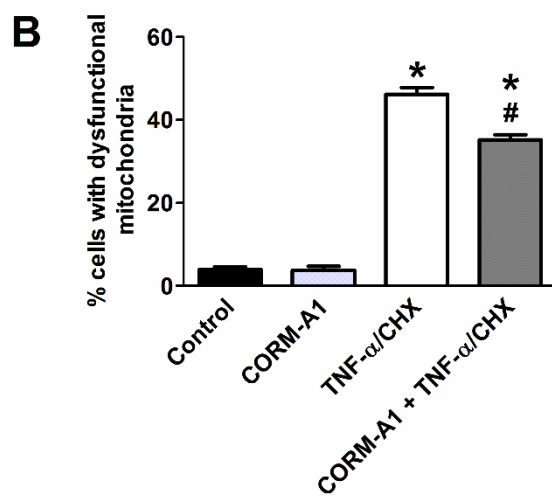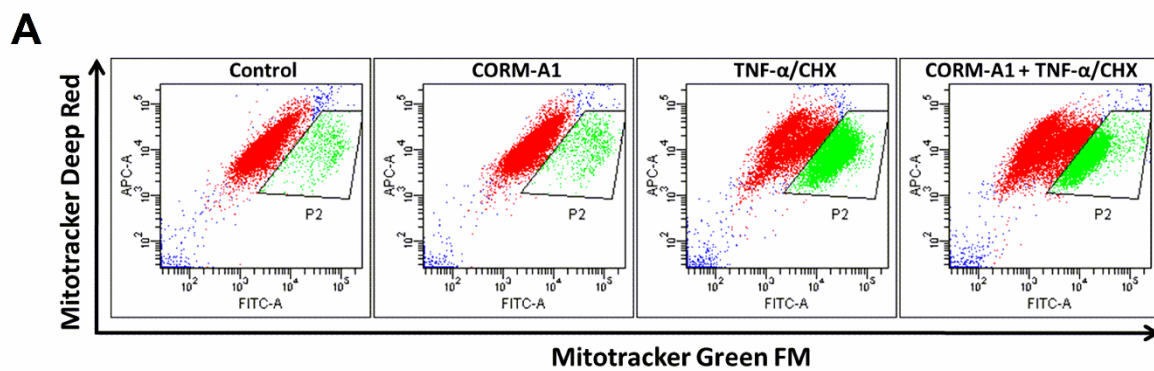
CORM-A1 and resveratrol on these pathways. The principal finding of this study is that CORM-A1 and resveratrol act on different sources of intracellular ROS production during their protection against TNF-α/CHX-induced cell death of MODE-K cells (see Table V.1 for a qualitative summary of the effects of CORM-A1 and resveratrol in basal conditions and versus TNF-α/CHX).

V.5.1 Mechanism of action of CORM-A1 during TNF-α/CHX-induced oxidative stress in MODE-K cells

Incubating MODE-K cells with 100 μM CORM-A1 from 1 h before exposure to TNF-α/CHX for 6 h partially reduced TNF-α/CHX-induced cell death. We previously reported that treatment of MODE-K cells with TNF-α/CHX induces a decrease in cellular oxygen consumption within 5 min of addition, a decrease in Ψ_m and an increase in mitochondrial dysregulation within 1 h of addition and an increase in intracellular total ROS and mitochondrial $O_2^{\bullet-}$ within 2 h of addition, the latter coinciding with the occurrence of apoptotic cell death (Babu *et al.*, 2012; Babu *et al.*, 2015). In several papers, the protection of cells by CO against oxidative insults has been related to inhibition of cytochrome c oxidase, the terminal enzyme within complex IV of the ETC, by competitive binding with oxygen resulting in a significant transient burst of mitochondria-derived ROS. The latter would create a state of preconditioning, inducing adaptive signaling towards subsequent oxidative stress (Taille *et al.*, 2005; Chin *et al.*, 2007; Zuckerbraun *et al.*, 2007; Kim *et al.*, 2008). However, in MODE-K cells, 100 μM CORM-A1 did not change mitochondrial ROS or $O_2^{\bullet-}$ levels even in the first hours after administration; only a higher CORM-A1 concentration of 200 μM increased mitochondrial $O_2^{\bullet-}$ levels temporarily at 1-2 h of incubation.

Fig. V.13 Effects of CORM-A1 (100 μM) or resveratrol (75 μM) on TNF-α (1 ng/ml)/CHX (10 μg/ml)-induced mitochondrial dysfunction in MODE-K cells measured by flow cytometry. **A-D** Influence of TNF-α/CHX, incubated for 6 h, on the amount of respiring mitochondria assessed with Mitotracker Green FM (FL1; FITC) and Mitotracker Deep Red FM (FL4; APC) staining in the absence and presence of CORM-A1 (A, B) or resveratrol (C, D). Control cells were incubated with serum free medium alone; the effect of CORM-A1 or resveratrol *per se* was also tested. **A** and **C** Representative dot plots of the flow cytometric analysis showing the effect of CORM-A1 (A) or resveratrol (Res; C) on the population of cells (gated on live cells) losing mitochondrial potential and with respiration-interrupted mitochondria (shift of cell population towards P2 gated region) after treatment with TNF-α/CHX. **B** and **D** Quantification of flow cytometric measurements (expressed as % of cells with dysfunctional mitochondria) of CORM-A1 (B) and resveratrol (Res; D). Mean ± SEM of three independent experiments. *$P < 0.05$ *vs.* control. #$P < 0.05$ *vs.* TNF-α/CHX alone.
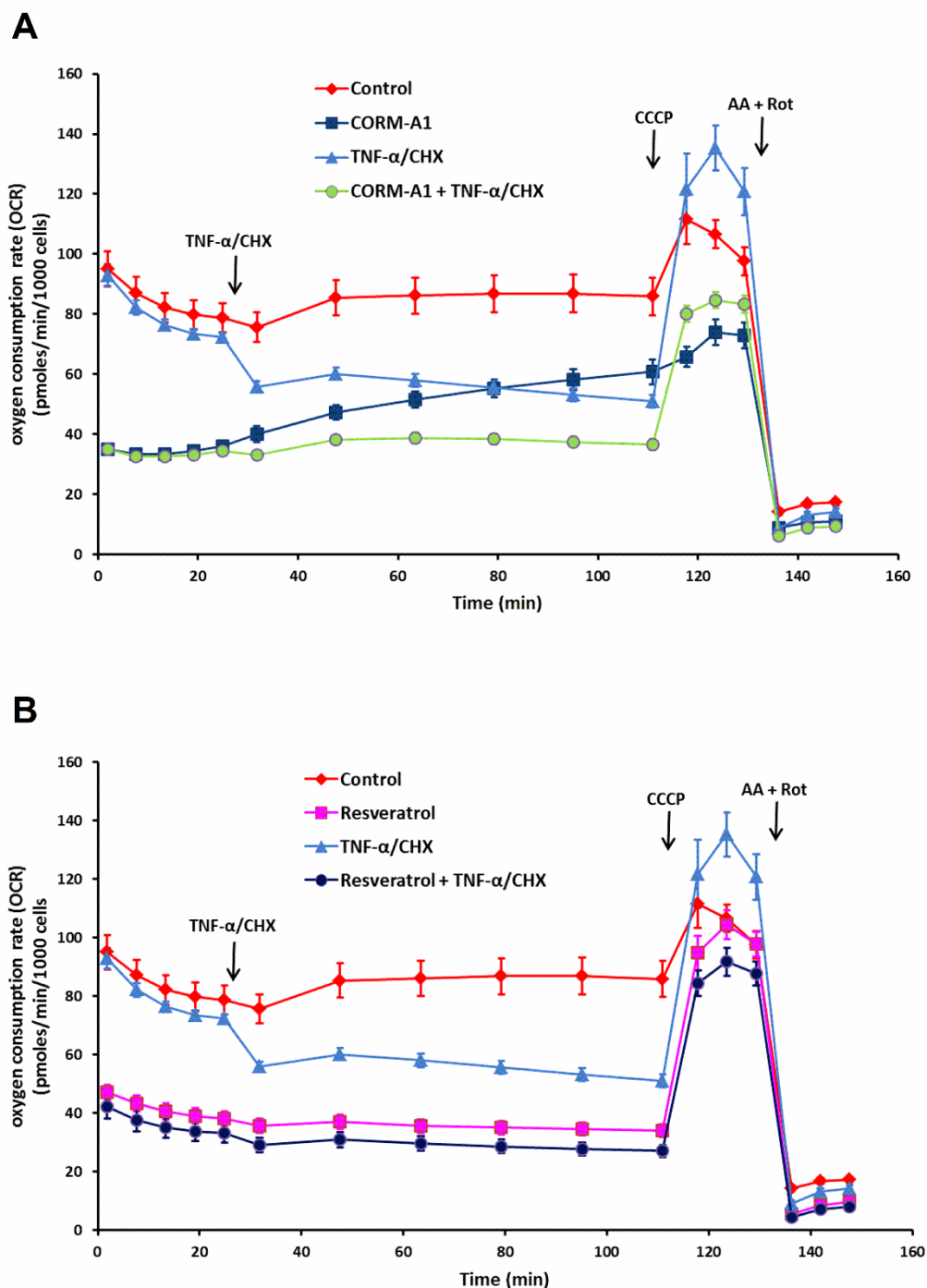
Fig. V.14 Acute effects of CORM-A1 (100 µM) or resveratrol (75 µM) on TNF-α (1 ng/ml)/CHX (10 µg/ml)-induced decrease in mitochondrial respiration in MODE-K cells. Influence of TNF-α/CHX, incubated for 2 h, on cellular oxygen consumption rate (OCR, expressed as pmoles/min) in the absence and presence of CORM-A1 (A) or resveratrol (B). CORM-A1 or resveratrol was incubated from 1 h before analysis of OCR. OCR was measured at different time points for 2.5 h. First, five consecutive measurements of respiration during incubation with medium alone were done for 30 min. Then, TNF-α/CHX was injected or not (control) followed by six consecutive measurements. At 115 min, the protonophore CCCP (50 µM) was added to measure maximal oxygen consumption for three measurements. At 130 min, the complex I inhibitor rotenone (2.5 µM) and the complex III inhibitor antimycin-A (5 µM) were injected, followed by three consecutive measurements to determine the non-mitochondrial respiration. Finally, the amount of viable cells (Hoechst[+]/PI^{-} cells) in the microchamber of each well was determined by automated imaging. The data represent the average of five replicates for each condition.
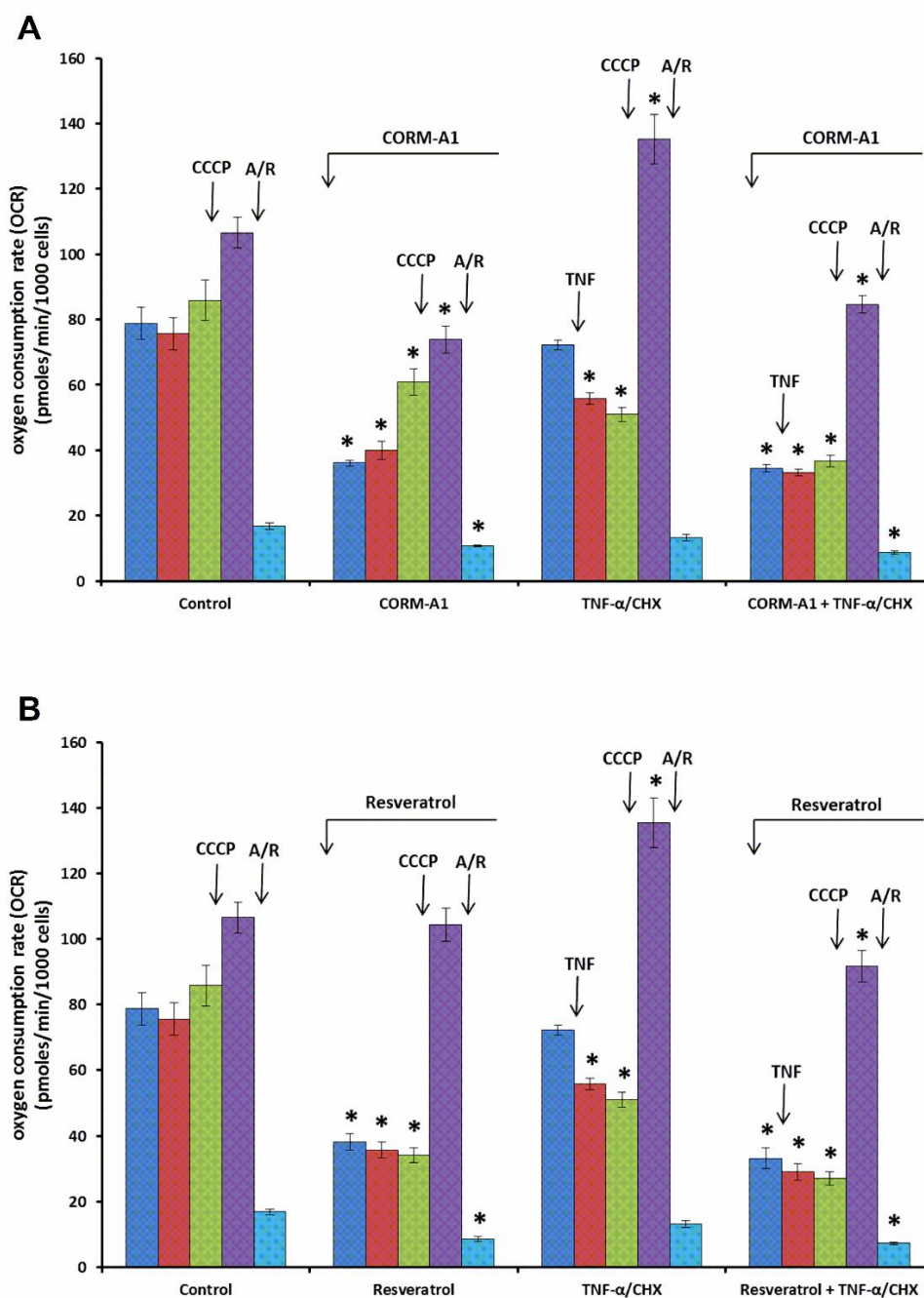
Fig. V.15 Acute effects of CORM-A1 (100 µM) or resveratrol (75 µM) on TNF-α (1 ng/ml)/CHX (10 µg/ml)-induced decrease in mitochondrial respiration in MODE-K cells. Influence of TNF-α/CHX, incubated for 2 h, on cellular oxygen consumption rate (OCR, expressed as pmoles/min) in the absence and presence of CORM-A1 (A) or resveratrol (B). CORM-A1 or resveratrol was incubated from 1 h before analysis of OCR. OCR was measured at different time points for 2.5 h. First, five consecutive measurements of respiration during incubation with medium alone were done for 30 min. Then, TNF-α/CHX was injected or not (control) followed by six consecutive measurements. At 115 min, the protonophore CCCP (50 µM) was added to measure maximal oxygen consumption for three measurements. At 130 min, the complex I inhibitor rotenone (2.5 µM) and the complex III inhibitor antimycin-A (5 µM) were injected, followed by three consecutive measurements to determine the non-mitochondrial respiration. Finally, the amount of viable cells (Hoechst[+]/PI^{-} cells) in the microchamber of each well was determined by automated imaging. OCR values are given for the measurements just before and after TNF-α/CHX administration (25 min and 32 min), for the measurement just before CCCP administration (111 min), for the second measurement after CCCP administration (124 min) and for the second measurement after administration of antimycin-A plus rotenone (142 min). A/R: Antimycin-A plus rotenone; TNF: TNF-α/CHX. * Significantly different from control.

Table V.1   Qualitative summary of the effects of CORM-A1 and resveratrol in basal conditions and versus TNF-α/CHX.

Parameter		Total ROS	Mitochondrial ROS	Mitochondrial $O_2^{\bullet-}$	Mitochondrial depolarization	Mitochondrial depolarization	Mitochondrial dysfunction
Probes		Carboxy-H$_2$DCFDA	DHR123	MitoSOX Red	TMRM	JC-10	MitoTracker Green/Deep Red
CORM-A1	Basal	=	=	=	=	=	=
	TNF-α/CHX	↓	=	=	↓	↓	↓
Resveratrol	Basal	↑	↓	↓	=	=	↓
	TNF-α/CHX	↓	↓	↓	↓	↓	↓

= Not influenced; ↑ Increased; ↓ Reduced; ↓ Abolished; ↓ Abolished and decreased under basal levels

Still, 100 µM CORM-A1 decreased cellular OCR in MODE-K cells with partial recuperation from this decrease from 90 min after its administration. In a previous study, a decrease in OCR was observed in isolated heart mitochondria treated with 100 µM CORM-3, while lower concentrations (1-20 µM) triggered an actual increase in OCR. However, the decrease in OCR with 100 µM CORM-3 was accompanied by inhibition of cytochrome c oxidase (complex IV) and increase in mitochondrial ROS production (Lo Iacono *et al.*, 2011). In contrast, we did not observe an increase in mitochondrial ROS production with 100 µM CORM-A1 in MODE-K cells. The difference in these results could be due to the chemical reactivity of CORM-3 and CORM-A1, the first being a transition metal carbonyl releasing CO with a fast rate, whereas the second being a boranocarbonate that generates spontaneously CO at physiological pH with a slow kinetic (Motterlini *et al.*, 2002; Motterlini *et al.*, 2005). In addition, we cannot exclude that the different results obtained are due to differences in technology, as Lo Iacono et al. (2011) measured OCR in isolated mitochondria using a Clark-type oxygen electrode and different substrates, compared to the intact cells in growth medium used in our study where OCR was measured using the Seahorse XF96 Analyzer. One has speculated that the cytoprotective effects of CO are independent of mitochondrial ROS generation, but related to partial or temporal inhibition of mitochondrial respiration (Almeida *et al.*, 2015). In HEK293 cells, both exogenous and endogenous CO were shown to reduce cellular respiration (D'Amico *et al.*, 2006) and it was suggested that this might contribute to its cytoprotective

effects, as reported for NO (Xu *et al.*, 2004). This might also explain why CORM-A1 partially recovered the decrease in Ψ_m and the increase in mitochondrial dysfunction by TNF-α/CHX observed in this study.

Although CORM-A1 is not preconditioning MODE-K cells by inducing *per se* mitochondrial ROS, it has antioxidant potential in the cells as illustrated by the partial reduction of TNF-α/CHX-induced and H_2O_2-induced intracellular total ROS. Modulation of ROS production is considered to be a main mechanism of CO-mediated cytoprotection (Motterlini *et al.*, 2012), the $O_2^{\bullet-}$ producing heme-containing proteins in mitochondria (cytochromes) and the NOX enzymes in the cells being the major targets of CO due to its higher affinity for heme (Foresti & Motterlini, 2010). In MODE-K cells, CORM-A1 was not able to reduce TNF-α/CHX-induced mitochondrial ROS or $O_2^{\bullet-}$ levels, excluding that this contributes to its partial protection from TNF-α/CHX-induced cytotoxicity. We previously showed that mitochondrial complexes I and II are the major mitochondrial ROS production sites during TNF-α/CHX-induced cell death in MODE-K cells (Babu *et al.*, 2015). CORM-A1 did not influence mitochondrial $O_2^{\bullet-}$ induced by the complex I inhibitor rotenone probably because rotenone-induced mitochondrial ROS are released into the mitochondrial matrix (Chen *et al.*, 2003; Rodriguez-Rocha *et al.*, 2013). Still, CORM-A1 was able to reduce antimycin-A-induced mitochondrial $O_2^{\bullet-}$. Antimycin-A-derived mitochondrial $O_2^{\bullet-}$ is reported to be fully (St-Pierre *et al.*, 2002) or at least partially (Han *et al.*, 2003) released into the mitochondrial intermembrane space. As myxothiazole, the Qo site inhibitor of complex III, partially reduced TNF-α/CHX-induced total ROS and cell death in MODE-K cells (Babu *et al.*, 2015), part of TNF-α/CHX-induced ROS must also be released into the mitochondrial intermembrane space. The lack of any effect of CORM-A1 versus TNF-α/CHX-induced mitochondrial ROS might be related to near full use of CORM-A1 derived CO in the cytoplasm to counteract NOX-derived ROS upon exposure to TNF-α. The latter ROS production site is not activated by antimycin-A, so that sufficient CO might reach the mitochondrial intermembrane space upon exposure of MODE-K cells to antimycin-A.

The partial reduction of TNF-α/CHX-induced intracellular total ROS by CORM-A1 is thus probably due to inhibition of NOX-derived ROS. In addition to mitochondrial complexes I and II, NOX are the second source of TNF-α/CHX-induced ROS, leading to apoptosis in MODE-K cells (Babu *et al.*, 2015). CO has been reported to inhibit NOX and decrease cytoplasmic $O_2^{\bullet-}$ production (Bilban *et al.*, 2006; Srisook *et al.*, 2006; Wang *et al.*, 2007;

Kelsen *et al.*, 2008), probably by binding to the heme-containing gp91phox (NOX2) subunit with subsequent decrease in NOX activity (Taille *et al.*, 2005; Nakahira *et al.*, 2006). Similarly, CORM-A1 inhibited TNF-α-induced NOX activation and apoptosis in cerebral microvascular endothelial cells (Basuroy *et al.*, 2009). As NOX are only one of the two major sources of TNF-α/CHX-induced ROS in MODE-K cells, and NOX activation might be sequential to mitochondrial ROS production (Babu *et al.*, 2015), the inhibitory effect of CORM-A1 on NOX can only lead to partial reduction of TNF-α/CHX-induced cell death.

V.5.2 *Mechanism of action of resveratrol during TNF-α/CHX-induced oxidative stress in MODE-K cells*

In contrast to CORM-A1, resveratrol decreased the basal levels of both mitochondrial ROS and mitochondrial $O_2^{\bullet-}$ in MODE-K cells. Moreover, the more pronounced reduction in TNF-α/CHX-induced cell death by resveratrol accompanied by abolishment of mitochondrial ROS/$O_2^{\bullet-}$ levels implies that the inhibitory action of this polyphenol on mitochondria-derived ROS contributes to its anti-apoptotic/cytoprotective effects in MODE-K cells. Attenuation of mitochondrial oxidative stress with resveratrol was also reported in coronary arterial endothelial cells (Ungvari *et al.*, 2009). Cytoprotection related to reduction of mitochondrial ROS has already been reported for several drugs (Reddy, 2006; Szeto, 2006; Plotnikov *et al.*, 2013) and a mitochondrial-targeted antioxidant has recently been shown to be beneficial in reducing intestinal epithelial barrier dysfunction (Wang *et al.*, 2014). In addition to decreasing mitochondrial $O_2^{\bullet-}$ levels, resveratrol effectively prevented the TNF-α/CHX-induced development of mitochondrial dysfunction and drop in Ψ_m in MODE-K cells. Resveratrol abolished both complex I- and complex III-induced ROS (as seen in experiments using rotenone and antimycin-A, respectively), which demonstrates the capacity of resveratrol in mitigating complex I and complex III-derived ROS. Owing to its lipophilicity, resveratrol might penetrate the mitochondrial matrix beyond the intermembrane space and thus could scavenge $O_2^{\bullet-}$ produced inside the matrix being available at the close proximity of $O_2^{\bullet-}$ generation. Additionally, resveratrol could induce an increased expression of mitochondrial superoxide dismutase (SOD)-2 as shown before in cultured neuronal cells (Fukui *et al.*, 2010).

In contrast to decreasing mitochondrial ROS, resveratrol increased intracellular total ROS production in MODE-K cells. Although well known as an antioxidant, the pro-oxidant effects of resveratrol have been reported in some cell types (de la Lastral & Villegas, 2007) and it has been suggested that this can create an intracellular environment preventing apoptotic cell death (Ahmad *et al.*, 2003). Resveratrol-induced ROS production in MODE-K is mediated through NOX1 (as evidenced by its abolishment in the presence of pan-NOX and Rac1 inhibitors), which is similar to its effect reported in endothelial cells (Schilder *et al.*, 2009). NOX-derived ROS production serves as a protective signal to increase the levels of intracellular antioxidant enzymes/scavenging molecules and has been implicated in stress-induced preconditioning (Bell *et al.*, 2005; Jiang *et al.*, 2011; Frasier *et al.*, 2013). The increase in the levels of NOX-derived ROS by pretreatment with resveratrol might exert such a "protective signaling" for MODE-K cells to raise their antioxidant defense to protect themselves from the successive cytokine (TNF-α) effect. Notably, resveratrol was shown in cultured hepatocytes to increase the activity of several antioxidant enzymes such as catalase and SOD via activation of nuclear factor-E2-related factor-2 (Rubiolo *et al.*, 2008). NOX-derived ROS has also been shown to play a role in epithelial cell proliferation (Brar *et al.*, 2002; Ranjan *et al.*, 2006). The role of NOX1-dependent ROS generation during proliferation of mouse small intestinal (Jones *et al.*, 2013) and colonic epithelium (Coant *et al.*, 2010) has been recently proposed. Hence, it seems plausible that ROS generation resulting from pre-treatment of MODE-K cells with resveratrol before exposure to TNF-α/CHX might have activated the proliferative machinery to defend against the successive stress insult.

We suggested that treatment of MODE-K cells with TNF-α/CHX might involve an early phase of mitochondria-derived ROS production inducing a later phase of NOX-derived ROS production as mitochondrial complex inhibitors show a more pronounced decrease in total ROS levels and cell death as compared to the moderate effect of the NOX inhibitor, VAS-2870 (Babu *et al.*, 2015). The pronounced cytoprotective effect of resveratrol concomitant with the abolishment of mitochondrial ROS/$O_2^{\bullet-}$, as compared to the moderate NOX-dependent cytoprotection observed with CORM-A1, further strengthens the notion of a possible sequential communication from mitochondria to NOX for ROS production in MODE-K cells.

In conclusion, the cytoprotective effect of resveratrol is predominantly due to mitigation of mitochondrial ROS while CORM-A1 acts solely on NOX-derived ROS to protect MODE-K cells from TNF-α/CHX-induced cell death. These data infer that interference of CORM-A1 and resveratrol with particular intracellular ROS production sites could have some therapeutic value and therefore should be further tested for the treatment of acute GI inflammatory diseases.

V.6   References

Aghdassi E, Wendland BE, Steinhart AH, Wolman SL, Jeejeebhoy K, Allard JP (2003). Antioxidant vitamin supplementation in Crohn's disease decreases oxidative stress. a randomized controlled trial. *Am J Gastroenterol* **98**, 348-353.

Ahmad KA, Clement MV, Pervaiz S (2003). Pro-oxidant activity of low doses of resveratrol inhibits hydrogen peroxide-induced apoptosis. *Ann N Y Acad Sci* **1010**, 365-373.

Ahn BO, Ko KH, Oh TY, Cho H, Kim WB, Lee KJ *et al.* (2001). Efficacy of use of colonoscopy in dextran sulfate sodium induced ulcerative colitis in rats: the evaluation of the effects of antioxidant by colonoscopy. *International Journal of Colorectal Disease* **16**, 174-181.

Almeida AS, Figueiredo-Pereira C, Vieira HL (2015). Carbon monoxide and mitochondria-modulation of cell metabolism, redox response and cell death. *Front Physiol* **6**, 33.

Anup R, Aparna V, Pulimood A, Balasubramanian KA (1999). Surgical stress and the small intestine: role of oxygen free radicals. *Surgery* **125**, 560-569.

Babu D, Leclercq G, Goossens V, Vanden Berghe T, Van Hamme E, Vandenabeele P *et al.* (2015). Mitochondria and NADPH oxidases are the major sources of TNF-alpha/cycloheximide-induced oxidative stress in murine intestinal epithelial MODE-K cells. *Cell Signal* **27**, 1141-1158.

Babu D, Motterlini R, Lefebvre RA (2014). CO and CO-releasing molecules (CO-RMs) in acute gastrointestinal inflammation. *Br J Pharmacol*.

Babu D, Soenen SJ, Raemdonck K, Leclercq G, De Backer O, Motterlini R *et al.* (2012). TNF-alpha/cycloheximide-induced oxidative stress and apoptosis in murine intestinal epithelial MODE-K cells. *Curr Pharm Des* **18**, 4414-4425.

Barbosa DS, Cecchini R, El Kadri MZ, Rodriguez MA, Burini RC, Dichi I (2003). Decreased oxidative stress in patients with ulcerative colitis supplemented with fish oil omega-3 fatty acids. *Nutrition* **19**, 837-842.

Baregamian N, Song J, Bailey CE, Papaconstantinou J, Evers BM, Chung DH (2009). Tumor necrosis factor-alpha and apoptosis signal-regulating kinase 1 control reactive oxygen species release, mitochondrial autophagy, and c-Jun N-terminal kinase/p38 phosphorylation during necrotizing enterocolitis. *Oxidative Medicine and Cellular Longevity* **2**, 297-306.

Basu Ball W, Kar S, Mukherjee M, Chande AG, Mukhopadhyaya R, Das PK (2011). Uncoupling protein 2 negatively regulates mitochondrial reactive oxygen species generation and induces phosphatase-mediated anti-inflammatory response in experimental visceral leishmaniasis. *J Immunol* **187**, 1322-1332.

Basuroy S, Bhattacharya S, Leffler CW, Parfenova H (2009). Nox4 NADPH oxidase mediates oxidative stress and apoptosis caused by TNF-alpha in cerebral vascular endothelial cells. *Am J Physiol Cell Physiol* **296**, C422-432.

Bell RM, Cave AC, Johar S, Hearse DJ, Shah AM, Shattock MJ (2005). Pivotal role of NOX-2-containing NADPH oxidase in early ischemic preconditioning. *Faseb Journal* **19**, 2037-2039.

Bereswill S, Munoz M, Fischer A, Plickert R, Haag LM, Otto B *et al.* (2010). Anti-inflammatory effects of resveratrol, curcumin and simvastatin in acute small intestinal inflammation. *PLoS One* **5**, e15099.

Bilban M, Bach FH, Otterbein SL, Ifedigbo E, d'Avila JC, Esterbauer H *et al.* (2006). Carbon monoxide orchestrates a protective response through PPARgamma. *Immunity* **24**, 601-610.

Bilban M, Haschemi A, Wegiel B, Chin BY, Wagner O, Otterbein LE (2008). Heme oxygenase and carbon monoxide initiate homeostatic signaling. *J Mol Med (Berl)* **86**, 267-279.

Brar SS, Kennedy TP, Sturrock AB, Huecksteadt TP, Quinn MT, Murphy TM *et al.* (2002). NADPH oxidase promotes NF-kappaB activation and proliferation in human airway smooth muscle. *Am J Physiol Lung Cell Mol Physiol* **282**, L782-795.

Cetinkaya A, Bulbuloglu E, Kurutas EB, Ciralik H, Kantarceken B, Buyukbese MA (2005). Beneficial effects of N-acetylcysteine on acetic acid-induced colitis in rats. *Tohoku Journal of Experimental Medicine* **206**, 131-139.

Chen Q, Vazquez EJ, Moghaddas S, Hoppel CL, Lesnefsky EJ (2003). Production of reactive oxygen species by mitochondria: central role of complex III. *J Biol Chem* **278**, 36027-36031.

Chin BY, Jiang G, Wegiel B, Wang HJ, Macdonald T, Zhang XC *et al.* (2007). Hypoxia-inducible factor 1alpha stabilization by carbon monoxide results in cytoprotective preconditioning. *Proc Natl Acad Sci U S A* **104**, 5109-5114.

Coant N, Ben Mkaddem S, Pedruzzi E, Guichard C, Treton X, Ducroc R *et al.* (2010). NADPH oxidase 1 modulates WNT and NOTCH1 signaling to control the fate of proliferative progenitor cells in the colon. *Mol Cell Biol* **30**, 2636-2650.

D'Amico G, Lam F, Hagen T, Moncada S (2006). Inhibition of cellular respiration by endogenously produced carbon monoxide. *J Cell Sci* **119**, 2291-2298.

Damiani CR, Benetton CA, Stoffel C, Bardini KC, Cardoso VH, Di Giunta G *et al.* (2007). Oxidative stress and metabolism in animal model of colitis induced by dextran sulfate sodium. *J Gastroenterol Hepatol* **22**, 1846-1851.

De Backer O, Elinck E, Blanckaert B, Leybaert L, Motterlini R, Lefebvre RA (2009). Water-soluble CO-releasing molecules reduce the development of postoperative ileus via modulation of MAPK/HO-1 signalling and reduction of oxidative stress. *Gut* **58**, 347-356.

de la Lastral CA & Villegas I (2007). Resveratrol as an antioxidant and pro-oxidant agent: mechanisms and clinical implications. *Biochemical Society Transactions* **35**, 1156-1160.

de Winter BY, van Nassauw L, de Man JG, de Jonge F, Bredenoord AJ, Seerden TC *et al.* (2005). Role of oxidative stress in the pathogenesis of septic ileus in mice. *Neurogastroenterol Motil* **17**, 251-261.

Duprez L, Takahashi N, Van Hauwermeiren F, Vandendriessche B, Goossens V, Vanden Berghe T *et al.* (2011). RIP kinase-dependent necrosis drives lethal systemic inflammatory response syndrome. *Immunity* **35**, 908-918.

Foresti R & Motterlini R (2010). Interaction of carbon monoxide with transition metals: evolutionary insights into drug target discovery. *Curr Drug Targets* **11**, 1595-1604.

Foti Cuzzola V, Ciurleo R, Giacoppo S, Marino S, Bramanti P (2011). Role of resveratrol and its analogues in the treatment of neurodegenerative diseases: focus on recent discoveries. *CNS Neurol Disord Drug Targets* **10**, 849-862.

Frasier CR, Moukdar F, Patel HD, Sloan RC, Stewart LM, Alleman RJ *et al.* (2013). Redox-dependent increases in glutathione reductase and exercise preconditioning: role of NADPH oxidase and mitochondria. *Cardiovascular Research* **98**, 47-55.

Fukui M, Choi HJ, Zhu BT (2010). Mechanism for the protective effect of resveratrol against oxidative stress-induced neuronal death. *Free Radic Biol Med* **49**, 800-813.

Guan Y, Worrell RT, Pritts TA, Montrose MH (2009). Intestinal ischemia-reperfusion injury: reversible and irreversible damage imaged in vivo. *Am J Physiol Gastrointest Liver Physiol* **297**, G187-196.

Han D, Canali R, Rettori D, Kaplowitz N (2003). Effect of glutathione depletion on sites and topology of superoxide and hydrogen peroxide production in mitochondria. *Mol Pharmacol* **64**, 1136-1144.

Holtmann MH, Schutz M, Galle PR, Neurath MF (2002). Functional relevance of soluble TNF-alpha, transmembrane TNF-alpha and TNF-signal transduction in gastrointestinal diseases with special reference to inflammatory bowel diseases. *Z Gastroenterol* **40**, 587-600.

Jiang F, Zhang Y, Dusting GJ (2011). NADPH oxidase-mediated redox signaling: roles in cellular stress response, stress tolerance, and tissue repair. *Pharmacological Reviews* **63**, 218-242.

Jin S, Ray RM, Johnson LR (2008). TNF-alpha/cycloheximide-induced apoptosis in intestinal epithelial cells requires Rac1-regulated reactive oxygen species. *Am J Physiol Gastrointest Liver Physiol* **294**, G928-937.

Jones RM, Luo L, Ardita CS, Richardson AN, Kwon YM, Mercante JW *et al.* (2013). Symbiotic lactobacilli stimulate gut epithelial proliferation via Nox-mediated generation of reactive oxygen species. *EMBO J* **32**, 3017-3028.

Kelsen S, Patel BJ, Parker LB, Vera T, Rimoldi JM, Gadepalli RS *et al.* (2008). Heme oxygenase attenuates angiotensin II-mediated superoxide production in cultured mouse thick ascending loop of Henle cells. *Am J Physiol Renal Physiol* **295**, F1158-1165.

Kim HS, Loughran PA, Rao J, Billiar TR, Zuckerbraun BS (2008). Carbon monoxide activates NF-kappaB via ROS generation and Akt pathways to protect against cell death of hepatocytes. *Am J Physiol Gastrointest Liver Physiol* **295**, G146-G152.

Kim YJ, Kim EH, Hahm KB (2012). Oxidative stress in inflammation-based gastrointestinal tract diseases: challenges and opportunities. *J Gastroenterol Hepatol* **27**, 1004-1010.

Lo Iacono L, Boczkowski J, Zini R, Salouage I, Berdeaux A, Motterlini R *et al.* (2011). A carbon monoxide-releasing molecule (CORM-3) uncouples mitochondrial respiration and modulates the production of reactive oxygen species. *Free Radic Biol Med* **50**, 1556-1564.

Millar AD, Rampton DS, Chander CL, Claxson AWD, Blades S, Coumbe A *et al.* (1996). Evaluating the antioxidant potential of new treatments for inflammatory bowel disease using a rat model of colitis. *Gut* **39**, 407-415.

Mittal M, Siddiqui MR, Tran K, Reddy SP, Malik AB (2014). Reactive oxygen species in inflammation and tissue injury. *Antioxid Redox Signal* **20**, 1126-1167.

Motterlini R, Clark JE, Foresti R, Sarathchandra P, Mann BE, Green CJ (2002). Carbon monoxide-releasing molecules: characterization of biochemical and vascular activities. *Circulation Research* **90**, E17-24.

Motterlini R, Haas B, Foresti R (2012). Emerging concepts on the anti-inflammatory actions of carbon monoxide-releasing molecules (CO-RMs). *Med Gas Res* **2**, 28.

Motterlini R & Otterbein LE (2010). The therapeutic potential of carbon monoxide. *Nat Rev Drug Discov* **9**, 728-743.

Motterlini R, Sawle P, Hammad J, Bains S, Alberto R, Foresti R *et al.* (2005). CORM-A1: a new pharmacologically active carbon monoxide-releasing molecule. *Faseb Journal* **19**, 284-286.

Nakahira K, Kim HP, Geng XH, Nakao A, Wang X, Murase N *et al.* (2006). Carbon monoxide differentially inhibits TLR signaling pathways by regulating ROS-induced trafficking of TLRs to lipid rafts. *J Exp Med* **203**, 2377-2389.

Nishikawa M, Oshitani N, Matsumoto T, Nishigami T, Arakawa T, Inoue M (2005). Accumulation of mitochondrial DNA mutation with colorectal carcinogenesis in ulcerative colitis. *Br J Cancer* **93**, 331-337.

Oshitani N, Kitano A, Okabe H, Nakamura S, Matsumoto T, Kobayashi K (1993). Location of Superoxide Anion Generation in Human Colonic Mucosa Obtained by Biopsy. *Gut* **34**, 936-938.

Ozkan OV, Yuzbasioglu MF, Ciralik H, Kurutas EB, Yonden Z, Aydin M *et al.* (2009). Resveratrol, a natural antioxidant, attenuates intestinal ischemia/reperfusion injury in rats. *Tohoku Journal of Experimental Medicine* **218**, 251-258.

Pastorelli L, De Salvo C, Mercado JR, Vecchi M, Pizarro TT (2013). Central role of the gut epithelial barrier in the pathogenesis of chronic intestinal inflammation: lessons learned from animal models and human genetics. *Front Immunol* **4**, 280.

Plotnikov EY, Morosanova MA, Pevzner IB, Zorova LD, Manskikh VN, Pulkova NV *et al.* (2013). Protective effect of mitochondria-targeted antioxidants in an acute bacterial infection. *Proc Natl Acad Sci U S A* **110**, E3100-3108.

Ranjan P, Anathy V, Burch PM, Weirather K, Lambeth JD, Heintz NH (2006). Redox-dependent expression of cyclin D1 and cell proliferation by Nox1 in mouse lung epithelial cells. *Antioxid Redox Signal* **8**, 1447-1459.

Reddy PH (2006). Mitochondrial oxidative damage in aging and Alzheimer's disease: implications for mitochondrially targeted antioxidant therapeutics. *J Biomed Biotechnol* **2006**, 31372.

Reifen R, Nissenkorn A, Matas Z, Bujanover Y (2004). 5-ASA and lycopene decrease the oxidative stress and inflammation induced by iron in rats with colitis. *Journal of Gastroenterology* **39**, 514-519.

Robinson KM, Janes MS, Pehar M, Monette JS, Ross MF, Hagen TM *et al.* (2006). Selective fluorescent imaging of superoxide in vivo using ethidium-based probes. *Proceedings of the National Academy of Sciences of the United States of America* **103**, 15038-15043.

Rodriguez-Rocha H, Garcia-Garcia A, Pickett C, Li S, Jones J, Chen H *et al.* (2013). Compartmentalized oxidative stress in dopaminergic cell death induced by pesticides and complex I inhibitors: distinct roles of superoxide anion and superoxide dismutases. *Free Radic Biol Med* **61**, 370-383.

Rubiolo JA, Mithieux G, Vega FV (2008). Resveratrol protects primary rat hepatocytes against oxidative stress damage: activation of the Nrf2 transcription factor and augmented activities of antioxidant enzymes. *European Journal of Pharmacology* **591**, 66-72.

Ryter SW, Alam J, Choi AM (2006). Heme oxygenase-1/carbon monoxide: from basic science to therapeutic applications. *Physiol Rev* **86**, 583-650.

Sawle P, Foresti R, Mann BE, Johnson TR, Green CJ, Motterlini R (2005). Carbon monoxide-releasing molecules (CO-RMs) attenuate the inflammatory response elicited by lipopolysaccharide in RAW264.7 murine macrophages. *Br J Pharmacol* **145**, 800-810.

Schilder YDC, Heiss EH, Schachner D, Ziegler J, Reznicek G, Sorescu D *et al.* (2009). NADPH oxidases 1 and 4 mediate cellular senescence induced by resveratrol in human endothelial cells. *Free Radical Biology and Medicine* **46**, 1598-1606.

Seidner DL, Lashner BA, Brzezinski A, Banks PL, Goldblum J, Fiocchi C *et al.* (2005). An oral supplement enriched with fish oil, soluble fiber, and antioxidants for corticosteroid sparing in ulcerative colitis: a randomized, controlled trial. *Clin Gastroenterol Hepatol* **3**, 358-369.

Sharma R & Tepas JJ, 3rd (2010). Microecology, intestinal epithelial barrier and necrotizing enterocolitis. *Pediatr Surg Int* **26**, 11-21.

Snoek SA, Dhawan S, van Bree SH, Cailotto C, van Diest SA, Duarte JM *et al.* (2012). Mast cells trigger epithelial barrier dysfunction, bacterial translocation and postoperative ileus in a mouse model. *Neurogastroenterol Motil* **24**, 172-184, e191.

Srisook K, Han SS, Choi HS, Li MH, Ueda H, Kim C *et al.* (2006). CO from enhanced HO activity or from CORM-2 inhibits both O-2(-) and NO production and downregulates HO-1 expression in LPS-stimulated macrophages. *Biochemical Pharmacology* **71**, 307-318.

St-Pierre J, Buckingham JA, Roebuck SJ, Brand MD (2002). Topology of superoxide production from different sites in the mitochondrial electron transport chain. *J Biol Chem* **277**, 44784-44790.

Szeto HH (2006). Cell-permeable, mitochondrial-targeted, peptide antioxidants. *AAPS J* **8**, E277-283.

Taille C, El-Benna J, Lanone S, Boczkowski J, Motterlini R (2005). Mitochondrial respiratory chain and NAD(P)H oxidase are targets for the antiproliferative effect of carbon monoxide in human airway smooth muscle. *J Biol Chem* **280**, 25350-25360.

Tiede LM, Cook EA, Morsey B, Fox HS (2011). Oxygen matters: tissue culture oxygen levels affect mitochondrial function and structure as well as responses to HIV viroproteins. *Cell Death Dis* **2**, e246.

Ungvari Z, Labinskyy N, Mukhopadhyay P, Pinto JT, Bagi Z, Ballabh P *et al.* (2009). Resveratrol attenuates mitochondrial oxidative stress in coronary arterial endothelial cells. *Am J Physiol Heart Circ Physiol* **297**, H1876-1881.

Vasina V, Broccoli M, Ursino MG, Canistro D, Valgimigli L, Soleti A *et al.* (2010). Non-peptidyl low molecular weight radical scavenger IAC attenuates DSS-induced colitis in rats. *World J Gastroenterol* **16**, 3642-3650.

Vidal K, Grosjean I, evillard JP, Gespach C, Kaiserlian D (1993). Immortalization of mouse intestinal epithelial cells by the SV40-large T gene. Phenotypic and immune characterization of the MODE-K cell line. *J Immunol Methods* **166**, 63-73.

Wang A, Keita AV, Phan V, McKay CM, Schoultz I, Lee J *et al.* (2014). Targeting mitochondria-derived reactive oxygen species to reduce epithelial barrier dysfunction and colitis. *Am J Pathol* **184**, 2516-2527.

Wang H, Yang YJ, Qian HY, Zhang Q, Xu H, Li JJ (2012). Resveratrol in cardiovascular disease: what is known from current research? *Heart Fail Rev* **17**, 437-448.

Wang X, Wang Y, Kim HP, Nakahira K, Ryter SW, Choi AM (2007). Carbon monoxide protects against hyperoxia-induced endothelial cell apoptosis by inhibiting reactive oxygen species formation. *J Biol Chem* **282**, 1718-1726.

Xu W, Liu L, Charles IG, Moncada S (2004). Nitric oxide induces coupling of mitochondrial signalling with the endoplasmic reticulum stress response. *Nat Cell Biol* **6**, 1129-1134.

Zhou R, Yazdi AS, Menu P, Tschopp J (2011). A role for mitochondria in NLRP3 inflammasome activation. *Nature* **469**, 221-225.

Zuckerbraun BS, Chin BY, Bilban M, d'Avila JC, Rao J, Billiar TR *et al.* (2007). Carbon monoxide signals via inhibition of cytochrome c oxidase and generation of mitochondrial reactive oxygen species. *FASEB J* **21**, 1099-1106.

Chapter VI

GENERAL DISCUSSION AND CONCLUSIONS

Chapter VI   General discussion and conclusions

Intestinal epithelial barrier dysfunction is involved in several acute GI inflammatory disease conditions such as POI and NEC. By intestinal epithelial barrier dysfunction, the gut can be a triggering factor in the progression of sepsis. The progression of sepsis to severe sepsis with MOF and to septic shock is related to an inflammatory/oxidative cascade involving production of inflammatory cytokines and ROS, I/R injury and mitochondrial dysfunction. Oxidative stress and inflammation can lead to disturbance of the intestinal epithelial barrier, accompanied by sepsis-induced ileus and allowing luminal bacterial content to penetrate in the body and aggravate the systemic inflammation. Several studies support that TNF-α, secreted by IECs themselves and by activated macrophages, is central to intestinal epithelial injury (Hausmann, 2010; Roulis *et al.*, 2011). Apart from its pro-inflammatory actions, there is also evidence that TNF-α increases oxidative stress in a variety of different cells (Shen & Pervaiz, 2006; Jin *et al.*, 2008). In a murine model of POI, a condition classically related to a muscular inflammatory reaction to the manipulation of the intestine, our laboratory has shown an increase in oxidative stress after intestinal manipulation occurring both in the mucosa and in the muscular layer, the increase in the mucosa in the early phase being more pronounced than in the muscular layer (De Backer *et al.*, 2009). This suggests that early epithelial oxidative stress, possibly inducing increased intestinal permeability, might contribute to the pathogenesis of POI. HO-1 is upregulated by oxidative stress and inflammatory mediators, and confers protection against oxidative stress and inflammation. This effect is mainly related to the products generated from the enzymatic activity of HO-1 i.e. biliverdin/bilirubin and still more CO. Several cytoprotective agents have been proposed to at least partially act via HO-1 induction; a frequently studied example between these agents is the polyphenol resveratrol. The aim of this thesis was therefore to establish an *in vitro* IEC model to assess the relation between TNF-α-induced oxidative stress and cell death, and to investigate the protective effects of HO-1-derived products, for CO using CO-RMs, and of resveratrol.

The murine IEC line MODE-K was used as it is a non-cancerous cell line derived from duodenum-jejunum of a normal mice bearing the characteristic features of normal

enterocytes (Vidal *et al.*, 1993). Additionally, data obtained with this cell line might be useful for targeted investigation in a murine *in vivo* model such as POI in subsequent projects. Preliminary experiments with TNF-α were done by testing its influence on cell viability. As in the case of many cell lines, including the GI ones (Beyaert *et al.*, 1993; Bhattacharya *et al.*, 2003; Pajak *et al.*, 2005; Minero *et al.*, 2013), we have found that TNF-α requires the combination with CHX to reduce cell viability in MODE-K cells. TNF-α is a pleiotropic cytokine that not only rapidly accelerates cell death, but also induces survival signals probably via activating the transcription factor NF-kB (Hayden & Ghosh, 2014). Addition of CHX suppresses the synthesis of short-lived cytoprotective proteins and blocks these protein synthesis-mediated survival effects. Therefore, the combination TNF-α/CHX was selected for further investigation.

Primary experiments involving treatment of MODE-K cells with 20 ng/ml TNF-α plus 25 µg/ml CHX, a classic cytotoxic apoptotic stimulus used in other IEC lines (Bhattacharya *et al.*, 2003; Naugler *et al.*, 2008; Greenspon *et al.*, 2009), decreased the cell viability to 10% of untreated cells. Moreover, this pronounced effect on cell viability was not influenced by any of the HO-1-related products. Treatment with 0.1 and 1 ng/ml TNF-α plus 10 µg/ml CHX decreased the cell viability to 50% and 20%, respectively. These results suggest that the MODE-K cell line is highly sensitive to the cytotoxic effects of TNF-α/CHX.

VI.1 Relation between TNF-α/CHX-induced oxidative stress and apoptotic cell death in MODE-K cells

Exposure of MODE-K cells to 0.1, 0.25, 0.5 and 1 ng/ml TNF-α plus 10 µg/ml CHX for 6 h decreased cell viability, increased caspase-3/7 activity and increased the number of apoptotic cells in a concentration-dependent manner. When incubated for 3 h, 0.1-1 ng/ml TNF-α plus 10 µg/ml CHX increased the intracellular ROS levels in a concentration-dependent manner as assessed with the most commonly used oxidant-sensitive fluorescent probe carboxy-H$_2$DCFDA. When investigating the time dependency of 1 ng/ml TNF-α plus 10 µg/ml, apoptosis started after 2 h of treatment with TNF-α/CHX corresponding with the onset of ROS production. The concentration-dependent induction of apoptosis by TNF-α/CHX at 6 h accompanied by a corresponding increase in caspase-3/7 activity suggests that a sequence of "*ROS production → caspase-3/7 activity → apoptosis*" might occur in MODE-K cells, similarly

as reported in rat IEC-6 cells (Jin *et al.*, 2008). The quantitation of apoptosis involved measurement of DNA hypoploidy after PI staining by flow cytometry while the quantitation of ROS production involved the measurement of fluorescence after carboxy-H_2DCFDA staining in wells of a microtiter plate reader, the fluorescence being contributed by both live and dead cells.

In the second project, intracellular ROS generation (by use of carboxy-H_2DCFDA) and cell death (by use of Sytox Red) were therefore measured simultaneously by flow cytometry, allowing selective measurement of ROS fluorescence in viable cells. This assay confirmed the concentration-dependent effect of 0.1, 0.25, 0.5 and 1 ng/ml TNF-α plus 10 μg/ml CHX on ROS production and cell death, as well as the time dependency for 1 ng/ml TNF-α plus 10 μg/ml CHX, with ROS increase and cell death both starting from 2 h of exposure. By use of annexin V and PI staining, it was illustrated again that TNF-α/CHX-induced cell death followed apoptotic kinetics, early apoptotic cells occurring from 2 h of exposure.

The onset of ROS production by TNF-α at 2 h in MODE-K cells is in apparent contrast with the rapid onset of ROS production at earlier time points observed in IECs from rat origin, i.e., 15 min in RIE-1 (Baregamian *et al.*, 2009) and 20 min in IEC-6 (Jin *et al.*, 2008) cells. Of note, MODE-K cells showed a significant increase in ROS production only when treated with a high concentration of exogenous H_2O_2 (0.5 mM) for a period of 40 min suggesting that MODE-K cells are highly resistant to the initial burst of oxidative stress by H_2O_2. These results suggest that the mouse IECs have the capacity to counteract the initial burst of oxidative stress up to a threshold time, beyond which the antioxidant defense can no longer be maintained and apoptotic cell death starts.

The significant reduction of both total ROS and cell death induced by TNF-α/CHX by a variety of antioxidants (like BHT, BHA, NAC and tiron) implies that ROS production contributes to TNF-α/CHX-induced cell death in MODE-K cells. The lipophilic antioxidants like BHT and BHA showed a more pronounced effect in decreasing TNF-α/CHX-induced ROS production and cell death as compared to the hydrophilic antioxidant NAC; these results suggest that the ROS produced might be predominantly released in the hydrophobic compartment of the mitochondrial membrane. This is corroborated by the lack of effect of the water-soluble mitochondria-targeted antioxidant Mito-TEMPO on both TNF-α/CHX-induced ROS production and cell death.

Each of the ROS species is a distinct chemical entity with its own reaction preferences, kinetics, rate and site of production, degradation and diffusion characteristics in biological systems. So, in biomedical research investigations, specifying the particular ROS thought to be responsible for the observed biological effect(s) with the direct measurement of a particular ROS would help in better understanding of the redox signaling under consideration (Murphy *et al.*, 2011). In this thesis, the abolishment of TNF-α/CHX-induced ROS production by iron chelators (DFO and SIH) without any effect on cell death excludes OH$^\bullet$ as the specific ROS causing TNF-α/CHX-induced cell death of MODE-K cells. The concentration-dependent increase in ROS production by TNF-α at 3 h was not paralleled by the decrease in the antioxidant GSH level; the latter occurred only at 6 h. Reduced GSH in mitochondria is the only antioxidant defense mechanism available to neutralize peroxides generated from the ETC through the GSH redox pool (Fernandez-Checa *et al.*, 1998). The decrease in GSH levels occurring only at 6 h suggests that ROS production in the form of H_2O_2 only starts after 3 h of TNF-α/CHX exposure, with other forms of ROS in particular $O_2^{\bullet-}$ being involved in the earlier apoptosis observed already from 2 h of exposure to TNF-α/CHX in MODE-K cells.

VI.2   Sources of TNF-α/CHX-induced oxidative stress in MODE-K cells

Activation of NOX, dysregulation of mitochondrial oxidative phosphorylation, the interaction xanthine/xanthine oxidase and uncoupled eNOS are the endogenous sources of ROS production in eukaryotic cells. A contribution of eNOS to TNF-α/CHX-induced oxidative stress in MODE-K cells can be excluded as it is not expressed in IECs (Chen *et al.*, 2002; Konig *et al.*, 2002). The lack of effect of allopurinol on both the TNF-α/CHX-induced ROS production and cell death excludes xanthine oxidase as a possible source of ROS production in MODE-K cells. NOX1 and DUOX1/2 are the three NOX isozymes present in the mouse small intestinal epithelium (Bedard & Krause, 2007; Jones *et al.*, 2013). During the screening study, the classical inhibitors of NOX (apocynin and DPI) showed differential effects on the TNF-α/CHX-induced decrease in cell viability. DPI reduced TNF-α-induced cytotoxicity at 0.1-0.5 ng but not at 1 ng TNF-α/CHX, while apocynin failed to influence the decrease in cell viability at all tested concentrations of TNF-α. The differential effect of apocynin and DPI does not exclude the involvement of NOX during TNF-α/CHX-induced ROS production in

MODE-K cells as apocynin was not effective in inhibiting NOX activity in certain cell types (Aldieri *et al.*, 2008). In the flow cytometric study, DPI was again found to not influence cell death (and also ROS production) by 1 ng TNF-α/CHX, but the decrease in the level of TNF-α/CHX-induced ROS production by the recently developed and well-validated pan-NOX inhibitor VAS-2870 indicates that NOX enzymes also contribute to ROS production by TNF-α in MODE-K cells. This is further corroborated by a relatively similar effect of NSC23766 to that of VAS-2870, implying that Rac1 mediated activation of NOX isozymes partly contributes to TNF-α/CHX-induced ROS production in MODE-K cells. This is in agreement with a study in rat IEC-6 cells (Jin *et al.*, 2008).

Mitochondria have been implicated as the principal source of ROS generation required for TNF-α-induced cytotoxicity of a variety of cells like mouse fibroblasts (Schulze-Osthoff *et al.*, 1993; Kamata *et al.*, 2005), human cervical adenocarcinoma cells (Kim *et al.*, 2010), macrophages (Roca & Ramakrishnan, 2013), neonatal rat ventricular myocytes (Suematsu *et al.*, 2003), liver cells (Kastl *et al.*, 2014), endothelial cells (Deshpande *et al.*, 2000; Corda *et al.*, 2001), cardiomyocytes (Roberge *et al.*, 2014) and IECs (Jin *et al.*, 2008; Baregamian *et al.*, 2009). A growing body of evidence suggests that ROS are physiologically generated at the level of complexes I and III of the mitochondrial respiratory chain. The involvement of different complexes of the respiratory chain in ROS-dependent signaling is cell type-dependent and stimulus-specific (Liu & Schubert, 2009; Kastl *et al.*, 2014). In the current study, the effects of the various inhibitors of the mitochondrial ETC complexes revealed the complex nature of ROS production in living MODE-K cells. The pronounced decrease in TNF-α/CHX-induced ROS production and cell death by amytal and TTFA suggests that the quinone binding sites of complexes I and II might be major mitochondrial contributors to ROS production during TNF-α/CHX-induced cell death. Interestingly, complex II was reported to contribute to hypoxia-induced ROS generation (Paddenberg *et al.*, 2003) and oxidative stress with associated tissue damage (Ralph *et al.*, 2011). Since treatment of MODE-K cells with TNF-α/CHX quickly induces decreased mitochondrial oxygen consumption, a similar mechanism as occurring during hypoxia could develop and contribution of complex II-induced ROS might come into play. Reverse electron transport from complex II to complex I is proposed to be a major pathway for mitochondrial ROS production during conditions involving oxidative stress (Drose, 2013). Correspondingly, in MODE-K cells, treatment of TTFA abolished TNF-α/CHX-induced ROS production suggesting

that the blockade of complex II at the Qp site by TTFA leads to a reduction of complex I related ROS production, generated by reverse electron transfer from complex II to complex I. Additionally, the partial reduction of TNF-α/CHX-induced ROS and cell death by myxothiazole indicates that the Qo site of complex III is also involved in TNF-α-induced ROS production. The partial reduction in TNF-α/CHX-induced ROS and cell death levels by cyanide and oligomycin implies that complex IV and V also participate in ROS production by TNF-α/CHX in MODE-K cells. As complex IV and V are not direct ROS production sites, the observed effect might probably be related to an indirect regulatory influence of complex IV and V on ROS production from the mitochondria. Similarly, the partial reduction of TNF-α/CHX-induced ROS and cell death levels by the proton ionophores CCCP and FCCP underlines the significance of the "uncoupling to survive" theory where "mild mitochondrial uncoupling" has been proposed to induce a protective antioxidant defense mechanism preventing cell death (Skulachev, 1996; Brand, 2000; Mailloux & Harper, 2011). In contrast to other mitochondrial complex inhibitors, inhibition of the Qi site of complex III with antimycin failed to inhibit TNF-α/CHX-induced ROS generation and cell death, excluding that $O_2^{\bullet-}$ released from the Qi site of complex III towards the matrix contributes to TNF-α/CHX-induced ROS production in MODE-K cells.

To gain further insight, we have assessed the contribution of mitochondrial ROS with MitoSOX Red to directly measure the primary species of intra-mitochondrial ROS, $O_2^{\bullet-}$. Indeed, TNF-α/CHX increased the levels of mitochondrial $O_2^{\bullet-}$ anion in MODE-K cells in a concentration-dependent manner. The onset of mitochondrial $O_2^{\bullet-}$ production also occurs at 2 h after exposure to TNF-α/CHX, the same time at which apoptotic cell death starts. This is in agreement with the involvement of mitochondrial ROS during TNF-α-induced ROS production in rat IECs reported previously (Jin *et al.*, 2008; Baregamian *et al.*, 2009). The contribution of complexes I and II to TNF-α/CHX-induced mitochondrial ROS production was confirmed by the observation that amytal and TTFA also decreased TNF-α/CHX-induced mitochondrial $O_2^{\bullet-}$ production.

Mitochondria play a critical role in cell survival as they are the main cellular sites controlling metabolism, cell cycle and apoptosis. Moreover, generation of ROS during apoptosis leads to mitochondrial damage associated with decreased Ψm. Treatment of MODE-K cells with TNF-α/CHX induced an increase in cells with depolarized mitochondria and increased the amount of respiration-interrupted mitochondria in a concentration- and

230

time-dependent manner. Additionally, our findings that treatment of MODE-K cells with TNF-α/CHX causes a rapid decrease in cellular oxygen consumption creating a hypoxic state (within 5 min of addition) and a decrease in Ψ_m (occurring within 60 min) and mitochondrial dysregulation (starting at 60 min) at earlier time points than ROS production and cell death (starting at 2 h), suggests that there could be a sequential link between these events.

Taken together, NOX and mitochondria are the major sources of TNF-α/CHX-induced oxidative stress in MODE-K cells.

VI.3 Influence of HO-1-derived products and resveratrol on TNF-α-induced oxidative stress and apoptotic cell death

HO-1 serves as a cytoprotective gene by virtue of its potent antioxidant, anti-apoptotic and anti-inflammatory properties, all attributed to the catalytic by-products of heme metabolism, namely, CO, biliverdin/bilirubin and iron/ferritin. Although HO-1 does not have a direct antioxidant enzymatic function, HO-1 and its product CO are believed to have indirect cytoprotective effects against oxidative stress (Vile *et al.*, 1994; Otterbein & Choi, 2000). However, studies to understand HO-1's potential in treating ROS-induced GI diseases are still in their infancy (Bhattacharyya *et al.*, 2014). Accumulating evidence indicates that CO mediates many of the biological functions of HO-1. The use of water soluble CO-RMs, CORM-3 and CORM-A1, with different CO-release kinetics that enable delivery of CO in a controllable manner could be of potential clinical utility for treatment of acute GI disorders like POI (De Backer *et al.*, 2009). So, the influence of the HO-1 related protective compounds (CORM-A1, CORM-3, biliverdin and bilirubin) was tested on the effects of the different concentrations of TNF-α plus CHX, on cell viability, oxidative stress (ROS and GSH levels) and apoptosis (caspase-3/7 activity and DNA hypoploidy). CORM-A1 seems to be the most promising protective agent among the tested compounds. The highest non-cytotoxic concentration of CORM-3 and CORM-A1 reduced the decrease of cell viability by TNF-α at all tested concentrations (0.1-1 ng TNF-α), while 100 µM bilirubin and 1 µM biliverdin had no influence. However, a lower concentration of 1 µM bilirubin partially prevented the decrease in cell viability by 0.1 and 0.25 ng/ml TNF-α plus CHX (10 µg/ml). Bilirubin (1 µM) partially reduced ROS production and caspase-3/7 activity by 1 ng/ml TNF-α plus 10 µg/ml CHX, but failed to prevent TNF-α/CHX-induced apoptosis. A similar effect of bilirubin with only mild

reduction in TNF-α/CHX-induced apoptosis despite having a pronounced effect on caspase-3 expression was already reported in cerebral vascular endothelial cells (Basuroy *et al.*, 2006). These results suggest that a caspase-independent pathway of apoptosis might also be involved during TNF-α/CHX-induced cell death of MODE-K cells. Correspondingly, caspase-independent apoptosis signaling of TNF-α has been reported in many different cell types including colonic IECs (Jones *et al.*, 2000; Wilson & Browning, 2002; Chen *et al.*, 2005; Alvarez *et al.*, 2011).

Low levels of HO-1 are expressed in the normal GI tract (Coeffier *et al.*, 2002; Barton *et al.*, 2003). In the GI tract, expression of HO-1 is increased in an experimental model of POI with surgical intestinal manipulation (De Backer *et al.*, 2009) and models of sepsis by an i.p. injection of LPS (Otani *et al.*, 2000), implying induction of HO-1 during stress conditions. However, in MODE-K cells, the baseline HO-1 protein level was decreased by treatment with TNF-α/CHX; this could at least partially be due to the presence of the protein synthesis inhibitor CHX. None of the previous investigations, where combination of TNF-α with CHX was used to induce cell death, investigated HO-1 expression (Beyaert *et al.*, 1993; Bhattacharya *et al.*, 2003; Pajak *et al.*, 2005; Minero *et al.*, 2013). In studies where TNF-α was used alone as an inflammatory trigger and not an apoptotic trigger, opposite effects have been obtained. In human chondrocytes (Fernandez *et al.*, 2003) and peripheral blood mononuclear cells (Kirino *et al.*, 2007), the expression of HO-1 protein was also decreased by TNF-α, similar to what we observed in our study. However, in human endothelial and monocytic cell lines, such as U937 and THP-1 (Muraosa & Shibahara, 1993; Terry *et al.*, 1998; Terry *et al.*, 1999; Udono-Fujimori *et al.*, 2004; Liang *et al.*, 2013), upregulation of HO-1 expression by TNF-α was reported. The reason for this difference is not clear.

Resveratrol showed the highest degree of cytoprotection against all tested concentrations of TNF-α/CHX. Resveratrol fully abolished TNF-α/CHX-induced ROS production and caspase-3/7 activity while only halving of TNF-α/CHX-induced apoptosis; these results further corroborate that TNF-α/CHX-induced apoptosis of MODE-K cells can occur via a ROS- and caspase-independent pathway. Apoptosis inducing factor (AIF) is a mammalian, caspase-independent death effector which, upon apoptosis induction, translocates from the mitochondria to the nucleus, causing chromatin condensation and DNA fragmentation (Cregan *et al.*, 2004). Treatment of rat RIE-6 cells with TNF-α was

reported to increase AIF expression (Baregamian *et al.*, 2009); a similar involvement of caspase-independent apoptotic induction by TNF-α might also exist in MODE-K cells.

Given the contribution of ROS production in TNF-α/CHX-induced apoptosis in MODE-K cells, with CORM-A1 and resveratrol reducing both these effects, the antioxidant mechanism of these two agents was subsequently studied.

VI.4 Mechanism of action of CORM-A1 during TNF-α/CHX-induced oxidative stress in MODE-K cells

Treatment of MODE-K cells with 100 µM CORM-A1 partially reduced TNF-α/CHX-induced cell death. The heme-containing proteins in mitochondria (cytochromes) and the NOX enzymes are the major cellular targets of CO due to its higher affinity for heme (Foresti & Motterlini, 2010). CO can partially and/or reversely inhibit cytochrome c oxidase (complex IV), leading to electron accumulation at complex III level, which facilitates $O_2^{\bullet-}$ generation. Such an induction of a mild transient burst of mitochondrial ROS by CO resulting in adaptive signaling ("ROS-induced preconditioning") towards subsequent oxidative insults is one of the most unified mechanisms proposed for the cytoprotective effect of CO (Queiroga *et al.*, 2012). However, the lack of induction of mitochondrial $O_2^{\bullet-}$ during the initial hours of incubation of MODE-K cells with 100 µM CORM-A1 implies that the antioxidant effect of CORM-A1 does not involve preconditioning through induction of a mitochondrial ROS burst. Still, there has been speculated that the cytoprotective effects of CO can be independent of mitochondrial ROS generation, but could be attributed to partial or temporal inhibition of mitochondrial respiration (Almeida *et al.*, 2015). Correspondingly, 100 µM CORM-A1 decreased cellular OCR in MODE-K cells with partial recuperation from this decrease from 90 min after its administration. This observation is in agreement with a finding in HEK293 cells showing reduced cellular respiration upon exposure to exogenous CO, which was suggested to contribute to cytoprotective effects of CO (D'Amico *et al.*, 2006). Moreover, one has recently speculated that CO can alter O_2 sensing and exert a "pseudo-hypoxic" state, providing a powerful cellular impact towards regeneration and increasing the cellular energy supply, thus leading to improved survival in the presence of cell stress and injury (Schallner & Otterbein, 2015). A similar effect on mitochondrial respiration might also explain the

partial recovery by CORM-A1 of the decrease in Ψ_m and the increase in mitochondrial dysfunction by TNF-α/CHX in MODE-K cells.

CORM-A1 partially reduced TNF-α/CHX-induced and H_2O_2-induced intracellular total ROS illustrating its antioxidant potential. Mitochondrial complexes I and II are identified to be the major mitochondrial ROS production sites during TNF-α/CHX-induced cell death in MODE-K cells. CORM-A1 did not affect the mitochondrial $O_2^{\bullet-}$ production induced by rotenone, the complex I inhibitor, which could be attributed to the fact that rotenone-induced mitochondrial ROS are released into the mitochondrial matrix (Chen *et al.*, 2003; Rodriguez-Rocha *et al.*, 2013). Still, CORM-A1 could partially reduce antimycin-A-induced mitochondrial $O_2^{\bullet-}$, which are reported to either fully (St-Pierre *et al.*, 2002) or at least partially (Han *et al.*, 2003) be released into the mitochondrial intermembrane space. However, CORM-A1 failed to influence TNF-α/CHX-induced mitochondrial ROS or $O_2^{\bullet-}$ level, excluding that modulation of mitochondrial ROS contributes to its partial protection from TNF-α/CHX-induced cytotoxicity. Inhibition of NOX is an additional and intriguing mechanism by which CO could modulate redox signaling (Boczkowski *et al.*, 2006). Several studies indicate that CO may directly inhibit NOX activity, probably by binding to the heme-containing gp91phox/Nox2 subunit, and thus can reduce ROS generation (Taille *et al.*, 2005; Matsumoto *et al.*, 2006; Nakahira *et al.*, 2006; Wang *et al.*, 2007). The partial reduction of TNF-α/CHX-induced intracellular total ROS by CORM-A1 is thus probably due to inhibition of NOX-derived ROS. Moreover, the full use of CORM-A1-derived CO in the cytoplasm to counteract NOX-derived ROS upon exposure to TNF-α might be the plausible reason for the lack of any effect of CORM-A1 against TNF-α/CHX-induced mitochondrial ROS production. As NOX enzymes are not involved in the ROS production by antimycin-A, sufficient CO derived from CORM-A1 might have reached the mitochondrial intermembrane space upon exposure of MODE-K cells to antimycin-A; this might explain why CORM-A1 could partially reduce antimycin-A-induced mitochondrial $O_2^{\bullet-}$.

Exogenous CO in the form of CORMs was reported to exert its protective effects through induction of HO-1 in many cell types like murine macrophages (Sawle *et al.*, 2005), mouse kidney tissue (Vera *et al.*, 2005), human and rat hepatocytes (Lee *et al.*, 2006), and rat endothelial cells (Rodella *et al.*, 2006). Moreover, the induction of HO-1 can provide a positive feedback loop (CO→ induction of HO-1→ more CO→ further induction of HO-1) resulting in the formation of biliverdin/bilirubin exerting ROS scavenging properties (Rodella

et al., 2006). However, in MODE-K cells, treatment with CORM-A1 did not induce HO-1 expression excluding the possibility that endogenous HO-1 induction contributes to the anti-apoptotic effect of CORM-A1 in MODE-K cells.

VI.5   Mechanism of action of resveratrol during TNF-α/CHX-induced oxidative stress in MODE-K cells

While resveratrol interacts with many important enzymes and receptor signaling pathways, the antioxidant properties of resveratrol are of particular interest because of the fundamental role that oxidative stress plays in numerous pathological conditions. In contrast to CORM-A1, the antioxidant potential of resveratrol in IECs has been previously identified in two studies but the mechanism remains unknown (Elamin *et al.*, 2013; Serra *et al.*, 2014). In the primary screening experiments using the fluorescence plate reader, resveratrol *per se* did not influence the basal ROS level while it abolished the TNF-α/CHX-induced increase in ROS production when measured after 3 h of apoptotic stimulus. However, in the experiments using the flow cytometer, resveratrol *per se* increased total ROS with only partial reduction of TNF-α/CHX-induced total ROS production measured after 6 h of apoptotic stimulus. This discrepancy could be attributed to the differences in technology, time point of measurement, contribution of dead cells to the ROS signal along with the type of ROS contributing to the fluorescence, and experimental steps involved (washing of the cells with HBSS before carboxy-H_2DCFDA loading in the cell culture plate for the plate reader measurement versus co-incubation of the dye with the cells without washing the cell culture plate in the flow cytometric analysis). Based on the flow cytometric measurements, resveratrol abolished TNF-α/CHX-induced mitochondrial ROS/$O_2^{\bullet-}$ production with a pronounced reduction of TNF-α/CHX-induced cell death; this suggests that inhibition of mitochondria-derived ROS contributes to the cytoprotective/anti-apoptotic effects of resveratrol in MODE-K cells. Additionally, resveratrol effectively prevented TNF-α/CHX-induced mitochondrial dysfunction and drop in Ψ_m in MODE-K cells. Moreover, resveratrol abolished both rotenone- and antimycin-A-induced ROS showing the potential of resveratrol in mitigating both complex I and complex III-derived ROS. All these effects of resveratrol with regard to the mitochondrial parameters could be attributed to the lipophilic nature of resveratrol enabling it to traverse through the mitochondrial intermembrane space and

reach the matrix, allowing scavenging of $O_2^{\bullet-}$ produced inside the matrix, immediately after its generation. Indeed, resveratrol was previously shown to suppress the formation of $O_2^{\bullet-}$ produced by murine resident peritoneal macrophages stimulated by LPS or phorbol esters (Martinez & Moreno, 2000). Even though resveratrol was known for its $OH^\bullet$ scavenging potential, it seems unlikely that resveratrol could act through this mechanism as we have previously identified that $OH^\bullet$ is not the ROS entity contributing to TNF-α/CHX-induced cell death in MODE-K cells.

With regard to the antioxidant defense, resveratrol can decrease oxidative stress through induction of MnSOD and HO-1 (Ungvari *et al.*, 2009; Ryan *et al.*, 2010; Kairisalo *et al.*, 2011). Resveratrol *per se* increased basal HO-1 protein expression in MODE-K cells, but it did not prevent the decrease by TNF-α/CHX, excluding HO-1 induction as the mechanism of action for its protective effect against TNF-α/CHX.

In recent years, it became evident that ROS are not only byproducts of cellular metabolism but also can act as second messengers to activate signaling pathways and hence lead to alterations in gene expression to regulate cellular functions. Contrary to decreasing mitochondrial ROS, resveratrol increased intracellular total ROS production in MODE-K cells, but still could decrease TNF-α/CHX-induced cell death. NOX1 seems to be the sole ROS production site of resveratrol in MODE-K cells as demonstrated by the abolishment of ROS by pan-NOX and Rac1 inhibitors. NOX-derived ROS production has been identified to exert stress-induced preconditioning with induction of antioxidant enzyme levels (Bell *et al.*, 2005; Jiang *et al.*, 2011; Frasier *et al.*, 2013); the increase in the NOX-derived ROS levels by pretreatment with resveratrol might have induced a similar "preconditioning" effect in MODE-K cells to protect themselves from the successive cell death trigger (TNF-α/CHX).

Interestingly, the mitochondrial complex I and II inhibitors showed a more pronounced effect in decreasing total cellular ROS and cell death as compared to the moderate effect of the NOX inhibitor VAS-2870; this might suggest that early ROS signaling from mitochondria can induce a later phase of NOX-derived ROS. Notably, resveratrol showed a pronounced cytoprotective effect against TNF-α/CHX concomitant with the abolishment of mitochondrial ROS/$O_2^{\bullet-}$, while the inhibitory effect of CORM-A1 on NOX only led to partial reduction of TNF-α/CHX-induced cell death. These results together reinforce the possibility of sequential communication from mitochondria to NOX for ROS production in MODE-K cells.

A schematic overview of the intracellular sources of ROS production induced by TNF-α along with the sites of ROS production influenced by CORM-A1 and resveratrol in MODE-K cells is shown in Fig. VI.1.
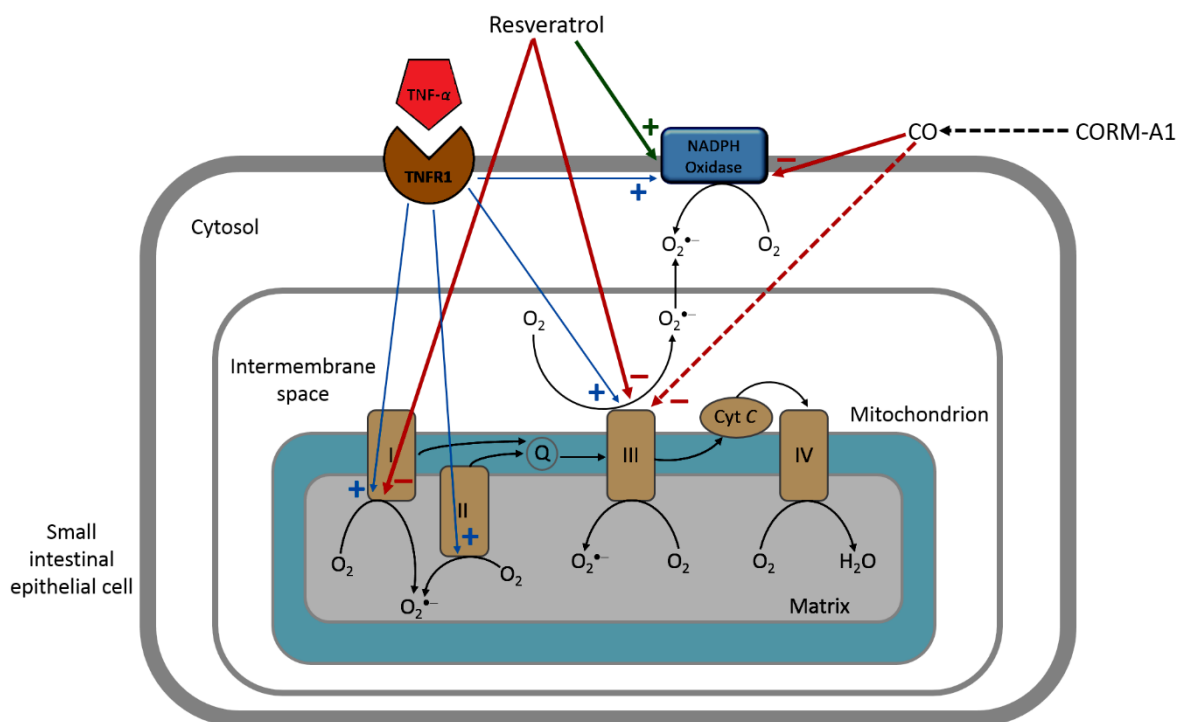

Fig. VI.1 Schematic overview of the intracellular sources of ROS production induced by TNF-α along with the sites of ROS production influenced by CORM-A1 and resveratrol in MODE-K cells. Binding of TNF-α to its receptor TNFR1 results in formation of $O_2^{\bullet-}$ from mitochondrial complexes I, II and III, and NOX. CORM-A1 reduces TNF-α-induced total ROS production through inhibition of NOX with partial reduction of antimycin-A-induced mitochondrial $O_2^{\bullet-}$ (influence of antimycin-A is not shown for clarity). Resveratrol *per se* induced total ROS production, mediated through NOX activation. Resveratrol abolished TNF-α-induced mitochondrial $O_2^{\bullet-}$ production. Resveratrol also abolished mitochondrial $O_2^{\bullet-}$ production from complexes I and III induced by rotenone and antimycin-A, respectively (not shown for clarity).

VI.6   Future perspectives

Although primary IECs can be prepared with high purity from intestinal tissue, their short survival in culture precludes their use in functional *ex vivo* studies (Bjerknes & Cheng, 1981; Cano-Gauci *et al.*, 1993; Lotz *et al.*, 2006). MODE-K is the most widely used mouse small IEC line in several research investigations in the literature to understand small intestinal mucosal pathophysiology, however, this cell line still suffers with the limitation that it does not develop measurable transepithelial resistance when grown in cultures (Iliev *et al.*, 2009). So, our findings with TNF-α toxicity and ROS generation in MODE-K cells should be ideally reassessed in another cell line like IEC-1, a recently established murine IEC line

bearing many functional features of the intestinal epithelium including the generation of increasing transepithelial electrical resistance during *in vitro* culture (Schwerk *et al.*, 2013). Following this, the effect of TNF-α/CHX in increasing the epithelial barrier permeability should be evaluated in IEC-1 cells both in the absence and presence of specific ROS inhibitors to strengthen the hypothesis that TNF-α-induced ROS production contributes to epithelial barrier dysfunction. The participation of mitochondrial ROS in TNF-α-induced cell death can be confirmed at the genetic level by using mtDNA-depleted ρ° cells generated from IEC-1 cells. In the present study, the involvement of mitochondrial complex I, the primary site of electron entry in the ETC, in TNF-α-induced mitochondrial ROS generation, has been identified based on pharmacological intervention. This finding should be investigated by a genetic approach with silencing of NADH dehydrogenase [ubiquinone] 1 beta subcomplex subunit 8 (NDUFB8), a mitochondrial complex I subunit, using siRNA; this should prevent the induction of ROS from mitochondria upon TNF-α exposure in MODE-K cells. The involvement of NOX in TNF-α-induced ROS production can also be assessed by performing studies with siRNA for NOX1 along with measurement of NOX activity. The ROS assessments after each of the above silencing experiments also would help to understand the proposed crosstalk between mitochondria and NOX. The mechanism of action of CORM-A1 through inhibition of NOX could be reevaluated in NOX1 silenced cells. Since induction of antioxidant enzymes is proposed to be a possible mechanism of action for the cytoprotective effect of resveratrol, gene/protein expression studies of MnSOD will further strengthen the role of antioxidant defense mechanism by resveratrol.

VI.7   General conclusion

In this thesis, a murine *in vitro* model of TNF-α-induced IEC death was established using MODE-K cells and the involvement of oxidative stress during cell death signaling by TNF-α was identified. The data indicate that MODE-K cells are highly sensitive to TNF-α-induced apoptosis involving caspase-3/7 activation when co-treated with CHX. Moreover, TNF-α/CHX-induced apoptosis of MODE-K cells corresponds with the production of ROS. Mitochondria and NOX are the two major sources of ROS overproduction during TNF-α/CHX-induced cell death in MODE-K cells with $O_2^{\bullet-}$ being the predominant ROS entity. From the results with mitochondrial complex inhibitors, the quinone-binding sites of mitochondrial

ETC complexes I (site I_Q) and II (site Q_P) seem to be the major ROS production sites of mitochondria. Resveratrol shows pronounced protection against TNF-α/CHX-induced cell death involving the abolishment of mitochondrial ROS/$O_2^{\bullet-}$; the moderate cytoprotection observed with CORM-A1 is NOX-dependent. This suggests a possible crosstalk of ROS signaling from mitochondria to NOX in MODE-K cells. Targeting ROS generation with agents like CORM-A1 and resveratrol interfering with particular intracellular ROS production sites should be further investigated for the treatment of acute GI inflammatory conditions.

VI.8 References

Aldieri E, Riganti C, Polimeni M, Gazzano E, Lussiana C, Campia I *et al.* (2008). Classical inhibitors of NOX NAD(P)H oxidases are not specific. *Curr Drug Metab* **9**, 686-696.

Almeida AS, Figueiredo-Pereira C, Vieira HL (2015). Carbon monoxide and mitochondria-modulation of cell metabolism, redox response and cell death. *Front Physiol* **6**, 33.

Alvarez S, Blanco A, Fresno M, Munoz-Fernandez MA (2011). TNF-alpha contributes to caspase-3 independent apoptosis in neuroblastoma cells: role of NFAT. *Plos One* **6**, e16100.

Baregamian N, Song J, Bailey CE, Papaconstantinou J, Evers BM, Chung DH (2009). Tumor necrosis factor-alpha and apoptosis signal-regulating kinase 1 control reactive oxygen species release, mitochondrial autophagy, and c-Jun N-terminal kinase/p38 phosphorylation during necrotizing enterocolitis. *Oxidative Medicine and Cellular Longevity* **2**, 297-306.

Barton SG, Rampton DS, Winrow VR, Domizio P, Feakins RM (2003). Expression of heat shock protein 32 (hemoxygenase-1) in the normal and inflamed human stomach and colon: an immunohistochemical study. *Cell Stress Chaperones* **8**, 329-334.

Basuroy S, Bhattacharya S, Tcheranova D, Qu Y, Regan RF, Leffler CW *et al.* (2006). HO-2 provides endogenous protection against oxidative stress and apoptosis caused by TNF-alpha in cerebral vascular endothelial cells. *Am J Physiol Cell Physiol* **291**, C897-908.

Bedard K & Krause KH (2007). The NOX family of ROS-generating NADPH oxidases: physiology and pathophysiology. *Physiol Rev* **87**, 245-313.

Bell RM, Cave AC, Johar S, Hearse DJ, Shah AM, Shattock MJ (2005). Pivotal role of NOX-2-containing NADPH oxidase in early ischemic preconditioning. *Faseb Journal* **19**, 2037-2039.

Beyaert R, Vanhaesebroeck B, Heyninck K, Boone E, De Valck D, Schulze-Osthoff K *et al.* (1993). Sensitization of tumor cells to tumor necrosis factor action by the protein kinase inhibitor staurosporine. *Cancer Res* **53**, 2623-2630.

Bhattacharya S, Ray RM, Viar MJ, Johnson LR (2003). Polyamines are required for activation of c-Jun NH2-terminal kinase and apoptosis in response to TNF-alpha in IEC-6 cells. *Am J Physiol Gastrointest Liver Physiol* **285**, G980-991.

Bhattacharyya A, Chattopadhyay R, Mitra S, Crowe SE (2014). Oxidative stress: an essential factor in the pathogenesis of gastrointestinal mucosal diseases. *Physiol Rev* **94**, 329-354.

Bjerknes M & Cheng H (1981). Methods for the isolation of intact epithelium from the mouse intestine. *Anatomical Record* **199**, 565-574.

Boczkowski J, Poderoso JJ, Motterlini R (2006). CO-metal interaction: Vital signaling from a lethal gas. *Trends Biochem Sci* **31**, 614-621.

Brand MD (2000). Uncoupling to survive? The role of mitochondrial inefficiency in ageing. *Exp Gerontol* **35**, 811-820.

Cano-Gauci DF, Lualdi JC, Ouellette AJ, Brady G, Iscove NN, Buick RN (1993). In vitro cDNA amplification from individual intestinal crypts: a novel approach to the study of differential gene expression along the crypt-villus axis. *Exp Cell Res* **208**, 344-349.

Chen Q, Vazquez EJ, Moghaddas S, Hoppel CL, Lesnefsky EJ (2003). Production of reactive oxygen species by mitochondria: central role of complex III. *J Biol Chem* **278**, 36027-36031.

Chen W, Li N, Chen T, Han Y, Li C, Wang Y *et al.* (2005). The lysosome-associated apoptosis-inducing protein containing the pleckstrin homology (PH) and FYVE domains (LAPF), representative of a novel family of PH and FYVE domain-containing proteins, induces caspase-independent apoptosis via the lysosomal-mitochondrial pathway. *J Biol Chem* **280**, 40985-40995.

Chen YM, Qian ZM, Zhang J, Chang YZ, Duan XL (2002). Distribution of constitutive nitric oxide synthase in the jejunum of adult rat. *World J Gastroenterol* **8**, 537-539.

Coeffier M, Le Pessot F, Leplingard A, Marion R, Lerebours E, Ducrotte P *et al.* (2002). Acute enteral glutamine infusion enhances heme oxygenase-1 expression in human duodenal mucosa. *J Nutr* **132**, 2570-2573.

Corda S, Laplace C, Vicaut E, Duranteau J (2001). Rapid reactive oxygen species production by mitochondria in endothelial cells exposed to tumor necrosis factor-alpha is mediated by ceramide. *Am J Respir Cell Mol Biol* **24**, 762-768.

Cregan SP, Dawson VL, Slack RS (2004). Role of AIF in caspase-dependent and caspase-independent cell death. *Oncogene* **23**, 2785-2796.

D'Amico G, Lam F, Hagen T, Moncada S (2006). Inhibition of cellular respiration by endogenously produced carbon monoxide. *J Cell Sci* **119**, 2291-2298.

De Backer O, Elinck E, Blanckaert B, Leybaert L, Motterlini R, Lefebvre RA (2009). Water-soluble CO-releasing molecules reduce the development of postoperative ileus via modulation of MAPK/HO-1 signalling and reduction of oxidative stress. *Gut* **58**, 347-356.

Deshpande SS, Angkeow P, Huang J, Ozaki M, Irani K (2000). Rac1 inhibits TNF-alpha-induced endothelial cell apoptosis: dual regulation by reactive oxygen species. *Faseb Journal* **14**, 1705-1714.

Drose S (2013). Differential effects of complex II on mitochondrial ROS production and their relation to cardioprotective pre- and postconditioning. *Biochim Biophys Acta* **1827**, 578-587.

Elamin E, Masclee A, Juuti-Uusitalo K, van Ijzendoorn S, Troost F, Pieters HJ *et al.* (2013). Fatty acid ethyl esters induce intestinal epithelial barrier dysfunction via a reactive oxygen species-dependent mechanism in a three-dimensional cell culture model. *Plos One* **8**, e58561.

Fernandez-Checa JC, Garcia-Ruiz C, Colell A, Morales A, Mari M, Miranda M *et al.* (1998). Oxidative stress: role of mitochondria and protection by glutathione. *Biofactors* **8**, 7-11.

Fernandez P, Guillen MI, Gomar F, Alcaraz MJ (2003). Expression of heme oxygenase-1 and regulation by cytokines in human osteoarthritic chondrocytes. *Biochem Pharmacol* **66**, 2049-2052.

Foresti R & Motterlini R (2010). Interaction of carbon monoxide with transition metals: evolutionary insights into drug target discovery. *Curr Drug Targets* **11**, 1595-1604.

Frasier CR, Moukdar F, Patel HD, Sloan RC, Stewart LM, Alleman RJ *et al.* (2013). Redox-dependent increases in glutathione reductase and exercise preconditioning: role of NADPH oxidase and mitochondria. *Cardiovascular Research* **98**, 47-55.

Greenspon J, Li RY, Xiao L, Rao JN, Marasa BS, Strauch ED *et al.* (2009). Sphingosine-1-Phosphate Protects Intestinal Epithelial Cells from Apoptosis Through the Akt Signaling Pathway. *Digestive Diseases and Sciences* **54**, 499-510.

Han D, Canali R, Rettori D, Kaplowitz N (2003). Effect of glutathione depletion on sites and topology of superoxide and hydrogen peroxide production in mitochondria. *Mol Pharmacol* **64**, 1136-1144.

Hausmann M (2010). How bacteria-induced apoptosis of intestinal epithelial cells contributes to mucosal inflammation. *Int J Inflam.*, 574568.

Hayden MS & Ghosh S (2014). Regulation of NF-kappa B by TNF family cytokines. *Semin Immunol* **26**, 253-266.

Iliev ID, Mileti E, Matteoli G, Chieppa M, Rescigno M (2009). Intestinal epithelial cells promote colitis-protective regulatory T-cell differentiation through dendritic cell conditioning. *Mucosal Immunol* **2**, 340-350.

Jiang F, Zhang Y, Dusting GJ (2011). NADPH oxidase-mediated redox signaling: roles in cellular stress response, stress tolerance, and tissue repair. *Pharmacological Reviews* **63**, 218-242.

Jin S, Ray RM, Johnson LR (2008). TNF-alpha/cycloheximide-induced apoptosis in intestinal epithelial cells requires Rac1-regulated reactive oxygen species. *Am J Physiol Gastrointest Liver Physiol* **294**, G928-937.

Jones BE, Lo CR, Liu H, Srinivasan A, Streetz K, Valentino KL *et al.* (2000). Hepatocytes sensitized to tumor necrosis factor-alpha cytotoxicity undergo apoptosis through caspase-dependent and caspase-independent pathways. *J Biol Chem* **275**, 705-712.

Jones RM, Luo L, Ardita CS, Richardson AN, Kwon YM, Mercante JW *et al.* (2013). Symbiotic lactobacilli stimulate gut epithelial proliferation via Nox-mediated generation of reactive oxygen species. *EMBO J* **32**, 3017-3028.

Kairisalo M, Bonomo A, Hyrskyluoto A, Mudo G, Belluardo N, Korhonen L *et al.* (2011). Resveratrol reduces oxidative stress and cell death and increases mitochondrial antioxidants and XIAP in PC6.3-cells. *Neurosci Lett* **488**, 263-266.

Kamata H, Honda S, Maeda S, Chang L, Hirata H, Karin M (2005). Reactive oxygen species promote TNFalpha-induced death and sustained JNK activation by inhibiting MAP kinase phosphatases. *Cell* **120**, 649-661.

Kastl L, Sauer SW, Ruppert T, Beissbarth T, Becker MS, Suss D *et al.* (2014). TNF-alpha mediates mitochondrial uncoupling and enhances ROS-dependent cell migration via NF-kappaB activation in liver cells. *FEBS Lett* **588**, 175-183.

Kim JJ, Lee SB, Park JK, Yoo YD (2010). TNF-alpha-induced ROS production triggering apoptosis is directly linked to Romo1 and Bcl-X(L). *Cell Death Differ* **17**, 1420-1434.

Kirino Y, Takeno M, Murakami S, Kobayashi M, Kobayashi H, Miura K *et al.* (2007). Tumor necrosis factor alpha acceleration of inflammatory responses by down-regulating heme oxygenase 1 in human peripheral monocytes. *Arthritis Rheum* **56**, 464-475.

Konig P, Dedio J, Muller-Esterl W, Kummer W (2002). Distribution of the novel eNOS-interacting protein NOSIP in the liver, pancreas, and gastrointestinal tract of the rat. *Gastroenterology* **123**, 314-324.

Lee SH, Seo GS, Kim HS, Woo SW, Ko G, Sohn DH (2006). 2',4',6'-Tris(methoxymethoxy) chalcone attenuates hepatic stellate cell proliferation by a heme oxygenase-dependent pathway. *Biochem Pharmacol* **72**, 1322-1333.

Liang C, Shu-Huei W, Pei-Jhen W, Jaw-Shiun T, Chau-Chung W, Chen Y-L (2013). Tumor necrosis factor-α regulates heme oxygenase-1 expression in endothelial cells via the phosphorylation of JNK/p38. *International Journal of Medical, Health, Biomedical and Pharmaceutical Engineering* **7**, 335-339.

Liu Y & Schubert DR (2009). The specificity of neuroprotection by antioxidants. *J Biomed Sci* **16**, 98.

Lotz M, Gutle D, Walther S, Menard S, Bogdan C, Hornef MW (2006). Postnatal acquisition of endotoxin tolerance in intestinal epithelial cells. *J Exp Med* **203**, 973-984.

Mailloux RJ & Harper ME (2011). Uncoupling proteins and the control of mitochondrial reactive oxygen species production. *Free Radic Biol Med* **51**, 1106-1115.

Martinez J & Moreno JJ (2000). Effect of resveratrol, a natural polyphenolic compound, on reactive oxygen species and prostaglandin production. *Biochem Pharmacol* **59**, 865-870.

Matsumoto H, Ishikawa K, Itabe H, Maruyama Y (2006). Carbon monoxide and bilirubin from heme oxygenase-1 suppresses reactive oxygen species generation and plasminogen activator inhibitor-1 induction. *Mol Cell Biochem* **291**, 21-28.

Minero VG, Khadjavi A, Costelli P, Baccino FM, Bonelli G (2013). JNK activation is required for TNF alpha-induced apoptosis in human hepatocarcinoma cells. *International Immunopharmacology* **17**, 92-98.

Muraosa Y & Shibahara S (1993). Identification of a cis-regulatory element and putative trans-acting factors responsible for 12-O-tetradecanoylphorbol-13-acetate (TPA)-mediated induction of heme oxygenase expression in myelomonocytic cell lines. *Mol Cell Biol* **13**, 7881-7891.

Murphy MP, Holmgren A, Larsson NG, Halliwell B, Chang CJ, Kalyanaraman B *et al.* (2011). Unraveling the Biological Roles of Reactive Oxygen Species. *Cell Metabolism* **13**, 361-366.

Nakahira K, Kim HP, Geng XH, Nakao A, Wang X, Murase N *et al.* (2006). Carbon monoxide differentially inhibits TLR signaling pathways by regulating ROS-induced trafficking of TLRs to lipid rafts. *J Exp Med* **203**, 2377-2389.

Naugler KM, Baer KA, Ropeleski MJ (2008). Interleukin-11 antagonizes Fas ligand-mediated apoptosis in IEC-18 intestinal epithelial crypt cells: role of MEK and Akt-dependent signaling. *Am J Physiol Gastrointest Liver Physiol* **294**, G728-737.

Otani K, Shimizu S, Chijiiwa K, Morisaki T, Yamaguchi T, Yamaguchi K *et al.* (2000). Administration of bacterial lipopolysaccharide to rats induces heme oxygenase-1 and formation of antioxidant bilirubin in the intestinal mucosa. *Dig Dis Sci* **45**, 2313-2319.

Otterbein LE & Choi AM (2000). Heme oxygenase: colors of defense against cellular stress. *Am J Physiol Lung Cell Mol Physiol* **279**, L1029-1037.

Paddenberg R, Ishaq B, Goldenberg A, Faulhammer P, Rose F, Weissmann N *et al.* (2003). Essential role of complex II of the respiratory chain in hypoxia-induced ROS generation in the pulmonary vasculature. *Am J Physiol Lung Cell Mol Physiol* **284**, L710-719.

Pajak B, Gajkowska B, Orzechowski A (2005). Cycloheximide-mediated sensitization to TNF-alpha-induced apoptosis in human colorectal cancer cell line COLO 205; role of FLIP and metabolic inhibitors. *J Physiol Pharmacol* **56 Suppl 3**, 101-118.

Queiroga CS, Almeida AS, Vieira HL (2012). Carbon monoxide targeting mitochondria. *Biochem Res Int* **2012**, 749845.

Ralph SJ, Moreno-Sanchez R, Neuzil J, Rodriguez-Enriquez S (2011). Inhibitors of succinate: quinone reductase/Complex II regulate production of mitochondrial reactive oxygen species and protect normal cells from ischemic damage but induce specific cancer cell death. *Pharm Res* **28**, 2695-2730.

Roberge S, Roussel J, Andersson DC, Meli AC, Vidal B, Blandel F *et al.* (2014). TNF-alpha-mediated caspase-8 activation induces ROS production and TRPM2 activation in adult ventricular myocytes. *Cardiovascular Research* **103**, 90-99.

Roca FJ & Ramakrishnan L (2013). TNF dually mediates resistance and susceptibility to mycobacteria via mitochondrial reactive oxygen species. *Cell* **153**, 521-534.

Rodella L, Lamon BD, Rezzani R, Sangras B, Goodman AI, Falck JR *et al.* (2006). Carbon monoxide and biliverdin prevent endothelial cell sloughing in rats with type I diabetes. *Free Radic Biol Med* **40**, 2198-2205.

Rodriguez-Rocha H, Garcia-Garcia A, Pickett C, Li S, Jones J, Chen H *et al.* (2013). Compartmentalized oxidative stress in dopaminergic cell death induced by pesticides and complex I inhibitors: distinct roles of superoxide anion and superoxide dismutases. *Free Radic Biol Med* **61**, 370-383.

Roulis M, Armaka M, Manoloukos M, Apostolaki M, Kollias G (2011). Intestinal epithelial cells as producers but not targets of chronic TNF suffice to cause murine Crohn-like pathology. *Proceedings of the National Academy of Sciences of the United States of America* **108**, 5396-5401.

Ryan MJ, Jackson JR, Hao Y, Williamson CL, Dabkowski ER, Hollander JM *et al.* (2010). Suppression of oxidative stress by resveratrol after isometric contractions in gastrocnemius muscles of aged mice. *J Gerontol A Biol Sci Med Sci* **65**, 815-831.

Sawle P, Foresti R, Mann BE, Johnson TR, Green CJ, Motterlini R (2005). Carbon monoxide-releasing molecules (CO-RMs) attenuate the inflammatory response elicited by lipopolysaccharide in RAW264.7 murine macrophages. *Br J Pharmacol* **145**, 800-810.

Schallner N & Otterbein LE (2015). Friend or foe? Carbon monoxide and the mitochondria. *Front Physiol* **6**, 17.

Schulze-Osthoff K, Beyaert R, Vandevoorde V, Haegeman G, Fiers W (1993). Depletion of the mitochondrial electron transport abrogates the cytotoxic and gene-inductive effects of TNF. *EMBO J* **12**, 3095-3104.

Schwerk J, Koster M, Hauser H, Rohde M, Fulde M, Hornef MW *et al.* (2013). Generation of Mouse Small Intestinal Epithelial Cell Lines That Allow the Analysis of Specific Innate Immune Functions. *Plos One* **8**.

Serra D, Rufino AT, Mendes AF, Almeida LM, Dinis TC (2014). Resveratrol modulates cytokine-induced Jak/STAT activation more efficiently than 5-aminosalicylic acid: an in vitro approach. *Plos One* **9**, e109048.

Shen HM & Pervaiz S (2006). TNF receptor superfamily-induced cell death: redox-dependent execution. *Faseb Journal* **20**, 1589-1598.

Skulachev VP (1996). Role of uncoupled and non-coupled oxidations in maintenance of safely low levels of oxygen and its one-electron reductants. *Q Rev Biophys* **29**, 169-202.

St-Pierre J, Buckingham JA, Roebuck SJ, Brand MD (2002). Topology of superoxide production from different sites in the mitochondrial electron transport chain. *J Biol Chem* **277**, 44784-44790.

Suematsu N, Tsutsui H, Wen J, Kang D, Ikeuchi M, Ide T *et al.* (2003). Oxidative stress mediates tumor necrosis factor-alpha-induced mitochondrial DNA damage and dysfunction in cardiac myocytes. *Circulation* **107**, 1418-1423.

Taille C, El-Benna J, Lanone S, Boczkowski J, Motterlini R (2005). Mitochondrial respiratory chain and NAD(P)H oxidase are targets for the antiproliferative effect of carbon monoxide in human airway smooth muscle. *J Biol Chem* **280**, 25350-25360.

Terry CM, Clikeman JA, Hoidal JR, Callahan KS (1998). Effect of tumor necrosis factor-alpha and interleukin-1 alpha on heme oxygenase-1 expression in human endothelial cells. *Am J Physiol* **274**, H883-891.

Terry CM, Clikeman JA, Hoidal JR, Callahan KS (1999). TNF-alpha and IL-1alpha induce heme oxygenase-1 via protein kinase C, Ca2+, and phospholipase A2 in endothelial cells. *Am J Physiol* **276**, H1493-1501.

Udono-Fujimori R, Takahashi K, Takeda K, Furuyama K, Kaneko K, Takahashi S *et al.* (2004). Expression of heme oxygenase-1 is repressed by interferon-gamma and induced by hypoxia in human retinal pigment epithelial cells. *European Journal of Biochemistry* **271**, 3076-3084.

Ungvari Z, Labinskyy N, Mukhopadhyay P, Pinto JT, Bagi Z, Ballabh P *et al.* (2009). Resveratrol attenuates mitochondrial oxidative stress in coronary arterial endothelial cells. *Am J Physiol Heart Circ Physiol* **297**, H1876-1881.

Vera T, Henegar JR, Drummond HA, Rimoldi JM, Stec DE (2005). Protective effect of carbon monoxide-releasing compounds in ischemia-induced acute renal failure. *J Am Soc Nephrol* **16**, 950-958.

Vidal K, Grosjean I, evillard JP, Gespach C, Kaiserlian D (1993). Immortalization of mouse intestinal epithelial cells by the SV40-large T gene. Phenotypic and immune characterization of the MODE-K cell line. *J Immunol Methods* **166**, 63-73.

Vile GF, Basu-Modak S, Waltner C, Tyrrell RM (1994). Heme oxygenase 1 mediates an adaptive response to oxidative stress in human skin fibroblasts. *Proc Natl Acad Sci U S A* **91**, 2607-2610.

Wang X, Wang Y, Kim HP, Nakahira K, Ryter SW, Choi AM (2007). Carbon monoxide protects against hyperoxia-induced endothelial cell apoptosis by inhibiting reactive oxygen species formation. *J Biol Chem* **282**, 1718-1726.

Wilson CA & Browning JL (2002). Death of HT29 adenocarcinoma cells induced by TNF family receptor activation is caspase-independent and displays features of both apoptosis and necrosis. *Cell Death Differ* **9**, 1321-1333.

Chapter VII

SUMMARY

Chapter VII Summary

A single layer of intestinal epithelial cells (IECs) in the gut provides a physical barrier between the organism and the luminal content. It allows the passage of nutrients and electrolytes but also forms the intestinal epithelial barrier preventing the passage of pathogens. The maintenance of its homeostasis is of prime importance for the survival of the organism. Apoptosis in the intestinal epithelium is an important regulator of mucosal homeostasis. Even though apoptotic cell death of IECs in the crypts and villi is continuously present during the physiological state, excessive apoptotic cell death has been implicated in gastrointestinal (GI) disorders. Disturbance of the intestinal epithelial barrier occurs during acute GI inflammatory disease conditions such as necrotizing enterocolitis (NEC), and can have a triggering role during sepsis. Sepsis is driven by a complex cascade initiated by bacteria-derived molecules with subsequent inflammation, oxidative stress and mitochondrial dysfunction. The disruption of the intestinal epithelial barrier results in invasion of commensal bacteria and the excessive production of inflammatory cytokines by mucosal immune cells, eventually leading to pathological inflammation during sepsis. This can be accompanied by sepsis-induced ileus, facilitating the passage of luminal content. Postoperative ileus (POI), occurring after abdominal surgery, is related to the occurrence of an inflammatory process in the muscular layer, induced by surgical handling of the intestine. In a mouse model of POI, our laboratory has shown the occurrence of an early 'oxidative burst' in the mucosa following intestinal manipulation. This might possibly lead to increased intestinal permeability, which then can contribute to or trigger the muscular inflammation. Tumor necrosis factor-α (TNF-α) is one of the early inflammatory cytokines known to play an important role during epithelial barrier dysfunction by induction of IEC apoptosis; it is also known to be one of the early inflammatory agents in the pathogenesis of POI. In addition to its pro-inflammatory effects, exposure to TNF-α has been shown to be associated with an increase in oxidative stress in many cell lines and thus could be expected to cause the same effect in IECs. Among the intracellular antioxidant pathways, heme oxygenase-1 (HO-1) is a stress-responsive protein known to be upregulated by oxidative stress and inflammatory signals; it is known to exert cytoprotection. The beneficial effect of HO-1 is mainly attributed to the products of HO-1 activity, namely biliverdin/bilirubin and still more to carbon

monoxide (CO). Emerging evidence reveals that CO can exert diverse biological and cytoprotective effects. The recent discovery of CO-releasing molecules (CO-RMs) which allow controlled CO delivery in biological systems highlights the potential use of this class of compounds to deliver CO for therapeutic purposes. In the GI tract, CO/CO-RMs protect against the development of POI and decrease inflammation and associated tissue damage during sepsis. In addition, CO has been shown to reduce ischemia/reperfusion injury of intestinal grafts and development of NEC. Another strategy to obtain the beneficial effects of HO-1 is to induce it by pharmacological means. A frequently studied cytoprotective compound, that at least in some models acts through induction of HO-1, is the plant polyphenol resveratrol.

The aim of this thesis was to establish an *in vitro* IEC model to assess TNF-α-induced oxidative stress, inflammation and cell death, and to investigate the protective effects of CO-RMs and resveratrol versus the TNF-α-induced dysfunction concentrating on their anti-oxidative effect.

The murine MODE-K IEC line was established as an *in vitro* model to assess TNF-α-induced oxidative stress and apoptotic cell death **(chapter III)**. Similar to many other cell types, TNF-α required a combination with the protein synthesis inhibitor cycloheximide (CHX) to induce cell death in MODE-K cells. TNF-α (0.1-1 ng)/CHX decreased cell viability, increased caspase-3/7 activity, induced apoptosis, decreased the level of reduced glutathione (GSH) and increased production of reactive oxygen species (ROS) in a concentration-dependent manner in MODE-K cells. TNF-α/CHX-induced apoptosis occurred in parallel with ROS production from 2 h after the start of exposure. CORM-A1 and resveratrol were the most effective cytoprotective agents tested among the set of HO-1-related products and antioxidant compounds, that was investigated; resveratrol abolished and CORM-A1 reduced TNF-α/CHX-induced ROS production. Treatment of MODE-K cells with TNF-α/CHX caused attenuation of basal HO-1 expression. None of the tested agents induced HO-1 in the presence of TNF-α/CHX in MODE-K cells; this suggests that the cytoprotection by CORM-A1 and resveratrol involves a HO-1 independent mechanism.

As TNF-α/CHX-induced ROS production occurred in parallel with cell death, the relation between TNF-α/CHX-induced cell death and ROS production was further investigated, assessing the sources of ROS production **(chapter IV)**. Using flow cytometry, simultaneous determination of the production of total ROS or mitochondrial superoxide

anion ($O_2^{\bullet-}$) and of cell death was assessed. Exposure to TNF-α/CHX time-dependently increased intracellular total ROS and mitochondrial $O_2^{\bullet-}$ production in MODE-K cells, starting from 2 h, which corresponds with the onset of apoptotic cell death. The significant reduction of TNF-α/CHX-induced ROS production and cell death by the antioxidants butylated hydroxytoluene, butylated hydroxyanisole, N-acetylcysteine and tiron underlines the important role of ROS production in cell death of MODE-K cells. By use of a set of inhibitors, it was shown that mitochondria and nicotinamide adenine dinucleotide phosphate oxidases (NOX) are the two major sources of ROS overproduction during TNF-α/CHX-induced cell death in MODE-K cells, with $O_2^{\bullet-}$ being the major type of ROS. Particularly, the quinone-binding sites of mitochondrial complex I (site I_Q) and complex II (site Q_P) seem to be the major sites of mitochondrial ROS production. TNF-α/CHX treatment caused an immediate decrease in mitochondrial respiration, and a loss of mitochondrial membrane potential and increase in mitochondrial dysfunction from 1 h of exposure on; this was followed by ROS production and cell death from 2 h on suggesting a possible sequential link between these cellular events.

Reducing oxidative stress in IECs may be a therapeutic approach to treat acute GI disorders. As ROS production corresponds to TNF-α/CHX-induced cell death in MODE-K cells, with CORM-A1 and resveratrol decreasing both these effects, the antioxidant mechanisms of these cytoprotective agents were investigated **(chapter V)**. While CORM-A1 did not influence basal levels of intracellular total or mitochondrial ROS, resveratrol increased total cellular ROS but decreased mitochondrial ROS production. Both CORM-A1 and resveratrol reduced total ROS production induced by TNF-α/CHX, but only resveratrol abolished the TNF-α/CHX-induced increase in mitochondrial ROS level. Resveratrol greatly reduced and abolished TNF-α/CHX-induced mitochondrial depolarization and mitochondrial dysfunction respectively, but CORM-A1 only mildly influenced these parameters. The cytoprotective effect of resveratrol versus TNF-α/CHX in MODE-K cells is thus predominantly due to mitigation of mitochondrial ROS production, while CORM-A1 acts solely on NOX-derived ROS to protect MODE-K cells. As the cytoprotective effect of resveratrol was clearly more pronounced than that of CORM-A1, this might correlate with a sequential communication from mitochondria to NOX for TNF-α/CHX-induced ROS production in MODE-K cells.

Conclusions

A murine *in vitro* model of TNF-α/CHX-induced oxidative stress and apoptosis was established using MODE-K cells, with ROS production corresponding to cell death. Mitochondria and NOX are the two major sources of ROS overproduction during TNF-α/CHX-induced cell death in MODE-K cells; $O_2^{\bullet-}$ was identified to be the predominant ROS. The quinone-binding sites of mitochondrial complexes I (site I_Q) and II (site Q_p) seem to be the major ROS production sites in the mitochondria. The pronounced cytoprotective effect of resveratrol against TNF-α/CHX-induced cell death involves the abolishment of mitochondrial ROS/$O_2^{\bullet-}$ while a NOX-dependent mechanism contributes to the moderate cytoprotection by CORM-A1. Taken together, these results imply that the antioxidant effects of CORM-A1 and resveratrol in IECs could be of potential therapeutic benefit to offer a solution for acute GI inflammatory conditions involving oxidative stress of the IEC layer.

Chapter VIII

SAMENVATTING

Chapter VIII   Samenvatting

Een enkele laag van intestinale epitheliale cellen (IECs) in de darm vormt een fysieke barrière tussen het organisme en de darminhoud. Ze laat de passage van voedingsbestanddelen en electrolieten toe maar vormt ook de intestinale epitheliale barrière welke de passage van pathogenen voorkomt. Het behoud van de homeostase van de intestinale epitheliale cellaag is van primair belang voor de overleving van het organisme. Apoptose in het intestinal epitheel is een belangrijke regulator van de mucosale homeostase. Weliswaar is celdood van IECs door apoptose in de krypten en villi continu aanwezig in fysiologische condities, maar overmatige celdood door apoptose kan betrokken zijn in gastro-intestinale (GI) aandoeningen. Verstoring van de intestinale epitheliale barrière treedt op tijdens acute GI inflammatoire aandoeningen zoals necrotizerende enterocolitis (NEC); dit kan ook een uitlokkende rol spelen tijdens sepsis. Sepsis wordt gedreven door een complexe cascade, in gang gestoken door van bacteriën afkomstige moleculen, met daarop volgend inflammatie, oxidatieve stress en mitochondriale dysfunctie. Het doorbreken van de intestinale epitheliale barrière leidt tot invasie van commensale bacteriën en overmatige productie van inflammatoire cytokinen door immuuncellen in de mucosa, wat uiteindelijk leidt tot pathologische inflammatie tijdens sepsis. Sepsis kan ook gepaard gaan met ileus, wat de passage van darminhoud doorheen de darmwand bevordert. Postoperatieve ileus (POI), die optreedt na abdominale chirurgie, wordt veroorzaakt door een inflammatoir proces in de spierlaag, uitgelokt door de manipulatie van de darm tijdens de operatie. In een model van POI bij de muis, werd in ons laboratorium voorheen aangetoond dat zich een vroege 'oxidatieve opstoot' voordoet in de mucosa na intestinale manipulatie. Dit kan mogelijk leiden tot verhoogde intestinale permeabiliteit, wat kan bijdragen aan de inflammatie in de spierlaag of deze zelfs kan uitlokken. Tumor necrosis factor-α (TNF-α) is één van de inflammatoire cytokinen, die een rol speelt in de dysfunctie van de epitheliale barrière door inductie van apoptose van de IECs; het is ook één van de vroege inflammatoire agentia in de pathogenese van POI. Naast zijn pro-inflammatoire effecten, is blootstelling aan TNF-α geassocieerd met een toename in oxidatieve stress in verschillende cellijnen zodat een gelijkaardig effect kan verwacht worden in IECs. Onder de intracellulaire anti-oxiderende signaalwegen, is heem oxygenase-1 (HO-1) een proteïne dat opgeregeld wordt

door oxidatieve stress en inflammatoire signalen; het heeft een cytoprotectief effect. Dit gunstig effect van HO-1 wordt hoofdzakelijk toegeschreven aan de producten bekomen door de enzymatische activiteit van HO-1, namelijk biliverdine/bilirubine en nog meer koolstofmonoxide (CO). Meer en meer evidentie ondersteunt dat CO talrijke biologische en cytoprotectieve effecten heeft. De recente ontwikkeling van CO-vrijstellende moleculen (CO-RMs) met gecontroleerde afgifte van CO in biologische systemen maakt toediening van CO voor therapeutische doeleinden mogelijk. In de GI tractus, beschermen CO/CO-RMs tegen de ontwikkeling van POI en zij verminderen de inflammatie en de geassocieerde weefselbeschadiging tijdens sepsis. Verder gaat CO letsels door ischemie/reperfusie van intestinale transplanten en de ontwikkeling van NEC tegen. Een andere strategie om de gunstige effecten van HO-1 te bekomen is het te induceren op farmacologische wijze. Een cytoprotectieve stof die reeds frequent werd bestudeerd, en althans in sommige modellen werkzaam is door inductie van HO-1, is het polyfenol resveratrol, dat aanwezig is in diverse planten.

De bedoeling van dit proefschrift was om een in vitro model van IECs te ontwikkelen ten einde de oxidatieve stress en celdood door TNF-α te onderzoeken. Verder werden de beschermende effecten van CO-RMs en resveratrol op deze door TNF-α uitgelokte dysfuncties onderzocht, hierbij concentrerend op hun anti-oxidatief effect.

The MODE-K IEC lijn, afkomstig van de muis, werd ontwikkeld als in vitro model voor onderzoek van oxidatieve stress en apoptotische celdood door TNF-α **(chapter III)**. Zoals voor vele andere celtypes, was het nodig om TNF-α te combineren met de proteïnesynthese-inhibitor cycloheximide (CHX) om celdood in MODE-K cellen uit te lokken. TNF-α (0.1-1 ng)/CHX verminderde de leefbaarheid van de cellen, verhoogde de caspase-3/7 activiteit, lokte apoptose uit, verminderde het gehalte aan gereduceerd glutathion (GSH) en verhoogde de productie van reactieve zuurstofspecies (ROS) op concentratie-afhankelijke manier. De door TNF-α/CHX-uitgelokte apoptose trad op in parallel met de productie van ROS vanaf 2 u na de start van de blootstelling. CORM-A1 en resveratrol waren de meest effectieve cytoprotectieve agentia onder de bestudeerde set van HO-1-afhankelijke producten en anti-oxiderende substanties; CORM-A1 veminderde de door TNF-α/CHX uitgelokte productie van ROS terwijl resveratrol ze ophief. Behandeling van MODE-K cellen met TNF-α/CHX veroorzaakte een daling van de basale expressie van HO-1. Geen enkele van de geteste substanties verhoogde de expressie van HO-1 in aanwezigheid van TNF-α/CHX in

de MODE-K cellen; dit suggereert dat de cytoprotectie door CORM-A1 en resveratrol plaats grijpt via een mechanisme dat onafhankelijk is van HO-1 .

Vermits de productie van ROS door TNF-α/CHX in parallel optreedt met de celdood, werd het verband tussen de door TNF-α/CHX uitgelokte celdood en productie van ROS verder bestudeerd, om de bronnen van de ROS te detecteren **(chapter IV)**. Door gebruik van "flow cytometry" werd simultaan de productie van totaal ROS of van mitochondriale superoxide anionen ($O_2^{\bullet-}$), en van celdood bestudeerd. Blootstelling aan TNF-α/CHX verhoogde tijdsafhankelijk de productie van intracellulair totaal ROS en van mitochondriale $O_2^{\bullet-}$ in MODE-K cellen, startende vanaf 2 u, wat overeenkomt met de start van de apoptotische celdood. De significante vermindering van de door TNF-α/CHX uitgelokte productie van ROS en celdood door de anti-oxiderende substanties gebutyleerd hydroxytolueen, gebutyleerd hydroxyanisol, N-acetylcysteïne en tiron bevestigt de belangrijke rol van ROS in de celdood van MODE-K cellen. Door studie van het effect van een set inhibitoren, werd aangetoond dat mitochondria en nicotinamide adenine dinucleotide fosfaat oxidasen (NOX) de 2 belangrijkste bronnen zijn van ROS tijdens de door TNF-α/CHX uitgelokte celdood in MODE-K cellen, met $O_2^{\bullet-}$ als belangrijkste ROS-type. De bindingsplaatsen van quinone in het mitochondriale complex I (site I_Q) en complex II (site Q_P) blijken de majeure mitochondriale productieplaatsen te zijn van mitochondriale ROS. Behandeling met TNF-α/CHX veroorzaakte een onmiddellijke daling in de mitochondriale respiratie, en vanaf 1 u een daling van de mitochondriale membraanpotentiaal en een toename in mitochondriale dysfunctie; dit werd gevolgd door productie van ROS en celdood vanaf 2 u wat een sequentieel verband tussen deze cellulaire fenomenen suggereert.

Vermindering van de oxidatieve stress in IECs zou een therapeutische benadering van acute GI aandoeningen kunnen vormen. Vermits de productie van ROS door TNF-α/CHX overeenkomt met de uitgelokte celdood in MODE-K cellen, en CORM-A1 en resveratrol beide effecten verminderen, werden de anti-oxiderende mechanismen van deze cytoprotectieve agentia verder onderzocht **(chapter V)**. Terwijl CORM-A1 de basale spiegels van intracellulair totaal ROS en mitochondriaal ROS niet beïnvloedde, verhoogde resveratrol totaal cellulair ROS maar verminderde het de basale spiegel van mitochondriaal ROS. Zowel CORM-A1 als resveratrol verminderde de productie van totaal ROS door TNF-α/CHX, maar alleen resveratrol hief de toename van mitochondriale ROS en $O_2^{\bullet-}$ door TNF-α/CHX op. Resveratrol verminderde uitgesproken de mitochondriale depolarizatie door TNF-α/CHX en

hief de mitochondriale dysfunctie op, terwijl CORM-A1 slechts een mild effect had op beide parameters. Het cytoprotectief effect van resveratrol versus TNF-α/CHX in MODE-K cellen berust dus hoofdzakelijk op onderdrukking van de mitochondriale productie van ROS, terwijl CORM-A1 enkel aangrijpt op NOX om de MODE-K cellen te beschermen. Vermits het cytoprotectief effect van resveratrol duidelijk meer uitgesproken was dan dit van CORM-A1, kan dit wijzen op een sequentiële communicatie van de mitochondria naar NOX toe tijdens de productie van ROS uitgelokt door TNF-α/CHX in MODE-K cellen.

Besluiten

Een in vitro model om oxidatieve stress en apoptose uitgelokt door TNF-α/CHX in IECs te bestuderen werd ontwikkeld door gebruik te maken van MODE-K cellen, afkomstig van de muis. De productie van ROS correleerde met het optreden van celdood. Mitochondria en NOX zijn de 2 majeure bronnen van overproductie van ROS tijdens door TNF-α/CHX uitgelokte celdood in MODE-K cellen; $O_2^{\bullet-}$ is het belangrijkste betrokken ROS. De bindingsplaatsen voor quinone van mitochondriaal complex I (site I_Q) en complex II (site Q_p) lijken de majeure productieplaatsen van ROS in de mitochondria. Het uitgesproken cytoprotectief effect van resveratrol versus TNF-α/CHX berust op de opheffing van de productie van mitochondriaal ROS/$O_2^{\bullet-}$ terwijl een NOX-afhankelijk mechanisme bijdraagt aan de matige cytoprotectie door CORM-A1. De anti-oxiderende effecten van CORM-A1 en resveratrol in IECs kunnen mogelijk therapeutisch nuttig zijn voor acute GI inflammatoire condities, waarin oxidatieve stress van de IEC-laag betrokken is.

Chapter IX

ACKNOWLEDGEMENTS

Acknowledgements

First of all, I am deeply grateful to my promoter, Prof. Dr. Romain Lefebvre, for providing me an opportunity to carry out my PhD research at the Heymans Institute of Pharmacology. I submit my respectable thanks for believing in my potential and performance. It was a great experience learning science under your leadership. Your consistent efforts with documentation to start my PhD in Gent was unforgettable; I am thankful to all your care and concern right from landing in Gent till the last toughest days of extended living supports during the completion of thesis. You have been a steady influence through my PhD life with your unwavering support and scholarly guidance. I am thankful for your constructive research ideas, feedbacks and suggestions during my PhD. I have always admired and looked up to your hard work, scientific expertise, writing skills and dedication to science; I will constantly strive to inculcate all these qualities which I learned from you throughout my career.

I am indebted to thank Prof. Dr. Georges Leclercq, without whom my PhD would not have been possible. Thank you for allowing me to work at the Department of Clinical Chemistry, Microbiology and Immunology. I should say that you cared about my PhD life as equal as Prof. Romain Lefebvre and adopted me as your own lab student. You always provided me with kind support, experimental assistance, constructive inputs whenever I needed during my research. I would also take this opportunity to thank the entire team (Els Van Ammel, Aline Van Acker, Dr. Sylvie Taveirne, Jessica Filtjens, Mandy Vanhees, Sophie Vermaut and Katia Reynvoet) for extending their support whenever I needed during my experiments; especially Els Van Ammel and Aline Van Acker for teaching me the techniques of basic immunology and isolation of primary intestinal epithelial cells. I already wish the new members of the lab, Filipa Martins Ribeiro and Sigrid Wahlen, success with their PhD.

I would like to thank all the members of the examination committee, Prof. Claude Cuvelier (chair), Prof. Van Ginneken Christa, Prof. Marc Bracke, Prof. Pieter Vanden Berghe, Prof. Anja Geerts, Prof. Mohammed Lamkanfi and Prof. Ken Bracke for their constructive comments and valuable suggestions to improve the quality of this thesis.

I want to thank all my lab colleagues for always being friendly which provided a good working environment for me. First of all, a big thanks goes to Els Van Deynse for her assistance in every aspect of my Belgian study life. She helped me right from searching for the accommodation before my arrival to Gent till the quick acclimatization of the lab life. Sorry for troubling you with many mailing queries and you patiently answered all of them despite your busy life. I really learned an organized working style from you and thanks for helping me all through the experiments of my first project. Many thanks to Dr. Ole De Backer for initiating an interesting project which laid the basis for my thesis. I could never get a better office colleague than Dr. Sarah Cosyns, who was always friendly at all the times during the lab life. Many chats, bike rides and dinners with Dr. Sabine Weninger was unforgettable and thanks Sabine for those good memories. Many thanks to Dr. Filip de Vin for his nice scientific talks and Sze Men Choi for her uninterrupted help all the time for my experiments. I also thank Valére Geers and Inge Van Colen for their friendliness which gave me the sense of oneness in the lab. Thanks to Jonas Van Dingenen for teaching me the intestinal ischemia-reperfusion model; I wish you and Vicky Pauwelyn all the best for your success with PhD.

A big thanks goes to Mrs. Annie De Smet, who helped me a lot with a lot of administrative tasks during my initial settling in Gent and Mrs. Danielle Woods, who was always extending her support with smile for the administrative tasks with regard to University. For all the technical support, I want to thank Bart Blanckaert, Samuel Tshitenge, Diego De Baere and especially Tom Vanthuyne, who helped a lot with all computer problems. Many thanks to Joscha Van Bree and Tjeu Pubben for their nice friendship.

My special thanks to Prof. Dr. Roberto Motterlini (INSERM U955, France) for providing us with CORMs and his scientific comments during the review and manuscript preparations.

For my first project, I had an opportunity to work in the lab of General Biochemistry and Physical Pharmacy and I am thankful to prof. Stefaan Desmedt for that. Many thanks to Bart Lucas, the lab manager, who provided me with the rights and access to utilize the facilities available in the lab. Thanks a lot to Dr. Koen Raemdonck and Dr. Stefaan Soenen for their supports during the experiments.

For my second project, I had the great opportunity to work in the lab of Prof. Peter Vandenabeele (molecular signaling and cell death unit, VIB). I have to thank Dr. Quinten Remijsen for initiating the collaboration with the unit. Even though I could not get a chance

to work with him during the experiments, his scientific discussions and positive words have always been a great support to complete my PhD. Thanks a lot to Vera Goossens for helping me with Seahorse experiments and Tom Vanden Berghe for interesting scientific suggestions. My thanks to Evelien Van Hamme and Eef Parthoens, who assisted me during daylong/late evening imaging experiments.

I owe my special thanks to all my friends in Ghent who made me feel at home during the whole PhD study life. Even though the list would appear long, I could not find any other place than here to extend my gratitude to all of them – Krishnan CMC, Sreeda krishnan, Sridhar Vepa, Vijaya Kameswari, Mokshada, Srikanth Lavu, Lalithya Pratti, Prasanna Ramaswamy, Farhan Azmat Ali, Neelam, Mahad, Muthahir, Ramanan Muthuraman, Saravana Kumar, Sriram Balusu, Vimal Kumar, Vijayaraj, Savita, Dharshana, Dhiya, Sreeparvathi, Swarnakamal Priyabadhini, Sreegovind, Pradeep Alava, Santosh Kadam, Megha, Visu, Srividhya Sundararaman, Tharakachand Ponnala, Sachin Sharma, Chetna, Kalkin, Abhishek Dixit, Richa, Ashwini Rajkumar, Srinath Govindarajan, Dhanyamithra, Jacob Sukumaran, Fenila, Shahid Kahloon, Vijayakumar Sukumaran and Jitesh Neupane.

I owe my respectable thanks to Mr. Sridhar Eswaran, my high school chemistry teacher, who seeded the zeal towards drug research and for being a constant source of inspiration all through my life so far.

Last but not the least, I would like to thank the family I am blessed and fortunate to be part of, for all their love and enormous encouragement. For my parents, thanks for letting me to lead the life what I want. Thanks a lot Kiran, my dear brother and Kavitha, my dear sister, for being there with our parents to take care of them in my absence and constantly support me to succeed in my research life.
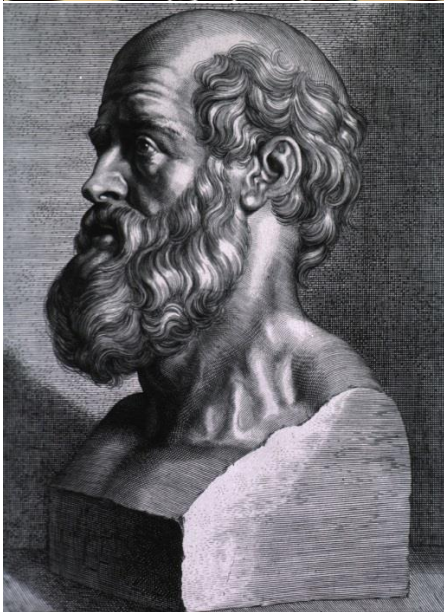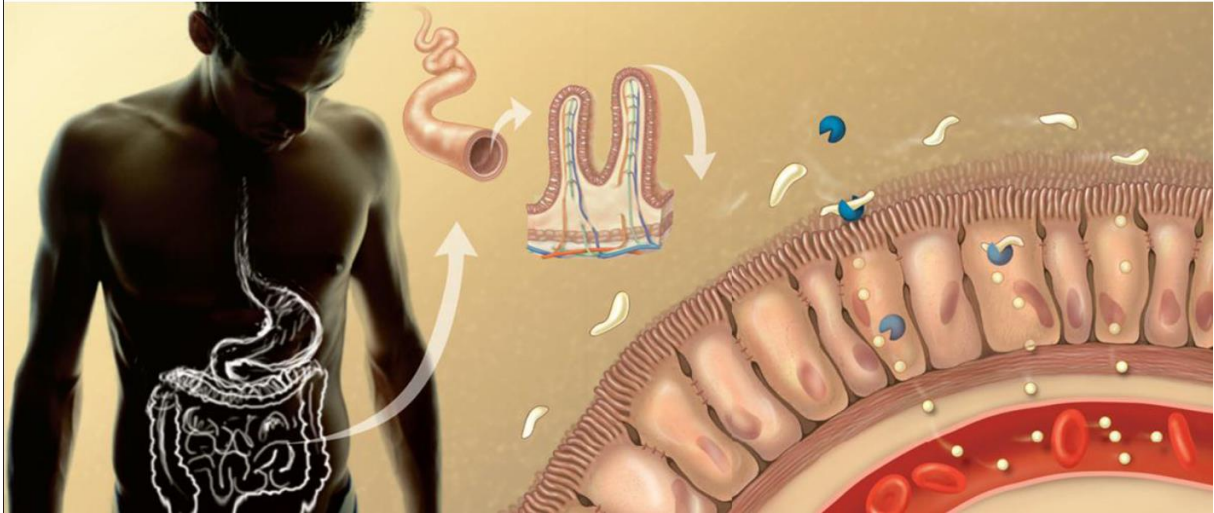
"All Disease Begins in The Gut!"
-Hippocrates